INFORMATION TO USERS

This manuscript has been reproduced from the microfilm master. UMI films the text directly from the original or copy submitted. Thus, some thesis and dissertation copies are in typewriter face, while others may be from any type of computer printer.

The quality of this reproduction is dependent upon the quality of the copy submitted. Broken or indistinct print, colored or poor quality illustrations and photographs, print bleedthrough, substandard margins, and improper alignment can adversely affect reproduction.

In the unlikely event that the author did not send UMI a complete manuscript and there are missing pages, these will be noted. Also, if unauthorized copyright material had to be removed, a note will indicate the deletion.

Oversize materials (e.g., maps, drawings, charts) are reproduced by sectioning the original, beginning at the upper left-hand corner and continuing from left to right in equal sections with small overlaps.

ProQuest Information and Learning
300 North Zeeb Road, Ann Arbor, MI 48106-1346 USA
800-521-0600

TURBO-BLAST
A NOVEL TECHNIQUE FOR MULTI-TRANSMIT AND MULTI-RECEIVE WIRELESS COMMUNICATIONS

By

MATHINI SELLATHURAI
B.SC. ENG., LICENTIATE ENG.

A Thesis
Submitted to the School of Graduate Studies
in Partial Fulfilment of the Requirements
for the Degree
Doctor of Philosophy

McMaster University

TURBO-BLAST

DOCTOR OF PHILOSOPHY (2001) MCMASTER UNIVERSITY

(Electrical and Computer Engineering) Hamilton, Ontario

TITLE: TURBO-BLAST
A Novel Technique for Multi-Transmit and Multi-Receive Wireless Communications

AUTHOR: Mathini Sellathurai
Licentiate of Eng. (KTH, Sweden)
B.Sc. Eng. Honors (Peradeniya)

SUPERVISOR: Prof. Simon Haykin

NUMBER OF PAGES: xx, 186

To my parents.

Abstract

Wireless communications technology is presently undergoing a tremendous expansion, which is brought on by the proliferation of many diverse and very compelling applications. These trends are continually pushing the demand for substantially increased information capacity, which can only be realized through the development of novel communication techniques.

In this context, we may mention a ground-breaking wireless communication technique that offers a tremendous potential to increase the information capacity of the channel, namely, the multi-transmit and multi-receive (MTMR) antenna system, which is popularized as the *Bell-Labs Layered Space-Time* (BLAST) architecture. In particular, the Diagonal-BLAST (D-BLAST) and the Vertical-BLAST (V-BLAST), developed by Bell labs of Lucent Technologies, permit signal processing complexity to grow linearly, with the capacity increase being made possible through the use of a large number of transmit and receive antennas. However, from a practical perspective, D-BLAST is inefficient for short packet transmissions due to its boundary space-time wastage. Meanwhile, V-BLAST suffers from error propagation due to deep fades in the wireless channel.

In this thesis, we propose Turbo-BLAST, a novel multi-transmit and multi-receive antenna system that can handle any configuration of transmit and receive antennas. It presents a framework of simple yet highly effective random space-time transmission and iterative joint-decoding receivers for BLAST architectures. Specifically, we show that the embodiment of turbo principles and the BLAST architecture provides a practical solution to the requirement of high data-rate transmission in a reliable manner for future wireless communication systems.

Acknowledgements

First and foremost, I wish to thank my supervisor Simon Haykin for guiding me through this thesis work. I have deep admiration for him and for his work. I consider it a great privilege to have had the opportunity to work with him. I would also like to thank the members of my supervisory committee Jim Reilly and Narayanaswamy Balakrishnan for their helpful comments and advice.

I would like to thank the members of the Wireless Communications Research organization at Bell Laboratories' Crawford Hill Lab in Holmdel for their support and for providing a conducive environment in which to perform parts of this research. I am indebted to Jerry Foschini for imparting to me his insights into information theory and for his inspiration as well as his confidence in my work; Reinaldo Valenzuela for his time and effort to establish this research collaboration and the necessary funding for the same; Mike Gans and Dragan Samardzija for the experimental measurements and advice; Linda Logsdon for her administrative help; and Kit August for providing a pleasant stay in NJ.

I would like to thank the members of the Communications Research Laboratory, McMaster University; I am indebted to Cheryl Gies, Helen Jachna, Lola Brooks and Terry Greenlay for their administrative support; and Sada Puthusserypady, Sabrina Quick, Eliana Yepez, Al Patel, Gaurav Patel, Chris Lesner, Kris Huber, Nelson Costa, Behnam Shahrrava for fruitful discussions and chats; and Chris Lesner for proofreading the thesis.

Most of all, I would like to thank Raty for introducing me to the wonderful world of wireless communications and his encouragement, insights, and support throughout the years.

Abbreviations

A/D	Analogue-to-Digital.
APP	*a posteriori* Probability.
AWGN	Additive White Gaussian Noise.
BCJR	Bahl, Cocke, Jelinek, and Raviv.
BER	Bit-Error Rate.
BPSK	Binary Phase Shift Keying.
BLAST	Bell-Labs Layered Space-Time.
CAI	Co-Antenna Interference.
CDF	Cumulative Distribution Functions.
CCI	Co-channel Interference.
CDMA	Code Division Multiple Access.
codec	Coder-Decoder.
CSI	Channel State Information.
D/A	Digital-to-Analogue.
D-BLAST	Diagonal-BLAST.
DEMUX	De-Multiplexer.
DSP	Digital Signal Processing.
FDMA	Frequency Division Multiple Access.
FEC	Forward Error-Correction.
FM	Frequency Modulation.

GF	Galois Field.
iid	Independent and Identically distributed.
ISI	Inter-Symbol Interferences.
IPSIC	Iterative Parallel Soft-Interference Canceler.
LAN	Local Area Networks.
LDPC	Low-density Parity-Check.
LLR	Log-Likelihood Ratio
LOS	Line Of Sight.
MAP	Maximum *a posteriori*.
MIPS	Million Instructions Per Second.
MRC	Maximum-Ratio-Combiner
MTMR	Multi-Transmit Multi-Receive.
MTSO	Mobile Telephone Switching Office.
ML	Maximum Likelihood.
MMSE	Minimum Mean-Squared Error.
MOD	Modulation.
MUX	Multiplexer.
PEP	Pairwise Error Probability.
PCS	Personal Communications Services.
PSIC	Parallel Soft Interference Canceler
PSTN	Public Switching Telephone Networks
QPSK	Quadrature Phase Shift Keying.
RF	Radio Frequency.
RSC	Recursive Systematic Convolutional.
RST	Random Space-Time.
RSTB	Random Space-Time Block.
SIC	Serial Interference Cancellation.
SISO	Soft-In/ Soft-Out.
SNR	Signal-to-Noise Ratio.

STC	Space-Time Code.
T-BLAST	Turbo-BLAST.
V-BLAST	Vertical-BLAST.
WLAN	Wireless Local Area Networks.
ZF	Zero-Forcing.

Notations

- a is a scalar.
- $\mathbf{a} = [a_1, a_2, \ldots, a_n]^T$ is a column vector.
- $\mathbf{A} = \begin{bmatrix} A_{11} & A_{12} \\ A_{21} & A_{22} \end{bmatrix}$ is a matrix.
- a^* is the conjugate of the complex scaler a.
- $(\mathbf{A})^T$ is the transpose of $\mathbf{A}$.
- $(\mathbf{A})^H$ is the complex conjugate transpose of $\mathbf{A}$.
- $\mathbf{a}_i$ is the i-th column of matrix $\mathbf{A}$.
- A_{ij} is the ij-th element of matrix $\mathbf{A}$.
- $\mathbf{I}_n$ is an $n \times n$ identity matrix.
- $a(t)$ is a as a function of t.
- $\det(\mathbf{A})$ is the determinant of matrix $\mathbf{A}$.
- $\mathrm{tr}(\mathbf{A})$ is the trace of matrix $\mathbf{A}$.
- $\mathrm{rank}(\mathbf{A})$ is the rank of matrix $\mathbf{A}$.
- $\mathbf{A}^+$ is the Moore-Penrose pseudo-inverse of matrix $\mathbf{A}$.
- $|a| = \sqrt{\Re(a)^2 + \Im(a)^2}$ is the absolute value of the complex scaler a.

- $\|\mathbf{a}\| = \sqrt{|a_1|^2 + \ldots + |a_n|^2}$ is the L_2-norm of the vector $\mathbf{a}$.
- $\|\mathbf{A}\| = \sqrt{\sum_{j=1}^{n} \sum_{i=1}^{m} |a_{ji}|^2}$ is the Frobenius-norm of the matrix $\mathbf{A}$ of size $n \times m$.
- $\mathcal{R}$ is the field of real numbers.
- $\mathcal{C}$ is the filed of complex numbers.
- $\mathcal{R}^n$ is the n-dimensional real space.
- $\mathcal{C}^n$ is the n-dimensional complex space.
- $P(A)$ is the probability of an event A.
- $P(A/B)$ is the conditional probability of the event A given that the event B has occurred.
- $f(a)$ is the probability density function of the random variable a.
- $\mathcal{E}(a)$ is the expected value of a.
- $\log a$ is the natural logarithm of $a > 0$, $a \in \mathcal{R}$.
- $\log_b a$ is the logarithm to the base b of a.

Contents

1 Introduction 1

1.1 Multi-Transmit Multi-Receiver Wireless Communications 1

1.2 Background 3

1.2.1 Succeeding Generations of Wireless System 3

1.2.2 Limits and Challenges of Wireless Channel 4

1.2.3 Traditional Wireless Channel 5

1.2.4 Multi-transmit, Multi-receive Channel Models 8

1.2.5 Diversity Techniques and Design Concepts 10

1.3 Outline of the Thesis 13

1.4 Significant Contributions of the Thesis 14

2 Multiple Antenna Techniques 16

2.1 Basic MTMR Scheme: Definitions and Notations 17

2.2 Information Theory of MTMR Systems 19

2.2.1 Rayleigh Fast-Fading Channel 20

2.2.2 Quasi-Fading Channel 20

2.3 BLAST Architecture 25

2.3.1 Diagonal-BLAST 28

2.3.2 Vertical-BLAST (V-BLAST) 32

2.3.3 Improved V-BLAST 37

2.3.4 Coded Vertical-BLAST 38

2.4 Space-Time Codes 43
2.4.1 Design Criterion 43
2.5 Low-Rate Space-Time Codes 45
2.5.1 Space-Time Trellis Codes 45
2.5.2 Space-Time Block Codes 47
2.6 High-Rate Space-Time Codes 49
2.7 Summary 50

3 The Turbo Principle **55**
3.1 History of Channel Coding 56
3.1.1 Channel coding / Feedforward Error-Correction Encoding 57
3.2 TURBO Coding 59
3.2.1 Parallel Concatenated Turbo Codes 60
3.2.2 Serial Concatenated Turbo Codes 65
3.3 SISO Decoders 68
3.3.1 Historical Remark 68
3.3.2 Generalized BCJR Algorithm 69
3.3.3 The MAP Algorithm in Log-Domain (LOG-MAP Algorithm) 74
3.4 Summary 77

4 TURBO-BLAST **78**
4.1 T-BLAST Transmitter 79
4.1.1 Assumptions 79
4.1.2 Notations 79
4.2 Random Space-Time Block (RSTB) Codes 81
4.2.1 Space-Time Interleaving 82
4.2.2 Intentional Time-Varying Channel 84
4.3 Optimal Detection 85
4.3.1 Optimal Decoding with No Interleavers 86
4.3.2 Optimal Decoding of RSTB Codes 87

4.4 Asymptotic Performance Analysis of RSTB Codes 87
4.5 Capacity of Correlated Channels 91
4.6 Iterative Decoders 93
4.6.1 Iterative Decoding Algorithm 99
4.7 Design and Performance of Soft in/Soft out Detectors 102
4.7.1 Performance Lower Bound 103
4.7.2 Detector based on Maximum *a posteriori* Probability Estimation . . 104
4.7.3 PSIC with Bootstrapping Channel Estimates 110
4.7.4 Minimum Mean-Square Error Receiver 114
4.8 Simulation Results 117
4.8.1 Performance of PSIC Receivers 118
4.8.2 Performance of MMSE Receivers 121
4.8.3 MMSE Vs MRC for T-BLAST 124
4.8.4 Interleaver Dependence 126
4.9 Summary 129

5 Experimental Verification of TURBO-BLAST **138**
5.1 The Bell Lab's BLAST Test-Bed 138
5.1.1 Indoor Test-Bed 139
5.1.2 Transmitter 139
5.1.3 Receiver 140
5.2 Performance Results 141
5.2.1 Experiments with (8,6)-BLAST 141
5.2.2 Experiments with (8,5)-BLAST 144
5.3 Summary 144

6 Spectral Efficiency of TURBO-BLAST **155**
6.1 System Description 156
6.1.1 T-BLAST System 156
6.1.2 Coded V-BLAST System 156

6.2 Indoor Environment 157
6.2.1 T-BLAST vs V-BLAST, $n_T = n_R = 8$ 157
6.2.2 T-BLAST vs V-BLAST, $n_T = 5, 6, 7$ and $n_R = 8$ 160
6.2.3 T-BLAST vs V-BLAST, $n_T = 8$ and $n_R = 5, 6, 7$ 161
6.2.4 Spectral Efficiency 165
6.3 Outdoor Environment 167
6.3.1 T-BLAST vs V-BLAST 167
6.3.2 Spectral Efficiencies 167
6.4 Summary 170

7 Conclusions **171**

List of Tables

2.1 4-PSK 4 state space-time code with 2 transmit antennas 46
6.1 Spectral efficiency of T-BLAST in an indoors environment. 166
6.2 Spectral efficiency of V-BLAST in an indoors environment. 166
6.3 Spectral efficiency of T-BLAST in an outdoors environment. 170
6.4 Spectral efficiency of V-BLAST in an outdoors environment. 170

List of Figures

1.1 Future wireless communications 4

1.2 A typical Rayleigh fading envelope with Doppler frequency =100 Hz, at 1 GHz carrier frequency and 100 Km/H vehicle speed. 7

1.3 Spatial diversity 12

2.1 An (n_T, n_R) system 18

2.2 Outage capacity of (N, N) system with N=1,2,4,8 and 16, $\rho = 18dB$. 23

2.3 Outage capacity of different $((n_T, n_R))$ systems, $\rho = 18dB$ 25

2.4 A BLAST system 26

2.5 Eye diagram 27

2.6 D-BLAST architecture 29

2.7 Diagonal coding 30

2.8 Uncoded V-BLAST architecture 33

2.9 Horizontal coded V-BLAST architecture 39

2.10 Vertical coded V-BLAST architecture 40

2.11 Concatenated coded V-BLAST architecture 41

2.12 Second-stage iterative receiver for V-BLAST 41

2.13 4-PSK 4 state space-time code with 2 transmit antennas 46

2.14 Space-Time Block Code with 2 transmit antennas 48

2.15 The 10% outage capacity of BLAST systems with $n_T = n_R = 8$ 50

3.1 Turbo codes 60

3.2 Turbo decoder 61

3.3 Serially concatenated convolutional codes 65
3.4 Iterative decoder for serially concatenated codes 66
3.5 Trellis section between time t and $t+1$ 70
4.1 T-BLAST transmitter 80
4.2 Receiving end 81
4.3 Diagonal interleaver. 83
4.4 T-BLAST transmitter and intentional time-varying channel. 84
4.5 Channel response before interleaving. 85
4.6 Channel response after interleaving. 86
4.7 Channel capacity vs correlation coefficient for n=2,4,8 and 16 at SNR = 30dB 93
4.8 Channel capacity vs correlation coefficient for (4,4) system at SNR =20dB and 30dB 94
4.9 The RSTB codes as serially concatenated codes. 95
4.10 Iterative decoder 97
4.11 Space-time turbo encoder 1. 98
4.12 Space-time turbo encoder 2. 98
4.13 Space-time turbo encoder 1. 99
4.14 Soft interference cancellation detector. 109
4.15 Performance of the proposed receivers for the encoded BLAST system. . . . 110
4.16 Parallel soft interference cancellation detector. 114
4.17 Quasi-static Rayleigh channel of eight transmit antennas 118
4.18 Slow fading Rayleigh channel of eight transmit antenna with Doppler frequency =10 Hz at 1 GHz carrier frequency and 10Km/H vehicle speed. . . 119
4.19 BER Vs. iterations, Doppler frequency = 0 Hz, SNR = 9dB 120
4.20 BER Vs. SNR, Doppler frequency = 0 Hz 120
4.21 BER vs iterations, Doppler frequency = 20 Hz, SNR = 9dB 122
4.22 BER Vs. SNR, Doppler frequency = 20 Hz 122
4.23 BER Vs. SNR, The continuous lines and dashed lines represent, respectively, the performance of the T-BLAST-MMSE 1 and 2 124

4.24 BER Vs. transmitters for T-BLAST-MMSE receiver 1, SNR = 8dB 125
4.25 BER Vs. SNR for time-invariant channel 126
4.26 BER Vs. SNR for time-varying channel 127
4.27 Performance comparison of D- and T-BLAST schemes 128
4.28 Performance variation with interleaver size L 129
5.1 Bit-error performance of T- BLAST, n_T=8 and n_R=6 with convolutional code of rate $R = 1/2$ and constraint length 3, and $\pi/4$-shifted QPSK modulated. 145
5.2 Number of errors vs packets in T-BLAST, n_T=8 and n_R=6 with convolutional code of rate $R = 1/2$ and constraint length 3, and $\pi/4$-shifted QPSK modulation. 146
5.3 Signal-space diagram at the receiver output in T-BLAST for packet 1, n_T=8 and n_R=6 with convolutional code of rate $R = 1/2$ and constraint length 3, and $\pi/4$-shifted QPSK modulation. 147
5.4 Mean-squared error at the receiver output of T-BLAST for packet 1, n_T=8 and n_R=6 with convolutional code of rate $R = 1/2$ and constraint length 3, and $\pi/4$-shifted QPSK modulation. 148
5.5 Signal-space diagram at the receiver output for packet 2 in T-BLAST, n_T=8 and n_R=6 with convolutional code of rate $R = 1/2$ and constraint length 3, and $\pi/4$-shifted QPSK modulation. 149
5.6 Mean-squared error at the receiver output of T-BLAST for packet 2, n_T=8 and n_R=6 with convolutional code of rate $R = 1/2$ and constraint length 3, and $\pi/4$-shifted QPSK modulation. 150
5.7 Average BER performance vs iterations of T-BLAST with and without encoding, n_T=8 and n_R=6 with convolutional code of rate $R = 1/2$ and constraint length 3, and $\pi/4$-shifted QPSK modulation. 151
5.8 Signal-space diagram at the receiver output for packet 1 in T-BLAST, n_T=8 and n_R=5 with convolutional code of rate $R = 1/2$ and constraint length 3, and $\pi/4$-shifted QPSK modulation. 152

5.9 Mean-squared error at the receiver output of T-BLAST for packet 1, n_T=8 and n_R=5 with convolutional code of rate $R = 1/2$ and constraint length 3, and $\pi/4$-shifted QPSK modulation. 153
5.10 Average BER performance vs iterations of T-BLAST with and without encoding, n_T=8 and n_R=5 with convolutional code of rate $R = 1/2$ and constraint length 3, and $\pi/4$-shifted QPSK modulation. 154
6.1 T-BLAST vs V-BLAST using real channel measurements for $n_T = n_R = 8$, using convolutional code with rate $R = 1/2$ and constraint length 3, and QPSK modulation. 158
6.2 BER performance of T-BLAST with increasing iterations, using the real channel measurements for $n_T = 8$ and $n_R = 8$, using convolutional code with rate $R = 1/2$ and constraint length 3, and QPSK modulation. 159
6.3 Convergence behavior of the T-BLAST receiver at SNR=4dB for (n_T=8, n_R=8), using convolutional code with rate $R = 1/2$ and constraint length 3, and QPSK modulation. 160
6.4 Bit error performance for n_T=5,6,7 and 8 and n_R=8, using convolutional code with rate $R = 1/2$ and constraint length 3, and QPSK modulation. . . 162
6.5 Convergence behavior of the T-BLAST receiver at SNR=4dB for n_T=7 and n_R=8, using convolutional code with rate $R = 1/2$ and constraint length 3, and QPSK modulation. 162
6.6 BER performance of T-BLAST with increasing iterations, for $n_T = 7$ and $n_R = 8$, using convolutional code with rate $R = 1/2$ and constraint length 3, and QPSK modulation. 163
6.7 Bit error performance for n_T=8 and n_R=5,6,7 and 8, using convolutional code with rate $R = 1/2$ and constraint length 3, and QPSK modulation. . . 164
6.8 Convergence of the T-BLAST receiver at SNR=4dB for (n_T=8, n_R=7), using convolutional code with rate $R = 1/2$ and constraint length 3, and QPSK modulation. 164

6.9 Bit error performance with number of iterations for n_T=8 and n_R=7, using convolutional code with rate $R = 1/2$ and constraint length 3, and QPSK modulation. 165
6.10 Bit error performance for $n_T = 5$ and $n_R = 7$, using convolutional code with rate $R = 1/2$ and constraint length 3, and QPSK modulation for outdoor channels. 168
6.11 Bit error performance for n_T=4 and n_R=7, using convolutional code with rate $R = 1/2$ and constraint length 3, and QPSK modulation for outdoor channels. 168
6.12 Bit error performance for n_T=3 and n_R=7, using convolutional code with rate $R = 1/2$ and constraint length 3, and QPSK modulation for outdoor channels. 169

Chapter 1

Introduction

1.1 Multi-Transmit Multi-Receiver Wireless Communications

We are in the midst of a communications revolution facilitated, in part, by advances in wireless communications, such as wireless internet and multimedia communications and leading to the next generation of wireless systems, i.e., "the fourth generation" (4G). As the wireless industry becomes ubiquitous and popular, the need for a high-data rate and large user capacity on a wireless platform is the key driver in developing *robust* communication techniques, which offer substantially increased information capacity.

The major concern in wireless communications research is to provide techniques that use the frequency spectrum — a scarce resource — efficiently. The basic information theory result reported in a pioneering paper [1] by Foschini and Gans showed enormous spectral efficiency can be achieved through the use of multi-transmit multi-receive (MTMR) antenna systems. The major conclusion of their work is that the capacity of an MTMR system far exceeds that of a single-antenna system. In particular, in a Rayleigh flat fading environment, an MTMR link has an asymptotic capacity that increases linearly with the number of transmit and receive antennas, provided that the complex-valued propagation coefficients between all pairs of transmit and receive antennas are statistically independent and known to the receiver antenna array.

In this context, we may mention an MTMR strategy that offers a tremendous potential to increase the information capacity of single user wireless communication systems, namely, the *Bell-Labs Layered Space-Time (BLAST)* architecture. The major challenge here is to design an efficient codec architecture that can closely realize the great capacity promised by information theory and yet maintain manageable system complexity. In this regard, three primary innovations are worth mentioning here.

The first version of BLAST system, proposed by Foschini [2], used a novel Diagonal Layered Space-Time architecture, hence the terminology *Diagonal-BLAST* or *D-BLAST*. The D-BLAST architecture can attain the channel capacity limits by using one-dimensional (1-D) codec technology. However, from a practical perspective, D-BLAST is inefficient for short packet transmissions due to its boundary space-time wastage (see Chapter 2 for explanation).

The next version of BLAST, *Vertical-BLAST*, described in [3]-[5], was the first practical system demonstrated in the literature. In Vertical-BLAST (V-BLAST), every antenna transmits its own independent stream of data, using a simple vector encoding and linear decoding structure. This architecture can achieve up to fifty percent channel capacity with no channel coding. However, V-BLAST has no built-in space-time codes to overcome deep fades from any of the transmit antennas.

The next major innovation was Turbo-BLAST [6]-[14], which uses a relatively simple space-time encoder and an iterative joint detector-decoder with turbo-like operation. The structure of the space-time encoder and the turbo-like operation allows Turbo-BLAST to realize the full benefits of BLAST in a computationally feasible manner. Furthermore, it offers

- high information capacity (efficiency)
- low bit-error rate (reliability)

This thesis is primarily concerned with the Turbo-BLAST architecture, or in short, T-BLAST. Specifically, we show that the combination of turbo principles and the BLAST

architecture is a practical and reliable solution to the requirement of high data-rate for wireless communication.

1.2 Background

1.2.1 Succeeding Generations of Wireless System

Over the past two decades, wireless communication technologies have moved through the first two generations of the wireless systems [15]-[16]. Technical interest in both generations of wireless systems was primarily focused on increasing capacity for voice and low data-rate services, such as email. The first generation services were based on frequency modulation (FM) and frequency division multiple access (FDMA). The second generation of wireless systems moved from analogue systems to micro and macro cellular digital systems. The market expansion, triggered by the emergence and popularity of new applications and services such as wireless internet and wireless multimedia communications, has driven the focus of technology improvement for wireless services in a new direction. The new wireless networks support not only cellular and personal communications services (PCS) but also fixed wireless packet oriented narrowband and broadband services. Currently, the third generation of wireless is being standardized for worldwide deployment [17] with emphasis on

- high mobility for 2 Mb/s broadband and 384 kb/s narrowband data services, and
- low mobility for 20-30 Mb/s broadband (5GHz) and 2 Mb/s narrowband data services.

Today, research focus is on the fourth generation of wireless system where mobile users are portable computers such as laptops with a compact wireless transceiver and with sufficient computing power for digital video and multimedia applications. Although, radios that operate in a burst and multi access mode at hundreds of Mb/s are not commercially available yet, they are the focus of most of the research projects. The fourth and higher generation systems will likely support [18]

- up to 20 Mb/s for moving vehicles, and
- up to 600 Mb/s for low mobility systems.

Figure 1.1 shows an overview of the fourth generation which consists of mobile users including laptop mobile terminals with access to multimedia services, just as wired local area networks (LANs) provide access to such services for personal computers and workstations.

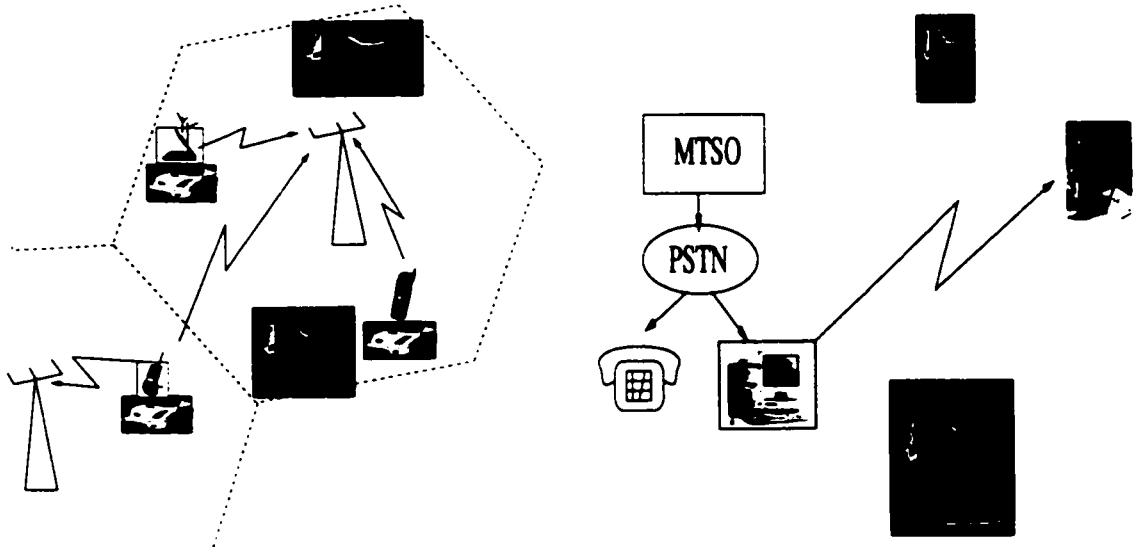

(a) Mobile Cellular Structures (b) Wireless Local Area Networks

Figure 1.1: Future wireless communications

1.2.2 Limits and Challenges of Wireless Channel

The physical limitation of the wireless channel poses a great challenge on the design of an MTMR antenna scheme. In a wireless communications system, information is carried from a transmitter to a receiver by electromagnetic waves through space and is affected by many factors including the speed of motion (mobile receiver) and severe obstructions between the transmitter and receiver. The propagation of radio waves through the physical environment involves diffraction, refraction, and reflection.

The major challenge is to find statistical models that closely approximate wireless channels. Unlike traditional wireless transmitters and receivers, a multi-transmit multi-receive antenna system involves multi-input, multi-output matrix wireless channels. To successfully design an MTMR system, it is important to develop/understand the statistical models of the matrix channel. In particular, the models must account for the physical impairment that characterizes the channels.

1.2.3 Traditional Wireless Channel

The mobile radio channel is characterized by shadowing, path loss, and multi-path fading [19]-[22].

- Shadowing is the fluctuation of mean signal strength, which depends on size of the obstructions between the transmitter and receiver, such as buildings. Shadowing is also referred to as slow fading and can be modeled by a stochastic process that follows a log-normal distribution. According to the central limit theorem, in the case of many obstructions, the logarithm of the sum of attenuation approaches a normal distribution[1].

- Path loss is due to dependence of the received signal on the distance between the transmitter and receiver. In ideal free space propagation, the received signal power is proportional to the inverse square of the distance between the transmitter and receiver. Only empirical models are available to characterize the path loss in an indoor environment. To characterize path loss we can use empirical models such as:

$$P(d) = K_p P_o d^{\eta_p} \tag{1.1}$$

where P_o is the transmitted power, d is the distance between the transmitter and the receiver, K_p is a constant and η_p is called the path loss exponent. A typical value for η_p ranges between 1.5 and 2 for line-of-sight channels and between 5 and 6 for

[1]That is, $10\log_{10}(P)$ follows the normal distribution, where P is the net attenuation

channels in cluttered areas [19].

- Multi-path fading: The waves propagating from the transmitter to the receiver do not travel simply through one particular path, but bounce and reflect off objects in the environment so that multiple replicas of the transmitted signal arrive at the receiver via many paths. The replicas arrive at the receiver at different times and interfere either constructively or destructively. This phenomenon causes fast fading, but small scale fluctuations in the received signal strength. An accepted probabilistic model for the fast fading random channel, when there is no line-of-sight path between the transmitter and receiver, is the Rayleigh distribution.

  According to the central limit theorem, when there is no line of sight path, the real and imaginary parts of the received random variables are independent Gaussians. The sum of two quadrature Gaussian noise signals obeys a Rayleigh distribution [24]:

$$\begin{aligned} h &= (h_1 + ih_2) \\ &= \alpha \cdot \exp(i\theta) \end{aligned} \tag{1.2}$$

  where h_1 and h_2 are independent Gaussian random variables with variance σ_1^2 and σ_2^2, respectively. The random variable θ represents the phase which is uniformly distributed from 0 to 2π, and the variable α has a Rayleigh distribution from 0 to ∞ with variance $\sigma^2 = \sigma_1^2 + \sigma_2^2$:

$$f_\alpha(r) = \begin{cases} \frac{r}{\sigma^2} \exp\left(\frac{-r^2}{2\sigma^2}\right) & r \geq 0 \\ 0 & \text{elsewhere} \end{cases} \tag{1.3}$$

  The Rayleigh distributed signal envelope as a function of time is shown in Figure 1.2. When a dominant stationary unfaded line-of-sight signal component exists, then the effect of dominant and the many weaker multi-path signals gives rise to a Ricean

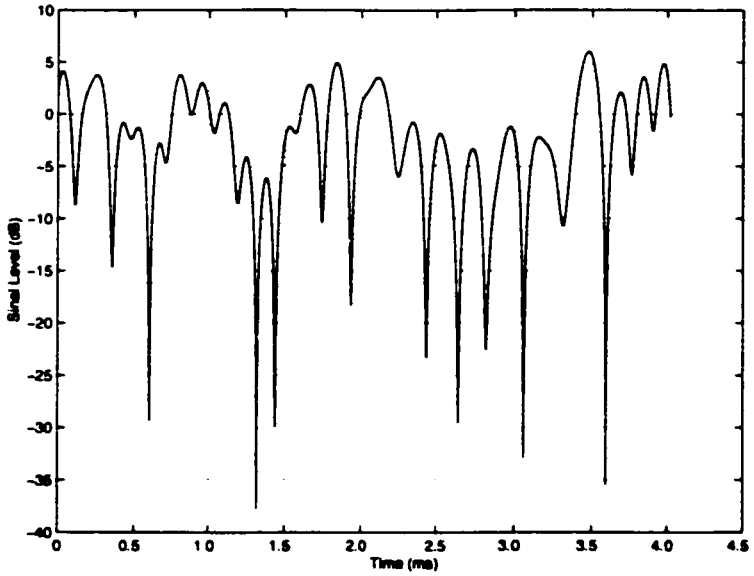

Figure 1.2: A typical Rayleigh fading envelope with Doppler frequency =100 Hz, at 1 GHz carrier frequency and 100 Km/H vehicle speed.

distribution of the fast fading signal envelope:

$$f_\alpha(r) = \frac{r}{\sigma^2} \exp\left(-\frac{r^2 + A^2}{2\sigma^2}\right) \mathrm{I}_0\left(\frac{Ar}{\sigma^2}\right) \tag{1.4}$$

where the parameter A denotes the peak amplitude of the dominant signal and I_0 is the modified Bessel function of the first kind and zero order. The parameter $K = A^2/(2\sigma^2)$ is known as the Ricean factor or K factor.

Moreover, the small-scale fading experienced by a signal propagating through a mobile wireless channel depends on the nature of the transmitted signal with respect to the following characteristics of the channel. In this context, we may mention the following:

- Flat and frequency Fading: The transmitted signals are scattered by buildings and hills, and arrive at the receiver as multiple replicas at different times. *Delay spread* is the second central moment of the *delay spectrum*. The reciprocal of the delay spread is called the *coherence bandwidth*. If the bandwidth of the transmitted signal is less than the coherence bandwidth then the channel is called a *flat-fading* channel; otherwise,

it is called a *frequency-selective fading* channel.

- Fast and slow fading: Motion, either of the mobile user or objects in the surrounding environment, causes a *Doppler shift* in the received signal, which is characterized by the rate of variation in the received signal level. The *Doppler spread* is the second central moment of the *Doppler spectrum*. The reciprocal of the Doppler spread is called the *channel coherence time*. If the transmitted signal duration is less than the channel coherence time then the fading is called *slow fading*; otherwise, it is called *fast fading*.

- Space-selective fading: Each propagation path reaches the receiver at different angles, which leads to *angle spread*. The inverse of the angle spread characterizes the channel *coherence distance*. If a signal is received by spatially separated antennas and the antennas are separated by *coherence distance* or more, then the received signals essentially have uncorrelated envelopes.

1.2.4 Multi-transmit, Multi-receive Channel Models

The biggest open questions in the area of modeling the MTMR channel deal with:

- indoor and outdoor space-time multi-path propagation characteristics at various spectrum ranges up to 60 GHz,

- reflection and transmission characteristics of various indoor construction materials and architectures,

- rain attenuation probability characteristics in outdoor environment.

The theoretical MTMR models validated with measured matrix channels of n_T transmit and n_R receive antennas can be classified as [25]-[28]:

- The uncorrelated high rank model [1], [25]: The fundamental model approximating each element in the matrix channel as an independent and identically distributed (iid) complex zero mean and unit variance entry:

- $H_{ij} = \mathcal{N}(0, 1/\sqrt{2}) + \sqrt{-1}\mathcal{N}(0, 1/\sqrt{2})$, that is $H_{ij} \sim \mathcal{CN}(0, 1)$
- $|H_{ij}|^2$ is a chi-squared (χ_2^2) variate but normalized to $\mathcal{E}[\,|H_{ij}|^2] = 1$.

- The uncorrelated low rank model [25]: In this model, the antenna elements at both transmitter and receiver sides have uncorrelated fading and yet have a rank deficient MTMR channel with reduced capacity. This channel model is described by

$$\mathbf{H} = \mathbf{h}_R \mathbf{h}_T^H \tag{1.5}$$

  where $\mathbf{h}_R$ and $\mathbf{h}_T$ are independent transmit and receive fading vectors with iid complex zero mean and unit variance entries $\mathbf{h}_T \sim \mathcal{CN}(0, \mathbf{I}_{n_R})$, $\mathbf{h}_T \sim \mathcal{CN}(0, \mathbf{I}_{n_T})$. This model assumes that the propagation scattering energy travels through a very thin air pipe, giving rise to the "pin hole" or "key hole" phenomenon. For this class of channel, the diversity gain is present, but there is no multiplexing gain.

- The correlated low rank model: If the antenna elements of either transmitter or receiver are correlated, then the MTMR system has a rank deficient channel matrix with reduced capacity. This channel model is described by

$$\mathbf{H} = h_R h_T^* \mathbf{u}_R \mathbf{u}_T^H \tag{1.6}$$

  where $h_R \sim \mathcal{CN}(0, 1)$, $h_T \sim \mathcal{CN}(0, 1)$ are independent random variables and $\mathbf{u}_R$ and $\mathbf{u}_T$ are fixed deterministic vectors of size $n_R \times 1$ and $n_T \times 1$ with unit modulus entries, respectively. In this situation, there is no diversity and multiplexing gain; only receiver array gain is present.

The initial experimental studies have successfully demonstrated that with a half-wavelength separation between the antenna elements at each transmit and receive end, rich scattering is almost always guaranteed in indoor channels. This confirmed that the entries of the channel matrix are independent complex Gaussian random variables. In this scenario, the MTMR matrix channels have high rank and hence achieve high capacity [3] and [25].

Despite this recent successful demonstration of the MTMR measurements in the indoor environment, the effective rank of the matrix channel depends on indoor structures and the distance between the transmitter and receiver. For instance, measurements taken in a long hallway at Lucent Technologies in Crawford Hill Labs shows that the presence of a strong line of sight component and the limited angular spread of the scatterers reduces the effective rank of the channel transfer matrix and therefore the ideal channel capacity cannot be achieved [27].

The realization of MTMR capacities in the outdoor environment is an open question. The matrix channel capacity is sensitive to both the fading correlation between individual antennas and the rank behavior of the channel. The probability of fading correlated and low-rank matrix channels is much higher in an outdoor environment.

1.2.5 Diversity Techniques and Design Concepts

Diversity is a powerful technique for combating the degrading effects of multi-path fading in wireless communications [29]-[31]. When the wireless channel experiences a deep fade, the bit errors occur in clusters and error-correcting codes cannot cope with this situation. In this scenario, by providing several, say ψ, versions of the same signal transmitted over independently faded channels, chances are good that at least one or more of these received signals will not be in a deep fade at any given time, and hence the signal reception can be enhanced. The conditional error probability over a Rayleigh fading channel can be approximated with

$$P \approx \kappa \cdot \rho^{\psi} \tag{1.7}$$

where the signal-to-noise ratio (SNR) of the Rayleigh faded channel is given by

$$\rho = \sum_{i=1}^{\psi} \rho_i \tag{1.8}$$

where ρ_i is the SNR of each independent path. Here the number of independent paths ψ is called the diversity order since the probability of error rate decreases with the ψth power of SNR.

To achieve the diversity gain, these independent signals must be combined in clever ways. In the decreasing order of performance, maximum ratio combining, equal gain combining and selection combining are well known diversity combining techniques. An overview of these diversity techniques is found in [29].

Independent fading can be created explicitly or implicitly. In the former case, the same signal is transmitted independently at the expense of resources to exploit a diversity channel. In the latter case, the signal is transmitted only once but in such a way so as to exploit the diversity effect induced by multi-path propagation. A good example of exploiting implicit diversity is MTMR, because Rayleigh flat fading is beneficial to MTMR. Paradoxically, the BLAST system exploits the multi-path by using scattering characteristics at both transmitter and receiver ends.

The spatial diversity provided in BLAST establishes a strong wireless link between the transmitter and receiver. Figure 1.3 illustrates the implicit diversity in BLAST, where eight independent fading signals are shown along with the average of all eight independent signals. The fades in the resulting signal are smooth and have a strong average power level at any given time.

Figure 1.3 clearly shows that communication systems that exploit diversity have many benefits. In an MTMR system, many diversity dimensions are exploited to combat the fading and co-antenna interferences path and time.

- Spatial diversity: In an MTMR system, to get sufficient spatial diversity channels or the uncorrelated fading channels, the antennas should be separated more than the coherence distance. The coherence distance is inversely proportional to the angle spread, thus the required spacing between the antennas depends on the degree of multi-path angle spread. Moreover, the coherence distance also increases with the antenna height. In the case of a mobile terminal, where the multi-path angle spread

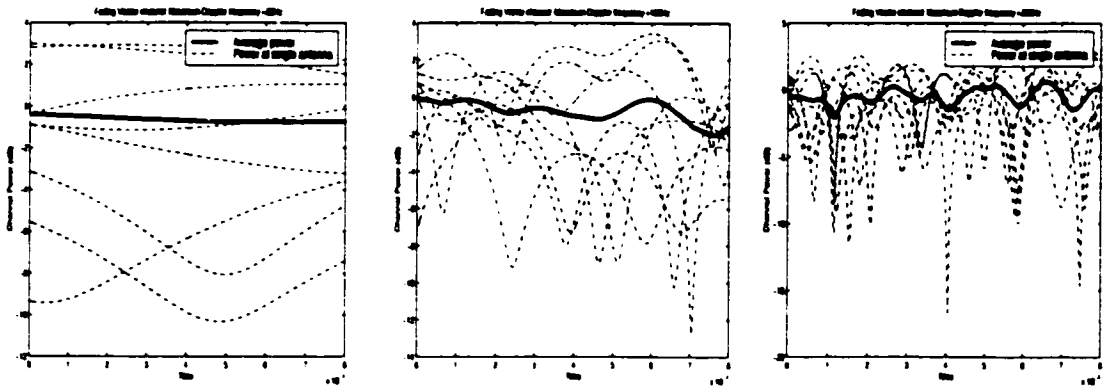

(a) *Slow fading* *Max. Doppler Freq.* = $20Hz$ (b) *Fast fading* $100Hz$ (c) *Very fast fading* $200Hz$

Figure 1.3: Spatial diversity

is sufficiently large, the antenna spacing in the order of 0.5-0.8 times the wavelength is adequate. On the other hand, at the base stations where the antennas are mounted at a higher points, the multi-path angle spread is small and the coherence distance is typically 10-20 times the wavelength.

- Polarization diversity: In addition to spatial diversity, implicit or explicit polarization diversity can also be used in MTMR to get higher gain. The multiple antennas can be polarized differently for reception/transmission to create channels that fade independently.

- Time diversity: Usually exploited via combined interleaving and forward-error correction coding and automatic-repeat requests (ARQ). The function of the interleaver is to spread errors and randomize their positions. However, due to the fading characteristics of wireless channels, under slow fading (slow moving), channel coding in combination with time interleaving is not effective. This thesis adds a space-time interleaving to MTMR system to boost performance in slow fading conditions. (see Chapter 4 for details).

- Frequency diversity: In narrowband systems, frequency diversity is not an option since the delay spread of the multi-path is small. However, for wideband MTMR systems,

frequency diversity may be used [32]-[37].

1.3 Outline of the Thesis

This thesis is motivated by the desire for developing a technique for high data rate that efficiently uses the scarce frequency spectrum in a computationally feasible manner. Technical challenges are yet to be solved in several areas. In particular, new physical-layer-related techniques (channel coding, modulation and diversity) that operate at bandwidth efficiencies that are multiples of those of current systems using MTMR schemes have yet to be investigated. Therefore, a prime motivation of this thesis is to provide a new T-BLAST architecture that is not only computationally efficient but also yields an error rate that is orders of magnitude smaller than traditional BLAST systems.

This thesis is composed of two parts. The first part, consisting of chapters one to three, reviews the literature and discusses the fundamental issues leading to the concept of T-BLAST. The second part, consisting of chapters four through seven, contains detailed descriptions of T-BLAST and the experimental results obtained. The experimental analyses include performance evaluation of the T-BLAST wireless communication system using the narrowband BLAST test-bed at the Bell-Labs of Lucent Technologies, Crawford Hill, New Jersey.

Chapter two details the current literature on MTMR techniques and describes some of the mathematical issues involved from the viewpoint of information theory. MTMR systems fall into three general cases: knowing the channel state information (CSI) at the receiver, knowing the CSI both at transmitter and receiver and blind schemes (no CSI at transmit and receive). The thesis deals with the first case, where we learn the CSI by transmitting training sequences potentially with each packet. Although the overhead reduces the efficiency of the system, it is proved to be the most practical way of recovering the signals in wireless communication systems. The existing BLAST architecture designs and space-time code designs fall under the first category. Here, the D-BLAST serves as the unique theoretical architecture that can attain the capacity limits of MTMR techniques,

and the V-BLAST is a simplified BLAST that has been demonstrated to work in real-life. We also discuss coded V-BLAST systems.

In chapter three, we review turbo principles. Here, we illustrate both the turbo encoding and decoding principles for serial and parallel concatenated convolutional codes. We also review maximum *a posteriori* (MAP) detection and the practical implementation of MAP symbol estimation developed by Bahl, Cocke, Jelinek, and Raviv (BCJR).

In chapter four, we introduce the T-BLAST architecture and theoretical aspects of the proposed turbo space-time codes. The analyses show that the proposed random space-time codes are capable of approaching capacity limits when we use global maximum likelihood (ML) solutions. We closely approximate the global ML with iterative decoders that are based on turbo principles. We also introduce suboptimal implementation of different iterative techniques. This includes a simple development of the T-BLAST algorithms and illustration of their properties using simulation results. In simulations, we used a quasi-static Raylcigh fading channel, where a matrix of independent Rayleigh fading coefficients are generated and the fading coefficients are fixed over a burst of symbols transmitted but they are changed considerably from one burst to the next, and Rayleigh slow fading channel, where independent Rayleigh fading channels are generated according to the modified Jakes model [38] with maximum Doppler frequency between 0 to 30 Hz.

In chapters five to six, we demonstrate T-BLAST performance using real-life data. Most importantly, the performance evaluations using real-life data are presented for both indoor and outdoor fixed wireless communications environments. Lastly, in chapter seven, we summarize all our contributions.

1.4 Significant Contributions of the Thesis

This thesis makes three significant contributions:

- A novel MTMR scheme, using a simple yet effective random space-time encoder, is derived. The proposed random space-time coding scheme can be viewed as a turbo space-time code that is implemented by using independent one-dimensional block

codes and space-time interleavers. In this framework, we use high-rate codes. Therefore, we increase the transmission rate of the system by increasing the number of transmit antennas. The codes can be designed simply by using traditional forward error-correction (FEC) coding schemes.

- Three sub-optimal turbo-like iterative decoders are derived, which perform joint channel estimation and decoding of the proposed space-time codes in an iterative and simple fashion. The net result is a new transmitter/receiver (transceiver), which is not only computationally efficient but it also yields a probability of error performance that is orders of magnitude smaller than the corresponding coded V-BLAST.

- These findings are confirmed by studying the performance of the new transceiver both theoretically and experimentally. The experimental analysis includes performance evaluation of T-BLAST in a real-life environment using the narrowband BLAST testbed at the Bell-Labs of Lucent Technologies, Crawford Hill, New Jersey. Using real-life experiments, we show that the Shannon capacity of MTMR schemes is achieved within a few dBs of average signal-to-noise ratio (SNR), which includes the losses due to practical coding schemes. Moreover, we show that a power gain of 2-4dBs is achieved over the corresponding coded V-BLAST system.

Chapter 2

Multiple Antenna Techniques

In recent years, multiple antenna techniques have become a pervasive idea that promises extremely high spectral efficiency for wireless communications. Two issues of concern here are:

- Information-theoretic aspects of data transmission using multi-transmit multi-receive (MTMR) antenna techniques with emphasis on spectral efficiency and information capacity.
- Practical feasibility of these techniques, aimed as the realization of a significant portion of capacity promised by information theory.

In this chapter, we first review the information theory behind MTMR techniques over Rayleigh fast fading and quasi-static fading channels. Then, we review the existing MTMR schemes characterized by the layered space-time concept, the so-called BLAST architecture. In this context, we present the D-BLAST architecture and prove that a D-BLAST system with whitened matched filters can attain Shannon's capacity bounds. Next, we consider a practical BLAST architecture called V-BLAST. The chapter also reviews the framework of space-time coding techniques. Popular low-rate space-time coding techniques, space-time trellis codes and space-time block codes, are described.

2.1 Basic MTMR Scheme: Definitions and Notations

Consider a discrete time MTMR wireless communication system with n_T transmit antenna elements and n_R receive antenna elements; the system is denoted by the pair (n_T, n_R). In Figure 2.1, we show an (n_T, n_R) system, using the following notation:

- $\mathbf{a}(t) = [a_1(t), a_2(t), \ldots, a_{n_T}(t)]^T$ is an n_T dimensional vector of fixed narrow-band transmitted complex signals drawn from a modulation constellation set

$$\mathcal{A} = \{\tilde{a}_1, \tilde{a}_2, \ldots, \tilde{a}_{N_l}\}$$

  The total power of $\mathbf{a}$ is constrained to P regardless of n_T, that is $R_{\mathbf{a}} = \mathcal{E}[\mathbf{a}\mathbf{a}^H] \leq P\mathbf{I}_{n_T}$.

- $\mathbf{H}(t) \in \mathcal{C}^{n_R \times n_T}$ is the normalized channel matrix. The normalization is done such that each element of $\mathbf{H}$ has a spatial average power loss of unity. The channel matrix $\mathbf{H}$ is drawn from the following independent and identically distributed (iid), complex, zero mean and unit variance entries:

  - $H_{ij} = \mathcal{N}(0, 1/\sqrt{2}) + \sqrt{-1}\mathcal{N}(0, 1/\sqrt{2})$
  - $|H_{ij}|^2$ is a normalized chi-squared (χ_2^2) variate, such that, $\mathcal{E}[\,|H_{ij}|^2] = 1$.

  The channel is assumed to exhibit Rayleigh flat fading, and the channel matrix is represented by $n_R \times n_T$ complex values that are constant over the band of interest. Moreover, the average channel gain grows linearly with the number of receive antennas, that is $\mathcal{E}[\|\mathbf{h}_i\|^2] = n_R$, where $\mathbf{h}_i$ is the ith column of channel matrix $\mathbf{H}$.

- $\mathbf{v}(t) = [v_1(t), v_2(t), \ldots, v_{n_R}(t)]^T$ is an n_R-dimensional complex additive white Gaussian noise (AWGN) with statistically independent components of power σ^2 at each of the n_R receiver inputs.

- $\mathbf{r}(t) = [r_1(t), r_2(t), \ldots, r_{n_R}(t)]^T$ is an n_R-dimensional received signal and the average SNR at each receiver input is $\rho = P/\sigma^2$, which is independent of n_T. When the channel is constant for at least L channel uses (quasi-static scenario), the received

signal is

$$\mathbf{r}(t) = \sqrt{\frac{\rho}{n_T}}\mathbf{H}\mathbf{a}(t) + \mathbf{v}(t), \quad t = 1, 2, \ldots, L \tag{2.1}$$

- Define $\mathbf{A} = [\mathbf{a}(1), \mathbf{a}(2), \ldots, \mathbf{a}(L)]$, $\mathbf{R} = [\mathbf{r}(1), \mathbf{r}(2), \ldots, \mathbf{r}(L)]$ and $\mathbf{V} = [\mathbf{v}(1), \mathbf{v}(2), \ldots, \mathbf{v}(L)]$. We obtain

$$\mathbf{R} = \sqrt{\frac{\rho}{n_T}}\mathbf{H}\mathbf{A} + \mathbf{V} \tag{2.2}$$

where $\mathbf{A} \in \mathcal{C}^{n_T \times L}$ obeys the power constraint $\mathrm{tr}(\mathcal{E}[\mathbf{A}^H\mathbf{A}]) \leq LP$, $\mathbf{R} \in \mathcal{C}^{n_R \times L}$ and $\mathbf{V} \in \mathcal{C}^{n_R \times L}$.

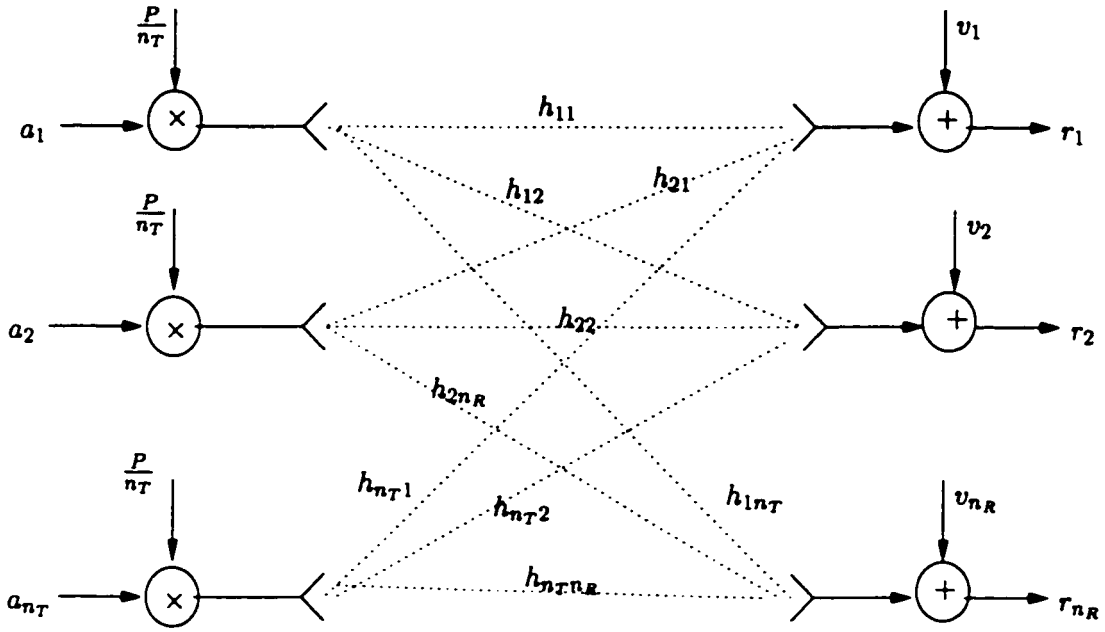

Figure 2.1: An (n_T, n_R) system

2.2 Information Theory of MTMR Systems

The expressions of channel capacity and the error exponent for MTMR schemes for a single user communication over Rayleigh fast-fading channels when each use of the channel employs an independent realization of $\mathbf{H}$, with the channel state information (CSI) available at the receiver, were derived by Teletar in [39].

Definition 1 Channel capacity, *C is the limit on the rate R at which data can be transmitted such that the probability of error $Pr(E)$ can be made arbitrarily small [40].*

Definition 2 The error exponent, *E_0, defines an upper bound on the probability of error achievable by random block codes of length L and rate R. The average error probability over the codebook of size* $\exp(LR)$, *and* $\forall\varsigma$ *in* $0 \leq \varsigma \leq 1$, *assuming maximum likelihood decoding satisfies [41]*

$$Pr(E) \leq \exp(-L[E_0(\varsigma) - \varsigma R]) \tag{2.3}$$

Definition 3 *The random coding exponent, $E_r(R)$, defines the tightest bound on the probability of error of the best block code of length L and rate R by choosing ς in (2.3) to maximize $E_0(\varsigma) - \varsigma R$:*

$$E_r(R) = \max_{0 \leq \varsigma \leq 1} E_0(\varsigma) - \varsigma R \tag{2.4}$$

where the random coding exponent, $E_r(R)$ is greater than zero for all rates $R < C$. Thus by choosing codes appropriately, the error probability can be made to approach zero exponentially with increasing block length for any rate less than capacity. However, the probability of error decreases only algebraically with decoding complexity:

$$Pr(E) \leq G^{-E_r(R)/R} \tag{2.5}$$

where G is the decoding complexity given by the order of the number of codewords $\exp(LR)$. *This poses the challenge of finding feasible decoding techniques for the best random codes.*

2.2.1 Rayleigh Fast-Fading Channel

In this section, we consider a discrete memoryless flat fading channel. For each use of channel, we draw an independent realization of $\mathbf{H} \in \mathcal{CN}^{n_R \times n_T}$, consisting of iid complex Gaussian elements. Channel capacity is defined as the maximum mutual information ($\mathcal{I}$). When the channel state information (CSI) is available at the receiver, we can write

$$C = \max_{R_{\mathbf{a}} \geq 0, \mathrm{tr}(R_{\mathbf{a}})=P} \mathcal{E}\left[\mathcal{I}(\mathbf{a};\mathbf{H}) + \mathcal{I}(\mathbf{a};\mathbf{r}|\mathbf{H})\right] \tag{2.6}$$

$$= \max_{R_{\mathbf{a}} \geq 0, \mathrm{tr}(R_{\mathbf{a}})=P} \mathcal{E}\left[\mathcal{I}(\mathbf{a};\mathbf{r}|\mathbf{H})\right] \tag{2.7}$$

where the maximization is made over all possible input probability distributions. The first term in (2.6) is zero due to the fact that the input signal is independent from the fading process. Teletar was the first to derive the capacity formula of this channel [39]

$$C = \mathcal{E}\left[\log_2 \det\left(\mathbf{I}_{n_R} + \frac{\rho}{n_T}\mathbf{H}\mathbf{H}^H\right)\right] \tag{2.8}$$

which is achieved with iid Gaussian input $\mathbf{a(t)}$ with $\mathcal{E}[\mathbf{a}(t)\mathbf{a}^H(t)] = \frac{P}{n_T}\mathbf{I}_{n_T}$.

For fixed n_R, when $n_T \to \infty$, due to the central limit theorem $\frac{1}{n_T}\mathbf{H}\mathbf{H}^H \to \mathbf{I}_{n_R}$. Consequently, the capacity in the limit is

$$\lim_{n_T \to \infty} C = n_R \log_2(1+\rho) \tag{2.9}$$

The corresponding lower bound on the error exponent is given by

$$E_0(\varsigma) = -\log_2 \mathcal{E}\left[\det\left(\mathbf{I}_{n_R} + \frac{\rho}{n_T(1+\varsigma)}\mathbf{H}\mathbf{H}^H\right)^{-\varsigma}\right] \tag{2.10}$$

2.2.2 Quasi-Fading Channel

Shannon's capacity is the limit on the maximum rate of error-free communication over a channel using bursts of long codes. However, practical wireless communications systems are quasi-static. Bursts are assumed to be short and the channel is assumed to be static

during a burst, although the channel may vary considerably from one burst to another (quasi-static).

Definition 4 *A stationary*[1] *stochastic process $X(t)$ is said to be an ergodic process if the statistical time averages of $X(t)$ are equal to their corresponding statistical ensemble averages. In the wireless channel process, ergodicity in the mean and ergodicity in the autocorrelation function are considered to be adequate for analytical purposes.*

Maximum mutual information measures the capacity when the channel is memoryless, that is, when each use of the channel employs an independent realization of **H** or when the process that generates **H** is ergodic. In direct contrast, if the channel is chosen randomly, and held fixed as in the case of a quasi-static scenario, then the channel capacity is not equal to the maximum mutual information because fading in a quasi-static environment is not a time ergodic process. This channel impairment leads to a new definition of capacity based on outage probability [39].

Definition 5 *For a given rate R and power P, there exists an outage probability $P_{out}(R, P)$ such that for a rate $R_1 < R$ and any $\delta > 0$, there exists a code, for which the error probability $Pr(E) \leq \delta$ for all but a set of quasi-static fading* **H** *whose probability is less than P_{out}.*

Foschini and Gans derived the formulas of outage channel capacity of MTMR schemes for quasi-static channels. They investigated the case of an independent Rayleigh faded path between antenna elements. The key result of their investigation reveals that Shannon's capacity for wireless communications can be increased at least by n times, where n is the number of the antenna elements at the transmit and receive ends, assumed to be the same. With multi-transmit multi-receive wireless systems, for every 3dB of signal-to-noise ratio (SNR) increase, the capacity increase is almost n bits transmission, whereas the classical Shannon capacity increase is 1 bit per transmission for every 3dB increase [1].

Furthermore, in the quasi-static fading environment, Foschini and Gans proved that the capacity of the MTMR scheme is a random variable.

[1] A stochastic process $\{X(t)\}$ is stationary if $\{X(t_1), X(t_2), \ldots, X(t_n)\}$ and $\{X(t_1 + \tau), X(t_2 + \tau), \ldots, X(t_n + \tau)\}$ have the same probability distribution for all $t_1, t_2, \ldots, t_n$ and τ.

The outage capacity computation involves two steps.

- First compute the random capacity of each chosen channel realization. For each realization of $\mathbf{H}$ chosen from a Rayleigh distribution, the capacity is given by

$$C = \log_2 \det\left(\mathbf{I}_{n_R} + \frac{\rho}{n_T}\mathbf{H}\mathbf{H}^H\right) \tag{2.11}$$

- Then evaluate the outage capacity by using Complimentary Cumulative Distribution Functions (CCDF).

Note that (2.9) holds even for the outage capacity of quasi-fading channels, that is, for large values of transmit and receive antennas, the random capacities converge to a fixed value.

Example 1 *For simplicity, we consider only systems with equal numbers of transmit and receive antennas (N). Figure 2.2 depicts the capacity CCDF, for $N = 1, 2, 4, 8$ and $N = 16$, at SNR=18dB. The figure reveals the significant capacity improvement, at different outage probability tails, by doubling the number of transmit and receive antennas. To generate this figure we used 10,000 realizations of $\mathbf{H}$ per run.*

Next we will consider the outage capacity of the following MTMR systems [1]:

No diversity, $n_t = n_R = 1$

$$C = \log_2[1 + \rho\chi_2^2] \tag{2.12}$$

where χ_2^2 is a chi-squared variate with two degrees of freedom

Single-antenna systems can achieve the capacity limits using 1-D codec technology. The irregular turbo codes [42]-[43] and the irregular low-density parity-check (LDPC) codes [44] with constraint random code ensembles are the closest known codes to the capacity limits with reasonable decoding complexity.

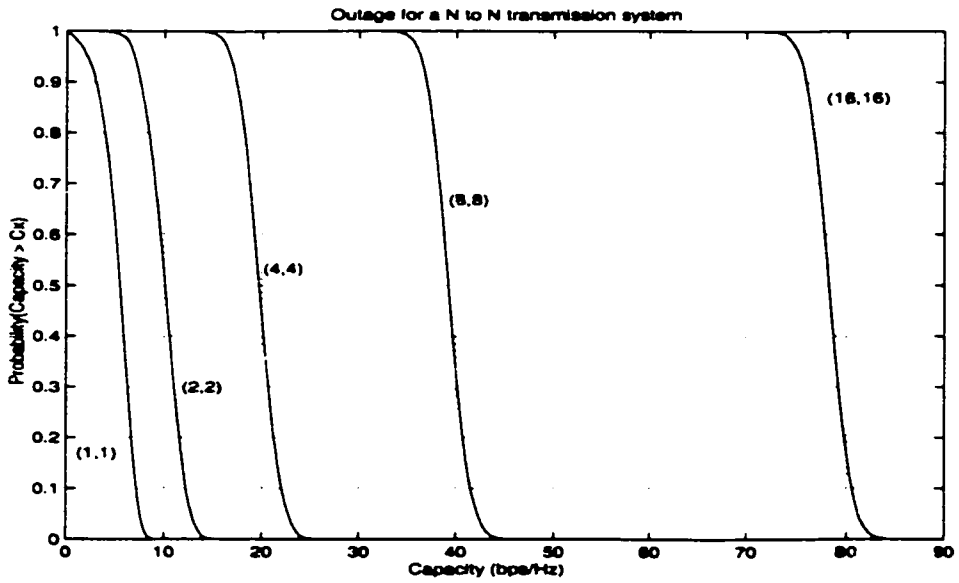

Figure 2.2: Outage capacity of (N, N) system with N=1,2,4,8 and 16, $\rho = 18dB$.

Receiver diversity, $n_T = 1$, $n_R = n$

Capacity for a system with n receive and one transmit antenna scales logarithmically with number of receive antennas n:

$$C = \log_2[1 + \rho\chi^2_{2n}] \tag{2.13}$$

where χ^2_{2n} is a chi-squared random variable that has $2n$ degrees of freedom. In general, the receiver diversity is obtained by simply using the well-established maximum-ratio combiner of the n independent versions of the transmitted signal. In rich scattering wireless environments, the use of multiple spatially separated and differently polarized antennas at the receiver is very effective in providing diversity gain against fading. Even though receiver diversity techniques create signal processing opportunities to suppress and equalize co-channel and inter-symbol interferences [45]-[47], the application of receiver diversity alone is limited with wireless communication scenarios because the mobile terminals can only be equipped with at most two or three antennas whereas the base station can have many transmit antennas.

Transmitter diversity, $n_T = n$, $n_R = 1$

$$C = \log_2[1 + \frac{\rho}{n}\chi^2_{2n}] \tag{2.14}$$

Transmit diversity, first introduced by Alamouti [48] is important in practice even though the capacity increment by using one transmit and n receive antennas is greater than the capacity increase from the use of n transmit and one receive antenna. Moreover, sophisticated techniques such as space-time coding are needed to achieve the full benefit of diversity [49]-[50].

Combined transmit and receive diversity or *BLAST* $n_T = n_R = n > 1$

The combined transmit and receive diversity in BLAST systems has $n \times n$ order. The capacity bounds for this class of MTMR schemes are [1]

$$\sum_{i=1}^{n} \log_2\left(1 + \frac{\rho}{n}\chi^2_{2(n-i+1)}\right) < C \leq \sum_{i=1}^{n} \log_2\left(1 + \frac{\rho}{n}\chi^2_{2n_i}\right) \tag{2.15}$$

where $\chi^2_{2n_i}$, $i = 1, 2, \ldots n$ are statistically independent chi-squared variates each with $2n$ degrees of freedom. Since χ^2_{2i} represents a fading channel with a diversity order of i, the lower bound can be viewed as the sum of the capacities of n independent channels with increasing diversity orders from 1 to n. The upper bound is achieved for the artificial case where each transmitted signal is received by a separate set of n_R receive antennas. In [2], Foschini suggested a layered space-time architecture concept that can attain the tight lower bound on capacity. In fact, in [51], it is shown that the Foschini's lower bound is the Shannon bound when the output SNR of the space-time processing in each layer is represented by the corresponding matched filter bound. The matched filter bound can be approached by using minimum-mean square error detectors[52].

Example 2 *Illustrated in Figure 2.3 is the outage capacity achieved by the different MTMR schemes described above for SNR=18dB. The figure reveals the importance of BLAST in*

high capacity wireless systems.

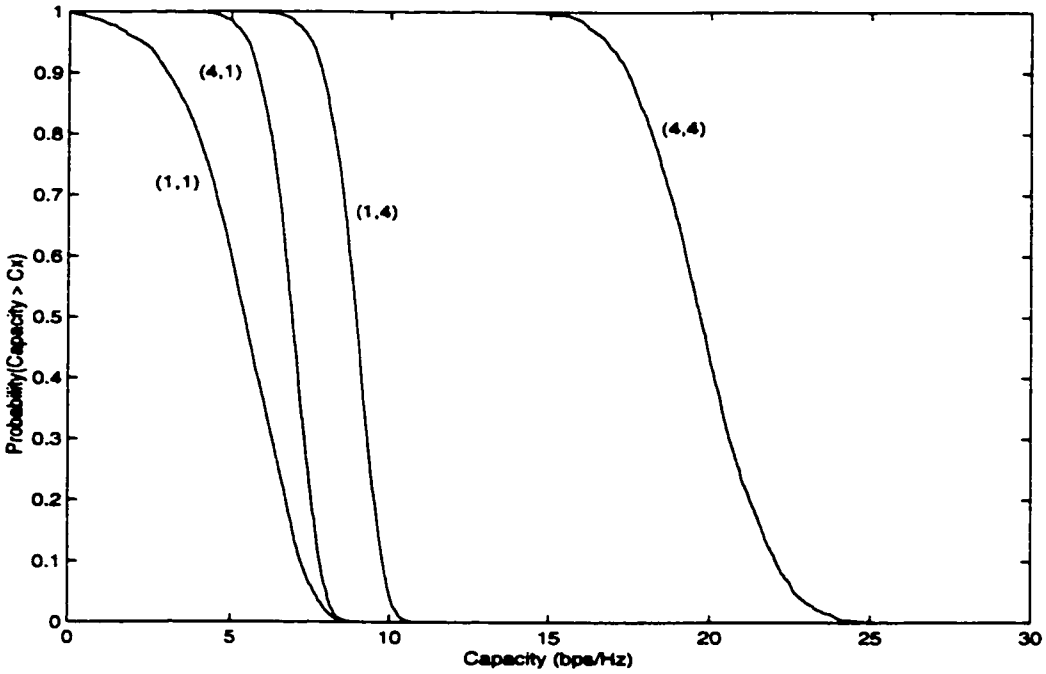

Figure 2.3: Outage capacity of different $((n_T, n_R))$ systems, $\rho = 18dB$

Remark 1 *For the capacity computation, it is assumed that the transmitter knows only the channel statistics and the receiver knows the CSI. In a quasi-static fading environment, the channel capacity of each packet is a random variable; thus the outage capacity is defined. However, we call the channel capacity C the "Shannon capacity" by assuming that the transmitter knows C at each packet of transmission.*

2.3 BLAST Architecture

The BLAST architecture consists of multiple antennas at both the transmitting and receiving ends of the system, as illustrated in Figure 2.4.

In this system, information-bearing signals are divided into multiple substreams and an array of antennas is used to launch the substreams simultaneously, using the same frequency bandwidth, with the total transmitted power always held constant. At the receiving end,

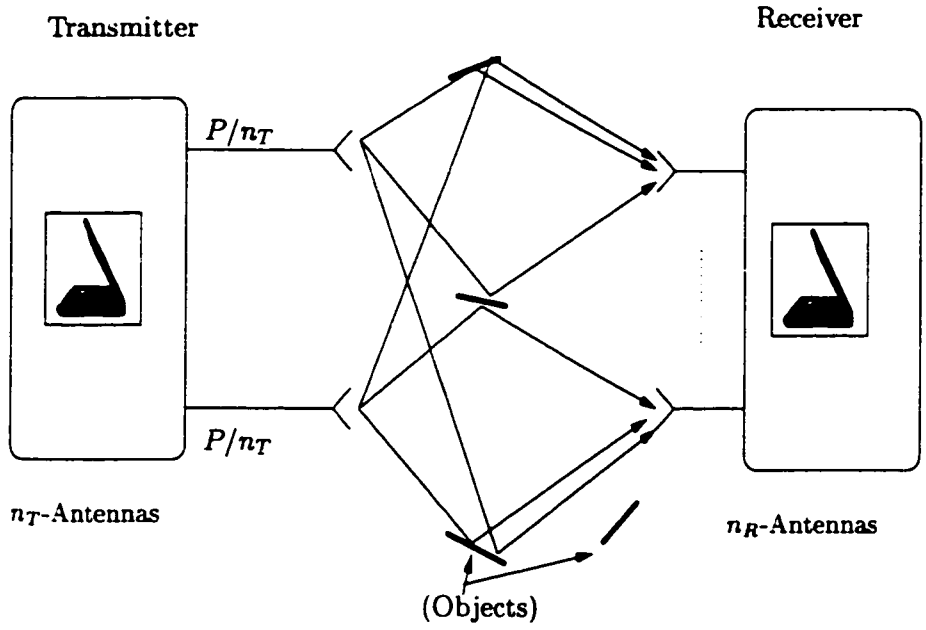

Figure 2.4: A BLAST system

the transmitted signals are picked up by a receiving antenna array. Each antenna receives all of the transmitted signals as one superimposed signal. Even though the signals are transmitted in the same frequency band, the signals from the different transmit antennas are located at different points in space, and each signal is scattered differently and hopefully the received signals at each receive antenna element still contains useful information about the transmitted signal. Since BLAST does not require additional spectrum resources to transmit parallel substreams, that is each antenna operates in a co-channel manner, the BLAST architecture is spectrally efficient. However, the spatial multiplexing and simultaneous use of the same portion of the spectrum leads to co-antenna interference which is the major source of channel impairment in the BLAST architecture. Figure 2.5 illustrates the effect of co-antenna interference (CAI) for one, two and eight simultaneous transmissions with single reception. For the eight simultaneous transmissions, the "eye" of the received signal is closed, which illustrates the major limitation of multiple transmission.

Optimal codecs for MTMR schemes are multi-dimensional and can be found through

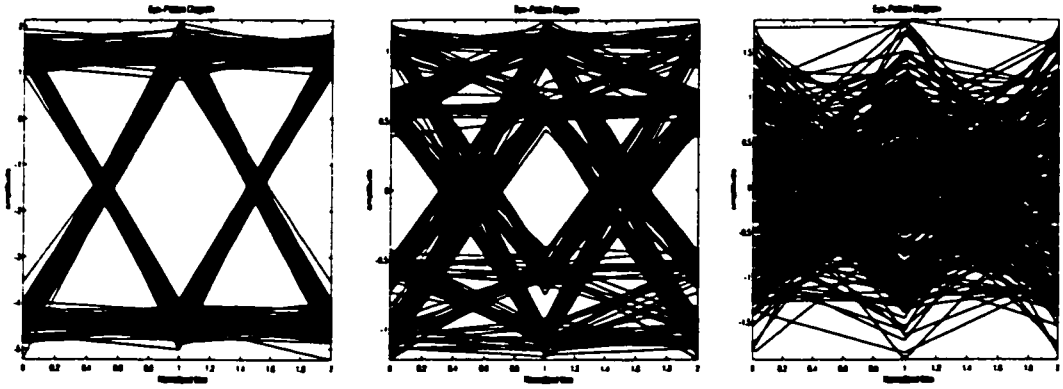

(a) 1 – *Transmitter* (b) 2 – *Transmitters* (c) 8 – *Transmitters*

Figure 2.5: Eye diagram

the exhaustive search methods as in the maximum likelihood algorithms [53]. However, the search complexity increases exponentially with the number of transmit antennas, the number of bits per modulation symbol and the burst size. For multi-dimensional codes, the number of $L \times n_T$ matrices **A** needed in a codebook can be large. The following example illustrates the computation needed for the optimal codec solution for (n_T, n_R) system.

Example 3 *Let R denote the rate in bits per channel; then the number of code matrices is 2^{RL}. For an example system with four transmit and receive antennas, the outage channel capacity at $\rho = 18$ is about 18 bits/channel use. Even with a relatively small block size of $L = 4$, the number of code matrices in the codebook is 2^{72}. Due to this huge number of constellations, the possibility of decoding using exhaustive search or maximum-likelihood decoding is not practical.*

The fundamental question raised by Foschini is: *Can one construct a BLAST system whose capacity scales linearly with the number of transmit antennas, using building blocks of n_T separately coded one-dimensional subsystems of equal capacity?* The motivation for raising this question is two-fold:

- The required codebook is only 2^{18} vectors of length $L = 4$.
- The system can be designed with the already developed 1-D codec technology.

This question was answered in [2]: Using Diagonal layered space-time or Diagonal-BLAST (D-BLAST), we can indeed achieve Shannon's capacity. D-BLAST processes two-dimensional signals in MTMR systems using the already developed one-dimensional codec technology. The first dimension refers to time and the second dimension refers to space. Note that, in general, the 1-D code involves many dimensions over the time domain.

2.3.1 Diagonal-BLAST

The aim of leveraging the already highly developed 1-D codec technology leads to the diagonally-layered space-time architecture, proposed in [2].

The diagonal layered space-time architecture concept attains a tight lower bound, given in (2.15), on the available capacity of MTMR schemes. In fact, following [51], we show that Foschini's lower bound is the Shannon bound when the output SNR of the space-time processing in each layer is represented by the corresponding matched filter bound.

The innovative feature of the D-BLAST transmitter is the space-time encoding structure constructed with n_T diagonal layering 1-D coded subsystems of equal capacity, which permit the decoding complexity to grow linearly with the number of transmit antennas. However, with this architecture requiring the use of diagonal layering, the space-time wasted at the start and end of a burst is significant for a practical burst length of few hundred symbols although this boundary waste becomes negligible as the burst length increases. Note that the use of a short packet size is important in wireless communications for two reasons:

1. Long packets require channel tracking inside a packet since the wireless channel varies with time.

2. Wireless communication is usually delay-limited.

The Diagonal-Layered Space-Time Codes

Figure 2.6 illustrates the D-BLAST transmitter. A data stream is demultiplexed into n_T data substreams of equal rate and each data substream is encoded independently using

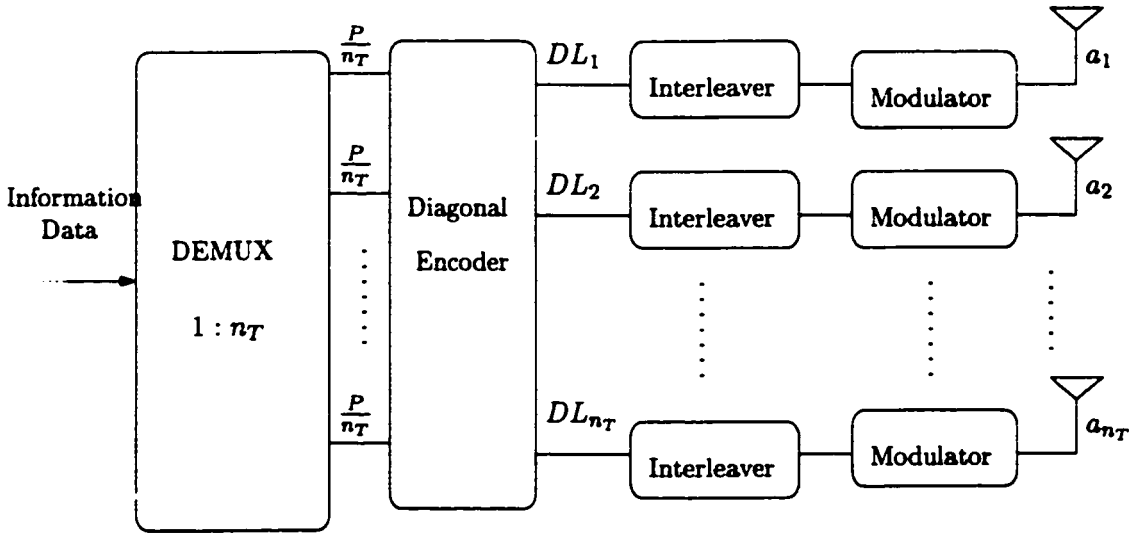

Figure 2.6: D-BLAST architecture

block encoders. Rather than committing each of the n_T coded substreams to an antenna, the bit stream per antenna association is periodically cycled [2]. The resulting diagonal layer codes due to the proposed periodic cycling of substreams are illustrated in Figure 2.7. Note the edge wastage that is associated with this architecture. The n_T-encoded diagonally layered substreams denoted by $\{DL_i\}_{i=1}^{n_T}$ share the following:

- a balanced presence over all n_T individual channel paths to the receiver; thus, each diagonal layer $\{DL_i\}_{i=1}^{n_T}$ has the same capacity $C_{DL_i} = C_D/n_T$, where C_D is the total capacity of D-BLAST, and
- a set of sub-layers, DL_{ij}, with high SNR and low SNR; thus the capacity obtained by each diagonal layer is equal to the sum of the SNR_k of n_T sublayers.

If we denote $\{SNR_{jk}\}_{k=1}^{n_T}$ as the generalized output SNR of sublayers $\{DL_{jk}\}_{k=1}^{n_T}$ of the diagonal layer DL_j, the capacity of the jth diagonal layer is:

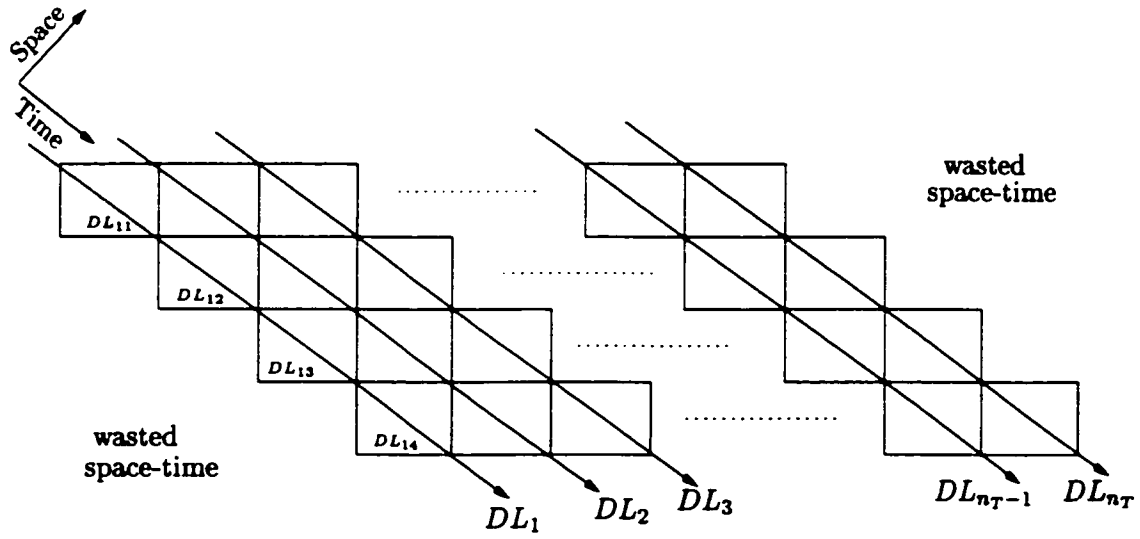

Figure 2.7: Diagonal coding

$$C_{DL_j} = \frac{1}{n_T} \sum_{k=1}^{n_T} \log_2[1 + SNR_{jk}] \tag{2.16}$$

Since each diagonal layer has virtually identical structure, the periodic signal-to-noise ratio experienced by each sublayer is identical. Thus, we denote $\{SNR_k\}_{k=1}^{n_T} = \{SNR_{jk}\}_{k=1}^{n_T}$ for all j, and the capacity of each sublayer reduces to:

$$C_{DL_j} = \frac{1}{n_T} \sum_{k=1}^{n_T} \log_2[1 + SNR_k], \quad j = 1, 2, \ldots n_T \tag{2.17}$$

Serial Interference Cancellation Decoder (SIC)

At the receiving end, the decoupling process for each of the n_T layers involves a combination of nulling out the interference from yet undetected signals and canceling out the interference from already detected signals. This receiver involves two steps:

1. Assume that the receiver has detected the last $a_{i+1}, \ldots, a_{n_T}$ correctly; then we can cancel the interference from the decided components of **a**.

We write the received signal as follows:

$$\mathbf{r} = (a_1\mathbf{h}_1 + a_2\mathbf{h}_2 + \ldots + a_{i-1}\mathbf{h}_{i-1}) + a_i\mathbf{h}_i + (a_{i+1}\mathbf{h}_{i+1} + a_{i+2}\mathbf{h}_{i+2} + \ldots + a_{n_T}\mathbf{h}_{n_T}) \tag{2.18}$$

The last bracketed sum involves only correctly detected signals and is subtracted from the received signal to get the modified received signal

$$\mathbf{r}_i = (a_1\mathbf{h}_1 + a_2\mathbf{h}_2 + \ldots + a_{i-1}\mathbf{h}_{i-1}) + a_i\mathbf{h}_i + \mathbf{v} \tag{2.19}$$

2. Interference nulling using the whitened matched filters. The current desired signal is a_i, and the remaining signals $[a_1 + a_2 + \ldots + a_{i-1}]$ are interferences. The channel vector corresponding to the desired signal is $\mathbf{h}_i$.

   When the receiver processing weights to suppress the remaining interferences in each layer are chosen to maximize the output signal-to-noise ratio, instead of using the nulling process presented in [2], one can achieve the maximum SNR available, known as the matched filter bound:

   - Spatial-whitening process (whitening of interferences and noise) [51]:

$$\mathbf{y}_i = \Psi_{i-1}^{-1/2}\mathbf{h}_i a_i + \nu_i \tag{2.20}$$

     where the vector ν_i has statistically independent complex Gaussian components with mean zero and variance one, and Ψ_i is the variance-covariance matrix of interference and additive white Gaussian noise, which is given by

$$\Psi_i = \frac{\rho}{n_T}\sum_{k=1}^{i}\mathbf{h}_k\mathbf{h}_k^H + \mathbf{I}_{n_R} \tag{2.21}$$

- The signal-to-noise ratio of the ith signal will be

$$\begin{aligned} \Upsilon_i &= \left[\Psi_{i-1}^{-1/2}\mathbf{h}_i a_i\right]^H \left[\Psi_{i-1}^{-1/2}\mathbf{h}_i a_i\right] \\ &= \mathbf{h}_i^H \Psi_{i-1}^{-1}\mathbf{h}_i \frac{\rho}{n_T} \end{aligned} \tag{2.22}$$

  where Υ_i is the maximum achievable SNR by any space-time processing receiver and is known as the matched filter bound.

Hence, the capacity achievable by the D-BLAST using the matched filtering receiver is given by

$$C_D = \sum_{k=1}^{n_T} \log_2[1 + \Upsilon_k] \tag{2.23}$$

Thus, each diagonal layering substreams can be coded using the already developed 1-D codec technology of equal capacity. This capacity of D-BLAST architecture is in fact the Shannon capacity. See appendix 2A for the proof.

Remark 2 *Foschini's lower bound is achieved by a combination of nulling (instead of whitened matched filtering) the interference from yet undetected signals and canceling the interference from the already detected signals. In the high SNR asymptote, the advantage of whitened SNR over the nulling process is negligible and Foschini's lower bound achieves Shannon's capacity.*

2.3.2 Vertical-BLAST (V-BLAST)

The uncoded BLAST architecture with optimally ordered serial interference cancellation (OSIC) detection is called Vertical-BLAST (V-BLAST) [3]. Real-time implementation of V-BLAST has been demonstrated, attaining spectral efficiencies of 20-40 b/s/Hz in an indoor propagation environment at 24dB - 34dB average SNR with eight transmit and twelve receive antennas.

The major difference between D-BLAST and V-BLAST transmitters is in the coding

scheme. D-BLAST uses a diagonal layering space-time code, whereas in V-BLAST a vector encoding process is used. The vector encoding process is simply a demultiplexing operation followed by independent bit-to-symbol mapping of each substream. Although no space-time coding can be employed in V-BLAST, a conventional 1-D channel coding of the individual substreams may certainly be applied.

The low-complexity sub-optimum nonlinear detector proposed [3] for V- BLAST is based primarily on a successive interference cancellation of hard decisions and a new scheme to find the order in which the substreams are to be detected for optimum performance. In this detection scheme, the substreams are first sorted according to the strength of each subchannel, then the strongest substream is detected and extracted from the total received signal, and the sorting and extraction are repeated until all the substreams are determined. A typical uncoded V-BLAST is shown in Figure 2.8.

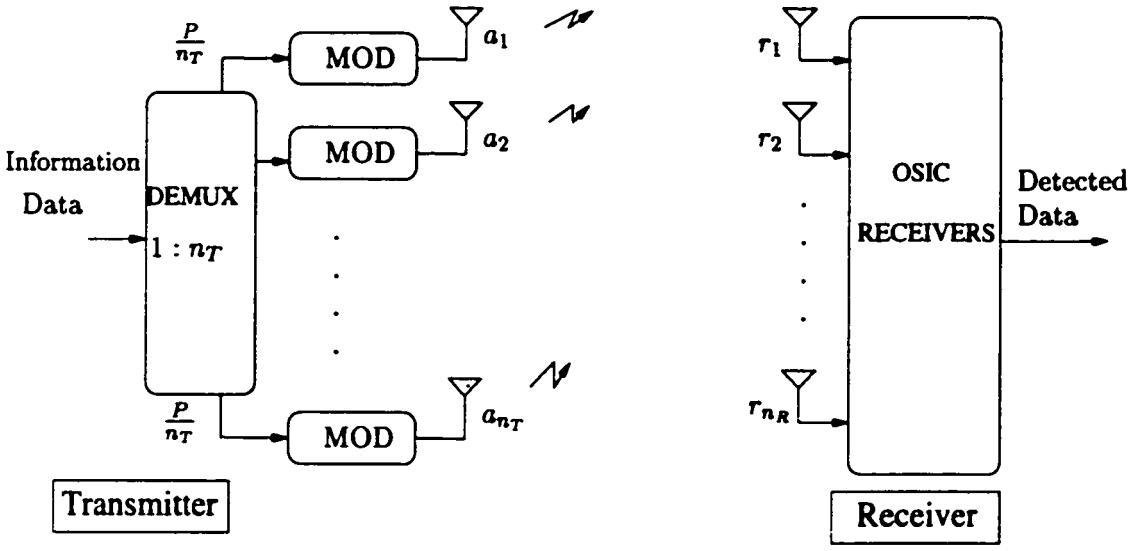

Figure 2.8: Uncoded V-BLAST architecture

OSIC Detection Algorithm [3]

Let the detection order

$$s = \{k_1, k_2, \ldots, k_{n_T}\} \tag{2.24}$$

be a permutation of integers $1, 2, \ldots n_T$. The detection process has three major steps as follows:

1. Form the soft decision statistics

$$y_{k_i} = \mathbf{w}_{k_i}^H \mathbf{r}_i \tag{2.25}$$

The weight vector $\mathbf{w}$ is obtained by using well-known linear filters such as zero-forcing (ZF)/nulling or minimum mean-squared error (MMSE)/whitened matched filtering, [54]:

Problem 1 (ZF): Given the model (2.1), estimate the user information sequence $\mathbf{a}$ by minimizing the following cost function

$$\min_{\mathbf{a}} \|\mathbf{r} - \mathbf{H}\mathbf{a}\|_{\mathbf{R}_v}^2 \tag{2.26}$$

where $\mathbf{R}_v = \mathcal{E}\{\underline{v}\underline{v}^H\} = \sigma^2\mathbf{I}$.

Solution to Problem 1 (ZF): Solution to this problem is given by

$$\hat{\mathbf{a}} = \mathbf{H}^+\mathbf{r} \tag{2.27}$$

The corresponding weight matrix is

$$\mathbf{w} = \mathbf{H}^+ \tag{2.28}$$

where $\mathbf{H}^+ = (\mathbf{H}^H\mathbf{H})^{-1}\mathbf{H}^H$ is pseudo-inverse [55]. Note that the ZF weight vector computation is inherently ill-posed.

Problem 2 (MMSE): Given the model (2.1), estimate the user information sequence $\mathbf{a}$ by minimizing the following cost function

$$\min_{\mathbf{a}} \|\mathbf{a} - \hat{\mathbf{a}}\|^2 \tag{2.29}$$

Solution to Problem 2 (MMSE): Solution to this second problem is given by

$$\hat{\mathbf{a}} = (\mathbf{H}^H\mathbf{H} + \sigma^2\mathbf{I})^{-1}\mathbf{H}^H\mathbf{r} \tag{2.30}$$

The corresponding weight matrix is

$$\mathbf{w} = (\mathbf{H}^H\mathbf{H} + \sigma^2\mathbf{I})^{-1}\mathbf{H}^H \tag{2.31}$$

2. Obtain the hard decisions $\hat{a}_{k_i}$ by finding the nearest point to y_{k_i} in the constellation coordinates, which minimizes the Euclidean distance based on the soft decisions

$$\hat{a}_{k_i} = Q(y_{k_i}) \tag{2.32}$$

3. Cancel the signal component due to $\hat{a}_{k_i}$ from the received vector $\mathbf{r}_i$

$$\mathbf{r}_{i+1} = \mathbf{r}_i - \hat{a}_{k_i}\mathbf{h}_{k_i} \tag{2.33}$$

where $\mathbf{h}_{k_i}$ denotes the k_ith column of $\mathbf{H}$.

Ordering of Substreams using Post Detection SNR

Post-detection SNR for the k_i-th detected component of $\mathbf{a}$ is given by

$$\rho_{k_i} = \frac{\mathcal{E}[\,|a_{k_i}|^2]}{\sigma^2\|\mathbf{w}_{k_i}\|^2} \tag{2.34}$$

where the expectation is taken over the constellation points. The larger the ρ_{k_i}, the smaller the nulling weights $\mathbf{w}_{k_i}$ are. Thus, the post detection SNR is maximized by the smallest nulling weight; detecting and canceling the signal with the smallest nulling weight improves the algorithm. V-BLAST with optimal ordering based on the smallest weight is described below [3].

- Initialization

$$\begin{aligned} i &\rightarrow 1 \\ \mathbf{G}_1 &= \mathbf{H}^+ \end{aligned} \tag{2.35}$$

- Recursion:

$$\begin{aligned} k_i &= \arg\{\min_{j \notin (k_1,\cdots,k_{i-1})} \|(\mathbf{G}_i)_j\|^2\} \\ \mathbf{w}_{k_i} &= ((\mathbf{G}_i)_{k_i})^T \\ y_{k_i} &= \mathbf{w}_{k_i}^H \mathbf{r}_i \\ \hat{a}_{k_i} &= Q(y_{k_i}) \\ \mathbf{r}_{i+1} &= \mathbf{r}_i - \hat{a}_{k_i} \mathbf{h}_{k_i} \\ \mathbf{G}_{i+1} &= \mathbf{H}_{\bar{k}_i}^+ \\ i &\leftarrow i+1 \end{aligned} \tag{2.36}$$

where $(\mathbf{G}_i)_{k_i}$ is the k_i-th row of $\mathbf{G}_i$, $\mathbf{H}_{\bar{k}_i}$ denotes the matrix obtained by zeroing columns $k_1, k_2, \ldots, k_i$ of $\mathbf{H}$, and $(\cdot)^+$ denotes the pseudo-inverse [55].

Remark 3 *To perform the optimal ordering process used in V-BLAST, the pseudo-inverse* $\mathbf{G}_i$ *must be computed for* $i = 1, 2, \ldots, n_T$, *which is sensitive with respect to a channel matrix* $\mathbf{H}$ *that has correlated columns: a small change in* $\mathbf{H}$ *may cause large and unpredictable variations in* $\mathbf{G}_i$. *Note that* $\mathbf{G}_i$ *is computed by zeroing* $n_T - i + 1$ *columns of* $\mathbf{H}$. *This sensitivity of the pseudo-inverse grows linearly with* $n_T - Rank(\mathbf{H})$ *[55] and [56]. Note that,*

this sensitivity may be reduced by setting the smaller singular values to zero but determining the numerical rank of this problem is challenging. Therefore, the ordering process may fail when $n_T \geq n_R$. Typically, for $n_T \leq n_R$ the columns of $\mathbf{H}$ *may be assumed to be independent.*

2.3.3 Improved V-BLAST

Many modifications have been proposed to improve V-BLAST. A channel based adaptive group detection (AGD) combined with OSIC is proposed in [57]. In the OSIC-AGD algorithm, the ZF/MMSE based interference nulling/ suppression is replaced with the AGD algorithm.

The AGD algorithm contains three steps: grouping based on the channel information, subspace projection and ML search within each group:

1. Several layers are grouped for processing together.
2. ML detection is performed within the groups.
3. Interference is canceled in a way that only part of the search results from each group is used as decisions.

Repeat Step 1 and 2 for the unprocessed layers until all the layers have been processed.

The complexity of ML detection over all n_T transmitters requires ${N_I}^{n_T}$ searches, where N_I is the size of the constellation used, which is beyond the limit of most systems today. The group detection is carried out within a group of n_g, where $n_g << n_T$, therefore the searching complexity is proportional to $N_I^{n_g}$, and can be maintained low by keeping group size n_g small.

Alternatively, a second-stage O_r-order processing of the detected V-BLAST signal is proposed in [56]:

- ML detection is performed on the soft decisions $y_{k_1}, \ldots, y_{k_{o_r}}$ to get improved decisions $\hat{a}_{k_1}, \ldots, \hat{a}_{k_{o_r}}$,

- Redetected signals are subtracted from the received signal

$$\mathbf{r}_{O_r+1} = \mathbf{r}_1 - \sum_{i=1}^{O_r} \hat{a}_{k_i} \mathbf{h}_{k_i} \tag{2.37}$$

The additional computational complexity of this processing is mainly the O_r-order ML reprocessing which is ${N_I}^{O_r}$ computations, where N_I is the size of constellations used.

2.3.4 Coded Vertical-BLAST

Three coded V-BLAST schemes exist in the literature, which are:

(1) V-BLAST with horizontal encoder V-BLAST-I [51]

(2) V-BLAST with vertical encoder V-BLAST-II [51]

(3) V-BLAST with concatenated coding V-BLAST-III [57]

In the horizontal encoding scheme, the substreams are independently encoded using 1-D channel codes as shown in Figure 2.9. The incoming data are first divided into $\mathbf{b}_1, \mathbf{b}_2, \ldots, \mathbf{b}_{n_T}$ and each part is encoded separately, interleaved, and symbol-mapped to generate the parallel substreams. The receiver performs OSIC detection and decoding. In this scheme, the receiver cancels interference using *decoded decisions* from previously decoded signals.

One possible shortcoming of horizontal coding over diagonal coding is that overall performance may be dominated by the weakest layer, particularly the first decoded layer, because it has the lowest diversity in V-BLAST decoding. Therefore, the capacity of such schemes is

$$C_{V\cdot} = \sum_{k=1}^{n_T} \log_2[1 + \underline{SNR}] \tag{2.38}$$

where

$$\underline{SNR} = \max \min[SNR_i, 1 \leq i \leq n_T] \tag{2.39}$$

This means that each layer of V-BLAST-I can only have an information rate $R \leq C_V$.

Note that in (2.39), we maximize the minimum SNR of the detection process. The first detection layer has the minimum SNR among the n_T possible layers, since it faces $n_T - 1$ interferences; the second detection layer has only $n_T - 2$ interferences and so on. The ordering process used in the V-BLAST OSIC receiver maximizes the minimum SNR by maximizing the post detection SNR [5].

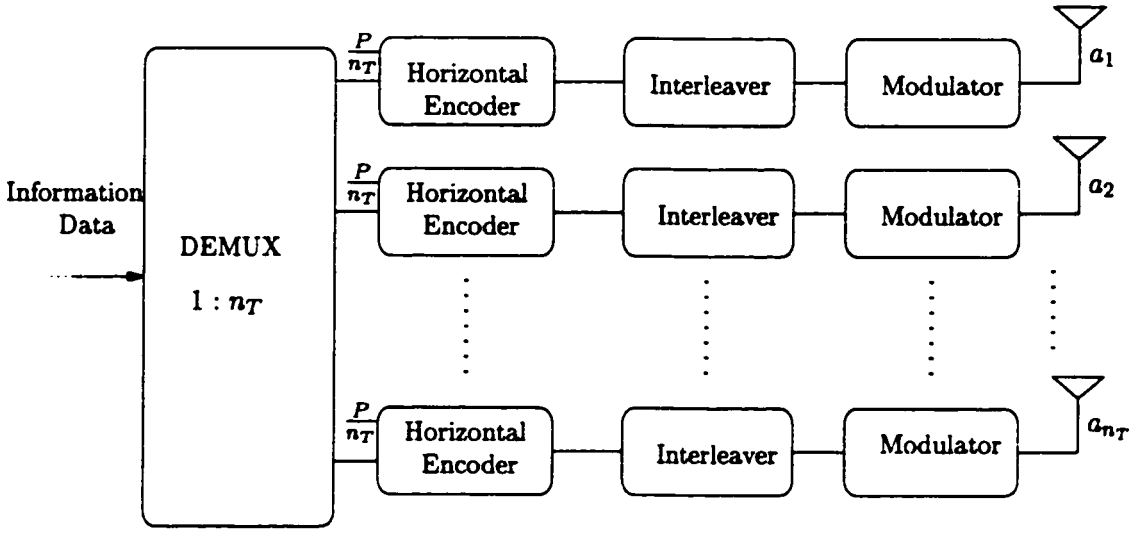

Figure 2.9: Horizontal coded V-BLAST architecture

In the vertical encoding approach (see Figure 2.10), a single code is used to encode all the signals, and the coded information bits are demultiplexed across the n_T parallel streams $\mathbf{a}_1, \mathbf{a}_2, \ldots, \mathbf{a}_{n_T}$. At the other end, the receiver first decouples the n_T data streams through interference nulling/cancellation as described for uncoded V-BLAST, then multiplexes and decodes all the n_T substreams as one information block. In this scheme, the effective SNR averaging across the antenna array may be achieved because all the layers are coded together. A serious drawback of vertical coding is that only the undecoded decisions are provided to the interference canceler since decoding cannot be done until all the layers are processed. Thus, vertical coding is more prone to decision errors than horizontal coding. Therefore, the rate of vertical encoding approaches $R_h < C_V$, where C_V is defined in (2.38)

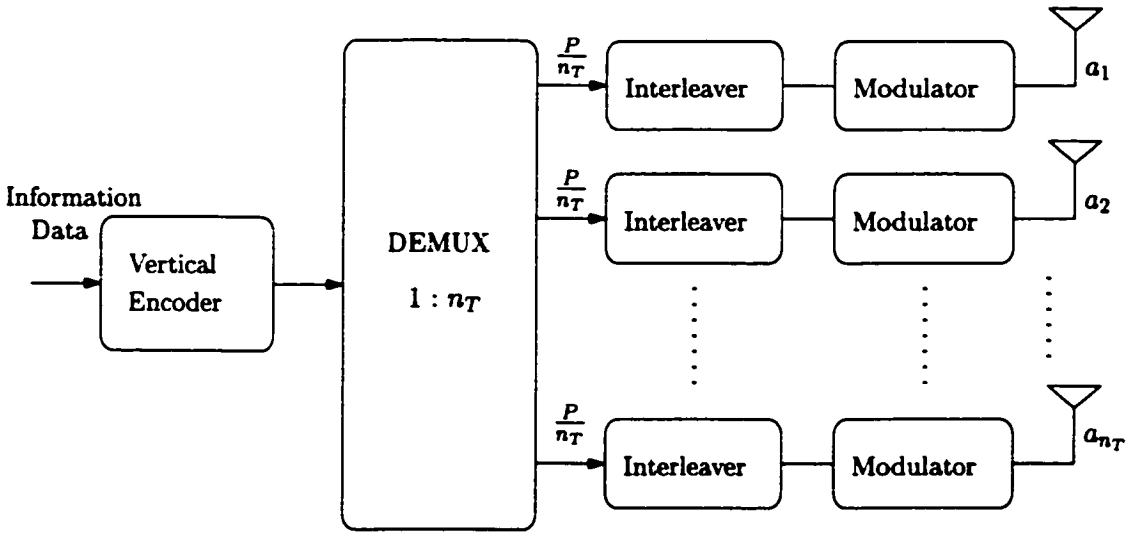

Figure 2.10: Vertical coded V-BLAST architecture

The third coding [57] is the concatenated approach shown in Figure 2.11. The horizontal coding layers are designed, typically with convolutional codes as inner codes, to facilitate the OSIC detection using decoded decisions whereas the vertical coding, with Reed-Soloman outer code, is included for SNR averaging across the antennas. A drawback of this scheme is a reduced information rate $R_{hv} < C_V$ due to the concatenation of two coding schemes.

In general, to minimize the effect of decision errors and to improve the joint detection and decoding gain, it is assumed that turbo processing is incorporated as a second round-processing as illustrated in Figure 2.12. Iterative detection used in second stage processing could improve the performance, if the performance due to the first processing is far from the capacity C_V. However, the ultimate capacity even with the second stage iterative processing is still limited by the V-BLAST capacity C_V given in (2.38).

Limitations of V-BLAST

1. V-BLAST detection algorithm has a computational complexity $O(n^4)$ where n is number of transmit and receive antennas. This is a major issue to be considered [59]. The V-BLAST scheme uses a sequential nulling and interference cancellation strategy;

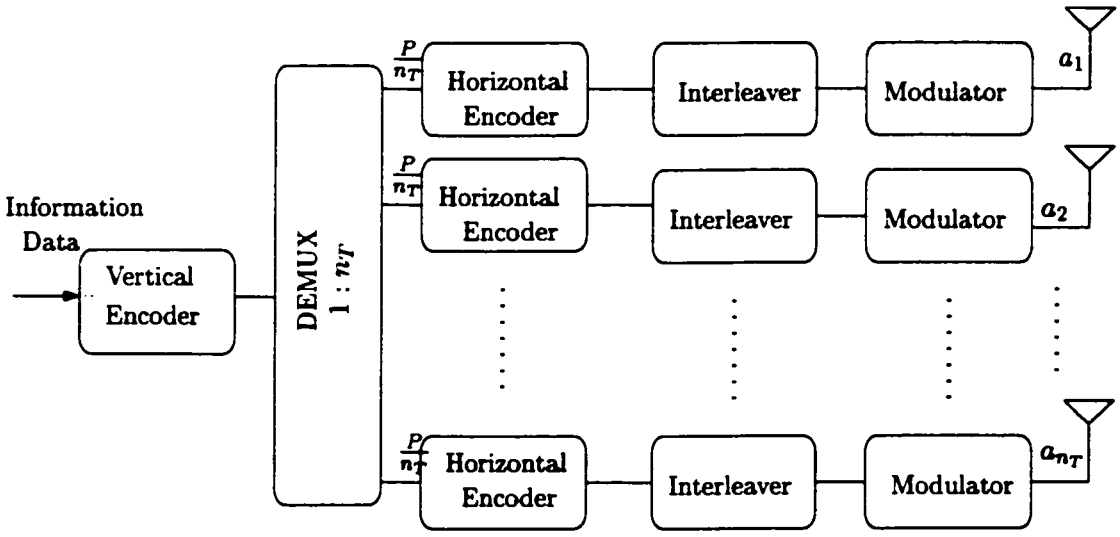

Figure 2.11: Concatenated coded V-BLAST architecture

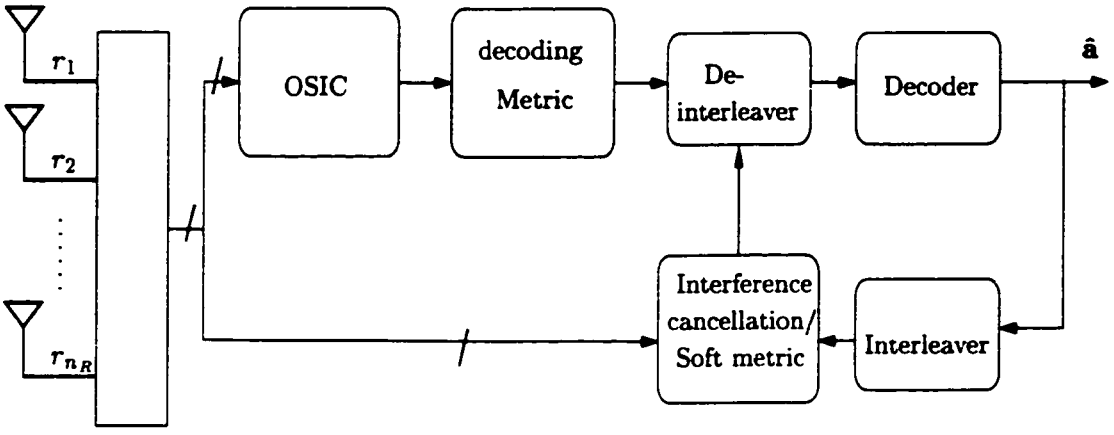

Figure 2.12: Second-stage iterative receiver for V-BLAST

decoding the strongest signal; canceling the interference due to the decoded signal; decoding the strongest signal of the remaining signals, and so on. In this receiving scheme, the optimal order of detection and the nulling vector has to be determined at each decoding step, which can be computationally expensive and numerically unstable. We may estimate the optimal ordering using the singular value decomposition (SVD), which is the most stable way of computing the pseudo-inverse. For an $n \times m$ matrix, whose entries are complex values, we note the following [55]:

- the singular value decomposition has a complexity of $2n^2m + 11m^3$, and
- the pseudo-inverse has a complexity $2nm^2$.

Since these steps have to be repeated m times in the sequential detection procedure with the matrix sizes of dimension $(n + k) \times k, \quad k = m, m - 1, \ldots, 1$, the total complexity is

$$\sum_{k=1}^{m} \{2(n+k)^2k + 11k^3 + 2(n+k)k^2\} = n^2m^2 + 2nm^3 + \frac{15}{4}m^4 \tag{2.40}$$

For an (n, n)-BLAST, the computations are on the order of n^4.

2. V-BLAST demands more receive antennas than transmit antennas. The ability to work with fewer receivers than transmitters is necessary in most cellular communications systems since the base station is typically designed with more antennas than the mobile unit.

3. V-BLAST does not use any transmit diversity naturally provided in the MTMR system. It has no built-in space-time codes to overcome deep fades from any of the transmit antennas and suffers from the problem of error propagation: a wrong decision made at the output leads to higher probability of error on subsequent decisions.

4. D-BLAST and V-BLAST are quite sensitive to the channel estimation errors since they use hard-decision based interference cancellation receivers. Note that, in practice, the

channel is learned by the receiver by using short training sequences transmitted by the transmitter with each packet of information symbols.

Remark 4 Complexity Reduction: *A cost efficient and numerically stable "square-root" algorithm has been proposed in [59] for V-BLAST architecture. This square-root algorithm has the following favorable features:*

- *the computational cost is reduced to* $0.7n$*, where* n *is number of transmitters,*
- *it uses only orthogonal transformations and is numerically stable, and*
- *it can be implemented using fixed-point digital signal processing (DSP) hardware. Note that the original V-BLAST algorithm demands floating point DSP.*

2.4 Space-Time Codes

Designing appropriate space-time coders and low-complex decoders for MTMR systems are addressed in the literature [60]. In this section, the design criterion of space-time codes for improving the data rate and the reliability of data communication is briefly discussed.

2.4.1 Design Criterion

We assume the channel is quasi-static over K time periods. The transmitted code vector sequence is

$$\mathbf{C} = [\mathbf{c}(1), \mathbf{c}(2), \ldots, \mathbf{c}(L)] \tag{2.41}$$

where the code vector at the lth time interval is

$$\mathbf{c}(l) = [c_1(l), c_2(l), \ldots, c_{n_T}(l)]^T \tag{2.42}$$

Definition 6 *The pairwise error probability: The probability of decoding the codeword* $\tilde{\mathbf{c}}$ *knowing that the codeword* $\mathbf{c}$ *is transmitted, when these two codewords are considered to be*

the only codewords of the codebook.

The pairwise error probability (PEP) $P(\mathbf{C} \rightarrow \tilde{\mathbf{C}}|\mathbf{H})$, assuming a perfect CSI, is [60]

$$P[\mathbf{C} \rightarrow \tilde{\mathbf{C}}|\mathbf{H}] \leq \exp(-d^2(\mathbf{C}, \tilde{\mathbf{C}})) \tag{2.43}$$

where $d^2(\mathbf{C}, \tilde{\mathbf{C}})$ defines the distance between $\mathbf{C}$ and $\tilde{\mathbf{C}}$:

$$d^2(\mathbf{C}, \tilde{\mathbf{C}}) = \frac{\rho}{4n_T} \sum_{i=1}^{n_R} \mathbf{h}_i \mathbf{A}(\mathbf{C}, \tilde{\mathbf{C}}) \mathbf{h}_i^H \tag{2.44}$$

where $\mathbf{h}_i$ is the ith row of the channel matrix $\mathbf{H}$, and $\mathbf{A}(\mathbf{C}, \tilde{\mathbf{C}})$ is defined as

$$\mathbf{A}(\mathbf{C}, \tilde{\mathbf{C}}) = \mathbf{B}(\mathbf{C}, \tilde{\mathbf{C}}) \mathbf{B}^H(\mathbf{C}, \tilde{\mathbf{C}}) \tag{2.45}$$

The matrix $\mathbf{B}(\mathbf{C}, \tilde{\mathbf{C}})$ is the error matrix between the transmitted code vector sequence $\mathbf{C}$ and the detected code vector $\tilde{\mathbf{C}}$ sequence:

$$\mathbf{B}(\mathbf{C}, \tilde{\mathbf{C}}) = \begin{bmatrix} c_1(1) - \tilde{c}_1(1) & c_1(2) - \tilde{c}_1(2) & \dots & c_1(L) - \tilde{c}_1(L) \\ c_2(1) - \tilde{c}_2(1) & c_2(2) - \tilde{c}_2(2) & \dots & c_2(L) - \tilde{c}_2(L) \\ \vdots & \vdots & \ddots & \vdots \\ c_{n_T}(1) - \tilde{c}_{n_T}(1) & c_{n_T}(2) - \tilde{c}_{n_T}(2) & \dots & c_{n_T}(L) - \tilde{c}_{n_T}(L) \end{bmatrix} \tag{2.46}$$

Let r be the rank of matrix $\mathbf{A}$ and $\lambda_1, \lambda_2, \dots \lambda_r$ be the nonzero eigenvalues of $\mathbf{A}$. Then by averaging over the Rayleigh fading variables, the PEP is given by

$$Pr\{\mathbf{C} \rightarrow \tilde{\mathbf{C}}\} \leq (\Pi_{i=1}^{r} \lambda_i)^{-n_R} \left(\frac{\rho}{4n_T}\right)^{-rn_R} \tag{2.47}$$

Thus a diversity gain of r and a coding gain of $(\lambda_1 \lambda_2 \dots \lambda_r)^{1/r}$ is achieved. Accordingly, the design criteria that minimize the PEP are equivalent to:

- Rank Criterion: The rank r of $\mathbf{B}$ is called the diversity gain of the space-time code and the diversity achieved with diversity gain r is rn_R. To achieve the maximum diversity

$n_T n_R$, the matrix $\mathbf{B}$ has to be full rank for any pair of codeword vector sequence $\mathbf{C}_1$ and $\mathbf{C}_2$.

- Determinant Criterion: If the diversity gain of the code is r, to obtain the best coding gain, the minimum of the rth root of the sum of determinants of all $r \times r$ principal cofactors of $\mathbf{A}$ taken over all pairs of distinct code vector sequence $\mathbf{C}_1$ and $\mathbf{C}_2$ must be maximized.

2.5 Low-Rate Space-Time Codes

In the design of space-time trellis and block codes, the above criterion is imposed by adding redundancy in the coding design, as described in [60]. We will give examples of redundant codes that achieve the full diversity with simple decoding structures at the expense of spectral efficiency. These redundancy codes have good fading resistance and simple decoding, but generally have poor capacity performance at high data rates [53].

2.5.1 Space-Time Trellis Codes

In Figure 2.13, we illustrate 4-PSK, 4-state space-time trellis codes for the transmission of 2b/s/Hz using two antennas. The encoding of the trellis codes is obvious with the exception that at the beginning and the end of each frame, the encoder is required to be in state zero. At each time l, depending on the state of the encoder and the input bits, a transition branch is chosen. Table 2.1 summarizes the input and the transmitted symbols from transmitter 1 and transmitter 2 for the 4-PSK, 4-state trellis space-time codes. If the current state is 0 and we receive symbol 1, then we transmit symbol 0 over one antenna and symbol 1 over the other.

The decoding of these codes is done, assuming that the CSI is perfectly known to the decoder. Given the received signal $\{\mathbf{r}(l)\}_{l=1}^{L}$, the receiver chooses the code vector sequence

$\tilde{\mathbf{C}}$ using the space-time maximum likelihood decoder:

$$\tilde{\mathbf{C}} = \arg\min_{\tilde{\mathbf{C}}} \sum_{l=1}^{L} \left\| \mathbf{r}(l) - \sqrt{\frac{\rho}{n_T}} \mathbf{H}(l)\tilde{\mathbf{c}}(l) \right\|^2 \tag{2.48}$$

The space-time maximum likelihood decoding is done using the Viterbi algorithm, [92][2], where the trellis path with the smallest accumulated metric is chosen.

The rank criterion for this code is verified over two time periods and it can be shown that the matrix **B** has full rank over all codeword pairs; thus the code can achieve the full gain of diversity. However, since each time a redundant symbol is transmitted, the rate of this code is only 1/2, and the effective transmission rate is only 1bit/s/Hz.

Input	0	1	2	3	2	2
Transmit antenna 1	0	0	1	2	3	2
Transmit antenna 2	0	1	2	3	2	2

Table 2.1: 4-PSK 4 state space-time code with 2 transmit antennas

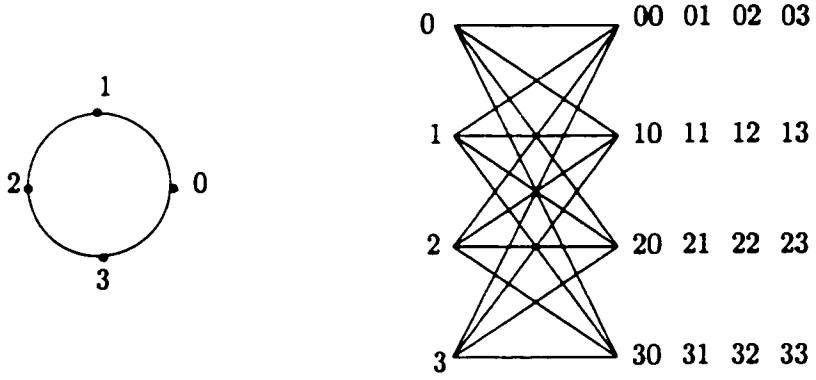

Figure 2.13: 4-PSK 4 state space-time code with 2 transmit antennas

[2]The Viterbi algorithm is a sequential trellis search algorithm for performing maximum likelihood sequence estimation, which is optimum for an AWGN channel.

2.5.2 Space-Time Block Codes

Yet another approach to the attainment of low-rate space-time coding over wireless fading channels has been inspired by Alamouti's transmit diversity scheme [48], which involves the use of two transmit antennas and a simple decoding algorithm. Alamouti's transmit diversity technique was generalized by Tarokh et al. [61] to an arbitrary number of transmit antennas as space-time block coding. Briefly, space-time block codes are designed to provide full diversity promised by the transmit and receive antennas under the constraint of using a simple decoding algorithm in the receiver. However, the limitation of these space-time codes is that they are not designed to achieve an additional coding gain. To do so, they have to be concatenated with an outer code.

A space-time block code is defined as $n_T \times L$ transmission matrix $\mathcal{G}$. For example, for two transmit antennas, $\mathcal{G}_2$ represents a code with rate 1/2, as shown by

$$\mathcal{G}_2 = \begin{bmatrix} c_1 & -c_2^* \\ c_2 & c_1^* \end{bmatrix} \tag{2.49}$$

If the channel is invariant for at least two symbol periods, the received signals at times l and $l+1$ are, respectively,

$$\begin{aligned} r(l) &= h_1 c_1 + h_2 c_2 + v(l) \\ r(l+1) &= -h_1 c_2^* + h_2 c_1^* + v(l+1) \end{aligned} \tag{2.50}$$

where h_1 and h_2 represent the channel coefficients between the receive antenna and transmit antennas 1 and 2, respectively. Equation (2.50) be represented in matrix form:

$$\begin{bmatrix} r(l) \\ r^*(l+1) \end{bmatrix} = \begin{bmatrix} h_1 & h_2 \\ h_2^* & -h_1^* \end{bmatrix} \begin{bmatrix} c_1 \\ c_2 \end{bmatrix} + \begin{bmatrix} v(l) \\ v^*(l+1) \end{bmatrix} = \mathcal{H}\mathbf{c} + \mathbf{v} \tag{2.51}$$

The use of maximum ratio combining, knowing the CSI at the receiver, yields

$$\begin{aligned} \tilde{\mathbf{c}} &= \mathcal{H}^H \mathcal{H}(\mathbf{c} + \mathbf{v}) \\ &= (h_1^2 + h_2^2)\mathbf{c} + \tilde{\mathbf{v}} \end{aligned} \tag{2.52}$$

The noise term $\tilde{\mathbf{v}}$ is still white since $\mathcal{H}$ is orthogonal, and c_1 and c_2 are detected independently with lower complexity. With n_R receive antennas, the diversity order of $2 * n_R$ can be obtained.

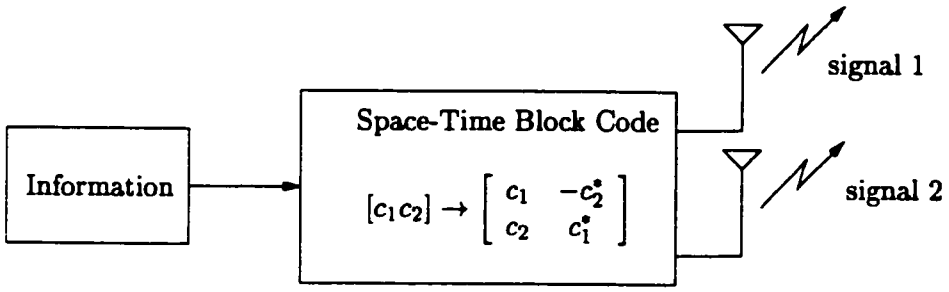

Figure 2.14: Space-Time Block Code with 2 transmit antennas

For the space-time block codes, the orthogonal design structure prohibits this scheme from achieving channel capacity. The capacity attainable with the space-time block code designs is limited by the orthogonal channel matrix $\mathcal{H}$ [53]. For the (n_T, n_R) systems, the space-time code design achieves

$$\begin{aligned} C_{ST} &= \frac{1}{n_T} \log_2 \det \left(\mathbf{I}_{n_T} + \frac{\rho}{n_T} \mathcal{H}^H \mathcal{H} \right) \\ &= \frac{1}{n_T} \log_2 \det \left(\mathbf{I}_{n_T} + \frac{\rho}{n_T} \left[\sum_{i=1}^{n_T} \sum_{j=1}^{n_R} H_{ij}^2 \right] \mathbf{I}_{n_T} \right) \\ &= \log_2 \det \left(1 + \frac{\rho}{n_T} \left[\sum_{i=1}^{n_T} \sum_{j=1}^{n_R} H_{ij}^2 \right] \right) \end{aligned} \tag{2.53}$$

where the factor $\frac{1}{n_T}$ in front of the log normalizes for the n_T channel uses spanned by the orthogonal design, and $\mathcal{H}$ is the orthogonal channel matrix that maximizes the diversity

gain.

Remark 5 *However, for the (2,1) case, the orthogonal design achieves the optimal channel capacity:*

$$\begin{aligned} C_{ST} &= \frac{1}{2}\log_2 \det\left(\mathbf{I}_2 + \frac{\rho}{2}\mathcal{H}^H\mathcal{H}\right) \\ &= \frac{1}{2}\log_2 \det\left(\mathbf{I}_2 + \frac{\rho}{2}(h_1^2 + h_2^2)\mathbf{I}_2\right) \\ &= \log_2\left(1 + \frac{\rho}{2}(h_1^2 + h_2^2)\right) \end{aligned} \tag{2.54}$$

These schemes have poor bandwidth efficiency since they use a form of repetition coding, but the codes are designed in such a way that the code matrix maximizes the diversity gain. Typically, the redundancy introduced in space-time coding schemes is a multiple of the number of transmit antennas. This motivates the use of high-rate space-time codes embodied in Turbo-BLAST as discussed next.

2.6 High-Rate Space-Time Codes

The Turbo-BLAST (T-BLAST) presented in this thesis uses a simple yet effective high-rate space-time code, and exploits the following ideas:

- The Bell-Labs Layered Space Time (BLAST) architecture.
- A novel space-time coding scheme by using the 1-D channel codes and space-time interleaving that are designed off-line.
- Sub-optimal turbo-like receiver that performs joint decoding of the proposed space-time codes in an iterative manner and, most important, simple fashion.

Simply put, T-BLAST combines the benefits of BLAST and turbo-principles in space-time coding design. Using computer simulations and tests with real-life data, we empirically show that T-BLAST attains near channel capacity.

Example 4 *Figure 2.15 illustrates the capacity margins of the various schemes analyzed in this chapter for* $n_T = n_R = 8$. *The capacity of a T-BLAST falls between the capacity upper bounds of D-BLAST (or the channel capacity) and V-BLAST.*

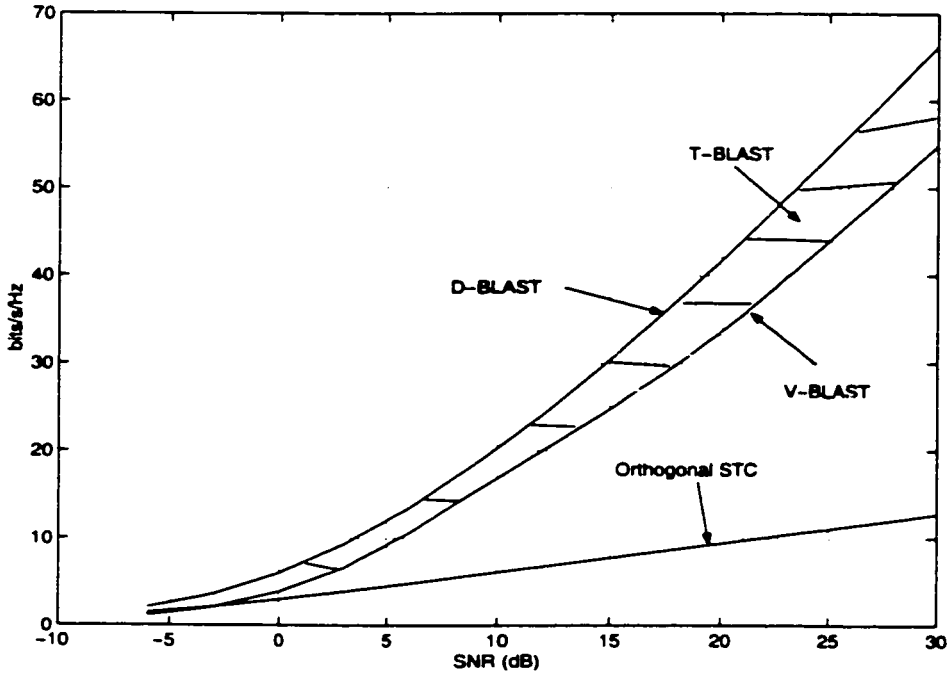

Figure 2.15: The 10% outage capacity of BLAST systems with $n_T = n_R = 8$

Before we move on to the T-BLAST system, we will describe the turbo-principles in the next chapter.

2.7 Summary

In this chapter, we discussed the fundamental limits of multi-transmit multi-receive wireless communications channels and reviewed existing MTMR architectures. Four popular MTMR systems were described. None of the four methods are without drawbacks:

- The D-BLAST architecture is a theoretical super structure attaining Shannon capacity with 1-D codec technology but unrealizable in practice.

- The V-BLAST architecture is susceptible to error propagation when any of its antennas enters a deep fade.
- A space-time concept has been used to mitigate the fading.
  - The Alamouti space-time code and its generalized Tarokh-Seshadri- Calderbank space-time codes, which use redundancy and thus suitable for low-rate coding.
  - T-BLAST, which uses simple yet effective high-rate space-time codes; the crucial innovation of T-BLAST is the combination of BLAST and turbo principles.

This thesis pioneers T-BLAST and backs its claims with solid empirical evidence.

Appendix of Chapter 2

2A. Optimality of D-BLAST

Consider an (M, N) system. The goal is to prove

$$\log_2 \det\left(\mathbf{I}_N + \frac{\rho}{M}\mathbf{H}\mathbf{H}^H\right) = \sum_{k=1}^{M} \log_2[1 + \Upsilon_k] \tag{2.55}$$

The above proof may be simplified as:

$$\det\left(\mathbf{I}_N + \frac{\rho}{M}\mathbf{H}\mathbf{H}^H\right) = \prod_{k=1}^{M} [1 + \Upsilon_k] \tag{2.56}$$

Define

$$\Omega_M = \left(\mathbf{I}_N + \frac{\rho}{M}\mathbf{H}\mathbf{H}^H\right) = \frac{\rho}{M}\sum_{i=1}^{M} \mathbf{h}_i\mathbf{h}_i^H + \mathbf{I}_N \tag{2.57}$$

where $\mathbf{h}_i$ is i-th column of matrix $\mathbf{H}$.

For single transmit and N receive antennas (receiver diversity only). It can be shown

$$\det\left(1 + \frac{\rho}{M}\mathbf{h}_1^H\mathbf{h}_1\right) = 1 + \Upsilon_1 \tag{2.58}$$

Let us assume that (2.56) is true for $m-1$ transmit antennas. Then we can write,

$$\det(\Omega_{m-1}) = \prod_{k=1}^{m-1}[1+\Upsilon_k] \tag{2.59}$$

From (2.57), we have

$$\Omega_m = \Omega_{m-1} + \frac{\rho}{M}\mathbf{h}_m\mathbf{h}_m^H \tag{2.60}$$

$$\mathbf{P} = \mathbf{Q} + \frac{\rho}{M}\mathbf{h}_m\mathbf{h}_m^H \tag{2.61}$$

where we have defined: $\mathbf{P} = \Omega_m$ and $\mathbf{Q} = \Omega_{m-1}$. Using the matrix inversion Lemma given in [52] and [62], we can show that

$$[\mathbf{Q} + \frac{\rho}{M}\mathbf{h}_m\mathbf{h}_m^H]^{-1}\mathbf{h}_m = \frac{\mathbf{Q}^{-1}\mathbf{h}_m}{1+\frac{\rho}{M}\mathbf{h}_m^H\mathbf{Q}^{-1}\mathbf{h}_m} \tag{2.62}$$

$$\mathbf{P}^{-1}\mathbf{h}_m = \frac{\mathbf{Q}^{-1}\mathbf{h}_m}{1+\Upsilon_m}$$

The matrix inverse $\mathbf{P}^{-1}$ is defined by [55]

$$\mathbf{P}^{-1} = \frac{\mathbf{P}_{adj}}{\det(\mathbf{P})} \tag{2.63}$$

where $\mathbf{P}_{adj}$ is the adjoint matrix of matrix $\mathbf{P}$; thus, we can rewrite (2.62) as

$$\frac{\mathbf{P}_{adj}}{\det(\mathbf{P})}\mathbf{h}_m = \frac{\mathbf{Q}_{adj}}{\det(\mathbf{Q})}\frac{\mathbf{h}_m}{1+\Upsilon_m} \tag{2.64}$$

$$= \mathbf{Q}_{adj}\frac{\mathbf{h}_m}{\prod_{i=1}^{m}(1+\Upsilon_i)} \tag{2.65}$$

where (2.65) is obtained by replacing $\det\mathbf{Q}$ using (2.59). Now, to prove (2.56), we have to show

$$\mathbf{P}_{adj}\mathbf{h}_m = \mathbf{Q}_{adj}\mathbf{h}_m \tag{2.66}$$

Expanding (2.61), we have

$$\begin{aligned} \mathbf{P} &= \mathbf{Q} + \frac{\rho}{M}\mathbf{h}_m\mathbf{h}_m^H \\ &= \left[\mathbf{q}_1 + \frac{\rho}{M}\mathbf{h}_m H_{m1}^*, \mathbf{q}_2 + \frac{\rho}{M}\mathbf{h}_m H_{m2}^*, \ldots, \mathbf{q}_N + \frac{\rho}{M}\mathbf{h}_m H_{mN}^*\right] \end{aligned} \tag{2.67}$$

where $\mathbf{q}_i, \forall i$ is the i-th column of $\mathbf{Q}$ and H_{ij} is the ijth element of matrix $\mathbf{H}$. We can prove (2.66) by showing the jth element of $\mathbf{P}_{adj}\mathbf{h}_m$ is equal to the jth element of $\mathbf{Q}_{adj}\mathbf{h}_m$ for $j = 1, \ldots, m$. The jth element of $\mathbf{P}_{adj}\mathbf{h}_m$ is given by $\det(\mathbf{P}_j)$, where $\mathbf{P}_j$ is obtained by replacing jth column of matrix $\mathbf{P}$ by $\mathbf{h}_m$. Similarly, the jth element of $\mathbf{Q}_{adj}\mathbf{h}_m$ is given by $\det(\mathbf{Q}_j)$. Accordingly, by replacing the j the column of (2.68) by $\mathbf{h}_m$, we get

$$\det(\mathbf{P}_j) = \det\left[\mathbf{q}_1 + \frac{\rho}{M}\mathbf{h}_m H_{m1}^*, \ldots, \mathbf{h}_m, \ldots, \mathbf{q}_N + \frac{\rho}{M}\mathbf{h}_m H_{mN}^*\right] \tag{2.68}$$

Using the fact that a determinant does not change if one column multiplied by a constant is added to another column, we can rewrite (2.68) as

$$\det(\mathbf{P}_j) = \det[\mathbf{q}_1, \mathbf{q}_2, \ldots, \mathbf{h}_m, \ldots, \mathbf{q}_N] \tag{2.69}$$

$$= \det(\mathbf{Q}_j) \tag{2.70}$$

Similarly, we can show that $\det(\mathbf{P}_j) = \det(\mathbf{Q}_j)$ for $i = 1, 2, \ldots, N, i \neq j$. This completes the proof of (2.55).

Chapter 3

The Turbo Principle

In 1948, Shannon laid down the foundation of information theory. In particular, he established the upper limit of the data transmission rate over a given channel and described channel coding as the means for achieving this limit: *For any communication channel there exist families of random block codes that achieve arbitrarily small probability of error at any information rate up to the capacity of the channel* [40]. However, for the proposed random codes, there is no practical coding or decoding algorithm because Shannon's proof was non-constructive. Since then, a fundamental research question has been: *How can we practically approach channel capacity using random block codes?* In practice, the key obstacle to approach the channel capacity is not the construction of good long random codes; rather, it is how to keep the decoding complexity reasonable. It is amazing to find that both turbo codes [63]-[66], and low-density parity-check (LDPC) codes [67]-[68], which are the closest known codes to the capacity limits with reasonable decoding complexity, have random code-like weight distribution. Most important, iterative decoders allow both of these codes to achieve their error performance within a hair's breadth of Shannon's theoretical limit on the channel capacity in a physically realizable fashion.

Again, the crucial innovation of LDPC and turbo codes was the introduction of message passing iterative decoding algorithms. Since then, iterative algorithms that employ the

turbo principles, [69]-[72] have found a wide range of applications including serial concatenation of codes [73]-[74], iterative equalization and decoding [82], iterative decoding of bit interleaved coded modulation [83], iterative multi-user detection [75]-[85], space-time turbo codes and TURBO-BLAST [6]-[14].

This thesis is about Turbo-BLAST, which is based on serially concatenated block codes and turbo processing. The goal of this chapter is to introduce the main ideas behind turbo coding and decoding structures. It begins by introducing the turbo-principle via the parallel and serial concatenated turbo codes and their iterative decoding structures. After establishing this principle, it introduces the generalized soft-in soft-out decoding module used in turbo decoders.

3.1 History of Channel Coding

The traditional algebraic coding designs, such as linear block codes and convolutional codes, have feasible maximum likelihood decoding structures. In the early sixties, it was considered that the combination of long randomly chosen convolutional codes with sequential decoding, a class of exhaustive tree search techniques, will essentially solve the complexity problem [86]. Decoding errors do not occur in long enough convolutional codes, but decoding failures can occur when the number of computations exceeds some practical complexity. Due to the exponential computational complexity of maximum likelihood decoders, increasing with the code-word length of a linear block code or the constraint length of a convolutional code, it is impossible to realistically achieve the Shannon capacity limits. Up to the early 1990s, the general view was that the effective channels capacity rate R_0 is smaller than the Shannon capacity and practical communication beyond R_0 was impossible. The sequential decoding [87], proved to be an efficient method of achieving zero error probability on any memoryless channel at any rate R_1 less than R_0.

In a series of innovative papers, concatenated coding schemes, landmarked by Forney [88] in 1966, were shown to achieve large coding gains by combining two or more relatively simple convolutional or block codes. Most important, the structure of the concatenated

coding permits relatively simple decoding structures.

Serial concatenation of Reed-Solomon outer code [75] followed by a convolutional inner code [91] was the most popular concatenated coding scheme until the new family of convolutional codes, known as turbo code, were invented by a group of researchers in France in 1993 [63]. Turbo codes are built from either parallel or serial concatenation of recursive systematic convolutional codes linked together by non-uniform interleaving.

Typically, the concatenation of codes splits the decoding problem into manageable steps. The crucial innovation of turbo decoding is not only to split the burden of decoding into steps but also to pass what has been learned from previous steps, and to do so iteratively. The discovery of turbo codes and iterative decoders rekindled interest in low-density parity-check (LDPC) codes. LDPC was originally invented and investigated in 1960 by Gallagar [67]; he was the first to show that iterative decoders are capable of achieving a significant fraction of Shannon's channel capacity with low complexity [67].

Turbo encoding and decoding has become popular due to its simple encoding structure that permits a lower complexity iterative decoding, yet performing within 0.7dB of the theoretical Shannon capacity limits at bit error rates of approximately 10^{-5}. The drawback of LDPC codes is that they have quadratic encoding complexity in the block length, whereas the encoding complexity of turbo codes is linear in block length. However, LDPC codes are serious competitors to turbo-codes since they have the potential to achieve a performance that is asymptotically better than turbo codes.

3.1.1 Channel coding / Feedforward Error-Correction Encoding

The function of the channel encoder is to add redundancy to user-information sequences, which can be used at the receiver to correct for the effect of wireless channel impairments. In particular, the channel encoder maps k information bits onto a unique n bit *codeword*, where $n \geq k$. The ratio $R = k/n$ is called the *code rate*, and the reciprocal of this ratio measures the added redundancy. There are two families of channel coding:

- Block codes: the codewords have fixed length n and 2^n codewords are possible for

binary codes. From these 2^n codewords, 2^k codewords are selected to form a code. The resulting block code is denoted as a (n, k) code. *A block code is said to be linear if any of two codewords in the code can be added in modulo-2 arithmetic to produce a third codeword in the code book.* Most of the traditional block codes are based on hard-decision algebraic decoders. This as we shall see is a disadvantage due to the possible loss of valuable information.

- Convolutional codes: Convolutional codes are non-block linear codes over a finite field. A convolutional code is generated by passing the information sequence through a linear finite-state machine that consists of an M-stage shift register and n linear algebraic function generators. The convolutional encoder has M bits of memory, and $\kappa = M + 1$ constraint length. Recursive systematic convolutional (RSC) codes constitute a special class of convolutional codes. For high code rates, RSC codes result in better error performance than conventional convolutional codes at any signal-to-noise ratio. There are two major differences between RSC codes and convolutional codes:

  - In the RSC codes, one or more of the tap outputs of the shift register are fed back to the input to make the internal state of the shift register depend on past outputs.
  - An RSC code is systematic, that is, an unaltered version of the information bits is included in the codewords.

Both convolutional codes and RSC codes can also be treated as block codes over certain infinite fields. An important parameter of the channel codes that characterizes the performance and the error correcting capability of block codes and block convolutional codes is the minimum distance property.

Definition 1 *The Hamming weight $w(c)$ of a code vector c is defined as the number of nonzero elements in the code vector.*

Definition 2 *The minimum distance $d_{\min}$ of a linear block code is defined as the smallest Hamming distance between any pair of codewords in a codebook. The Hamming distance $d(\mathbf{c}_i, \mathbf{c}_j)$ between any two codewords $\mathbf{c}_i$ and $\mathbf{c}_j$ is defined as the number of locations in which their respective elements differ. Thus the minimum distance of a linear block code is the smallest Hamming weight of the non zero codewords in the codebook.*

The difficulty with linear block codes and convolutional codes is that the block size of a linear block code or the constraint length of a convolutional code has to be increased to design a large minimum distance code, which, in turn, causes the computational complexity of a maximum likelihood decoder to increase exponentially.

In contrast to traditional code designs using the algebraic structures and their corresponding feasible decoding schemes, turbo codes provide a new framework for constructing random codes and decoding them with feasible complexity. Moreover, the random code framework uses quite *short constraint* block convolutional codes and an interleaver[1] as its building blocks. Thus, the well known coder-decoder structures developed for convolutional codes are utilized to achieve a good performance. The resulting random codes minimize the probability of occurrence of low weight codewords, thus improving the bit-error performance.

3.2 TURBO Coding

A turbo encoder is a combination of two simple convolutional encoders. A block of bits is encoded by two simple recursive convolutional codes, each with a relatively small number of states. The input to the second encoder is an interleaved (i.e., pseudo-randomized) version of the bits output from the first encoder.

A turbo code is the combination of the uncoded bits and the parity bits generated by the two encoders. An innovative feature of turbo codes is the use of a random interleaver, which permutes the original block of bits before application to the second encoder. The

[1] An interleaver is an input-output device that permutes the ordering of a block symbols in a pseudo-random fashion.

high error correcting power of turbo codes originates from random-like coding achieved by random interleaving in conjunction with concatenated coding and iterative decoding using uncorrelated extrinsic information. The random-like structure of turbo codes has resulted in outstanding performance by providing small error rates at information rates close to theoretical channel capacity. The structure and complexity of turbo encoder design is restricted by the system parameters such as *decoding delay* and *coding gain*.

3.2.1 Parallel Concatenated Turbo Codes

Turbo principles were first applied to parallel concatenated turbo-codes. In this case two systematic convolutional codes with rates R_1 and R_2 are concatenated in parallel in the form shown in Figure 3.1. Moreover, the block of L bits is fed directly to the first encoder. For the second encoder the same block of data is permuted using a pseudo-block interleaver, Π. These two encoders are not necessarily identical, but for best decoding performance, $R_1 \leq R_2$.

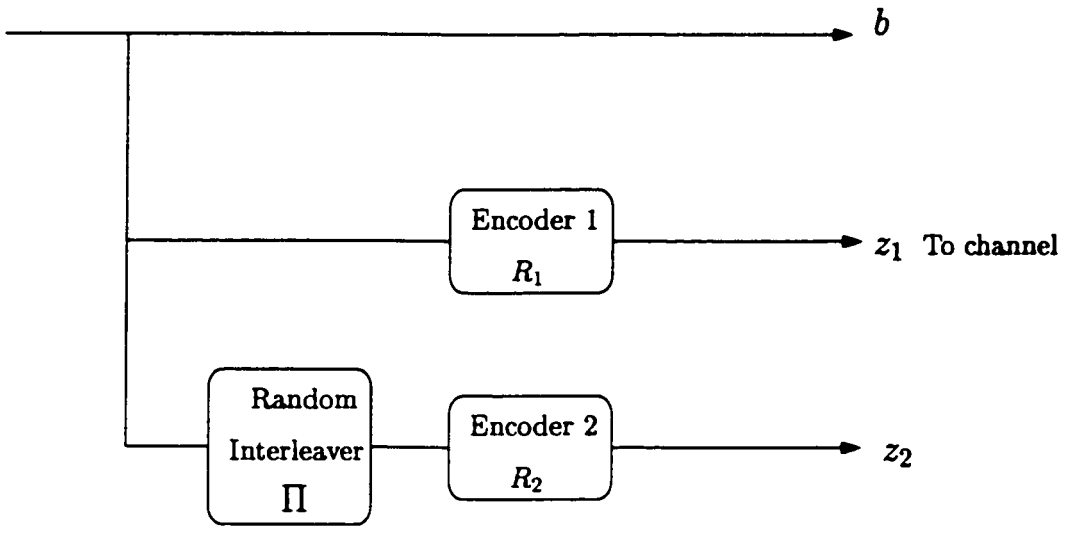

Figure 3.1: Turbo codes

The block diagram of iterative decoder, depicted in Figure 3.2, is made up of two elementary soft in/soft out decoder modules denoted by "SISO", one for each encoder,

an interleaver and a deinterleaver performing the inverse permutation with respect to the interleaver.

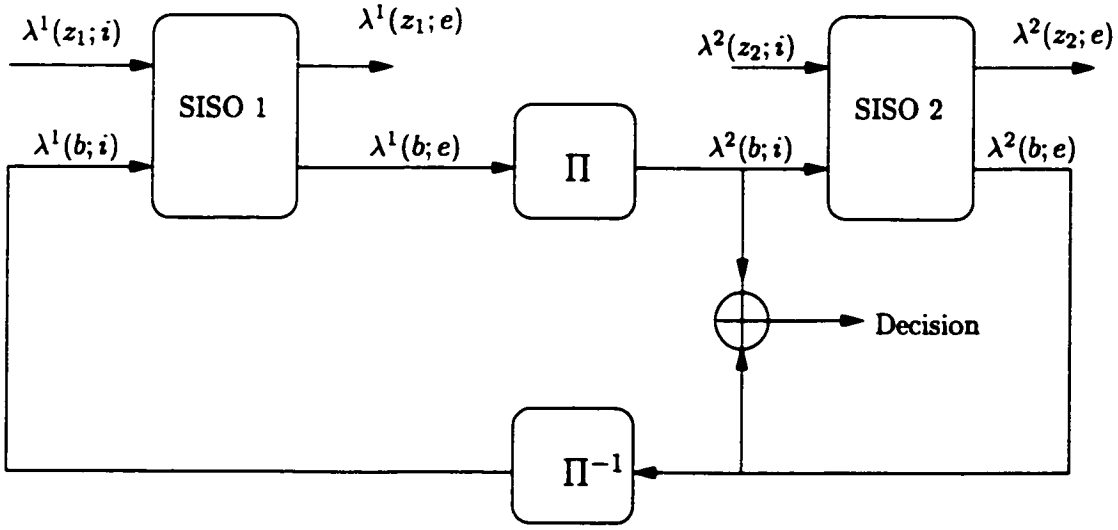

Figure 3.2: Turbo decoder

At the core of the decoding algorithm is the SISO module. A SISO module is a four-port device that accepts the probability distributions or the corresponding likelihood ratios of the information and noisy encoded symbols as inputs, and provides an update of these probability distributions based upon the code constraint as outputs [73]. The symbols $\lambda(:,i)$ and $\lambda(:,e)$ at the input and output ports of the SISO module refer to the *intrinsic* and *extrinsic* information described as log-likelihood ratios (LLR).

Definition 3 *The LLR of a binary random variable U in GF(2) with the elements $\{+1,-1\}$ is defined as*

$$\lambda(u) = \log \frac{P(u=+1)}{P(u=-1)} \tag{3.1}$$

The sign and the magnitude of $\lambda(u)$ corresponds to a hard decision and its reliability.

Notations used in LLR: The first argument refers to the information symbols (u) or the parity bits (z_1 or z_2). The second argument refers to *intrinsic* (i), *extrinsic* (e) or *a*

posteriori (p) information. Finally, the superscripts 1 and 2 refer to the SISO decoders 1 and 2, respectively.

The turbo principle makes use of the concepts of intrinsic and extrinsic information to increase the independence of the inputs from one processing stage to next. A SISO module accepts *intrinsic* or *a priori* values and provides the *a posteriori* and *extrinsic* information. Before proceeding to describe the operation of the turbo decoder in detail, we define the notions of *intrinsic* and *extrinsic* information.

Definition 4 *Intrinsic* information refers to the soft information inherent in a bit as received over the channel. Typically, it is the sample *a priori* values prior to decoding, i.e unconstrained probability:

$$\lambda(u;i) = \log \frac{P\{u=+1\}}{P\{u=-1\}} \tag{3.2}$$

Definition 5 The *a posteriori* information is the information provided about a bit u from the received bits according to the code constraint:

$$\lambda(u;p) = \log \frac{P\{u=+1|decoding\}}{P\{u=-1|decoding\}} \tag{3.3}$$

where $P\{u|decoding\}$ is the probability of information bit u computed by the decoder using the knowledge of channel code constraint.

Definition 6 The *extrinsic* information is the information provided about a bit u from the other received bits according to the constraint imposed by the FEC code. It is formally defined as the difference between the *a posteriori* information and the *intrinsic* information fed back at the input of the decoding stage:

$$\lambda(u;e) = \lambda(u;p) - \lambda(u;i) \tag{3.4}$$

The exchange of extrinsic informations between the decoding stages of the receiver assists in the task of a slow but steady convergence of the iterative decoding process. With increasing

iterations, the extrinsic values achieve better and better confidence levels. At convergence, the extrinsic informations will be directed towards the sign of the information bits and with high reliability. (See [71].)

The iterative decoder illustrated in the Figure 3.2 depicts the flow of message passing between the SISO modules. The SISO module operations can be explained using the following three steps:

1. The first SISO module generates soft estimates of the systematic bits $b(l)$, $l = 1, 2, \ldots, L$:

   - First, estimate the *a posteriori information*

$$\lambda^1(b(l);p) = \log \frac{P\{b(l) = +1 | \lambda^1(\mathbf{z_1};i), \lambda^1(\mathbf{b};i), decoding\}}{P\{b(l) = -1 | \lambda^1(\mathbf{z_1};i), \lambda^1(\mathbf{b};i), decoding\}}, \quad l = 1, 2, \ldots L \tag{3.5}$$

     During the first iteration $\lambda^1(\mathbf{z_1};i)$ and $\lambda^1(\mathbf{b};i)$ are initialized with the soft outputs consisting of the log-likelihood ratios of the information symbols $\mathbf{b}$ and the first set of parity check bits $\mathbf{z_1}$ for the received channel signal [71].

   - Compute the extrinsic information

$$\lambda^1(\mathbf{b};e) = \lambda^1(\mathbf{b};p) - \lambda^1(\mathbf{b};i) \tag{3.6}$$

   - The $\lambda^1(\mathbf{b};e)$ is the extrinsic information about the set of message bits $\mathbf{b}$ derived from the first decoding stage and fed to the second decoding stage as the intrinsic information. Before application to the second decoding stage, the extrinsic information is reordered to compensate for the pseudo-random interleaving introduced in the turbo encoder:

$$\lambda^2(\mathbf{b};i) = \Pi\{\lambda^1(\mathbf{b};e)\} \tag{3.7}$$

2. Similarly, the second SISO module associated with the second encoder performs a

further refined estimate of the systematic bit $b(l)$ using the soft outputs consisting of the LLR's of the interleaved information symbols $\mathbf{b}$ and the second set of parity check bits $\mathbf{z}_2$ for the received channel signal [71].

The output of the second stage provides *intrinsic* information to the first stage after re-ordering to compensate for the random interleaving:

$$\lambda^1(\mathbf{b}; i) = \Pi^{-1}\{\lambda^2(\mathbf{b}; e)\} \tag{3.8}$$

Steps 1 and 2 are repeated until the algorithm converges [2].

3. Estimate of the message bits $\mathbf{b}$ is obtained by hard limiting the LLR $\lambda^2(\mathbf{b}; p)$ at the output of the second stage

$$\hat{\mathbf{b}} = \text{sgn}\{\lambda^2(\mathbf{b}; p)\} \tag{3.9}$$

Note the following:

- The estimate $\hat{\mathbf{b}}$ approaches the global maximum *a posteriori* (MAP) solution as the number of iterations approaches infinity, if the bit probabilities remain independent between iterations of the decoding process. Here, we mean "global MAP" by decoding a single Markov process (trellis) modeled for the turbo code, which includes the effects of the interleaver.

- The fundamental principle for feeding back the *extrinsic* information from one decoder to another is to never feedback decoder information that stems from itself. The feedback of *extrinsic* information prevents the enhancement of highly correlated input and output corruptions. Typically, for cases encountered in practice, the feedback of *extrinsic* information maintains the statistical independence between stages.

[2] In practice, we may do one of two things: Either the steps 1 and 2 are repeated for a fixed number of times, or appropriate stopping criteria are used [74].

- Finally, the separation of extrinsic information from the estimate of *a posteriori* probabilities holds only if the inputs to the decoders are independent. If the channel has memory, the independence assumption is not valid; therefore, interleaving between the decoder stages is important. For better performance, either an outer interleaver or two interleavers as described in irregular turbo codes may be used.

3.2.2 Serial Concatenated Turbo Codes

An alternative to turbo codes is serially concatenated convolutional codes formed by concatenating two systematic convolutional codes in the form shown in Figure 3.3. The block of information bits are encoded by the first encoder, then interleaver permutes the output codewords of the outer code before passing them to the inner code [73]:

$$\mathbf{b}^i = \Pi(\mathbf{c}^o) \tag{3.10}$$

These codes are viewed as a new class of turbo codes since they can be decoded using iterative decoders.

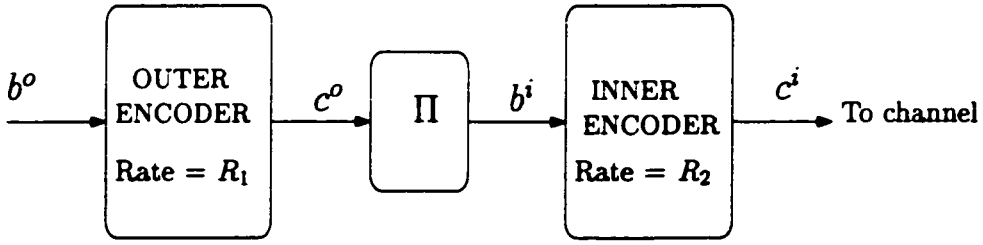

Figure 3.3: Serially concatenated convolutional codes

The decoder for the serially concatenated codes is a concatenation of inner and outer SISO modules as shown in Figure 3.4. The figure clearly depicts the flow of message passing between the inner and outer SISO modules. The decoder processing involves the following computations:

1. The inner SISO module generates a soft estimate of the information bits $\mathbf{b}^i$ conditioned

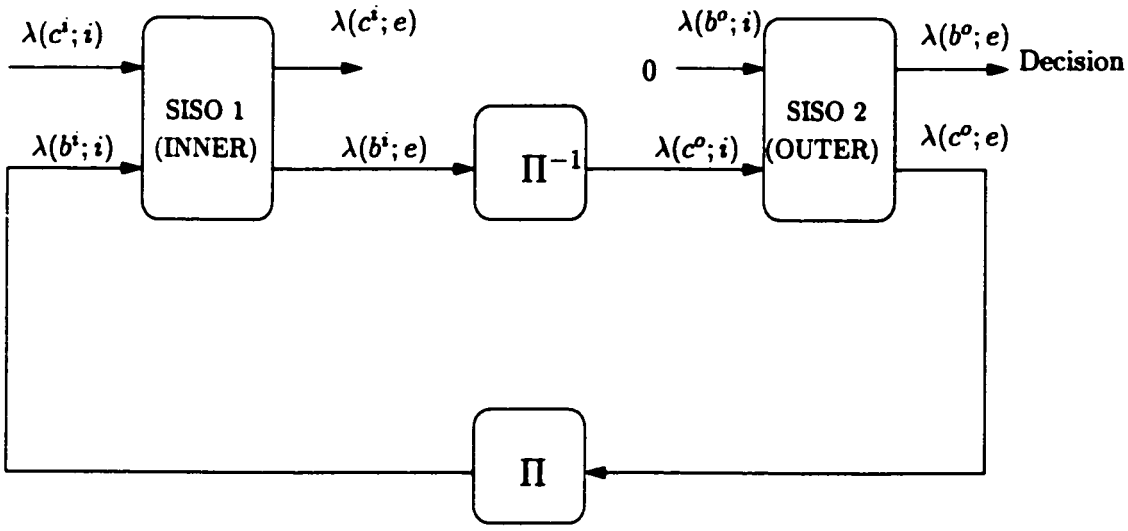

Figure 3.4: Iterative decoder for serially concatenated codes

on the inner code constraint:

- Estimation of the *a posteriori* information:

$$\lambda(b^i(l);p) = \log \frac{P\{b^i(l) = +1|\lambda(\mathbf{c}^i;i), \lambda(\mathbf{b}^i;i), decoding\}}{P\{b^i(l) = -1|\lambda(\mathbf{c}^i;i), \lambda(\mathbf{b}^i;i), decoding\}}, \quad l = 1, 2, \ldots L \tag{3.11}$$

  During the first iteration, $\lambda(\mathbf{c}^i;i)$ is initialized with the soft outputs consisting of the LLR's of symbols received from the channel. The second input $\lambda(\mathbf{b},i)$ is initialized to zero since no *a priori* information is available of the input symbols $\mathbf{b}$.

- Computation of the *extrinsic* information

$$\lambda(\mathbf{b}^i;e) = \lambda(\mathbf{b}^i;p) - \lambda(\mathbf{b}^i;i) \tag{3.12}$$

- The $\lambda(\mathbf{b}^i;e)$ is the *extrinsic* information about the set of message bits $\mathbf{b}^i$ of the inner encoder and fed back to the outer decoder as the intrinsic information of its

coded bits. Before the application of the outer decoder, the extrinsic information is reordered to compensate for the pseudo-random interleaving introduced in the turbo encoder.

$$\lambda(\mathbf{c}^o; i) = \Pi^{-1}\{\lambda(\mathbf{b}^i; e)\} \tag{3.13}$$

2. The outer SISO, in turn, processes the LLR's $\lambda(\mathbf{c}^o; i)$ and computes the LLR's of both code and information symbols based on the outer code constraints.

   - The *a posteriori* information for information and code symbols are given by

$$\lambda(b^o(l); p) = \log \frac{P\{b^o(l) = +1 | \lambda(\mathbf{c}^o; i), \lambda(\mathbf{b}^o; i), decoding\}}{P\{b^o(l) = -1 | \lambda(\mathbf{c}^o; i), \lambda(\mathbf{b}^o; i), decoding\}}, \quad l = 1, 2, \ldots L \tag{3.14}$$

$$\lambda(c^o(l); p) = \log \frac{P\{c^o(l) = +1 | \lambda(\mathbf{c}^o; i), \lambda(\mathbf{b}^o; i), decoding\}}{P\{c^o(l) = -1 | \lambda(\mathbf{c}^o; i), \lambda(\mathbf{b}^o; i), decoding\}}, \quad l = 1, 2, \ldots L \tag{3.15}$$

   The input $\lambda(\mathbf{b}^o, i)$ is always initialized to zero assuming equally likely source information symbols.

   - Extrinsic information of both the information and the code symbols:

$$\lambda(\mathbf{b}^o; e) = \lambda(\mathbf{b}^o; p) - \lambda(\mathbf{b}^o; i) \tag{3.16}$$

$$\lambda(\mathbf{c}^o; e) = \lambda(\mathbf{c}^o; p) - \lambda(\mathbf{c}^o; i) \tag{3.17}$$

The output of the outer decoder provides *intrinsic* information to the inner decoder

after re-ordering to compensate for the random interleaving:

$$\lambda(\mathbf{b}^i; i) = \Pi\{\lambda(\mathbf{c}^o; e)\} \tag{3.18}$$

Steps 1 and 2 are repeated until the algorithm converges.

3. Estimation of the message bits $\mathbf{b}^o$ by hard limiting the LLR $\lambda(\mathbf{b}^o; p)$ at the output of the outer SISO:

$$\hat{\mathbf{b}^o} = \text{sgn}(\lambda(\mathbf{b}^o; p)) \tag{3.19}$$

Note the following:

- In contrast to the turbo decoder used for traditional turbo codes, which updates only the LLR of systematic symbols, the iterative decoder associated with the serially concatenated turbo codes updates LLR of both information and code symbols based on the code constraint.
- The interleaver gain of serially concatenated codes, defined as the factor that decreases the bit error probability as a function of interleaver size, can be made significantly higher than that of traditional turbo codes [73].

3.3 SISO Decoders

This section introduces a key feature in the iterative decoders; the MAP-based soft-in/ soft-out module and, in particular, the implementation technique known as a generalized BCJR algorithm [73].

3.3.1 Historical Remark

In 1974, the pioneering work of Bahl, Cocke, Jelinek and Raviv (BCJR) established the symbol-by-symbol MAP algorithm as an alternative to the Viterbi algorithm for decoding convolutional codes. The MAP algorithm performs forward and backward recursion

which, in [94], was used for canceling intersymbol interference (ISI). Later in 1970, a similar technique was used to perform forward recursion only for canceling ISI, but typically had higher memory and complexity requirements [95]. The MAP algorithm requires the whole sequence for decoding, and thus can only be used in block-mode decoding. Despite a long delay, the memory requirement and computational complexity grow only linearly with the sequence length. However, the algorithm requires a forward recursion; hence its memory and computational complexity grow exponentially with decoding delay.

3.3.2 Generalized BCJR Algorithm

The SISO modules used in the turbo processing uses the BCJR algorithm, so called in honor of its four inventors: Bahl, Cocke, Jelinek, and Raviv (BCJR) [93]. The BCJR is fundamentally different from the Viterbi algorithm:

- The Viterbi algorithm is a maximum likelihood sequence estimator in that it maximizes the likelihood function for the whole sequence (usually a code word). Thus, it minimizes the sequence or codeword error rate of a communication system.

- The BCJR algorithm is a MAP decoder in that it minimizes the bit errors by estimating the *a posteriori* probabilities of the individual bits in a code word. The average bit error rate of BCJR algorithm can be slightly better than the Viterbi algorithm, but it can never be worse.

The formulation of the BCJR algorithm relies on the assumption that the channel is memoryless and the channel encoder and the channel coding can be completely described by a Markov process. This means that if a code can be represented as trellis, then the present state of the trellis depends only on the past state and the input bit [24]. The trellis of a block code or convolutional code can be always made to start and end in the zero state by adding zero bits to the information sequence appropriately. Moreover, the dynamics of the time-invariant trellis are completely specified by a trellis section [73]. A trellis section is depicted in Figure 3.5.

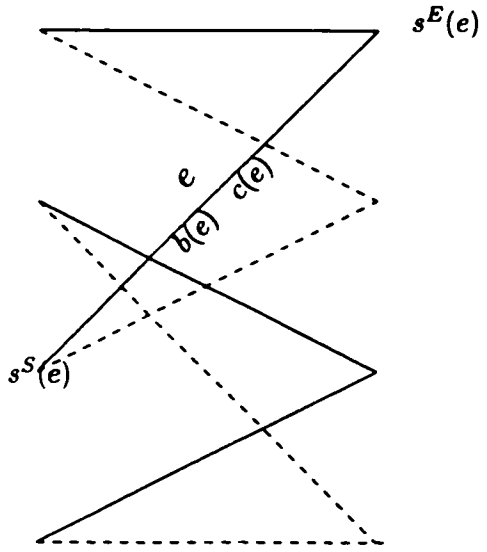

Figure 3.5: Trellis section between time t and $t+1$

Let $\mathbf{b} = \{b(t)\}_{t=1}^{T}$ be the input to a trellis encoder drawn from the alphabet $\mathcal{B} = \{b_1, \ldots, b_{N_I}\}$, and $\mathbf{c} = \{c(t)\}_{t=1}^{T}$ be the sequence of output or code from the trellis encoder drawn from the alphabet $\mathcal{C} = \{c_1, \ldots, c_{N_O}\}$, and $\mathbf{y} = \{y(t)\}_{t=1}^{T}$ be the corresponding output observed at the receiver.

Definition 7 *A trellis section can be characterized by a set of N_s states $\mathcal{S} = \{s_1, \ldots, s_{N_s}\}$ and a set of N_I edges $\mathcal{E} = \{e_1, \ldots, e_{N_s \times N_I}\}$ between the states of the trellis at time t and $t+1$. An edge can be identified by the information symbol $b(e)$ and code symbol $c(e)$ associated with the edge, and the starting (S) and ending (E) states of the edge are denoted as $s^S(e)$ and $s^E(e)$, respectively.*

We consider a new generalized form of BCJR algorithm which is suitable for any component or block codes represented by a trellis [73]. The generalized BCJR algorithm can cope with codes having trellis with parallel edges. Note that the original BCJR algorithm could not cope with a trellis having parallel edges.

Consider a trellis section between time t and $t+1$. The BCJR algorithm first computes the probability $P(s^S(e) \rightarrow s^E(e))$ of each valid state transition given the noisy channel

observations $\mathbf{y}$:

$$P(s^S(e) \rightarrow s^E(e))|\mathbf{y}) = \frac{P(s^S(e) \rightarrow s^E(e), \mathbf{y})}{P(\mathbf{y})} \tag{3.20}$$

This joint probability $P(s^S(e) \rightarrow s^E(e), \mathbf{y})$ can be partitioned using the properties of a Markov process [78], [85]

$$P(s^S(e) \rightarrow s^E(e), \mathbf{y}) = \alpha_t(s^S(e))\gamma_t(s^S(e) \rightarrow s^E(e))\beta_{t+1}(s^E(e)) \tag{3.21}$$

where

$$\alpha_t(s^S(e)) = P(s^S(e), (y_0, \ldots y_{t-1})) \tag{3.22}$$

$$\gamma_t(s^S(e) \rightarrow s^E(e)) = P(s^E(e), y_t|s^S(e)) \tag{3.23}$$

$$\beta_{t+1}(s^E(e)) = P((y_{t+1}, \ldots y_\tau)|s^E(e)) \tag{3.24}$$

and the state transition probability can be expressed as

$$\gamma_t(s^S(e) \rightarrow s^E(e)) = P(s^E(e)|s^S(e))P(y_t|s^S(e) \rightarrow s^E(e)) \tag{3.25}$$

The first factor on the right hand side of (3.25) follows from the fact that, given $s^S(e)$, the probability of going to state $s^E(e)$ depends only on the probability of the information bit at time t. The second factor on the right hand side follows from the fact that, if we know $s^S(e)$ and $s^E(e)$ then, since the code is deterministic, the code symbol is known. Thus (3.25) reduces to

$$\gamma_t(s^S(e) \rightarrow s^E(e)) = P(b(e))P(y_t|c(e)) \tag{3.26}$$

Forward and Backward Recursions

The forward and backward estimates can be determined recursively as follows, respectively:

$$\begin{aligned}\alpha_t(s) &= \sum_{e:s^E(e)=s} \alpha_{t-1}[s^S(e)]\gamma_{t-1}[s^S(e) \to s^E(e)] \\ &= \sum_{e:s^E(e)=s} \alpha_{t-1}[s^S(e)]P_t[b(e),i]P_t[c(e);i], t = 1,2,\ldots,\tau\end{aligned} \tag{3.27}$$

$$\begin{aligned}\beta_t(s) &= \sum_{e:s^S(e)=s} \beta_{t+1}[s^E(e)]\gamma_t[s^S(e) \to s^E(e)] \\ &= \sum_{e:s^S(e)=s} \beta_{t+1}[s^E(e)]P_{t+1}[b(e);i]P_{t+1}[c(e);i], t = \tau-1,\tau-2,\ldots 0\end{aligned} \tag{3.28}$$

$$\alpha_0(s) = \begin{cases} 1 & s = S_0 \\ 0 & \text{otherwise} \end{cases} \tag{3.29}$$

$$\beta_\tau(s) = \begin{cases} 1 & s = S_\tau \\ 0 & \text{otherwise} \end{cases} \tag{3.30}$$

A Posteriori Probabilities (APP)

At time t, the output *a posteriori* probabilities of the information and code bits are found according to the following two formulas, respectively:

$$P_t(c;p) = \sum_{e:c(e)=c} \alpha_{t-1}[s^S(e)]P_t[b(e);i]P_t[c(e);i]\beta_t[s^E(e)] \tag{3.31}$$

$$P_t(b;p) = \sum_{e:b(e)=b} \alpha_{t-1}[s^S(e)]P_t[b(e);i]P_t[c(e);i]\beta_t[s^E(e)] \tag{3.32}$$

Extrinsic Information

From the APP defined in (3.31) and (3.32), the extrinsic information can be obtained by extracting $P_t(c(e),i)$ and $P_t(b(e),i)$, respectively. Note $P_t(c(e),i)$ and $P_t(b(e),i)$ do not depend on e, and thus, can be extracted.

$$P_t[c;e] = A_c \frac{P_t(c;p)}{P_t(c;i)} \tag{3.33}$$

$$P_t(b;e) = A_b \frac{P_t(b;p)}{P_t(b;i)} \tag{3.34}$$

The normalization constant A_b is obtained such that the sum of the probabilities of information bits equal to 1:

$$A_b \leftarrow \sum_b P_t(b;e) = 1 \tag{3.35}$$

Similarly, the normalization constant A_c is:

$$A_c \leftarrow \sum_c P_t(c;e) = 1 \tag{3.36}$$

The corresponding extrinsic information becomes

$$P_t(c;e) = A_c \sum_{e:c(e)=c} \alpha_{t-1}[s^S(e)]P_t[b(e);e]\beta_t[s^E(e)] \tag{3.37}$$

$$P_t(u;e) = A_u \sum_{e:u(e)=u} \alpha_{t-1}[s^S(e)] P_t[c(e);i] \beta_t[s^E(e)] \tag{3.38}$$

3.3.3 The MAP Algorithm in Log-Domain (LOG-MAP Algorithm)

The MAP algorithm has high computational complexity: $2 \times N_s \times N_I$ multiplications and additions per bit. This can be reduced by performing the algorithm in the log domain where multiplication becomes summation [97]. First we define the following:

1. The transition probability

$$\begin{aligned} \bar{\gamma}_{t-1}[s^S(e) \to s^E(e)] &= \log \gamma_{t-1}[s^S(e) \to s^E(e)] \\ &= \log P_t[b(e),i] + \log P_t[c(e);i] \\ &= \pi_t[b(e),i] + \pi_t[c(e);i] \end{aligned} \tag{3.39}$$

2. The forward estimator for $t = 1, 2, \ldots, \tau$

$$\begin{aligned} \bar{\alpha}_t(s) &= \log \alpha_t(s^S(e)) \\ &= \log \left[\sum_{e:s^E(e)=s} \{\alpha_{t-1}[s^S(e)] \cdot P_t[b(e);i] \cdot P_t[c(e);i]\} \right] \\ &= \log \left[\sum_{e:s^E(e)=s} \exp\{\bar{\alpha}_{t-1}[s^S(e)] + \pi_t[b(e);i] + \pi_t[c(e);i]\} \right] \\ &= \max^*_{e:s^E(e)=s} \{\bar{\alpha}_{t-1}[s^S(e)] + \pi_t[b(e);i] + \pi_t[c(e);i]\} \end{aligned} \tag{3.40}$$

with initial values

$$\bar{\alpha}_0(s) = \begin{cases} 0 & s = S_0 \\ -\infty & \text{otherwise} \end{cases} \tag{3.41}$$

3. The backward estimator for $t = \tau - 1, \tau - 2, \ldots, 0$

$$\begin{aligned}
\bar{\beta}_t(s) &= \log \beta_t(s) \qquad (3.42)\\
&= \log\left[\sum_{e:s^S(e)=s} \{\beta_{t+1}[s^E(e)] \cdot P_{t+1}[b(e);i] \cdot P_{t+1}[c(e);i]\}\right]\\
&= \log\left[\sum_{e:s^S(e)=s} \exp\{\bar{\beta}_{t+1}[s^E(e)] + \pi_{t+1}[b(e);i] + \pi_{t+1}[c(e);i]\}\right]\\
&= \max^{*}_{e:s^S(e)=s} \{\bar{\beta}_{t+1}[s^E(e)] + \pi_{t+1}[b(e);i] + \pi_{t+1}[c(e);i]\}
\end{aligned}$$

with initial values

$$\bar{\beta}_\tau(s) = \begin{cases} 0 & s = S_\tau \\ -\infty & \text{otherwise} \end{cases} \qquad (3.43)$$

Once forward and backward estimates are computed, the output extrinsic information is found by using the following two formulas:

$$\begin{aligned}
\pi_t(c;e) &= \log\left[\sum_{e:c(e)=c} \{\alpha_{t-1}[s^S(e)] \cdot P_t[b(e);i] \cdot \beta_{t+1}[s^E(e)]\}\right] + a_c \qquad (3.44)\\
&= \log\left[\sum_{e:c(e)=c} \exp\{\bar{\alpha}_{t-1}[s^S(e)] + \pi_t[b(e);i] + \bar{\beta}_{t+1}[s^E(e)]\}\right] + a_c\\
&= \max^{*}_{e:c(e)=c} \{\bar{\alpha}_{t-1}[s^S(e)] + \pi_t[b(e);i] + \bar{\beta}_{t+1}[s^E(e)]\} + a_c
\end{aligned}$$

$$\begin{aligned}\pi_t(b;e) &= \log\left[\sum_{e:u(e)=u}\{\alpha_{t-1}[s^S(e)]\cdot P_t[c(e);i]\cdot\beta_{t+1}[s^E(e)]\}\right]+a_b \qquad (3.45)\\ &= \log\left[\sum_{e:u(e)=u}\exp\{\bar{\alpha}_{t-1}[s^S(e)]+\pi_t[c(e);i]+\bar{\beta}_{t+1}[s^E(e)]\}\right]+a_b\\ &= \max^{*}_{e:u(e)=u}\{\bar{\alpha}_{t-1}[s^S(e)]+\pi_t[c(e);i]+\bar{\beta}_{t+1}[s^E(e)]\}+a_b\end{aligned}$$

where the quantities a_c and a_b are normalization quantities needed to prevent the excessive growth of $\bar{\alpha}$ and $\bar{\beta}$ and the operator $\max^*$ is defined as

$$\max^{*}_{i}(a_i) = \log\left[\sum_{i=1}^{I}\exp(a_i)\right] \qquad (3.46)$$

The major task in the LOG-MAP algorithm is to compute the logarithm of the sum of exponentials, which, in practice, can be approximated as

$$\begin{aligned}\max^{*}_{i}(a_i) &= \max_{i}(a_i)+\delta(a_1,a_2,\ldots,a_I) \qquad (3.47)\\ &\simeq \max_{i} a_i \qquad (3.48)\end{aligned}$$

Algorithms using the approximation given in (3.47) and (3.48) are referred to as MAX-LOG-MAP algorithms.

- The term $\delta(a_1,a_2,\ldots,a_I)$ in (3.47) is a correction term that can be computed recursively using a 1-D lookup table [85].
- The approximation in (3.48) can be performed without undue performance degradation between medium to high SNRs, if $a_{\max} >> a_i, \forall a_i \neq a_{\max}$, where $a_{\max} = \max_i(a_i)$.
- Using max-log-map algorithm, good performance can be achieved without undue computational complexity.

3.4 Summary

This chapter has discussed the turbo principle. In particular, we described

- serial and parallel concatenated turbo codes and their iterative decoders,
- soft-in/soft-out modules, which are exemplified by the BCJR algorithm that performs maximum *a posteriori* estimation on a bit-by-bit basis in the decoding of turbo codes and their lower complexity and numerically less sensitive approximations, and
- the extraction of extrinsic information which we believe is behind the success of turbo principles.

With these descriptions in hand, our discussion in the next chapter turns to the T-BLAST, the main theme of the thesis.

Chapter 4

TURBO-BLAST

Foschini [2] posed a fundamental question: *using the building blocks of separately coded one-dimensional subsystems of equal capacity, is it possible to construct a BLAST system whose capacity grows linearly with number of transmit antennas?* This is precisely what is done in D-BLAST; however, D-BLAST is impractical.

In this chapter, we show that Turbo-BLAST, or T-BLAST for short, built on the combination of BLAST and turbo principles provides a practical answer to Foschini's fundamental question. Specifically, T-BLAST attains near Shannon capacity of MTMR systems using building blocks of separately coded one-dimensional subsystems of equal capacity.

This chapter is organized as follows: In section 4.1, we describe the base-line T-BLAST transmitter, some basic assumptions, and our notations. In section 4.2, the proposed random space-time (RST) coding for T-BLAST is explained. Sections 4.3 and 4.4, dealing with the T-BLAST optimal detection scheme, prove the optimality of the proposed codes, when using global Maximum Likelihood (ML) receivers. Note that, here we consider both uncorrelated and the highly correlated channel environments. In section 4.5, we derive the explicit capacity formula for a simple correlated channel which shows how the channel capacity may change with correlation coefficient. In section 4.6, the proposed near-optimal iterative decoder scheme for the T-BLAST is given. Here we introduce the important concepts of *intrinsic* and *extrinsic* information. Finally, in section 4.7, the performances of

various T-BLAST schemes proposed in this chapter are examined.

4.1 T-BLAST Transmitter

4.1.1 Assumptions

We consider an MTMR system that has n_T transmitting and n_R receiving antennas. Throughout this chapter, we assume:

- The n_T-transmitters operate with synchronized symbol timing, at the rate of $1/T$ symbol per second, and the sampling times of n_R receivers are symbol-synchronous.
- A quasi-static Rayleigh fading process, which means that channel variation is assumed to be negligible over L symbol periods. Therefore, we can learn the channel matrix by sending a training sequence within each packet.
- A narrowband frequency-flat fading communication environment, which implies no delay spread.

4.1.2 Notations

Figure 4.1 illustrates a high-level description of the BLAST architecture, which employs the proposed random space-time (RST) codes and having n_T transmitting and n_R receiving antenna elements.

The encoding process involves:

- De-multiplexing the user information bits into n_T substreams $\{\mathbf{b}_k\}_{k=1}^{n_T}$ of equal data rate.
- Independent block-encoding of each data substream, which uses the same predetermined linear block forward error correction (FEC) code with a weighted distribution of minimum weight equal to d_{min}:

$$\mathbf{C} = [\mathbf{b}_1\mathbf{G}, \mathbf{b}_2\mathbf{G}, \ldots, \mathbf{b}_{n_T}\mathbf{G}] = [\mathbf{c}_1, \mathbf{c}_2, \ldots, \mathbf{c}_{n_T}]^T \tag{4.1}$$

where $\mathbf{G}$ is $K \times L$ binary code generator and the $\{\mathbf{b}_k\}_{k=1}^{n_T}$ are K-dimensional information sequences, and the $\{\mathbf{c}_k\}_{k=1}^{n_T}$ are L-dimensional code sequences.

- The encoded substreams are bit-interleaved using an off-line designed space-time random permuter Π. We use $\{\tilde{\mathbf{c}}_k\}_{k=1}^{n_T}$ to denote the permuted substreams, where

$$\tilde{\mathbf{C}} = \Pi(\mathbf{C}) \tag{4.2}$$

- The space-time interleaved substreams are independently mapped into M-ary PSK symbols $\{\mathbf{a}_k\}_{k=1}^{n_T}$, where

$$\mathbf{A} = f(\tilde{\mathbf{C}}) \tag{4.3}$$

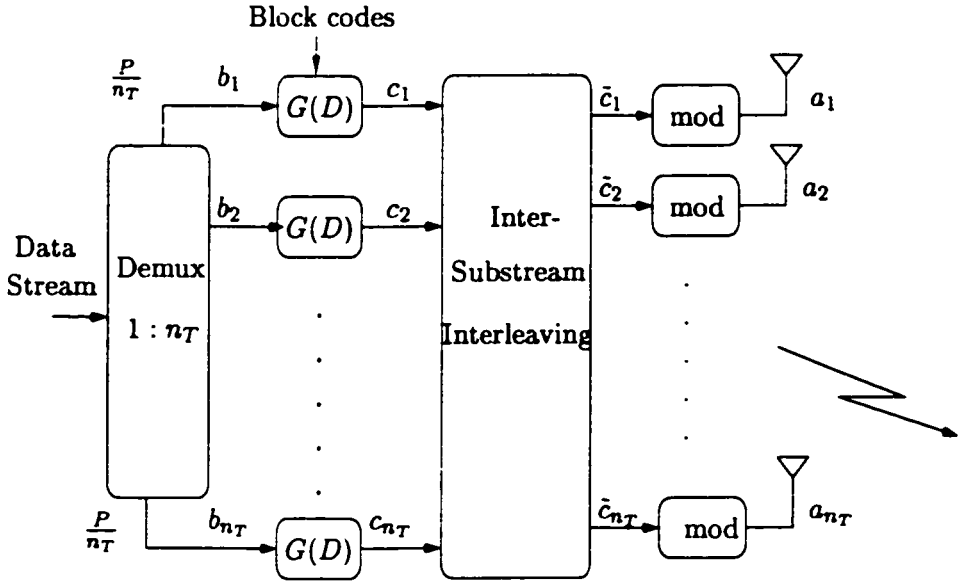

Figure 4.1: T-BLAST transmitter

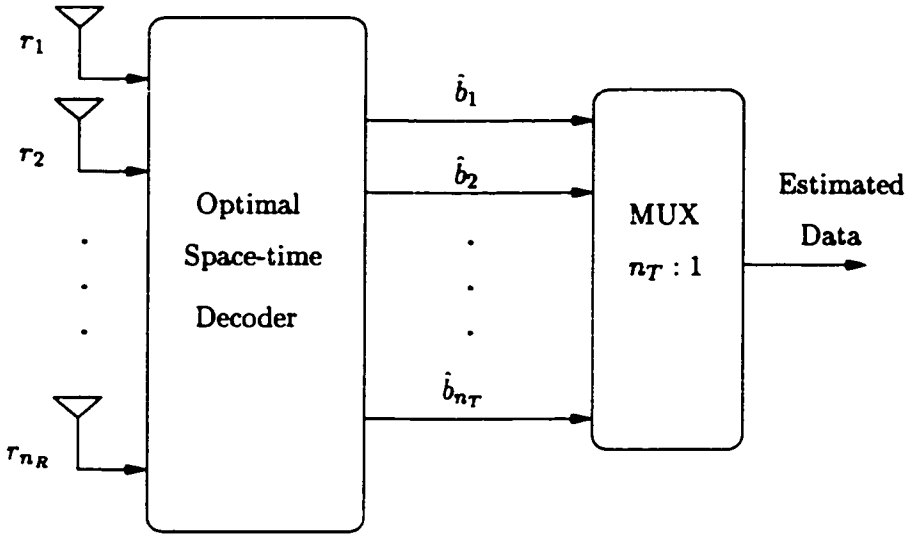

Figure 4.2: Receiving end

4.2 Random Space-Time Block (RSTB) Codes

The combined use of block codes and interleaving provides the basis for the *random block codes*, namely, parallel and serially concatenated turbo codes. Using this principle, for MTMR systems, we propose turbo space-time codes by concatenating block codes and space-time interleavers.

The random space-time coding is composed of two parts:

(1) independent forward error-correction (FEC) encoding of substreams using 1-D block codes, and

(2) inter-substream permutation of independently coded substreams using space-time interleavers that are designed off-line. Note that, the block size of the RSTB code is determined by the size of the interleaver.

For random space-time code design we consider only probabilistic block codes, which rely on a probabilistic (soft-in/soft-out) method for their decoding at the receiver. The reasons for the use of soft-in/soft out decoding are:

- A power gain of 2-2.5dB can be achieved by using the soft- decision decoding as compared to hard-decision decoding for rate 1/2 codes [85]. Here, we recall an important principle of information theory, which states: *preserve the information learned from the receiver until the very end where estimation of the transmitted symbols is made.*

- We derive a near optimal space-time iterative decoder (similar to turbo decoders) for the proposed random space-time codes.

The codes that can be considered for the RSTB code design are block-based convolutional or recursive systematic convolutional (RSC) codes, turbo codes, or low-density parity-check codes. Note that this new scheme does not necessarily use traditional turbo encoding. Rather, it uses fundamental ideas in turbo decoders to decode the proposed random space-time coding in a near-optimal way and with low complexity. Hence we call the new random space-time code a "turbo space-time code" and the MTMR wireless system that uses it "Turbo-BLAST".

4.2.1 Space-Time Interleaving

Random Space-Time Interleavers

We propose two types of random space-time interleaving schemes for the T-BLAST architecture:

- a random inter-substream interleaving of size $n_T \times L$.

- space-time interleaving made up of two stages:

  - Stage 1: time-interleaving using n_T different and independent random permuters of size L

  - Stage 2: space-interleaving using L different and independent random permuters of size n_T, and vice versa.

Diagonal Layered Space-Interleavers

The space interleaving proposed in T-BLAST is used for spatial cycling of each substream over all possible sub-channels. A deterministic space-interleaver based on diagonal layering of each independently coded substream is shown in the Figure 4.3. The interleaving procedure is simply a permutation operation over the L columns according to the interleaver. Note that unlike D-BLAST, we do not experience any boundary waste in this diagonal layering structure. The benefits of T-BLAST using diagonal space-time interleavers include the following:

- Diagonal layering space interleaving guarantees the equal use of each sub-channel by each independently coded substream,
- Each substream can be coded using 1-D code blocks of equal rates.

Without explicit knowledge of the channel matrix at the transmitter end, this may be the best we can achieve for any set of sub-channels.

C_1	C_6	C_5	C_4	C_3	C_2	C_1	C_6	C_5	C_4	C_3
C_2	C_1	C_6	C_5	C_4	C_3	C_2	C_1	C_6	C_5	C_4
C_3	C_2	C_1	C_6	C_5	C_4	C_3	C_2	C_1	C_6	C_5
C_4	C_3	C_2	C_1	C_6	C_5	C_4	C_3	C_2	C_1	C_6
C_5	C_4	C_3	C_2	C_1	C_6	C_5	C_4	C_3	C_2	C_1
C_6	C_5	C_4	C_3	C_2	C_1	C_6	C_5	C_4	C_3	C_2

Figure 4.3: Diagonal interleaver.

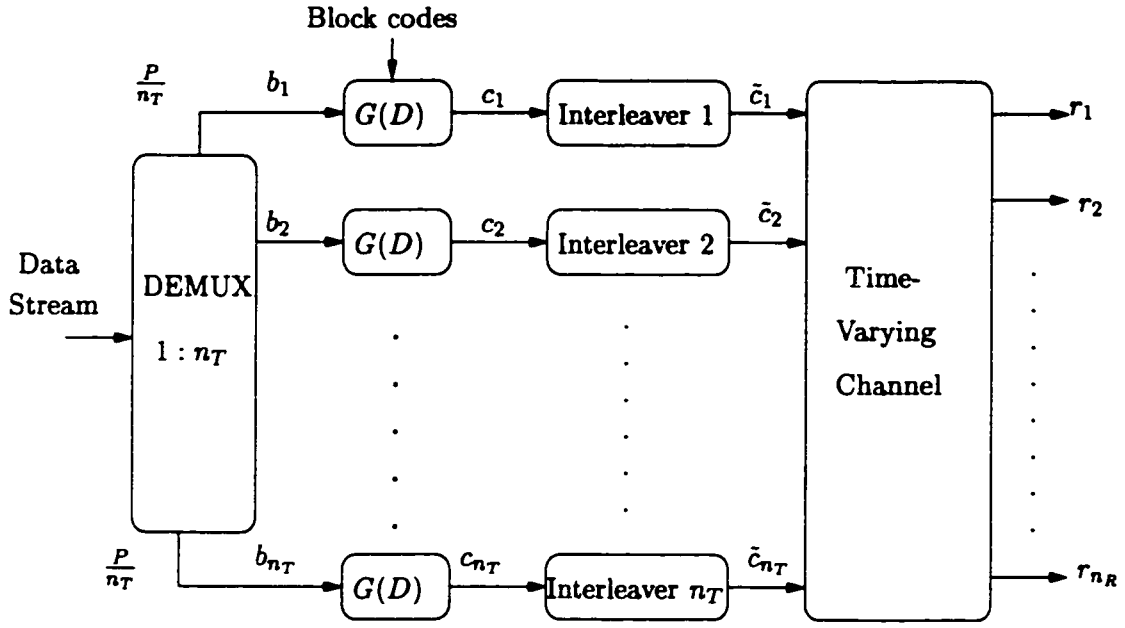

Figure 4.4: T-BLAST transmitter and intentional time-varying channel.

4.2.2 Intentional Time-Varying Channel

Figure 4.4 illustrates another view of the proposed random space-time block codes. In this representation, we include the effect of diagonal-interleaving with the quasi-static Rayleigh matrix channel. The combination of diagonal-interleaving and the quasi-static Rayleigh matrix channel introduces an "intentional" time-varying/selective channel.

In Figures 4.5 and 4.6, we show the artificially generated time-varying channel process using diagonal-interleaving. Figure 4.5 illustrates the original subchannels that connect the n_T transmitters with n_R receivers. The channel is generated for a (16,16)-BLAST system; note that each subchannel is static within the packet of interest. In Figure 4.6, we show the time-varying subchannels generated by the inter-substream interleaving process. Only three subchannels (out of 16) are shown here for simplicity.

The artificial time-varying process is generated by cycling the underlying independent channels; for sufficiently large number of transmitters, a highly time-varying channel can be achieved even in delay-limited and non-ergodic systems. Moreover, the time averages

of each independent channels in Figure 4.6 will approach their corresponding ensemble averages in the limit as the observation interval T and the number of transmit antennas n_T approach infinity; thus the space-time interleaver generates an artificial ergodic process from the non-ergodic quasi-static Rayleigh fading MTMR channels. Note that in Figure 4.5, each subchannel is non-ergodic since it does not change with time.

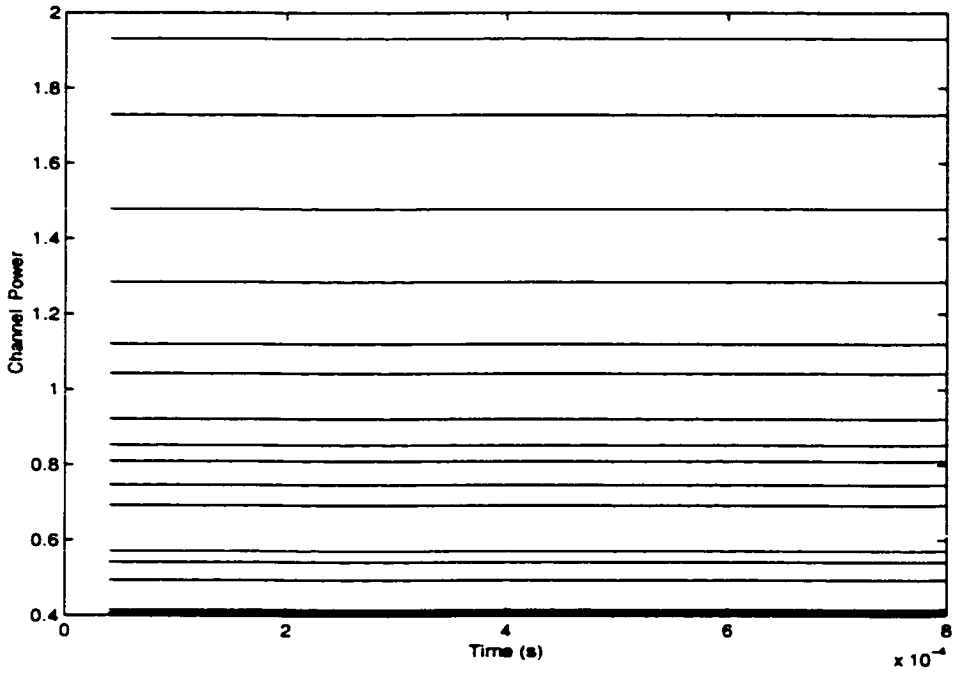

Figure 4.5: Channel response before interleaving.

4.3 Optimal Detection

With no delay spread, the discrete-time model of the received signal is given by:

$$\mathbf{R} = \sqrt{\frac{\rho}{n_T}}\tilde{\mathbf{H}}\mathbf{A} + \mathbf{V} \tag{4.4}$$

where $\tilde{\mathbf{H}} \in \mathcal{C}^{n_R \times n_T}$ is is the known intentional time varying channel. $\mathbf{A} \in \mathcal{C}^{n_T \times L}$ is the transmitted information, $\mathbf{R} \in \mathcal{C}^{n_R \times L}$ is the received signal, $\mathbf{V} \in \mathcal{C}^{n_R \times L}$ is Gaussian noise, and the SNR received at each receiving antenna is ρ. The components of the noise vector

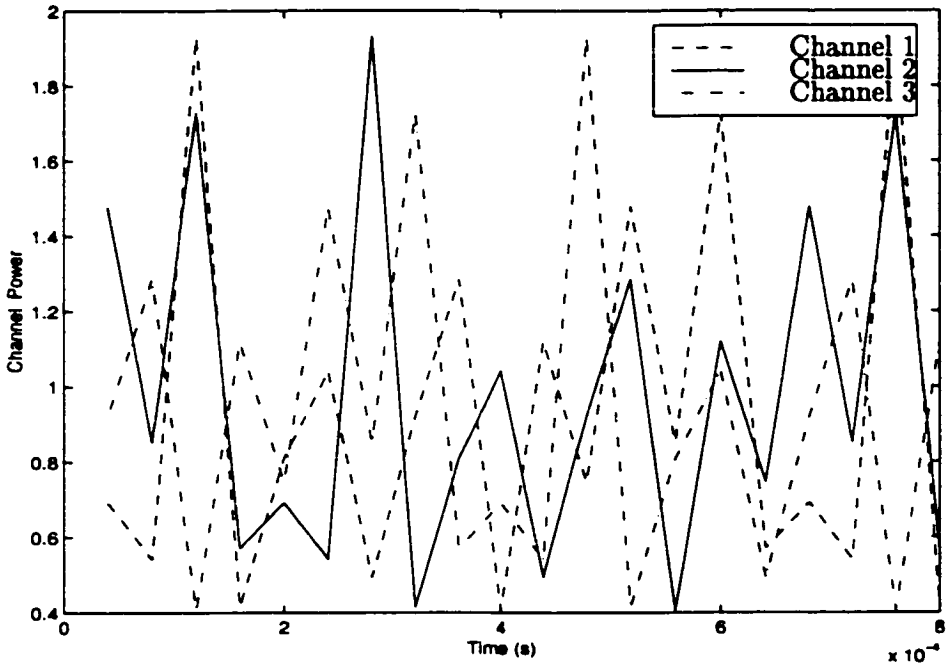

Figure 4.6: Channel response after interleaving.

are uncorrelated zero-mean complex white Gaussian random variables with zero mean and variance σ^2.

4.3.1 Optimal Decoding with No Interleavers

The optimal receiver performs an exhaustive search to determine $\mathbf{A}$ from the received signal $\mathbf{R}$:

$$\hat{\mathbf{A}} = \arg\min_{\mathbf{A}} \left\| \mathbf{R} - \sqrt{\frac{\rho}{n_T}} \tilde{\mathbf{H}} \mathbf{A} \right\|^2 \tag{4.5}$$

It is easy to see that the computational complexity of this search increases exponentially with the number of transmit antennas, n_T, and the number of information bits in the modulation and the block size L.

4.3.2 Optimal Decoding of RSTB Codes

In theory, it is possible to model the proposed RSTB code as a single Markov process, and a trellis can be formed to include the effect of interleaving. Such a trellis representation is extremely complex and does not lend itself to feasible decoding algorithms [78].

4.4 Asymptotic Performance Analysis of RSTB Codes

For simplicity, we consider an (n, n) system. We assume that we use the same 1-D linear block codes with minimum distance $d_{\min}$ to encode each substream separately. In the case of convolutional codes, $d_{\min}$ will be the free distance d_{free}. Define the noiseless input to the receiver as:

$$\mathbf{S}(\mathbf{A}) = \sqrt{\frac{P}{n}}\tilde{\mathbf{H}}\mathbf{A} \tag{4.6}$$

The asymptotic probability of error[1] is determined by the minimum Euclidean distance between any pair of information sequences $\mathbf{A}$ and $\tilde{\mathbf{A}}$ is given by [98] (see Appendix 4A, Lemma 4A.1)

$$\lim_{\sigma^2 \to 0} P(E) = Q\left(\sqrt{\frac{d^2_{ST,\min}}{\sigma^2}}\right) \tag{4.7}$$

where the minimum distance of the RSTB code is defined as:

$$d^2_{ST,\min}(\mathbf{A}, \tilde{\mathbf{A}}) \;=\; \min_{\mathbf{A},\tilde{\mathbf{A}}} \left\| \frac{\mathbf{S}(\mathbf{A}) - \mathbf{S}(\tilde{\mathbf{A}})}{2} \right\|^2 \tag{4.8}$$

and the Q function is given by

$$Q(x) = \frac{1}{\sqrt{2\pi}} \int_x^\infty e^{-t^2/2} dt, \quad x \geq 0 \tag{4.9}$$

[1] The limit of the probability of error as the receiver AWGN goes to zero

■

The bounds of the probability of error $P(E)$ is $0 \leq P(E) \leq 1/2$. The upper bound is achieved either the minimum distance $d_{ST} \to 0$ or the noise variance $\sigma^2 \to \infty$. The lower bound is achieved either the minimum distance becomes large ($d_{ST} \to d_{ST,\min}$) or the noise variance $\sigma^2 \to 0$.

From Lemma 4A.2 (see Appendix 4A), the minimum distance of the RSTB code is equivalent to

$$d^2_{ST,\min}(\mathbf{A}, \tilde{\mathbf{A}}) = \min_{\mathbf{e}\neq\mathbf{0}} \sum_{l=1}^{L} \mathbf{e}(l)^T \Delta \mathbf{e}(l) \tag{4.10}$$

where $\mathbf{e}(l) \in \{-1, 0, +1\}^n$ is the error vector defined as $\frac{\mathbf{a}_l - \tilde{\mathbf{a}}_l}{2}$, where $\mathbf{a}_l$ is lth column of matrix $\mathbf{A}$, and the channel cross-correlation matrix Δ is

$$\Delta = \begin{bmatrix} 1 & \delta_{1,2} & \dots & \delta_{1,n} \\ \delta_{2,1} & 1 & \dots & \delta_{2,n} \\ \vdots & \vdots & \ddots & \vdots \\ \delta_{n,1} & \delta_{n,2} & \dots & 1 \end{bmatrix}, \qquad \delta_{i,j} < 1, \forall i, j \tag{4.11}$$

In the sequel, we show that the minimum distance properties of the RSTB code can be made equal to $d_{\min}$ by using random interleavers. The decision distance d^2_{ST} of RST codes simplifies to (see Appendix 4A, Lemma 4A.2):

$$\begin{aligned} d^2_{ST} &= \sum_{l=1}^{L} \mathbf{e}(l)^T \Delta \mathbf{e}(l) \\ &= \sum_{l=1}^{L} \left\{ \sum_{j=1}^{n} \mathbf{e}_j^2(l) + 2 \sum_{i<j} \delta_{ij} \mathbf{e}_i(l) \mathbf{e}_j(l) \right\} \end{aligned} \tag{4.12}$$

Note, if $n = 1$ then the minimum distance is $d_{ST,\min} = d_{\min}$. However, for $n > 1$, it is not trivial to preserve the minimum distance without interleaving. From the channel cross-correlation matrix Δ, we have $\delta_{ij} < 1$ for $i \neq j, \forall i, j$. Consequently, the lower bound on the

minimum distance of ST becomes:

$$d_{ST}^2 > \sum_{l=1}^{L} \left\{ \sum_{j=1}^{n} \mathbf{e}_j^2(l) - 2 \sum_{i<j} |\mathbf{e}_i(l)| \, |\mathbf{e}_j(l)| \right\} \tag{4.13}$$

When only ν substreams are having non-zero error events of weight $d_{\min}$ among the n possible substreams, (4.13) reduces to

$$d_{ST}^2 > \sum_{l=1}^{L} \left\{ \sum_{j=1}^{\nu} \mathbf{e}_j^2(l) - 2 \sum_{i<j} |\mathbf{e}_i(l)| \, |\mathbf{e}_j(l)| \right\} \tag{4.14}$$

Proposition 1 *The minimum distance property of the RSTB code will be lower bounded by zero if no interleaving is used. Moreover, this lower bound is achieved when there is an even number of non-zero error events occurring in the RSTB code. In this case, if pairs of error events* $\mathbf{e}(l)$ *can be aligned in time such that they are the negative of another, then the minimum distance of the RSTB code can be made zero. This is because the negative of any codeword difference is a permissible codeword difference, which is the property of linear block codes.* ■

Proposition 2 With interleaving: *Consider the time-interleaving operation before the space-interleaving so that we can include the space-interleaving with the channel matrix to get intentional time-varying channel. In this case, we can align an error event with another, only at one bit intervals, by independent random time-interleaving of each substream separately. The probability of more bits aligned is a function dependent on the length of the interleavers. For random interleaving, we have the following:*

$$\begin{aligned} P\{\, |\mathbf{e}_j(l)| = 1\} &= \frac{d_{\min}}{L} \\ P\{\, |\mathbf{e}_j(l)| = 0\} &= 1 - \frac{d_{\min}}{L} \end{aligned} \tag{4.15}$$

and the expectation of the minimum distance of RSTB code is given as

$$\mathcal{E}\{d^2_{ST,\min}\} > \sum_{l=1}^{L}\left\{\sum_{j=1}^{\nu}\mathbf{e}_j^2(l) - n(n-1)\frac{d^2_{\min}}{L^2}\right\} - 2\nu \tag{4.16}$$

$$= \nu d_{\min} - n(n-1)\frac{d^2_{\min}}{L} - 2\nu$$

where $\nu > 0$ represents the ability to align ν bits of ν substreams errors.
To achieve the minimum decision distance $d_{\min}$ of 1-D linear block codes, we should have $\mathcal{E}\{d^2_{ST,\min}\} > d_{\min}$. Given that the length of the interleaving must be

$$L > \frac{n(n-1)d^2_{\min}}{(\nu-1)d_{\min} - 2\nu}, \tag{4.17}$$

the minimum of this condition is achieved for $\nu = 2$ and $d_{\min} > 4$. Therefore, a sufficient condition to preserve the minimum distance property of the RSTB code is

$$L > n(n-1)d^2_{\min} \tag{4.18}$$

and $d_{\min} > 4$. ■

This means that, with sufficient space-time interleaving, the minimum distance property of 1-D channel codes can be preserved in multi-transmit multi-receive antenna schemes. By using interleaving and ML decoding, the asymptotic error performance of an MTMR scheme can be made equivalent to that of a single transmit antenna scheme. A similar analysis can be found in [78] for an CDMA multiuser detection using iterative decoders in AWGN channel. The space interleaving in RSTB code provides additional freedom for the interleaving depth as well as time-selective fading for each decoder to achieve the optimal performance on each substream.

4.5 Capacity of Correlated Channels

The above analysis shows that the proposed random space-time code achieves optimal performance even in a highly correlated environment. The capacity of MTMR schemes strongly depends on the cross-correlation between the subchannels. However, finding an explicit closed-form expression of the channel capacity as a function of the channel correlation is rather difficult in general. To simplify matters, we consider an $n \times n$ channel matrix with the symmetric cross-correlation matrix, so called n-symmetric channel [77]:

$$\Delta = \begin{bmatrix} 1 & \delta & \dots & \delta \\ \delta & 1 & \dots & \delta \\ \vdots & \vdots & \ddots & \vdots \\ \delta & \delta & \dots & 1 \end{bmatrix}, \qquad \frac{-1}{n-1} < \delta < 1, \forall i, j \tag{4.19}$$

and a channel gain matrix of $\mathbf{W}^{1/2} = \sqrt{n}\mathbf{I}_n$.

Theorem 1 *The capacity of a n-symmetric channel is given by*

$$C = n \log_2 (1 + \rho(1-\delta)) + \log_2 \left(1 + \frac{n\rho\delta}{1+\rho(1-\delta)}\right) \tag{4.20}$$

■

Proof

The capacity of MTMR scheme is defined as

$$C = \log_2 \det \left(\mathbf{I}_n + \frac{\rho}{n}\mathbf{W}^{1/2}\Delta\mathbf{W}^{1/2}\right) \tag{4.21}$$

By substituting $\mathbf{W}^{1/2} = \sqrt{n}\mathbf{I}_n$, we get

$$\begin{aligned} C &= \log_2 \det (\mathbf{I}_n + \rho\Delta) \\ &= \log_2 E \end{aligned} \tag{4.22}$$

The determinant of E is given by (see Lemma 4A.3, Appendix 4A)

$$\det(E) = \left[(1+\rho(1-\delta))^n \cdot \left(1+\frac{n\rho\delta}{1+\rho(1-\delta)}\right)\right] \tag{4.23}$$

Hence the capacity reduces to

$$\begin{aligned} C &= \log_2\left[(1+\rho(1-\delta))^n \cdot \left(1+\frac{n\rho\delta}{1+\rho(1-\delta)}\right)\right] \\ &= n\log_2(1+\rho(1-\delta)) + \log_2\left(1+\frac{n\rho\delta}{1+\rho(1-\delta)}\right) \end{aligned} \tag{4.24}$$

■

Equation (4.24) demonstrates the explicit dependence of channel capacity on channel correlation.

Remark 6 *This result also confirms some of the claims made in [39].*

- *In the limit of* $\delta \to 0$,

$$C = n\log_2(1+\rho) \tag{4.25}$$

  That is, the capacity scales linearly with the number of transmit antennas. In this case, we have orthogonal parallel channels.

- *In the limit of* $\delta \to 1$, *that is, in a highly correlated environment,*

$$C = \log_2(1+n\rho) \tag{4.26}$$

- *For* $n = 2$, *the capacity reduces to [99]:*

$$C = \log_2\left(1+2\rho+(1-\delta^2)\rho^2\right) \tag{4.27}$$

Example 1 *Figure 4.7 illustrates the BLAST channel capacity against the channel correlation coefficient for $\rho = 30dB$ and for the number of transmit and receive antennas $n = 2, 4, 8$ and 16. For $n = 4$, Figure 4.8 shows the BLAST channel capacity against the channel correlation coefficient for $\rho = 20dB$ and $\rho = 30dB$. These two figures explain how the channel capacity of an MTMR scheme changes with the correlation parameter. In a highly varying environment, the capacity of the system varies drastically. The channel coding rate must be constantly adapted to reach the capacity limits [100]. With such a scheme, the system does not waste spectral resources under any channel conditions.*

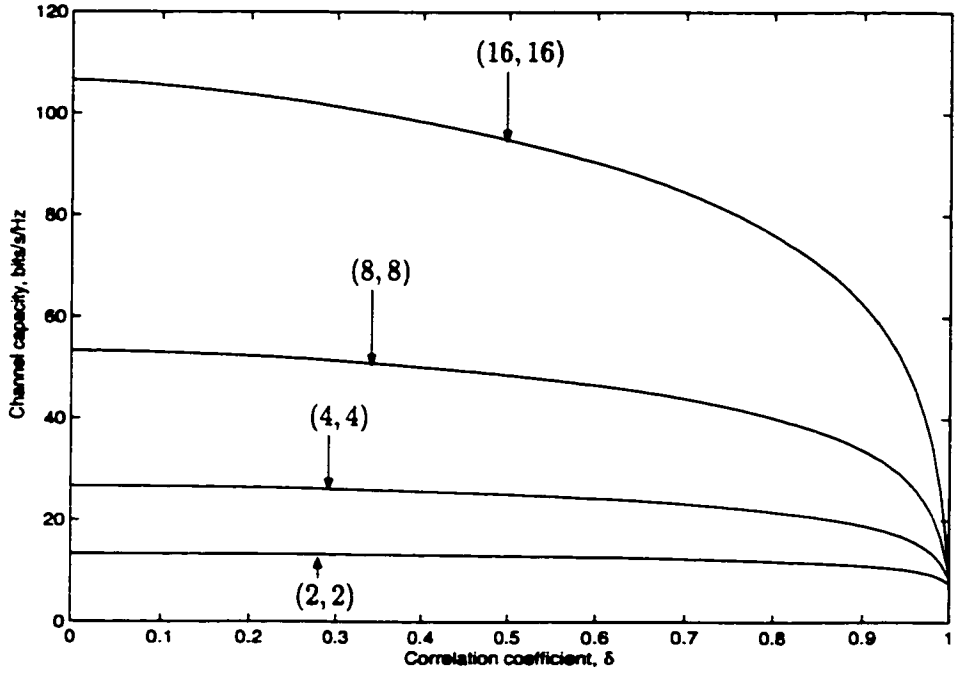

Figure 4.7: Channel capacity vs correlation coefficient for n=2,4,8 and 16 at SNR = 30dB

4.6 Iterative Decoders

In the previous section, we have shown that the proposed RSTB codes can decouple the parallel antenna substreams. However, the optimum detection of these codes is not practical. This section proposes a practical sub-optimum detection scheme based on iterative "turbo"

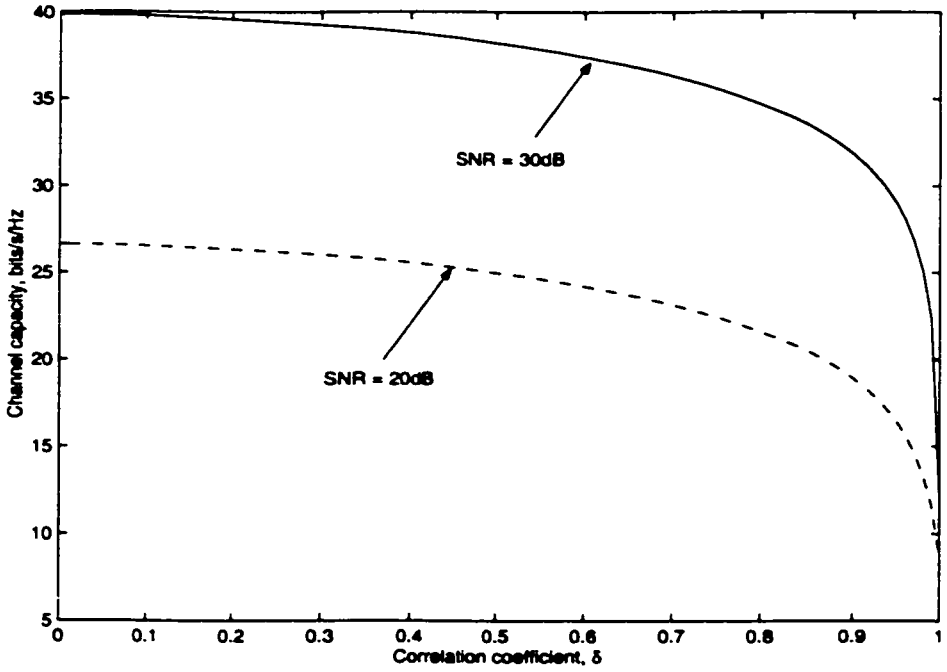

Figure 4.8: Channel capacity vs correlation coefficient for (4,4) system at SNR =20dB and 30dB

detection principles. The inter-substream coding proposed as independent encoding and space-time interleaving can be viewed as a serially concatenated code as illustrated in Figure 4.9:

- Inner code: n_T parallel channel codes
- Outer code: time-varying matrix channel

The inner and outer codes are separated by n_T parallel interleavers. The concatenated code can be decoded using a lower complexity iterative receiver similar to the iterative schemes proposed for serially concatenated turbo codes.

In the iterative decoding scheme, we separate the optimal decoding problem into two stages and exchange all information learned from one stage to another iteratively until the receiver converges. The two decoding stages are:

- *Inner decoder:* SISO detector

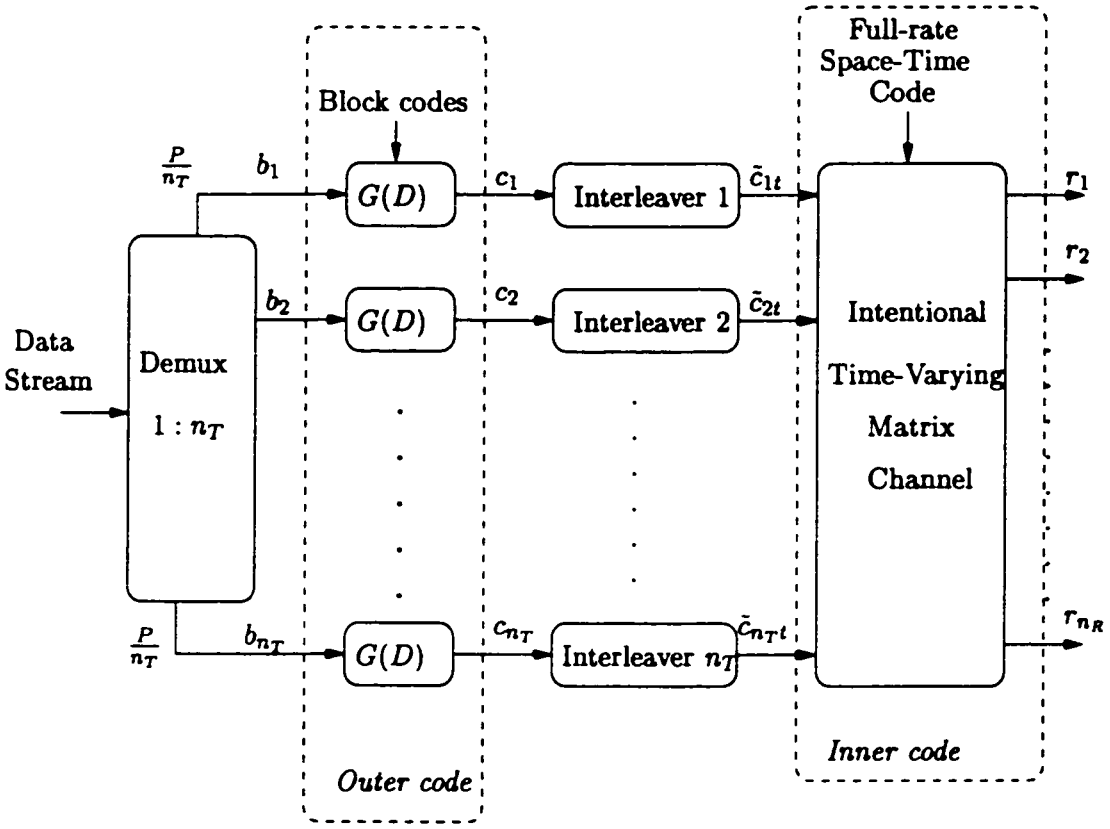

Figure 4.9: The RSTB codes as serially concatenated codes.

- *Outer decoders:* A set of n_T parallel soft-input/ soft-output (SISO) channel decoders.

The detector and decoder stages are separated by space-time interleavers and de-interleavers. The interleavers and de-interleavers are used to compensate for the interleaving operation used in the transmitter as well as to decorrelate the correlated outputs before feeding them to the next decoding stage. The iterative receiver produces new and better estimates at each iteration and repeats the information exchange process a number of times to improve the decisions. Note that the design of our inter-substream coding uses independent coding of each substream; hence the receiver needs to select only one of 2^L sequences for each n_T sequence separately without increasing the probability of symbol error significantly. The iterative decoder is shown in Figure 4.10.

Remark 7 *Recently several versions of modified turbo codes for MTMR schemes with two transmit antennas, based on parallel concatenated turbo codes, have been proposed in the literature [102] -[111], namely, space-time turbo codes. The space-time turbo codes proposed in [102]-[108] can be classified into three classes as shown in Figures 4.13-4.12. In the first class (Figure 4.13), the outputs of a turbo code are transmitted using multiple antennas. In the second class, (Figure 4.11), the outputs of a turbo code are bit interleaved and mapped to QPSK symbols and transmitted using multiple transmit antennas. In the third class, (Figure 4.12), the transmitter is composed of a turbo encoder followed by the operations of puncturing[2] channel interleaving, and multiplexing. Multiple transmit antennas are used to transmit the output of the multiplexer. However, the generalization of these algorithms for more than two transmit antennas is not obvious.*

Moreover, serial concatenated space-time codes and iterative decoders have also been proposed in [109]-[111]. These are based on the low-rate space-time block codes and trellis codes. Typically, the space-time block codes are concatenated with 1-D channel codes such as convolutional and Reed-Soloman codes, to achieve the coding gain. One criticism of these techniques is that they have low information rates; thus they do not attain the full channel capacity.

[2]Deleting certain parity check bits, thereby increasing the data rate.

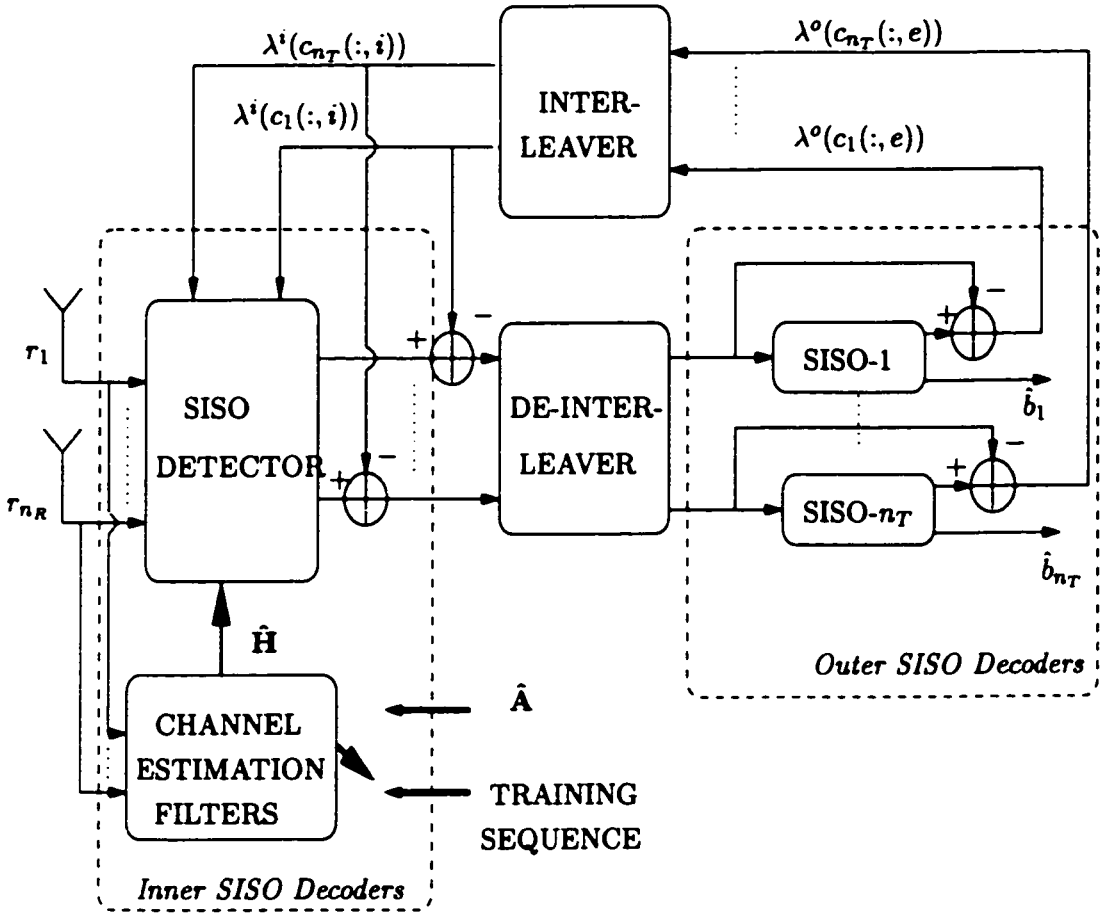

Figure 4.10: Iterative decoder

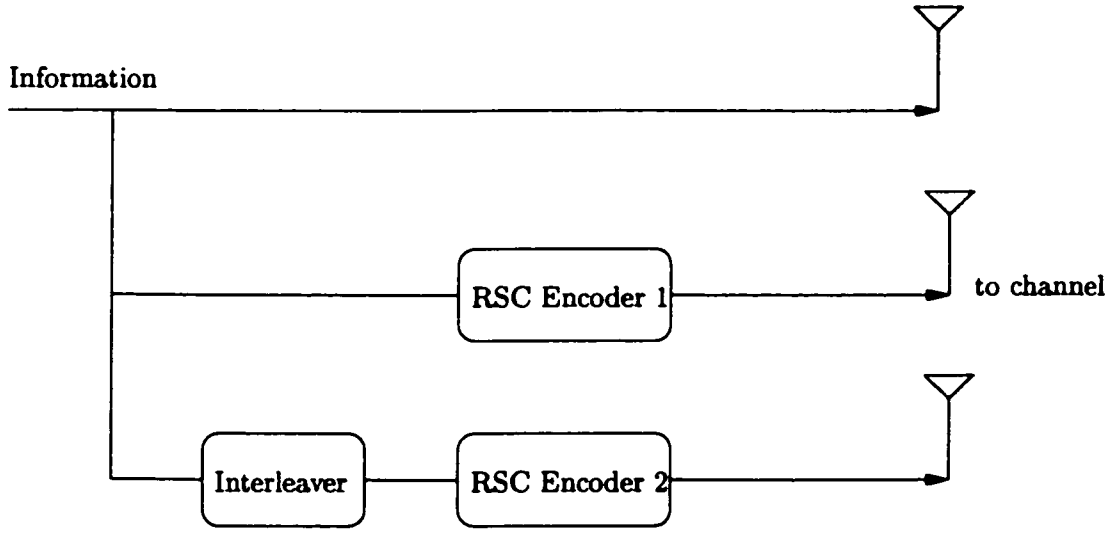

Figure 4.11: Space-time turbo encoder 1.

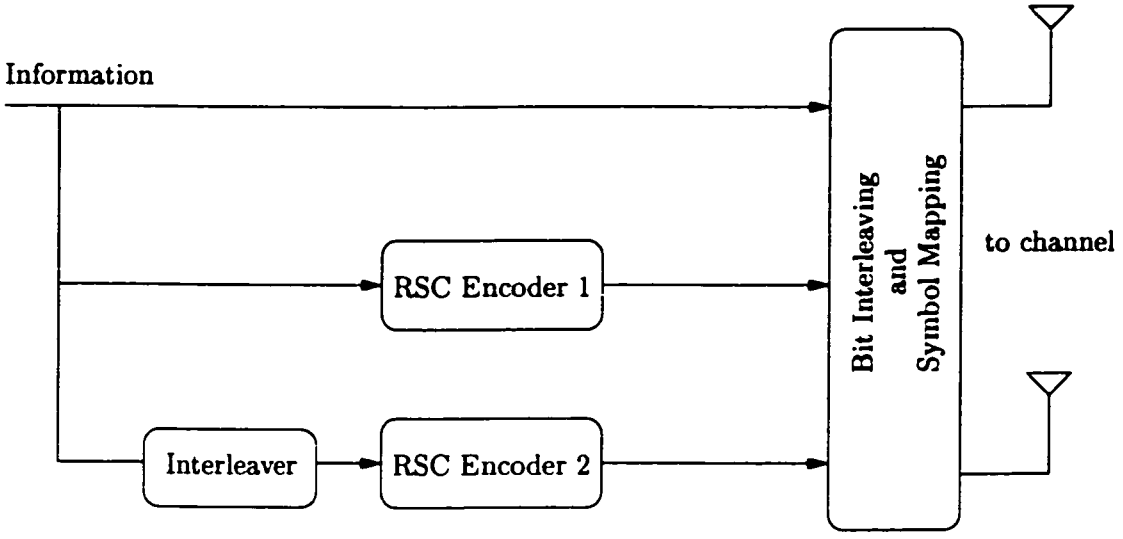

Figure 4.12: Space-time turbo encoder 2.

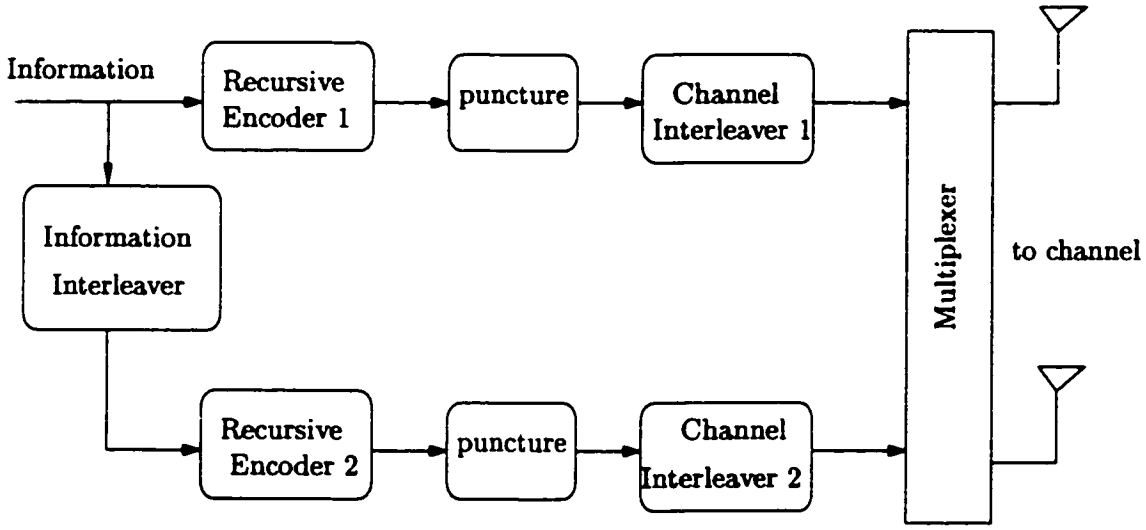

Figure 4.13: Space-time turbo encoder 1.

4.6.1 Iterative Decoding Algorithm

In this section, we describe the iterative decoding scheme of T-BLAST. From Section 3.2 of Chapter 3 we recall that the iterative decoding structure of serially concatenated turbo codes provides the principal model for this iterative decoder. Specifically, we use the following notations to explain the iterative decoders of serially concatenated turbo codes: the log-likelihood ratio (LLR) λ^i and λ^o, with superscripts i and o denote the LLR associated with the inner decoder and the outer decoder of the decoding process, respectively. The symbols $\lambda(:,i)$, $\lambda(:,e)$ and $\lambda(:,p)$ at the output and input of the SISO modules refer to *intrinsic*, *extrinsic* and *a posteriori* information formulated as log-likelihood ratios.

First, we define the *a posteriori* log-likelihood ratio (LLR) of a transmitted bit symbol for a BPSK modulated symbol $c_j(l)$, $j = 1, 2, \ldots n_T$ and $l = 1, 2, \ldots, L$:

$$\lambda(c_j(l); p) = \log \frac{P\{c_j(l) = +1|\mathbf{r}\}}{P\{c_j(l) = -1|\mathbf{r}\}} \tag{4.28}$$

Using Bayes' rule, (4.28) can be rewritten as

$$\lambda(c_j(l);p) = \log\frac{P\{\mathbf{r}(t)|c_j(l)=+1\}}{P\{\mathbf{r}(t)|c_j(l)=-1\}} + \log\frac{P\{c_j(l)=+1\}}{P\{c_j(l)=-1\}} \tag{4.29}$$

$$= \lambda(c_j(l);e) + \lambda(c_j(l);i)$$

The first term $\lambda(c_j(l);e)$ in (4.29) constitutes *extrinsic* information, and the second term denoted by $\lambda(c_j(l);i)$ constitutes *a priori/intrinsic* information of the code bit $c_j(l)$.

The iterative decoder, illustrated in Figure 4.10, depicts message passing between the inner/detector and outer/decoder SISO modules:

1. The SISO detector (inner SISO module) generates a soft estimate of the code/transmitted bits $c_j(l)$ conditional on the received signal $\mathbf{r}(t)$, and the *a priori* information about all the code/transmitted bits $c_k(l), \forall k, k \neq j$ and $c_j(t), \forall t, t \neq l$. Note that the soft information of $c_j(l)$ as computed by the SISO detector is influenced by the *a priori* information of $\lambda(c_j(l);i)$ from the previous stage (SISO decoders):

   - Estimate the *a posteriori information*

$$\lambda^i(c_j(l);p) = \log\frac{P\{c_j(l)=+1|\mathbf{r},\lambda^i(\mathbf{C};i)\}}{P\{c_j(l)=-1|\mathbf{r},\lambda^i(\mathbf{C};i)\}} \tag{4.30}$$

$$j = 1,2,\ldots n_T, l = 1,2,\ldots,L$$

     During the first iteration, the initial *a priori* probabilities of all symbol bits are assumed to be 1/2 (i.e., equally likely). Thus, $\lambda(\mathbf{c}_j(l);i) = 0, \quad \forall j,l.$

   - Compute the extrinsic information

$$\lambda^i(\mathbf{C};e) = \lambda^i(\mathbf{C};p) - \lambda^i(\mathbf{C};i) \tag{4.31}$$

     where $\lambda^i(\mathbf{C};e)$ is the extrinsic information about the set of code/transmitted

bits $\mathbf{C}$ of the SISO detector and fed back to the outer decoder as the intrinsic information of its coded bits. Before application to the outer decoder, the extrinsic information is reordered to compensate for the pseudo-random interleaving introduced in the turbo encoder:

$$\lambda^o(\mathbf{C};i) = \Pi^{-1}\{\lambda^i(\mathbf{C};e)\} \tag{4.32}$$

2. The n_T outer SISO modules, in turn, process the soft information $\lambda^o(\mathbf{c}_j(l);i)$, and compute refined estimates of soft information of both code $\mathbf{c}_j(l)$, information symbols $\mathbf{b}_j(l)$, and based on the trellis structure of the channel codes, which is the channel code constraint:

   - The *a posteriori information* for information and code symbols is, respectively,

$$\lambda^o(b_j(l);p) = \log\frac{P\{b_j(l)=+1|\lambda^o(\mathbf{C};i),\lambda^o(\mathbf{B};i),decoding\}}{P\{b_j(l)=-1|\lambda^o(\mathbf{C};i),\lambda^o(\mathbf{B};i),decoding\}} \tag{4.33}$$

$$j = 1,2,\ldots n_T, l = 1,2,\ldots,L$$

$$\lambda^o(c_j(l);p) = \log\frac{P\{c_j(l)=+1|\lambda^o(\mathbf{C};i),\lambda^o(\mathbf{B};i),decoding\}}{P\{c_j(l)=-1|\lambda^o(\mathbf{C};i),\lambda^o(\mathbf{B};i),decoding\}} \tag{4.34}$$

$$j = 1,2,\ldots n_T, l = 1,2,\ldots,L$$

   The input $\lambda^o(\mathbf{B},i)$ is always initialized to zero, assuming equally likely source information symbols.

   - Extrinsic information of information and code symbols is, respectively,

$$\lambda^o(\mathbf{B};e) = \lambda^o(\mathbf{B};p) - \lambda^o(\mathbf{B};i) \tag{4.35}$$

$$\lambda^o(\mathbf{C};e) = \lambda^o(\mathbf{C};p) - \lambda^o(\mathbf{C};i) \tag{4.36}$$

The output, that is, the *extrinsic* information of the n_T outer decoders provides *intrinsic* information to the inner/detector SISO module after reordering to compensate for the random interleaving.

$$\lambda^i(\mathbf{C};i) = \Pi\{\lambda^o(\mathbf{C};e)\} \tag{4.37}$$

Steps 1 and 2 are repeated until the algorithm converges.

3. Estimate of the message bits $\mathbf{B}$ is obtained by hard limiting the LLR $\lambda^o(\mathbf{B};p)$ at the output of the outer decoder:

$$\hat{\mathbf{B}} = \text{sgn}\{\lambda^o(\mathbf{B};p)\} \tag{4.38}$$

Remark 8 *Note that the outer decoder of the iterative algorithm is made up of n_T parallel SISO channel decoders implemented by using the generalized BCJR algorithm. A detailed explanation of the generalized BCJR algorithm was presented in Chapter 3, Section 3.3. The following section describes the design of inner SISO decoders/ SISO detectors.*

4.7 Design and Performance of Soft in/Soft out Detectors

An issue of interest is the criterion used to optimize the inner/detector SISO module in the iterative decoders. In this section, we design the inner/detector SISO module using the following:

- maximum *a posteriori* (MAP) probability estimation,
- mean-square error minimization (MMSE), and
- parallel soft-interference cancellation (PSIC).

4.7.1 Performance Lower Bound

Consider a system that is equivalent to each of n_T transmitted signals received by a separate set of n_R antennas in such a way that each signal component is received with no interference from the others. Each transmitted signal can be viewed as a $(1, n_R)$-BLAST signal with transmit power P/n_T, where P is the total transmitted power of the (n_T, n_R)- BLAST scheme. Let the ratio $P/\sigma^2 = \rho$ denote the total transmitted SNR. The total average received SNR of the kth information bit is

$$\begin{aligned} \bar{\rho} &= \frac{\rho}{n_T}\mathcal{E}[\|\mathbf{h}_k\|^2] \\ &= \rho\frac{n_R}{n_T} \end{aligned} \tag{4.39}$$

since $\mathcal{E}[\|\mathbf{h}_k\|^2] = n_R$.

This system can also be viewed as (1,1)-BLAST scheme with average received SNR=$\bar{\rho}$. Hence, we may express the probability of error in terms of the average SNR per bit for a single transmit-receive antenna system. The bit error rate (BER) performance of a single transmit-receive antenna system with average received SNR=$\bar{\rho}$ for uncoded BPSK in a fixed and known fading environment is given by [30]

$$\text{BER} = Q(\sqrt{2\bar{\rho}}) \tag{4.40}$$

Since we use a soft decoding scheme in the receiver, we have an additional coding gain of $10\log_{10}(R_c d_{\min})$ in calculating the lower bound for the BER, where R_c and $d_{\min}$ are the code rate and free distance of the FEC, respectively. Note, for convolutional codes, d_{free} will be used. This is a lower bound on BER performance of a T-BLAST scheme. ■

4.7.2 Detector based on Maximum *a posteriori* Probability Estimation

To derive a simplified optimum receiver, we maximize the *a posteriori* metric of individual substreams separately. The received signal $\mathbf{r}(i) \in \mathcal{C}^{n_R \times 1}$ at the receive array at time i is

$$\mathbf{r}(i) = \mathbf{H}(i)\mathbf{a}(i) + \mathbf{v}(i) \tag{4.41}$$

where $\mathbf{H}(i) \in \mathcal{C}^{n_R \times n_T}$, $\mathbf{a}(i) \in \mathcal{C}^{n_T \times 1}$ and $\mathbf{v}(i) = \in \mathcal{C}^{n_R \times 1}$. Let $a_k(i)$ be the desired signal

$$\mathbf{r}(i) = \mathbf{h}_k(i)a_k(i) + \mathbf{H}_k(i)\mathbf{a}_k(i) + \mathbf{v}(i) \tag{4.42}$$

where $\mathbf{H}_k(i) = [\mathbf{h}_1(i), \mathbf{h}_2(i), \ldots, \mathbf{h}_{k-1}(i), \mathbf{h}_{k+1}(i), \ldots, \mathbf{h}_n(i)] \in \mathcal{C}^{n_R \times n_T - 1}$. The decision statistic of the kth substream using matched filtering is

$$y_k(i) = \underbrace{\mathbf{h}_k^H \mathbf{h}_k a_k(i)}_{d_k} + \underbrace{\mathbf{h}_k^H \mathbf{H}_k \mathbf{a}_k(i)}_{u_k} + \underbrace{\mathbf{h}_k^H \mathbf{v}(i)}_{\bar{v}_k} \tag{4.43}$$

where d_k, u_k and $\bar{v}_k$ are the desired response obtained by the linear beamformer, the CAI, and phase-rotated noise, respectively.

The soft output of MAP detector for the kth substream is given by:

$$\hat{a}_k = \arg\max_{a_k} P(a_k|y_k) \tag{4.44}$$

For brevity, we omit the sampling time index (i) in the equations. Let the interference of the kth substream be denoted by $\mathbf{u}_k \in U_k$, where $U_k = \{(a_1, a_2, \ldots, a_{k-1}, 0, a_{k+1}, \ldots, , a_{n_T}) : a_j \in \{+1, -1\}, j \neq k\}$, a set that spans $2^{n_T - 1}$ dimensions, and $\mathbf{u}_k$ is any $(n_T - 1)$-dimensional interference vector of the kth substream. The *a posteriori* probability of the kth substream is defined by

$$P(a_k|y_k) = P(y_k, a_k)/P(y_k) \tag{4.45}$$

where

$$P(y_k, a_k) = \sum_{\mathbf{u}_k \in U_k} P(y_k, a_k, \mathbf{u}_k) \tag{4.46}$$

and

$$\begin{aligned} P(y_k, a_k, \mathbf{u}_k) &= P(y_k|a_k, \mathbf{u}_k) P(a_k, \mathbf{u}_k) \\ &= P(y_k|a_k, \mathbf{u}_k) \prod_{j=1}^{n_T} P(a_j) \end{aligned} \tag{4.47}$$

Here the probability distribution of the kth substream is formed by averaging out the contributions of interfering substreams. In the kth substream, $(n_T - 1)$ interferences may be present and therefore there are 2^{n_T-1} possible interference patterns. In order to achieve the individual MAP decisions, we need knowledge of the *a priori* probability of the interfering substreams $P(a_j), \ \forall j$. We use n_T-parallel soft-in/soft-out (SISO) decoders to provide the *a priori* probabilities of the interfering substreams to the MAP detectors.

The corresponding log-likelihood ratios (LLR) for the MAP SISO detectors are formed as sums rather than products of independent metrics. We define the log-likelihood metric as:

$$\lambda(a_k|y_k) = \lambda(y_k|a_k) + \lambda(a_k) \tag{4.48}$$

where

$$\lambda(a_k) = \log \frac{P(a_k = +1)}{P(a_k = -1)} \tag{4.49}$$

and

$$\begin{aligned}\lambda(y_k|a_k) &= \log\frac{P(y_k|a_k=+1)}{P(y_k|a_k=-1)}\\ &= \log\frac{\sum_{\mathbf{u}_k\in U_k}P(y_k|a_k=+1,u_k)P(\mathbf{u}_k)}{\sum_{\mathbf{u}_k\in U_k}P(y_k|a_k=-1,u_k)P(\mathbf{u}_k)}\\ &= \log\frac{\sum_{\mathbf{u}_k\in U_k}\exp\left[-\frac{1}{2\sigma^2}(y_k-d_k-u_k)^2\right]\prod_{j\neq k}P(a_j)}{\sum_{\mathbf{u}_k\in U_k}\exp\left[-\frac{1}{2\sigma^2}(y_k+d_k-u_k)^2\right]\prod_{j\neq k}P(a_j)}\\ &= \lambda_{a_k}(a_k)+\lambda_{\mathbf{u}_k}(a_k) \qquad (4.50)\end{aligned}$$

where

$$\lambda_{a_k}(a_k)=\frac{2d_ky_k}{\sigma^2} \qquad (4.51)$$

and

$$\lambda_{\mathbf{u}_k}(a_k)=\log\frac{\sum_{\mathbf{u}_k\in U_k}P(\mathbf{u}_k)\exp\left(\frac{-1}{2\sigma^2}(u_k^2-2u_k(y_k-d_k))\right)}{\sum_{\mathbf{u}_k\in U_k}P(\mathbf{u}_k)\exp\left(\frac{-1}{2\sigma^2}(u_k^2-2u_k(y_k+d_k))\right)} \qquad (4.52)$$

However, the computational complexity of the MAP detector is exponential in terms of the number of transmit antennas. One way of reducing the complexity is to use a sub-optimal interference cancellation scheme as described next.

Parallel Soft Interference Cancellation Receivers

A sub-optimal solution may be found by using the max-log principle (see chapter 3, section 3.3.3). Specifically, the logarithm of sum of exponentials in the numerator and the denominator of (4.50) can be approximated by the maximum of the exponents when the maximum of the exponents is much higher than the other exponent terms:

$$\lambda(y_k|a_k)\approx\frac{2d_ky_k}{\sigma^2}+\log\frac{\max_{\mathbf{u}_k\in U_k}P(\mathbf{u}_k)\exp\left(\frac{-1}{2\sigma^2}(u_k^2-2u_k(y_k-d_k))\right)}{\max_{\mathbf{u}_k\in U_k}P(\mathbf{u}_k)\exp\left(\frac{-1}{2\sigma^2}(u_k^2-2u_k(y_k+d_k))\right)} \qquad (4.53)$$

Note that in (4.53), the numerator and the denominator are Gaussian distributions centered at $(u_k + d_k)$ and $(u_k - d_k)$, respectively, and the corresponding optimization problems may yield different solutions for the interference vector $\mathbf{u}_k$, which is clearly undesirable. However, if one assumes that the bit estimates from the previous iterations are highly reliable for all substreams, then for each substream, there exists a unique interference pattern $\mathbf{u}_k$ such that $P(\mathbf{u}_k) \approx 1$. Thus, we can further approximate (4.53) as

$$\lambda(y_k|a_k) \approx \underbrace{\frac{2d_k y_k}{\sigma^2}}_{\lambda_{a_k}(a_k)} + \underbrace{\log \frac{P(\mathbf{u}_k)\exp\left(\frac{-1}{2\sigma^2}(u_k^2 - 2u_k(y_k - d_k))\right)}{P(\mathbf{u}_k)\exp\left(\frac{-1}{2\sigma^2}(u_k^2 - 2u_k(y_k + d_k))\right)}}_{\lambda_{\mathbf{u}_k}(a_k)} \tag{4.54}$$

$$= \frac{2d_k y_k}{\sigma^2} - \frac{2}{\sigma^2} d_k(u_k) \tag{4.55}$$

Since we only have expectations of the interfering symbols, we replace the exact information of the interfering substreams by the expectation of the interferences:

$$\lambda_{\mathbf{u}_k}(a_k) = -\frac{2}{\sigma^2} d_k \mathcal{E}(u_k) \tag{4.56}$$

where

$$\mathcal{E}(u_k) = \sum_{j \neq k} \mathbf{h}_k^H \mathbf{h}_j \mathcal{E}(a_j) \tag{4.57}$$

SISO Decoders

We use n_T-parallel SISO decoders to provide the *a priori* probabilities of the transmitted substreams (for details of SISO decoders, see chapter 3, section 3.3). Consider the log-likelihood ratio (LLR) of symbol a_j provided by the SISO decoder $\lambda(a_j)$. Since $\lambda(a_j) = \log \frac{P(a_j=+1)}{P(a_j=-1)}$, we have the following relation:

$$\frac{P(a_j = +1)}{P(a_j = -1)} = \exp(\lambda(a_j)) \tag{4.58}$$

Further, by using the fact that $P(a_j = +1) + P(a_j = -1) = 1$, we get the following component-wise relation:

$$P(a_j = +1) = \frac{\exp(\lambda(a_j))}{1 + \exp(\lambda(a_j))} \tag{4.59}$$

and

$$P(a_j = -1) = \frac{1}{1 + \exp(\lambda(a_j))} \tag{4.60}$$

Hence, we have the expectations

$$\begin{aligned} \mathcal{E}[a_j] &= \frac{(+1)\exp(\lambda(a_j))}{1 + \exp(\lambda(a_j))} + \frac{(-1)}{1 + \exp(\lambda(a_j))} \\ &= \tanh(\lambda(a_j)/2) \quad j = 1, 2, \ldots, n_T \end{aligned} \tag{4.61}$$

Accordingly, the MAP formulation reduces to a soft interference cancellation scheme using the hyperbolic tangent function, as shown by

$$\lambda(y_k|a_k) = \frac{2d_k}{\sigma^2}\left[y_k - \sum_{j \neq k} \mathbf{h}_k^H \mathbf{h}_j \tanh(\lambda(a_j)/2)\right] \tag{4.62}$$

The resulting soft-interference cancellation receiver is shown in Figure 4.14.

Experiment 1: Performance of Map Based Receivers

In this experiment, we compare the performance of the MAP based iterative receiver to the sub-optimal soft interference canceling receiver. Figure 4.15 presents the results of computer simulation performed on four receiver configurations:

- (1,1)- system for an AWGN channel
- (8,12)- coded V-BLAST system that relies on hard decisions in the receiver

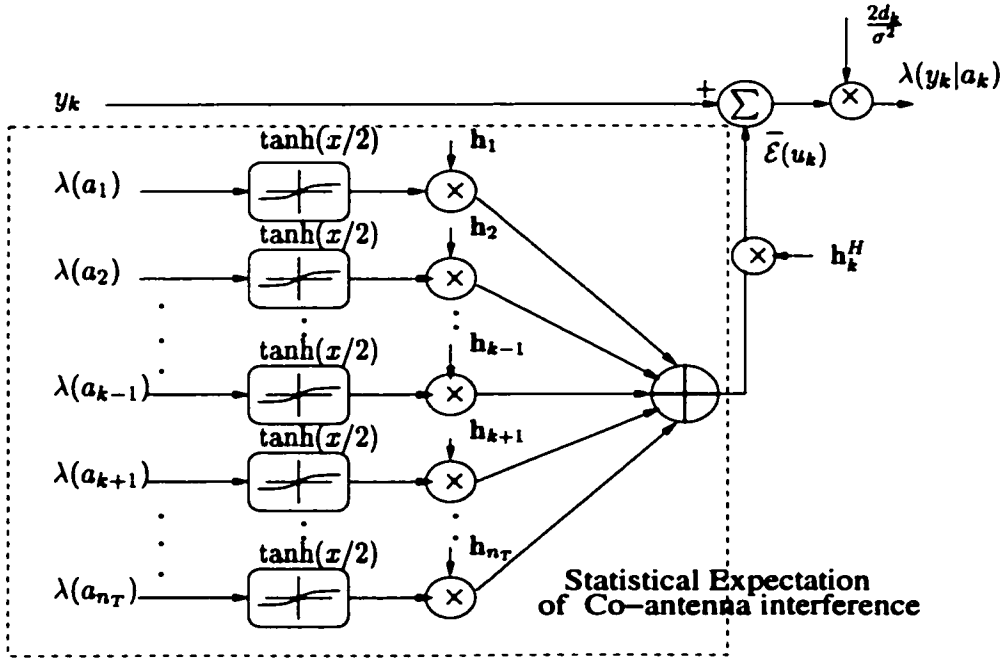

Figure 4.14: Soft interference cancellation detector.

- (8,12)- T-BLAST with MAP-based SISO detector
- (8,12)- T-BLAST sub-optimum soft interference cancellation detector

The transmitted power is maintained constant in all four configurations. The first receiver is noise-limited, whereas the other three BLAST configurations are called co-antenna interference- and fading-limited. The burst length L is 100 symbols, 20 of which are used for training. Each of the 8 substreams utilized rate 1/2 convolutionally coded BPSK. The code generator used is (7,5) and eight different pseudo-random interleavers are used.

In Figure 4.15, the bit error rate (BER) is plotted versus the number of iterations at SNR = 7dB. We observe the following:

- Naturally, the single antenna system and V-BLAST system that rely on hard decisions, are both independent of the number of iterations.
- In direct contrast, the performances of both Turbo-BLAST systems (reliant on soft

decisions) improve with increasing number of iterations, approaching that of the noise-limited single antenna system in about 5 iterations.

- The performance of sub-optimal T-BLAST is close to that of the optimum one.

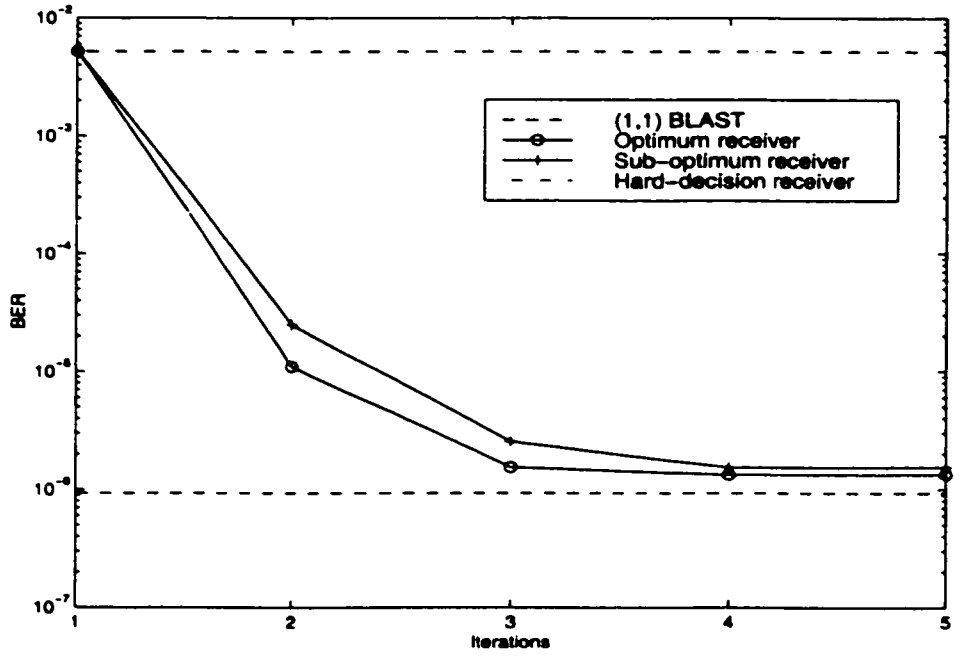

Figure 4.15: Performance of the proposed receivers for the encoded BLAST system.

Note that even with MAP detectors used as the inner decoders, iterative decoding can still provide a performance gain. The reason is that the MAP-based inner decoders are still sub-optimal compared to the global MAP solution; the iterative decoders are used as a practical solution to the global MAP receiver. Moreover, the turbo iterative process applies equally well to the sub-optimal inner decoders; a soft interference-cancellation inner decoder has a performance close to that of the MAP-based inner decoder, which is the motivation for designing the simplified inner decoders.

4.7.3 PSIC with Bootstrapping Channel Estimates

To extract the desired signal, we may use a simple spatial matched filtering scheme. We use the maximum-ratio-combining (MRC) scheme since it is a simple and effective technique.

In MRC, the beamforming weight vector is simply the estimated channel vector. In the following to simplify the presentation, we assume that we have exact channel estimates. The decision statistic for the kth substream at the ith sampling interval obtained by the MRC is

$$\begin{aligned} y_k(i) &= \underbrace{\mathbf{h}_k^H \mathbf{h}_k a_k(i)}_{d_k} + \underbrace{\sum_{j \neq k} \mathbf{h}_k^H \mathbf{h}_j a_j(i)}_{u_k} + \underbrace{\mathbf{h}_k^H \mathbf{v}(i)}_{\bar{v}_k} \\ &= d_k(i) + u_k(i) + \bar{v}_k(i) \end{aligned} \tag{4.63}$$

The terms corresponding to d_k, u_k and $\bar{v}_k$ are the desired response obtained by the MRC, the CAI, and phase-rotated noise, respectively. The receive-diversity gain achieved by the MRC is only $(n_R - n_T + 1)$, since $n_T - 1$ interferes are present. The MRC is known to be the optimum linear filter to combat multi-path fading, provided that there is no co-channel interference. Unfortunately, in a correlated channel environment exemplified by BLAST, MRC is an inefficient way to extract the desired signals. In order to exploit the optimal behavior of MRC, we use a robust nonlinear interference canceler in front of the MRC, as described next.

Iterative Parallel Soft-Interference Canceler (IPSIC)

The soft interference cancellation detector stage has three learning strategies:

(i) An iterative soft-interference cancellation scheme, which makes use of the implicit form of supervision provided by the FEC code via an iterative scheme.

(ii) A spatial channel matched filtering operation, which is based on maximum ratio combining of the channel outputs since it is simple and effective. (For strategies (i) and (ii), we use a short training sequence to estimate the channel matrix.)

(iii) Re-estimation of channel matrix, which uses the training sequence provided by the complete set of decoded information at each iteration.

Parallel Soft-Interference Canceler

In this scheme, the CAI is removed from the received signal before the receiver performs MRC to extract each desired signal. After canceling the interferers, the MRC exploits knowledge of the channel matrix to achieve n_R-fold diversity reception of each of the transmitted signals. Assume that we have a preliminary symbol estimate of each substream $\{\hat{a}_j\}$, $j = 1, 2, \ldots, n_T$. In the following, we omit the sampling index (i) to simplify notation.

The interference-free received vector pertaining to the kth substream is:

$$\mathbf{r}_k = \mathbf{r} - \sum_{j \neq k} \mathbf{h}_j \hat{a}_j \tag{4.64}$$

The decision statistic of the kth substream obtained by performing the MRC on the interference free received vector is given by

$$\begin{aligned} x_k &= \underbrace{\mathbf{h}_k^H \mathbf{h}_k a_k}_{d_k} + \underbrace{\sum_{j \neq k} \mathbf{h}_k^H \mathbf{h}_j (a_j - \hat{a}_j)}_{\delta_k} + \underbrace{\mathbf{h}_k^H \mathbf{v}}_{\bar{v}_k} \\ &= d_k + \delta_k + \bar{v}_k \end{aligned} \tag{4.65}$$

If we have exact knowledge of the interference, $\delta_k \to 0$ and x_k reduces to

$$x_k = \underbrace{\mathbf{h}_k^H \mathbf{h}_k a_k}_{d_k} + \underbrace{\mathbf{h}_k^H \mathbf{v}}_{\bar{v}_k} = |\mathbf{h}_k|^2 a_k + \bar{v}_k \tag{4.66}$$

where $\|\mathbf{h}_k\|^2$ is a chi-squared variate with $2n_R$ degrees of freedom. We normalize the channel such that $\mathcal{E}[\,|H_{kl}|^2] = 1$, and thereby achieve n_R-fold receive diversity for each transmitted signal. However, since we do not know the actual symbol estimates of the transmitted substreams, we replace the exact symbol estimates $\{\hat{a}_j\}$ by their expectations $\mathcal{E}[a_j]$. We

use the *a priori* probabilities of the substreams to estimate the $\mathcal{E}[a_j]$, as shown by

$$\mathcal{E}[a_j] = \sum_{a_j \in \{+1,-1\}} a_j P(a_j), \quad j = 1, 2, \ldots, n_T \tag{4.67}$$

Accordingly, we rewrite (4.65) as

$$\begin{aligned} x_k &= \underbrace{\mathbf{h}_k^H \mathbf{h}_k a_k}_{d_k} + \underbrace{\sum_{j \neq k} \mathbf{h}_k^H \mathbf{h}_j (a_j - \mathcal{E}(a_j))}_{\hat{\delta}_k} + \underbrace{\mathbf{h}_k^H \mathbf{v}(i)}_{\bar{v}_k} \\ &= d_k + \hat{\delta}_k + \bar{v}_k \end{aligned} \tag{4.68}$$

The expectation of the interference estimation can be obtained from (4.61), and the interference estimate is

$$\begin{aligned} \mathcal{E}(u_k) &= \sum_{j \neq k} \mathbf{h}_k \mathbf{h}_j \mathcal{E}(a_j) \\ &= \sum_{j \neq k} \mathbf{h}_k \mathbf{h}_j \tanh(\lambda(a_j)/2) \end{aligned} \tag{4.69}$$

Figure 4.16 shows the resulting structure of the soft interference-cancellation scheme.

Channel Re-Estimation

In practice, we need to estimate the channel matrix in order to use the interference-cancellation scheme. During the first iteration of the receiver, we use a short training sequence to estimate a preliminary channel matrix. When performing linear beamforming and parallel soft-interference cancellation, we benefit from a good estimate of the channel matrix. With a short training sequence, it may be difficult to achieve a good estimate for slowly time-varying channel in a BLAST system. In order to achieve a good performance for slowly time-varying (within the packet) channel, we re-estimate the channel matrix using all estimated symbols of the packet at each subsequent iteration. This newly estimated

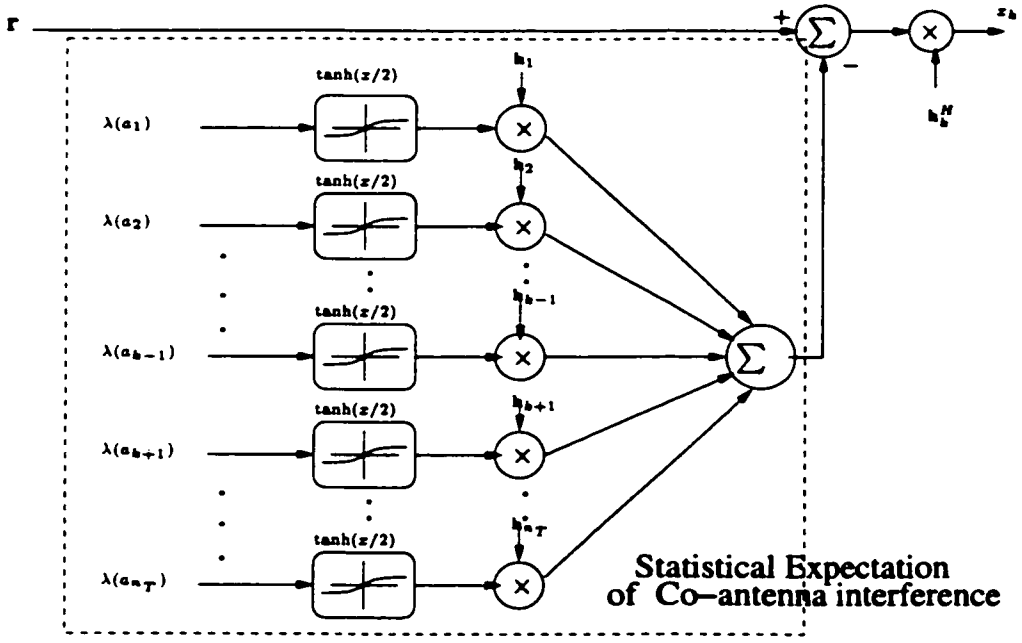

Figure 4.16: Parallel soft interference cancellation detector.

matrix channel is used by the detector to estimate spatial match filter weights and interferences. The bootstrapping technique described herein is performed in a manner that tends to maximally squeeze information out of each packet; the training overheads per information packet are thereby reduced.

Soft interference cancellation suffers from large error floors in correlated environments. In the next section, we propose MMSE based detectors which are mathematically tractable and avoid this error floor problem [81].

4.7.4 Minimum Mean-Square Error Receiver

Finally, we propose a multi-substream detector based on MMSE detectors and soft interference cancellation, which optimizes the interference estimate and the weights of the linear detector jointly by using the MMSE criterion.

In the interference cancellation MRC, we remove CAI from the linear beamformer output

y_k. Accordingly, we write:

$$x_k = \mathbf{w}_k^H \mathbf{r} - u_k \tag{4.70}$$

where u_k is a linear combination of interfering substreams: $u_k = \mathbf{w}_2^H \hat{\mathbf{a}}_k$, and x_k is an improved estimate of transmitted symbol a_k. For brevity, we omit the sampling index (i). The performance of the estimator is measured by the error $e_k = (a_k - x_k)$. We need to minimize $\mathcal{E}[e_k e_k^*]$. The weights $\mathbf{w}_k \in \mathcal{C}^{n_T \times 1}$ and the interference estimate u_k are optimized by minimizing the mean-square of the error between each substream and its estimate.

Problem 1 *Given (4.41) and (4.70), find the weight vectors* $\mathbf{w}_k$ *and* u_k *by minimizing the following cost function:*

$$(\hat{\mathbf{w}}_k, \hat{u}_k) = \arg \min_{(\mathbf{w}_k, u_k)} \mathcal{E}\left[\|a_k - x_k\|^2\right] \tag{4.71}$$

where the expectation is taken over the noise and the statistics of the data sequence. ■

Solution 1 *The Solution to* **Problem 1** *is given by*

$$\hat{\mathbf{w}}_k = (\mathbf{P} + \mathbf{Q} + \Sigma_{n_R})^{-1} \mathbf{h}_k \tag{4.72}$$

$$\hat{u}_k = \mathbf{w}_k^H \mathbf{z} \tag{4.73}$$

Where

$$\begin{aligned}
&\mathbf{P} = \mathbf{h}_k \mathbf{h}_k^H && \in \mathcal{C}^{n_R} \\
&\mathbf{Q} = \mathbf{H}_k \left[\mathbf{I}_{(n_T-1)} - \mathrm{Diag}(\mathcal{E}[\mathbf{a}_k]\mathcal{E}[\mathbf{a}_k]^H)\right] \mathbf{H}_k^H && \in \mathcal{C}^{n_R} \\
&\Sigma_{n_R} = \sigma^2 \mathbf{I}_{n_R}, \quad \sigma^2 > 0 && \in \mathcal{C}^{n_R} \\
&\mathbf{z} = \mathbf{H}_k \mathcal{E}[\mathbf{a}_k] && \in \mathcal{C}^{n_R \times 1}
\end{aligned}$$

■

We used standard minimization techniques to solve the optimization problem formulated

in (4.71) (see Lemma 4A.4 in Appendix 4A). In arriving at this solution, we used

$$\mathcal{E}[\mathbf{v}\mathbf{v}^T] = \sigma^2\mathbf{I}_{n_R}; \quad \mathcal{E}[\mathbf{a}\mathbf{v}] = \mathbf{0}; \quad \mathcal{E}[a_i a_j] = \mathcal{E}[a_i]\mathcal{E}[a_j] \ \ \forall i \neq j \tag{4.74}$$

These conditions are achieved by independent and different space-interleaving and time-interleaving applied at the transmitter.

- For the first iteration, we assume $\mathcal{E}[\mathbf{a}_k] = \mathbf{0}$ and (4.70) reduces to the linear MMSE receiver for substream k:

$$x_k(i) = \mathbf{h}_k^H(\mathbf{H}\mathbf{H}^H + \sigma^2\mathbf{I})^{-1}\mathbf{r}(i) \tag{4.75}$$

- In the limit of $\mathcal{E}[\mathbf{a}_k] \rightarrow \mathbf{a}_k$, and (4.70) simplifies to a perfect interference canceler:

$$x_k(i) = (\mathbf{h}_k^H\mathbf{h}_k + \sigma^2)^{-1}\mathbf{h}_k^H(\mathbf{r}(i) - \mathbf{H}_k\mathbf{a}_k) \tag{4.76}$$

Solution 2 *The MMSE solution to the weight vector* $\mathbf{w}_k$ *requires inversion of* $n_R \times n_R$ *matrices. A sub-optimum solution to* **Problem 1** *is obtained by ignoring the matrix* $\mathbf{Q}$ *in* $\mathbf{w}_k$*, as follows:*

$$\begin{aligned} x_k &= \mathbf{h}_k^H((\mathbf{h}_k\mathbf{h}_k^H + \sigma^2\mathbf{I})^{-1})^H(\mathbf{r}(i) - \mathbf{H}_k\mathcal{E}[\mathbf{a}_k]) \\ &= ((\mathbf{h}_k^H\mathbf{h}_k + \sigma^2)^{-1}\mathbf{h}_k^H(\mathbf{r}(i) - \mathbf{H}_k\mathcal{E}[\mathbf{a}_k]) \end{aligned} \tag{4.77}$$

■

This solution requires a scalar inversion only. Note that the matrix $\mathbf{Q}$ represents the variance-covariance of the residual interferences.

To acquire the expectations of interfering substreams modulated as QPSK signals, we use n_T-parallel SISO decoders to provide the *a priori* probabilities of the transmitted substreams. The *a priori* probabilities are obtained from the decoder soft outputs of the

previous iterations using the following relationship:

$$P(\Re\{a_j\} = +1) = \frac{\exp(\lambda(\Re\{a_j\}))}{1 + \exp(\lambda(\Re\{a_j\}))} \tag{4.78}$$

$$P(\Re\{a_j\} = -1) = \frac{1}{1 + \exp(\lambda(\Re\{a_j\}))} \tag{4.79}$$

where $\lambda(\Re\{a_j\})$ is the soft output (formalized as log-likelihood ratio) of symbol $\Re\{a_j\}$ provided by the SISO decoder. The expectations are:

$$\begin{aligned} \mathcal{E}[\Re\{a_j\}] &= \frac{(+1)\exp(\lambda(\Re\{a_j\}))}{1 + \exp(\lambda(\Re\{a_j\}))} + \frac{(-1)}{1 + \exp(\lambda(\Re\{a_j\}))} \\ &= \tanh(\lambda(\Re\{a_j\})/2), \qquad j = 1, 2, \ldots, n_T \end{aligned} \tag{4.80}$$

where $a_j = \Re\{a_j\} + \sqrt{-1}\Im\{a_j\}$. Similarly, $\mathcal{E}[\Im\{a_j\}]$ can be estimated. Accordingly, the interference estimate reduces to

$$\begin{aligned} \hat{u}_k &= \mathbf{h}_k^H \mathcal{E}\{\mathbf{a}_k\} \\ &= \sum_{j \neq k} \mathbf{h}_k^H \mathbf{h}_j [\tanh(\lambda(\Re\{a_j\})/2) + \sqrt{-1}\tanh(\lambda(\Im\{a_j\})/2)] \end{aligned} \tag{4.81}$$

4.8 Simulation Results

The BLAST scheme considered for the simulation presented herein is a (16, 16) system. The packet length is 120 symbols, 20 of which are training symbols. Each of the 16 substreams uses a rate 1/2 convolutionally coded BPSK. The code generator used is (7,5). For simplicity, we use BPSK/QPSK modulation. The space-time interleavers are chosen randomly and no attempt is made to optimize their design.

In validating the T-BLAST proposed in this thesis, we used the following channel models:

- Quasi-static Rayleigh fading channel as depicted in Figure 4.17: A matrix of independent Rayleigh fading coefficients are generated and the fading coefficients are fixed over bursts of L symbols but are varied from one burst to the next.

- Slow fading Rayleigh fading channel as depicted in Figure 4.18: Independent Rayleigh fading channels are generated according to the modified Jakes model [38] with maximum Doppler frequency between 0 to 30 Hz.

For each run (packet), a new realization of channel is chosen.

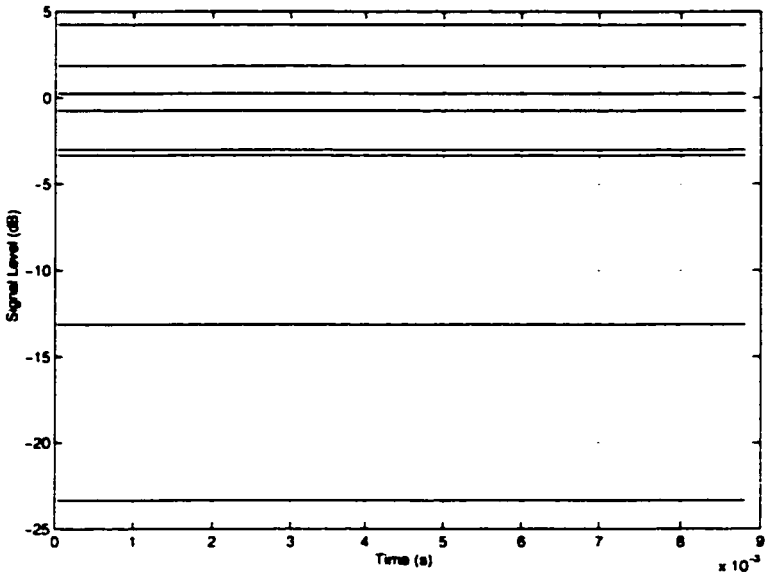

Figure 4.17: Quasi-static Rayleigh channel of eight transmit antennas

4.8.1 Performance of PSIC Receivers

In this experiment, we compare the performance of the parallel soft-interference cancellation receiver with and without bootstrapping channel re-estimation. Computer simulations are performed on the following BLAST configurations with BPSK modulation:

- V-BLAST receiver that uses hard decisions in the receiver,
- T-BLAST receiver that uses iterative soft interference-cancellation (T-BLAST-MRC 1), and
- T-BLAST receiver that uses iterative soft interference-cancellation with bootstrapping channel estimation (T-BLAST-MRC 2).

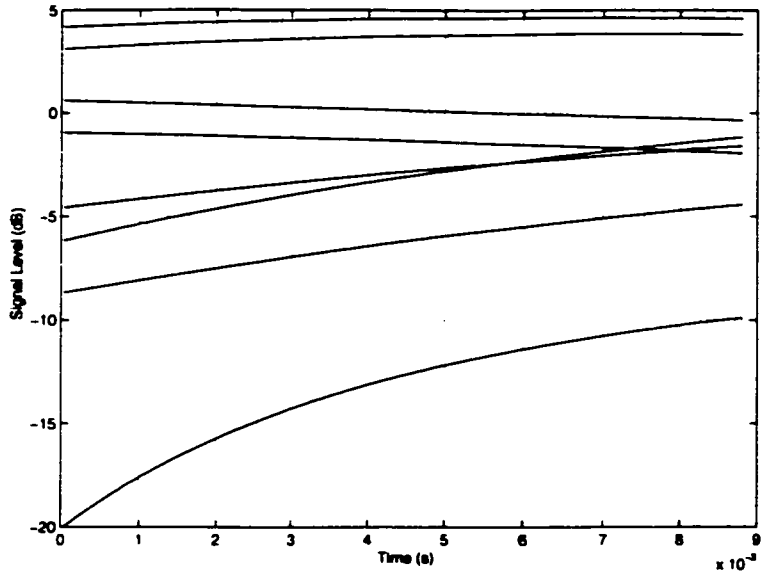

Figure 4.18: Slow fading Rayleigh channel of eight transmit antenna with Doppler frequency =10 Hz at 1 GHz carrier frequency and 10Km/H vehicle speed.

Experiment 2: Time-invariant channel

In this experiment, we consider independent channels that are time invariant for the duration of a packet.

Figure 4.19 shows the BER versus the number of iterations for SNR=9dB. Naturally, the single antenna system and the V-BLAST system are both independent of the number of iterations. In direct contrast, the performance of both T-BLAST-MRC 1 and 2 improves with increasing number of iterations, with T-BLAST-MRC 2 performing slightly better than receiver MRC 1. In particular, the performance of both T-BLAST receivers approaches that of the noise-limited single antenna system (lower-bound) in about 4 to 5 iterations.

In Figure 4.20, we show the BER performance versus SNR for V-BLAST and T-BLAST-MRC 2. The performance of T-BLAST-MRC 2 is shown for 1,2,3,4 and 7 iterations. As expected, the performance of both V-BLAST and T-BLAST improves with increasing SNR. The T-BLAST scheme approaches the performance of the single-antenna system (lower-bound) in about 4 iterations. The performance of T-BLAST exceeds that of V-BLAST in 2 iterations.

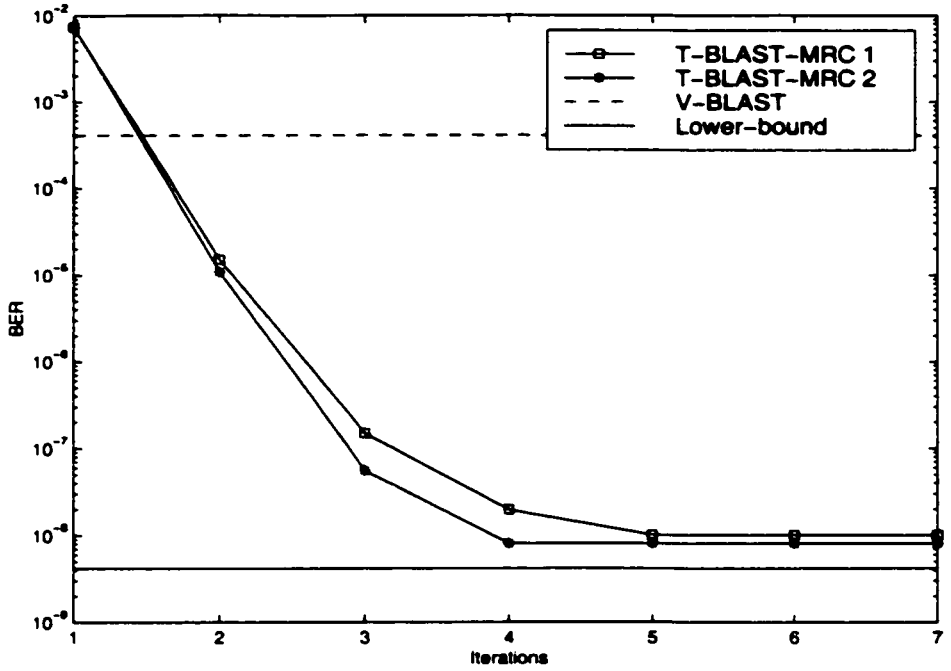

Figure 4.19: BER Vs. iterations, Doppler frequency = 0 Hz, SNR = 9dB

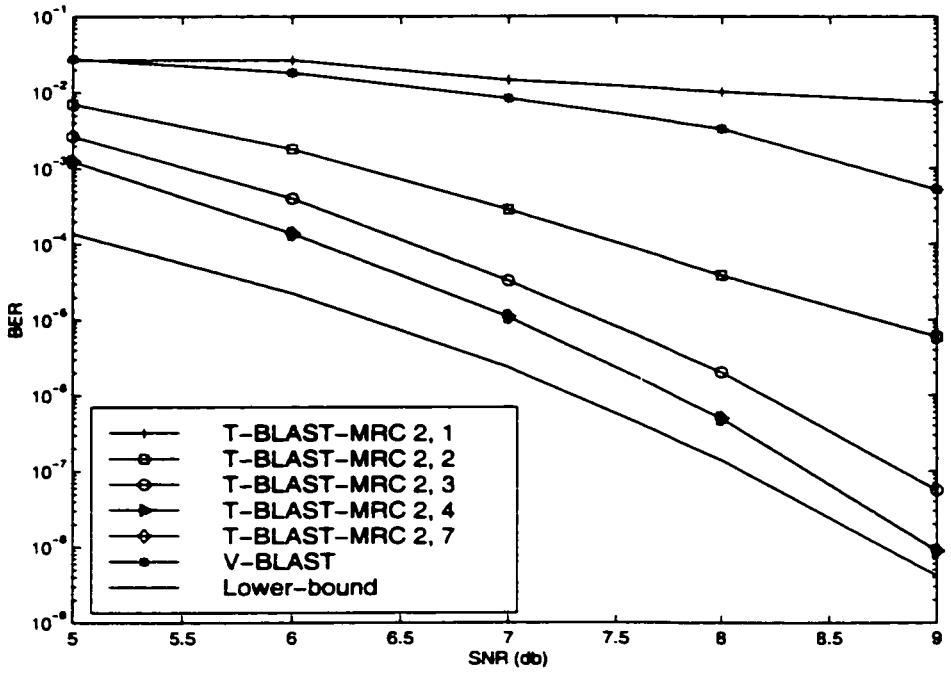

Figure 4.20: BER Vs. SNR, Doppler frequency = 0 Hz

Experiment 3: Slowly time-varying channel

We repeated Experiment 2 with independent channels that are varying slowly in time within a burst (packet). The maximum Doppler frequency considered here is 20Hz. Figures 4.21 and 4.22 show the BER versus number of iterations and the BER versus SNR for 1,2,4 and 7 iterations for the T-BLAST-MRC receiver 1 and receiver 2. From these figures, we make the following observations:

- The performance of both T-BLAST-MRC receivers improves with increasing number of iterations, with T-BLAST-MRC 2 outperforming T-BLAST-MRC 1. Both T-BLAST-MRC receivers outperform V-BLAST.
- After about 4 to 5 iterations, the T-BLAST-MRC receiver reaches a steady state but falls short of the single-antenna system (lower-bound) in performance by a wider margin than in Experiment 2. This fall is because a fixed matrix inadequately represents the time-varying channel matrix. For highly time-varying channels, the performance may be further decreased.

4.8.2 Performance of MMSE Receivers

In this section, we examine the performance of MMSE based T-BLAST systems. Computer simulations are performed on the following BLAST configurations:

- coded V-BLAST that relies on hard decisions,
- T-BLAST using Solution 1 (T-BLAST-MMSE 1), and
- T-BLAST using Solution 2 (T-BLAST-MMSE 2).

Experiment 4: Performance with varying SNR

Figure 4.23 shows the BER performance versus SNR for V-BLAST and T-BLAST-MMSE 1 and 2 for a 16×16 BLAST scheme. We observe the following:

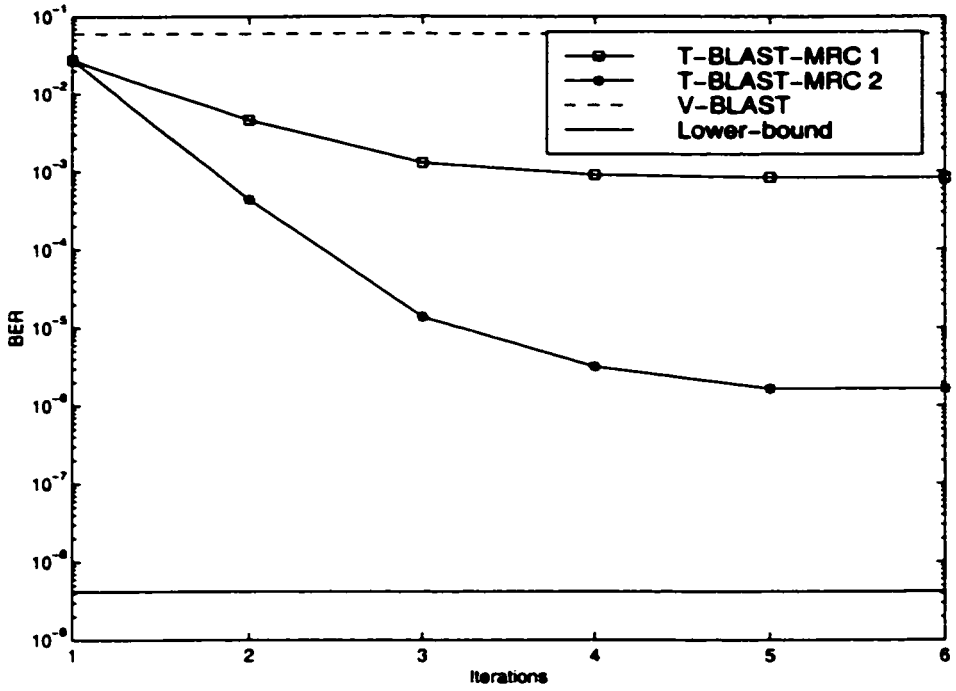

Figure 4.21: BER vs iterations, Doppler frequency = 20 Hz, SNR = 9dB

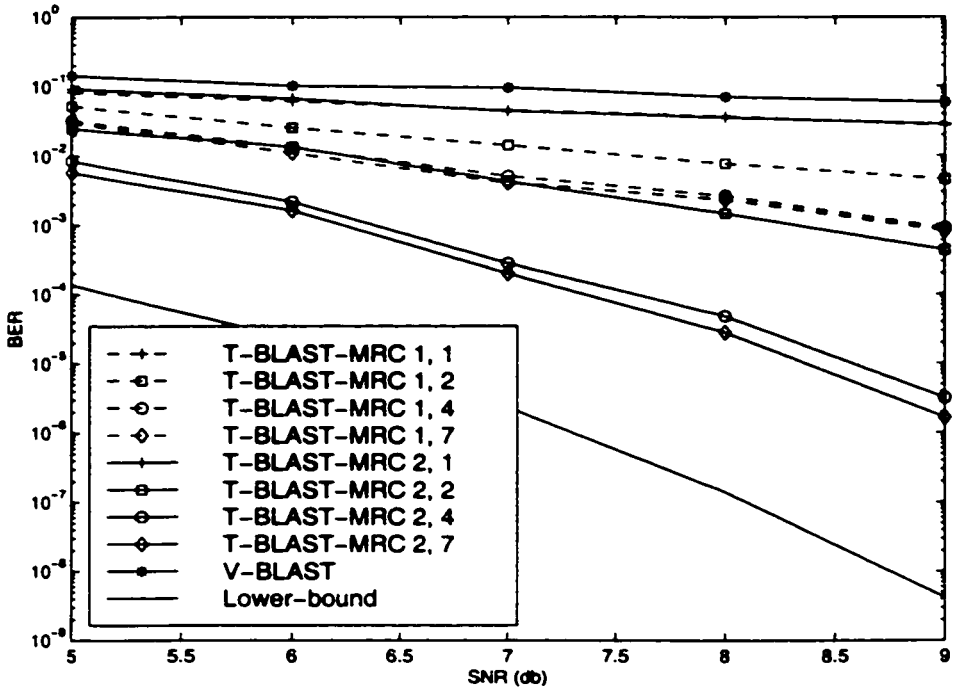

Figure 4.22: BER Vs. SNR, Doppler frequency = 20 Hz

- The performance of both V-BLAST and T-BLAST-MMSE improves with increasing SNR.
- The performances of both T-BLAST-MMSE receivers 1 and 2 improve with the increasing number of iterations, with T-BLAST-MMSE 2 performing slightly better than T-BLAST-MMSE 1, for high SNR.
- The performance of T-BLAST exceeds that of V-BLAST in 2 iterations.

Experiment 5: Performance with increasing number of transmitters

Figure 4.24 shows the BER versus the number of transmitters for V-BLAST and T-BLAST-MMSE 2 for iterations 2 and 4 at SNR=8dB. The number of transmitters considered is 2, 4, 8 and 16. From the figure, we note:

- The T-BLAST-MMSE 2 outperforms V-BLAST.
- The performance of T-BLAST receivers improves significantly with increasing number of transmitters. A significant performance increment is achieved for T-BLAST scheme with 16 transmit and 16 receive antennas compared to the T-BLAST scheme with 2 transmit and 2 receive antennas for the same operating conditions and same total transmit power.
- The performance of V-BLAST increases from the 2×2 scheme to the 8×8 scheme. In fact, this improvement diminishes and a performance decrement is observed for the 16×16 antenna scheme compare to that of the 8×8 antenna scheme.

This example illustrates the robustness of the T-BLAST scheme in the presence of co-antenna interferences. T-BLAST performs better for large number of transmitters and achieves a significant diversity and coding gain. The larger the interleaver depth, the higher the coding gain. Since the decoder outputs are used to estimate the soft-interferences, the scheme is also guaranteed to achieve the maximum receiver diversity. In direct contrast, the performance of a V-BLAST system decreases for higher number of transmit antennas due

to the increased amount of co-channel interference. Since V-BLAST does not utilize any transmit diversity, it has no additional means to compensate for the increased co-channel interference.

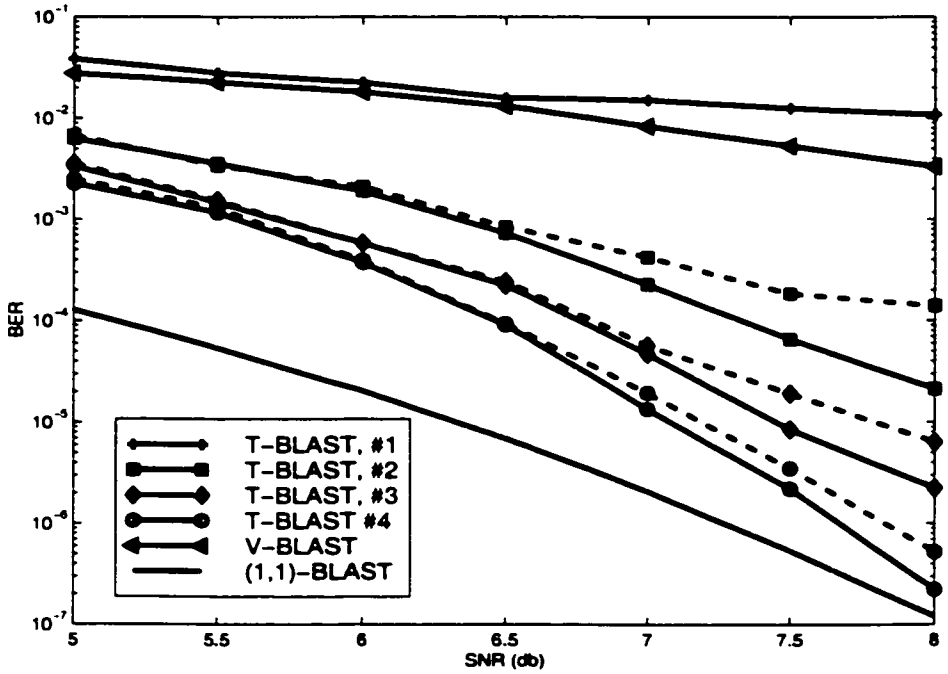

Figure 4.23: BER Vs. SNR, The continuous lines and dashed lines represent, respectively, the performance of the T-BLAST-MMSE 1 and 2

4.8.3 MMSE Vs MRC for T-BLAST

We compare the performance of MRC based soft interference cancellation receivers with MMSE based receivers. Computer simulations are performed on the following BLAST configurations with QPSK modulation:

(1) D-BLAST with no edge waste and relies on hard decisions,

(2) T-BLAST-MMSE-1, and

(3) T-BLAST-MRC- 2.

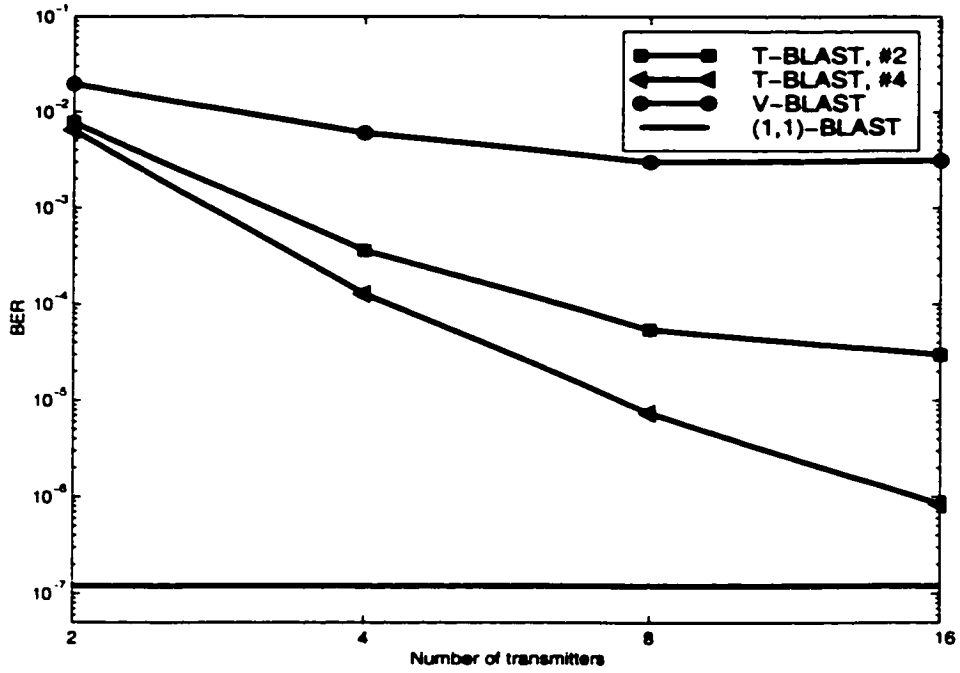

Figure 4.24: BER Vs. transmitters for T-BLAST-MMSE receiver 1, SNR = 8dB

Experiment 6: Performance with time-invariant channel

Figure 4.25 shows the BER performance versus SNR for D-BLAST and T-BLAST receivers for iterations 1,2 and 5. As expected, the performance of both D-BLAST and T-BLAST improves with increasing SNR. The performance of both T-BLAST receivers improves with increasing iterations and exceeds that of D-BLAST in 2 iterations. A significant gain (7dB) is achieved by the T-BLAST scheme over D-BLAST. The T-BLAST-MMSE performs around 0.75dB better than T-BLAST-MRC.

Experiment 7: Performance in a time-varying channel

We repeated Experiment 6 with independent channels that are varying slowly in time within a burst (packet). The maximum Doppler frequency considered here is 20Hz. Figure 4.26 shows the BER performance after 5 iterations versus SNR for T-BLAST-MMSE and T-BLAST-MRC. From this figure we note that the performance of both T-BLAST receivers

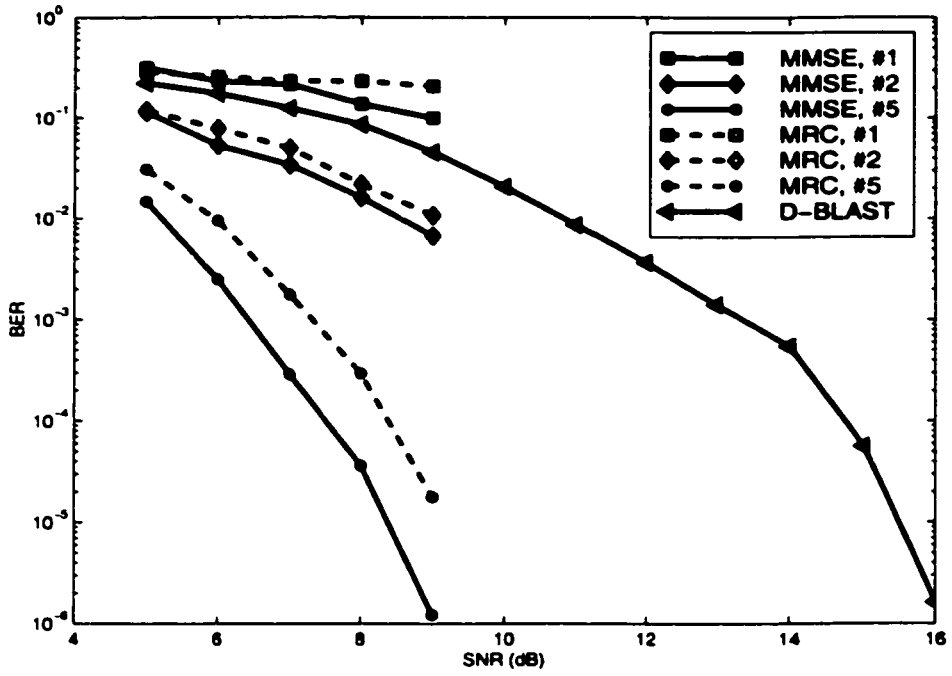

Figure 4.25: BER Vs. SNR for time-invariant channel

improves with SNR, with T-BLAST-MMSE outperforming T-BLAST-MRC by a wide margin (2dB). This illustrates the robustness of the MMSE receiver for channel estimation errors. Moreover, a performance decrement of about 6dB is observed from Figure 4.25 compared to Figure 4.26 due to possible channel estimation errors present in the time-varying channel.

4.8.4 Interleaver Dependence

Computer simulations were performed on the following configurations with QPSK modulation for time-invariant channel:

- T-BLAST (random interleavers),
- T-BLAST with diagonal layering interleavers with no edge waste (T-D-BLAST),
- Traditional D-BLAST but with no edge waste.

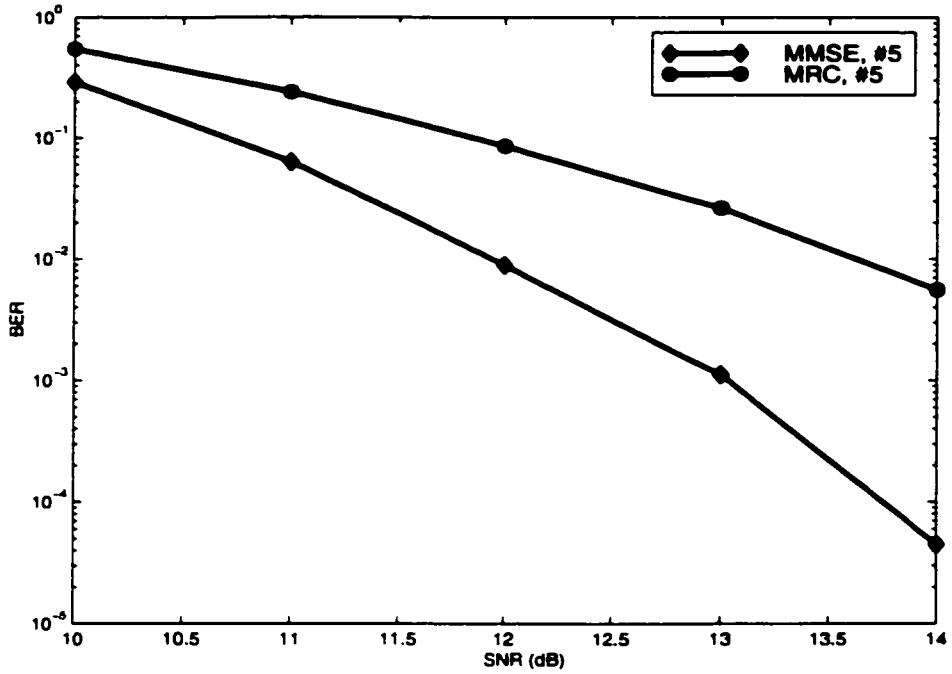

Figure 4.26: BER Vs. SNR for time-varying channel

Experiment 8: Interleaver Design Dependence

Figure 4.27 shows the BER performance versus SNR for the T-D-BLAST and T-BLAST, for iterations 1,2,4 and 5. The figure also shows the performance of traditional D-BLAST. From this figure, we note:

- T-BLAST and T-D-BLAST outperform traditional D-BLAST in two iterations. In particular, at the 10^{-4} BER level, traditional D-BLAST performs 7dB worse compared to the D-BLAST with an iterative receiver.
- The performance of both T-BLAST and T-D-BLAST is virtually identical.

The second observation illustrates that random interleaving is sufficient for T-BLAST since the independent subchannels are random and vary from packet to packet.

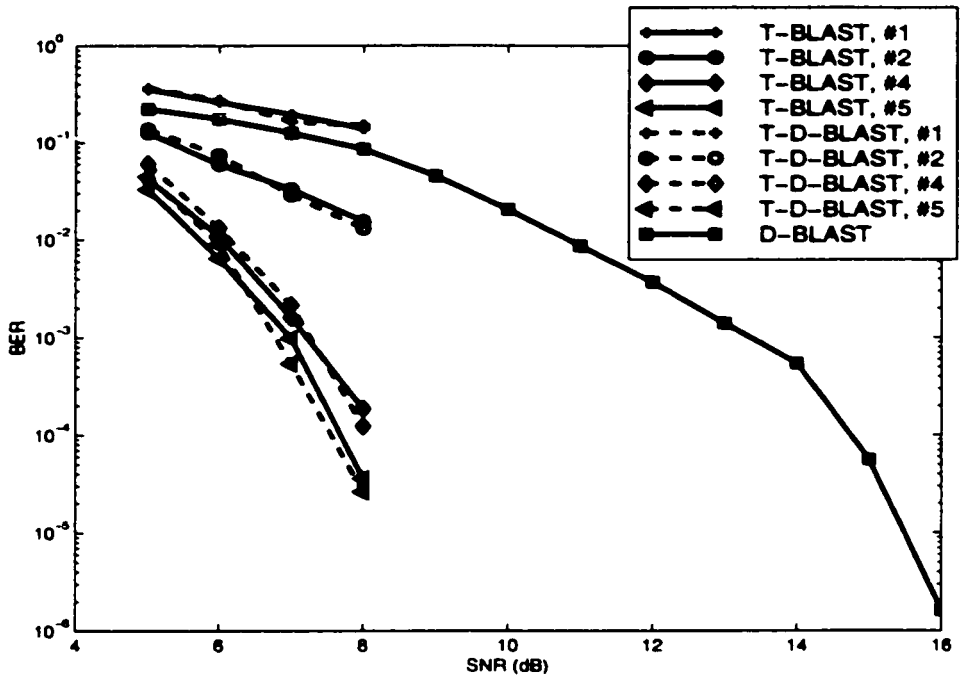

Figure 4.27: Performance comparison of D- and T-BLAST schemes

Experiment 9: Interleaver size dependence

In Figure 4.28, we show the BER performance at iteration 5 versus SNR for different sizes of interleavers by varying the length of the interleaver. Note that the width of the interleaver equals the number of transmitters, which is 16 for the scenario considered herein. We observe again that the performances of both T-BLAST and T-D-BLAST schemes are identical.

The performance of the schemes improves with interleaver size. Note that interleaver sizes 100, 200 and 400 correspond to packet sizes 25, 50 and 100 of modulated signals. The packet size 100 is the most preferable scenario in wireless communications, for which we achieve the best performance among the other sizes considered. In particular, at 10^{-5} BER level, the T-D-BLAST with interleaver size of 400 gains 5dB and 1.5dB SNR over the T-D-BLAST with interleaver sizes 100 and 200, respectively. This gain in SNR can be due to many factors. One reason may be the possible but rare presence of bad interleavers as the interleaver size increases.

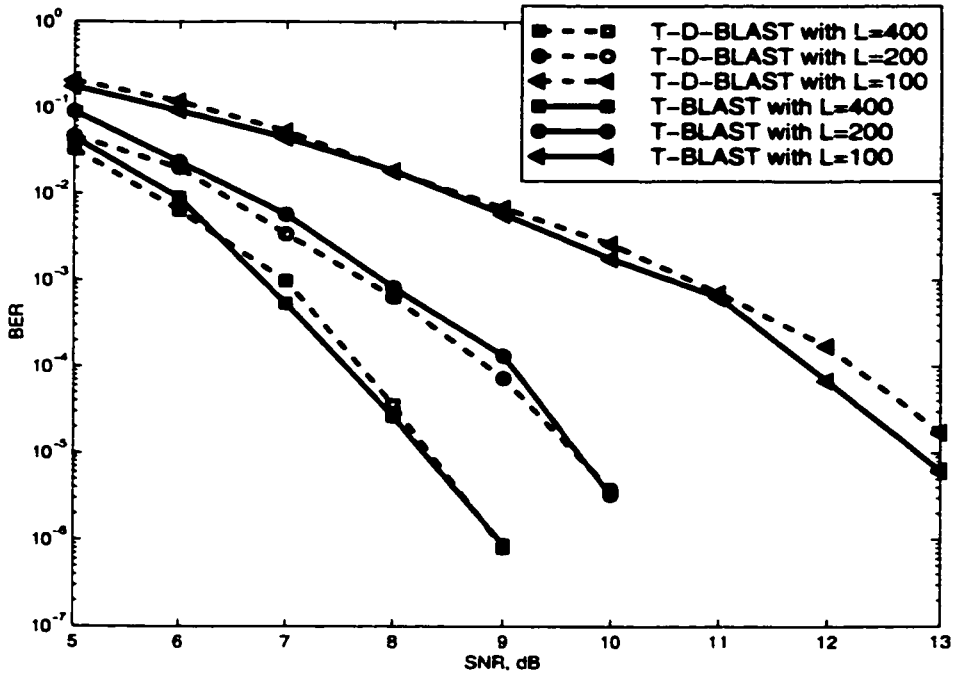

Figure 4.28: Performance variation with interleaver size L

Remark 9 *The iterative process may seem to increase the complexity of the entire receiver. With the iterative detection, we can use suboptimal methods for signal detection and therefore reduce the overall complexity. In particular, T-BLAST has no optimal ordering step that contributes to the computational complexity (growing as the 4th power of n_T) of V-BLAST scheme.*

4.9 Summary

In this chapter, we have proposed and studied a new MTMR system called T-BLAST. Specifically, we showed that the combination of BLAST and turbo principles in an intelligent manner provides a reliable and practical solution to high data-rate transmission for wireless communication. The distinguishing features of T-BLAST include:

- It is a close approximation to the global maximum likelihood (ML) solution realized via a practical iterative decoder, which uses the *extrinsic* and *intrinsic* information

concepts developed to explain turbo decoding.

- The complete system is constructed using building blocks of separately coded one-dimensional subsystems of equal capacity that allow one-dimensional signal processing at the receiving end, and yet are capable of approaching the theoretical capacity limits.

The above properties and the excellent performance of T-BLAST were demonstrated in a Rayleigh slow-fading environment. Three different BLAST algorithms, T-BLAST, D-BLAST with no edge waste, and V-BLAST, were evaluated and we found T-BLAST to be superior to the other two by a wide margin (2-7dB).

Finally, the convergence of the iterative decoder is not yet proved theoretically, although it converges in the cases encountered in practice. To further confirm this observation, we demonstrate the performance of T-BLAST using real-life data in the next two chapters.

Appendix of Chapter 4

Lemma 4A.1: Asymptotic probability of error

The asymptotic probability of error is given by

$$P(E) = Q\left(\sqrt{\frac{d_{\min}^2}{\sigma^2}}\right) \tag{4.82}$$

Proof

The received signal is given by

$$\mathbf{r}(t) = \sqrt{\frac{\rho}{n_T}}\tilde{\mathbf{H}}\mathbf{a}(t) + \mathbf{v}(t) = \mathbf{s}(\mathbf{a}, t) + \mathbf{v}(t) \tag{4.83}$$

Using the standard hypothesis test, an error occurs if [78]

$$\|\mathbf{r}(t) - \mathbf{s}(\mathbf{a}, t)\|^2 > \|\mathbf{r} - \mathbf{s}(\tilde{\mathbf{a}}, t)\|^2 \tag{4.84}$$

which is equivalent to

$$\begin{aligned} \|\mathbf{v}(t)\|^2 &> \|\mathbf{s}(\mathbf{a}, t) + \mathbf{v}(t) - \mathbf{s}(\tilde{\mathbf{a}}, t)\|^2 \\ &= \|\mathbf{s}(\mathbf{a}, t) - \mathbf{s}(\tilde{\mathbf{a}}, t)\|^2 + \|\mathbf{v}(t)\|^2 + 2\int_{-\infty}^{\infty} [\mathbf{s}(\mathbf{a}, t) - \mathbf{s}(\tilde{\mathbf{a}}, t)]^H \mathbf{v}(t) dt \end{aligned} \tag{4.85}$$

The decision distance between any two signals $\mathbf{a}$ and $\tilde{\mathbf{a}}$ is defined as

$$d^2(\mathbf{a}, \tilde{\mathbf{a}}) = \left|\left| \frac{\mathbf{s}(\mathbf{a}, t) - \mathbf{s}(\tilde{\mathbf{a}}, t)}{2} \right|\right|^2 \tag{4.86}$$

The decision error occurs if

$$d^2(\mathbf{a}, \tilde{\mathbf{a}}) \leq -\frac{1}{2} \int_{-\infty}^{\infty} [\mathbf{s}(\mathbf{a}, t) - \mathbf{s}(\tilde{\mathbf{a}}, t)]^H \mathbf{v} = \omega \tag{4.87}$$

If the noise is white Gaussian with variance σ^2, then the right hand side of (4.87) can be assumed as Gaussian with variance $\sigma^2 d^2$. Consequently, the pairwise error probability is given by

$$P(E) = P\left[d^2 < \omega\right] = Q\left(\sqrt{\frac{d^2}{\sigma^2}}\right) \tag{4.88}$$

As $\sigma \to 0$, $\min(d^2) = d^2_{\min}$, the asymptotic probability of error reduces to ([78] and [98])

$$\lim_{\sigma^2 \to 0} P(E) = Q\left(\sqrt{\frac{d^2_{\min}}{\sigma^2}}\right) \tag{4.89}$$

Lemma 4A.2: Minimum distance of RST codes

For optimal decoding of the RST, the minimum distance is:

$$d^2_{ST,\min}(\mathbf{A}, \tilde{\mathbf{A}}) = \min_{\mathbf{e} \neq \mathbf{0}} \sum_{l=1}^{L} \mathbf{e}(l)^T \Delta \mathbf{e}(l) \tag{4.90}$$

■

Proof

The decision distance between any two signals $\mathbf{A}$ and $\tilde{\mathbf{A}}$ is defined as

$$d_{ST}^2(\mathbf{A},\tilde{\mathbf{A}}) = \left\| \frac{\mathbf{S}(\mathbf{A},t) - \mathbf{S}(\tilde{\mathbf{A}},t)}{2} \right\|^2 \tag{4.91}$$

By substituting $\mathbf{S}(\mathbf{A},t)$ and $\mathbf{S}(\tilde{\mathbf{A}},t)$ into (4.91), we get

$$\begin{aligned} d_{ST}^2(\mathbf{A},\tilde{\mathbf{A}}) &= \frac{P}{4n}\|\mathbf{HA} - \mathbf{H}\tilde{\mathbf{A}}\|^2 \\ &= \frac{P}{4n}\sum_{l=1}^{L}\sum_{j=1}^{n} |H_{j1}[a_1(l) - \tilde{a}_1(l)] + \ldots + H_{jn}[a_n(l) - \tilde{a}_n(l)]\,|^2 \\ &= \sum_{l=1}^{L} \frac{(\mathbf{a}_l - \tilde{\mathbf{a}}_l)^H}{2}\mathbf{W}^{1/2}\mathbf{H}^H\mathbf{H}\mathbf{W}^{1/2}\frac{(\mathbf{a}_l - \tilde{\mathbf{a}}_l)}{2} \end{aligned} \tag{4.92}$$

where $\mathbf{a}_l$ is lth column of matrix $\mathbf{A}$ and the channel gain matrix of $\mathbf{W}^{1/2} = \sqrt{\frac{P}{n}}\mathbf{I}_n$. The $d_{ST}^2(\mathbf{A},\tilde{\mathbf{A}})$ can be simplified as:

$$\begin{aligned} d_{ST}^2(\mathbf{A},\tilde{\mathbf{A}}) &= \sum_{l=1}^{L} \frac{(\mathbf{a}_l - \tilde{\mathbf{a}}_l)^H}{2}\mathbf{W}^{1/2}\mathbf{H}^H\mathbf{H}\mathbf{W}^{1/2}\frac{(\mathbf{a}_l - \tilde{\mathbf{a}}_l)}{2} \\ &= \sum_{l=1}^{L} \mathbf{e}(l)^H\Delta\mathbf{e}(l) \end{aligned} \tag{4.93}$$

where $\mathbf{e}(l) \in \{-1,0,+1\}^n$ is the error vector defined as $\frac{\mathbf{a}_l - \tilde{\mathbf{a}}_l}{2}$, where $\mathbf{a}_l$ is lth column of matrix $\mathbf{A}$, and the channel cross-correlation matrix is

$$\Delta = \mathbf{W}^{1/2}\mathcal{E}[\mathbf{H}^H\mathbf{H}]\mathbf{W}^{1/2} = \begin{bmatrix} 1 & \delta_{1,2} & \ldots & \delta_{1,n} \\ \delta_{2,1} & 1 & \ldots & \delta_{2,n} \\ \vdots & \vdots & \ddots & \vdots \\ \delta_{n,1} & \delta_{n,2} & \ldots & 1 \end{bmatrix}, \quad \delta_{i,j} < 1, \forall i,j \tag{4.94}$$

Equation (4.94) is because the channel is normalized such that $\mathcal{E}[\ |H_{ij}\ |^2] = 1$. We also normalized the power $P = 1$. Consequently, the minimum distance is defined as

$$\min(d_{ST}^2) = d_{ST,\min}^2(\mathbf{A}, \tilde{\mathbf{A}}) \quad = \quad \min_{\mathbf{e}\neq\mathbf{0}} \sum_{l=1}^{L} \mathbf{e}(l)^T \Delta \mathbf{e}(l) \tag{4.95}$$

■

Lemma 4A.3: Capacity of Correlated Channels

The determinant of E

$$E = (\mathbf{I}_n + \rho\Delta) \tag{4.96}$$

is given by

$$\det(E) = \left[(1+\rho(1-\delta))^n \cdot \left(1 + \frac{n\rho\delta}{1+\rho(1-\delta)}\right)\right] \tag{4.97}$$

■

Proof

Following [78] and [112]:

$$\det(\mathbf{A})\det(\mathbf{D} + \mathbf{C}\mathbf{A}^{-1}\mathbf{B}) = \det(\mathbf{D})\det(\mathbf{A} + \mathbf{B}\mathbf{D}^{-1}\mathbf{C}) \tag{4.98}$$

where $\mathbf{A} \in \mathcal{R}^{m\times m}$, $\mathbf{D} \in \mathcal{R}^{n\times n}$, $\mathbf{B} \in \mathcal{R}^{m\times n}$ and $\mathbf{C} \in \mathcal{R}^{n\times m}$. Note that $\mathbf{A}$ and $\mathbf{D}$ are non-singular. We can represent (4.96) as follows:

$$\det(E) = \det\left((1+\rho(1-\delta))\,\mathbf{I} + \delta\rho \begin{bmatrix} 1 \\ 1 \\ \vdots \\ 1 \end{bmatrix} \begin{bmatrix} 1 & 1 & \dots & 1 \end{bmatrix}\right) \tag{4.99}$$

$$= (1+\rho(1-\delta))^n \det\left(\mathbf{I}_n + \frac{\delta\rho}{1+\rho(1-\delta)} \begin{bmatrix} 1 \\ 1 \\ \vdots \\ 1 \end{bmatrix} \begin{bmatrix} 1 & 1 & \dots & 1 \end{bmatrix}\right)$$

Let $\mathbf{A} = 1$, $\mathbf{D} = \mathbf{I}_n$, $\mathbf{C} = \begin{bmatrix} 1 \\ 1 \\ \vdots \\ 1 \end{bmatrix}$, and $\mathbf{B} = \frac{\delta\rho}{1+\rho(1-\delta)} \begin{bmatrix} 1 & 1 & \dots & 1 \end{bmatrix}$. Thus the determinant of E reduces to

$$\begin{aligned} \det(E) &= (1+\rho(1-\delta))^n \det(\mathbf{I}_n) \det(1 + \mathbf{B}\mathbf{I}_n\mathbf{C}) \\ &= \left[(1+\rho(1-\delta))^n \cdot \left(1 + \frac{n\rho\delta}{1+\rho(1-\delta)}\right)\right] \end{aligned} \tag{4.100}$$

■

Lemma 4A.4: Derivation of MMSE detectors

Given (4.41) and (4.70), find the weight vectors $\mathbf{w}_k$ and u_k by minimizing the cost (convex) function:

$$(\hat{\mathbf{w}}_k, \hat{u}_k) = \arg \min_{(\mathbf{w}_k, u_k)} \mathcal{E}\left[\|a_k - x_k\|^2\right] \tag{4.101}$$

where the expectation is taken over noise and the statistics of the data sequence. ■

Proof

The cost function is written as

$$\begin{aligned} C &= \mathcal{E}\left[\|x_k - a_k\|^2\right] \\ &= \mathcal{E}\left[\|(\mathbf{w}_k^H \mathbf{r} - u_k - a_k)\|^2\right] \\ &= \mathbf{w}_k^H \mathcal{E}[\mathbf{r}\mathbf{r}^H]\mathbf{w}_k - \mathbf{w}_k^H \mathcal{E}[\mathbf{r}(u+a)^*] - \mathcal{E}[\mathbf{r}(u_k+a_k)^*]^H \mathbf{w}_k + \mathcal{E}[(u_k+a_k)^2] \end{aligned} \tag{4.102}$$

where

$$\begin{aligned} \mathcal{E}[\mathbf{r}\mathbf{r}^H] &= \mathcal{E}[[\mathbf{h}_k a_k + \bar{\mathbf{H}}_k \mathbf{a}_k + \mathbf{v}][\mathbf{h}_k a_k + \bar{\mathbf{H}}_k \mathbf{a}_k + \mathbf{v}]^H] \\ &= \mathbf{h}_k \mathbf{h}_k^H + \bar{\mathbf{H}}_k \mathcal{E}[\mathbf{a}_k \mathbf{a}_k^H] \bar{\mathbf{H}}_k^H + \mathcal{E}[\mathbf{v}\mathbf{v}^H] \end{aligned} \tag{4.103}$$

and

$$\begin{aligned} \mathcal{E}[\mathbf{r}(u_k + a_k)^*] &= \mathcal{E}[[\mathbf{h}_k a_k + \bar{\mathbf{H}}_k \mathbf{a}_k + \mathbf{v}](u_k + a_k)^*] \\ &= \mathbf{h}_k + \bar{\mathbf{H}}_k \mathcal{E}[\mathbf{a}_k] u_k^* \end{aligned} \tag{4.104}$$

and $n_T - 1 \times n_T - 1$ matrix:

$$\mathcal{E}[\mathbf{a}_k \mathbf{a}_k^H] = \begin{bmatrix} 1 & \mathcal{E}(a_1 a_2^*) & \dots & \mathcal{E}(a_1 a_{n_T}^*) \\ \mathcal{E}(a_2 a_1^*) & 1 & \dots & \mathcal{E}(a_2 a_{n_T}^*) \\ \vdots & \vdots & \ddots & \vdots \\ \mathcal{E}(a_{n_T} a_1^*) & \mathcal{E}(a_{n_T} a_2^*) & \dots & 1 \end{bmatrix} \tag{4.105}$$

By assuming that the soft outputs of different substreams are independent, we can obtain

$$\begin{aligned}\mathcal{E}[\mathbf{a}_k\mathbf{a}_k^H] &= \begin{bmatrix} 1 & \mathcal{E}(a_1)\mathcal{E}(a_2^*) & \dots & \mathcal{E}(a_1)\mathcal{E}(a_{n_T}^*) \\ \mathcal{E}(a_2)\mathcal{E}(a_1^*) & 1 & \dots & \mathcal{E}(a_2)\mathcal{E}(a_{n_T}^*) \\ \vdots & \vdots & \ddots & \\ \mathcal{E}(a_{n_T})\mathcal{E}(a_1^*) & \mathcal{E}(a_{n_T})\mathcal{E}(a_2^*) & \dots & 1 \end{bmatrix} \\ &= \mathbf{I}_{n_T-1} - \mathrm{Diag}[\mathcal{E}[\mathbf{a}_k][\mathbf{a}_k]^H] + \mathcal{E}[\mathbf{a}_k]\mathcal{E}[\mathbf{a}_k]^H \end{aligned} \tag{4.106}$$

We use standard minimization techniques to solve the optimization problem formulated in (4.101). By setting $\frac{\partial C}{\partial u_k} = 0$ and $\frac{\partial C}{\partial \mathbf{w}_k} = 0$, and using (4.74), we get the following:

$$\begin{aligned} u_k - \mathbf{w}_k^H \bar{\mathbf{H}}_k \mathcal{E}[\mathbf{a}_k] &= 0 \\ u_k &= \mathbf{w}_k^H \mathbf{z} \end{aligned} \tag{4.107}$$

and

$$\begin{aligned} \left[\mathbf{h}_k\mathbf{h}_k^H + \bar{\mathbf{H}}_k(\mathcal{E}[\mathbf{a}_k\mathbf{a}_k^H])\bar{\mathbf{H}}_k^H + \mathcal{E}[\mathbf{v}\mathbf{v}^H]\right]\mathbf{w}_k - \bar{\mathbf{H}}_k\mathcal{E}[\mathbf{a}_k]u_k^* &= \mathbf{h}_k \\ (\mathbf{P} + \mathbf{S} + \Sigma_{n_R})\mathbf{w}_k - \mathbf{z}u_k^* &= \mathbf{h}_k \end{aligned} \tag{4.108}$$

Solving (4.107) and (4.108), we get

$$\mathbf{w}_k = (\mathbf{P} + \mathbf{Q} + \Sigma_{n_R})^{-1}\mathbf{h}_k \tag{4.109}$$

This completes the proof of (4.72). ■

Chapter 5

Experimental Verification of TURBO-BLAST

In the previous chapter, we proposed a novel multi-transmit multi-receive (MTMR) antenna system for wireless communications. This system, called T-BLAST, uses a random space-time encoder and a turbo-like iterative decoder. Most important, the proposed system achieves a superior performance compared to V-BLAST after 2 to 4 iterations of the receiver.

The goal of this chapter is to present experimental results, based on real-life data collected using the Bell-Labs experimental multiple antenna system with eight transmit and five to six receive antennas. The results confirm the virtues of T-BLAST.

This chapter begins by describing the indoor narrow-band test-bed and the Digital Signal Processing (DSP) operations at the receiver. Then the bit error and frame error performances of T-BLAST configuration are presented for the eight transmit and five to six receive antennas.

5.1 The Bell Lab's BLAST Test-Bed

The data set was acquired with the cooperation of the Department of Wireless Communications Research, Lucent Technologies, Bell Laboratories at Holmdel, New Jersey and was

collected using the indoor narrow-band BLAST test-bed located on the 2nd floor of the Crawford-Hills Laboratory [1].

5.1.1 Indoor Test-Bed

The hardware components of the test-bed consist of a radio frequency (RF) front-end with an antenna array and the corresponding array of analog RF transmitters and receivers. The antenna arrays consist of wire dipoles mounted in various (horizontal and vertical polarizations) arrangements, with about half-wavelength separation between adjacent elements. The system operates at a carrier frequency of 1.95 GHz with 30 kHz signal bandwidth.

The DSP multiprocessor system used to execute the baseband digital signal processing is a Pentek 4285, which consists of eight Texas Instrument's TM320C40 DSP's. The total processing power of the DSP is 400 MIPS. The analog RF transmitters and receivers are interfaced to the baseband inputs and outputs, using a system of multi-channel A/D (Pentek 4275) and D/A (Pentek 4253) converters. The maximum sampling rate is 100 kHz per baseband channel. A detailed description of this BLAST test-bed is given in [3] and [26].

5.1.2 Transmitter

In the experiment, 100 different channel conditions are considered. At each channel condition, packets of 132 $\pi/4$-shifted QPSK modulated symbols per antenna are transmitted at a rate of 25 kilo-symbols/s. Among those 132 symbols, the first 32 symbols are dedicated to synchronization and training:

1. Synchronization: The first 16 symbols are used for frame and symbol timing recovery.

2. Training Sequence: The next 16 symbols (symbols 17 to 32) are for matrix channel response estimation. For each substream, mutually orthogonal and equal power training sequences are generated by using 16-dimensional Hadamard sequences.

[1] The experiments were carried out during September to December, 2000, while the author of this thesis was an intern at Luecnt. The cooperation and help provided by personnel of Lucent are gratefully acknowledged.

3. Information Symbols: The last 100 symbols (200 bits) are for information transmission. In the transmit end, each substream of 100 information bits is independently encoded using a convolutional code with rate $R = 1/2$, constraint length 3, and then interleaved using space-time interleavers. The space interleavers are designed according to the diagonal-BLAST architecture but with no edge wastage [9]. The time interleavers are chosen randomly and no attempt is made to optimize their design.

5.1.3 Receiver

At the receiving end, the signal detection process involves the following operations:

1. Frame initialization: The receiver waits until it finds a sufficiently strong signal to indicate the start of data transmission.

2. Symbol synchronization: The sampled received signal is cross-correlated with a predefined synchronization sequence and the condition that results in highest cross correlation is used to establish symbol synchronization. The received signal is oversampled with four samples per symbol period. Binary Barker sequences are used for synchronization because of their good autocorrelation properties.

3. Hardware induced inter-symbol interference (ISI) mitigation: The spectrum shaped with an analog low-pass filter is usually distorted by the radio-frequency front-end of the transmitter during the transmission process. The ISI caused by the spectrum shaping and its distortions is mitigated by a precalculated fixed-coefficient FIR filter.

4. Channel Estimation: The matrix channel response is estimated by using a mutually orthogonal 16-dimensional Hadamard sequence transmitted for training purpose between the parallel antennas.

5. Information Recovery: An iterative decoder is used to recover the transmitted signals. In this scheme, we separate the receiver into two stages: soft interference cancellation detector, and a set of parallel soft-input/soft-output (SISO) channel decoders. Extrinsic information learned from one stage is applied to the other stage iteratively

until the receiver converges. These two stages of processing are separated by the corresponding space-time interleavers and de-interleavers. Detailed explanations of the algorithm can be found in chapter 4. In particular, the algorithm used in this experiment is given in equation (4.77).

5.2 Performance Results

The tests were carried out in an indoor environment with about ten meters separation between the transmitter and receiver. The experimental results are summarized as follows:

5.2.1 Experiments with (8,6)-BLAST

This section discusses the performance of T-BLAST using the Bell-Labs test-bed with eight transmit and six receive antennas.

Bit Error Rate

Figure 5.1 displays the bit error rate performance of T-BLAST at each iteration of the receiver. Here the instantaneous (broken trace) and average (solid trace) BER are demonstrated at each iteration.

Subplots 1 and 2 show the bit error performance, respectively, before decoding the detected coded signals (200 bits/packet) and the decoded information signals (100 bits/packet) at the first iteration. As expected, the second scheme performs better due to the coding gain. However, the performance at the first iteration is poor since each substream (transmit antenna) sees all the other (seven) parallel substreams as interference. The subsequent subplots 3-6 show the bit error performance at iterations 2-5. These figures clearly illustrate a significant performance improvement in the course of a few iterations. The first three iterations are sufficient to achieve a significant performance gain. Evidently, the performance gain due to the subsequent iterations (4 and 5) is minimal.

Frame Error

In Figure 5.2, we show the corresponding bit error traces in each packet and the packets in error. In accordance with Figure 5.1, subplot 1 shows the receiver bit error trace (out of 200 bits/packet) at each packet with no channel encoding. The subsequent subplots 2-6 show the bit error traces (out of 98 information bits/packet) at iterations 1-5. The iterative action of the receiver significantly reduces the packet error rate.

With no channel encoding, 100-150 bits were detected incorrectly in each packet; indeed a hundred percent packet error rate was occasionally observed. With channel encoding, the number of errors in each packet is reduced to below 15 and the packet error rate is reduced by over twenty five percentage. In fact, the packet error rate is reduced further to seventeen percent at iteration 2. Thereafter, only about 4 packets are corrupted and among the corrupted packets only 1-2 bits, are in error per packet. Even though the frame error performance is converged at iteration 3, the appearance and the disappearance of errors is observed between packets, from iteration 3 to 6. However, a packet error rate of $4 - 5\%$ is maintained. For example, at iteration 3, packets 7, 35, 50 and 75 are in error whereas at the iteration 5, packets 15, 35, 50 and 75 are in error.

Signal-Space Diagram

Another measure of convergence of the iterative receiver is the mean-squared error (MSE) between the detected signals and the transmitted constellation points in the signal-space diagram. Here we consider two examples. First, we show a packet of data that has converged to zero bit error in three iterations. The second example shows the appearance and the disappearance of errors from one iteration to the next.

Example 1: Perfect Convergence

In this example we illustrate a perfect convergence behavior. Figure 5.3 displays the soft-decoded signals in the signal-space diagram for packet 1. Here the x and y axes represent the real and imaginary parts of the $\pi/4$-shifted QPSK signal, respectively. Subplot 1 shows

the positions of the 200×8 coded bits, whereas subplots 2-9 show the positions of the 98×8 decoded bits at iterations 1-8 of the T-BLAST receiver.

The corresponding MSEs of the detected soft bits are shown in Figure 5.4. A bit error occurs if the MSE exceeds 1. MSE between 0 and 1 means that a bit is classified appropriately but has residual error that can propagate through the soft interference cancellation receiver. Subplot 1 shows the MSE before decoding and almost all the bits have residual error and about thirty percent of them are detected incorrectly. The figure illustrates how the test error decreases as iterations are added to the receiver. In particular, all the bits have been detected correctly in three iterations.

Example 2: Appearance and Disappearance of errors

In this example, we illustrate the appearance and disappearance of errors from one iteration to the next. Figure 5.5 displays the soft decoded signals in the signal-space diagram for packet 2. The corresponding MSEs of the detected soft bits are shown in Figure 5.6. From the figures, we observe the following:

- The residual errors do not converge within eight iterations.
- All the bit errors are corrected at iteration 3. However, a single bit error appears in the fourth, sixth, and eight iterations and disappears during the fifth and seventh iterations, which shows the appearance and disappearance of errors in the course of convergence.

In both examples, little benefit results from increasing the number of iterations beyond three; thus it is reasonable to accept this number as the practical number of iterations in terms of both error reduction and receiver complexity. Moreover, this point is also borne out by the average performance, Figure 5.7, over the hundred packets versus the number of iterations (solid trace). Note that the broken trace shows the performance assuming no channel coding.

5.2.2 Experiments with (8,5)-BLAST

The above tests were repeated with eight transmit and five receive antennas. Even though the performance decreased from the previous experiment, good convergence behavior is still observed. Figures 5.8 and 5.9 display the soft-decoded signals in the signal-space diagram and the corresponding MSEs of the detected soft bits, respectively. In contrast to the previous experiment, five iterations were needed to achieve a perfect convergence. This point is also borne out by the average performance, Figure 5.10, over the hundred packets versus the number of iterations (solid trace). The broken trace shows performance without channel coding.

5.3 Summary

Previously, the BLAST test-bed has been used to demonstrate uncoded V-BLAST architecture [3] for 8 transmit and 12 receive antennas. However, a major limitation of V-BLAST is its inability to work with fewer receive antennas than transmit antennas. The ability to work with fewer receivers than transmitters is necessary in most cellular systems since the base station is typically designed with more antennas than mobile transceivers.

In contrast, T-BLAST accommodates any multiple antenna configuration, including the case of fewer receive antennas than transmit antennas with manageable computational complexity. The experimental results using real-life indoor wireless communication data presented herein confirm the practical virtues of T-BLAST.

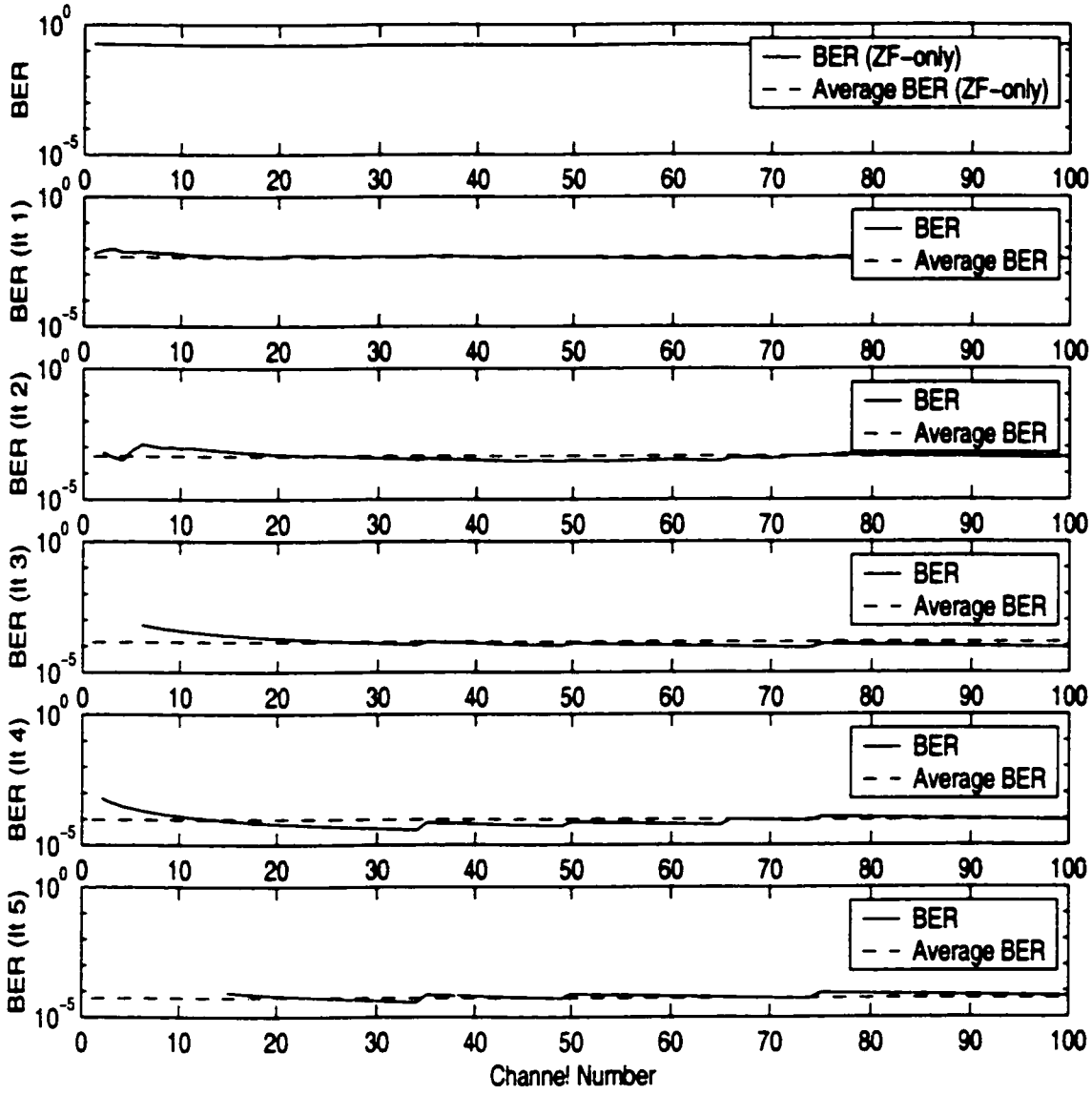

Figure 5.1: Bit-error performance of T- BLAST, n_T=8 and n_R=6 with convolutional code of rate $R = 1/2$ and constraint length 3, and $\pi/4$-shifted QPSK modulated.

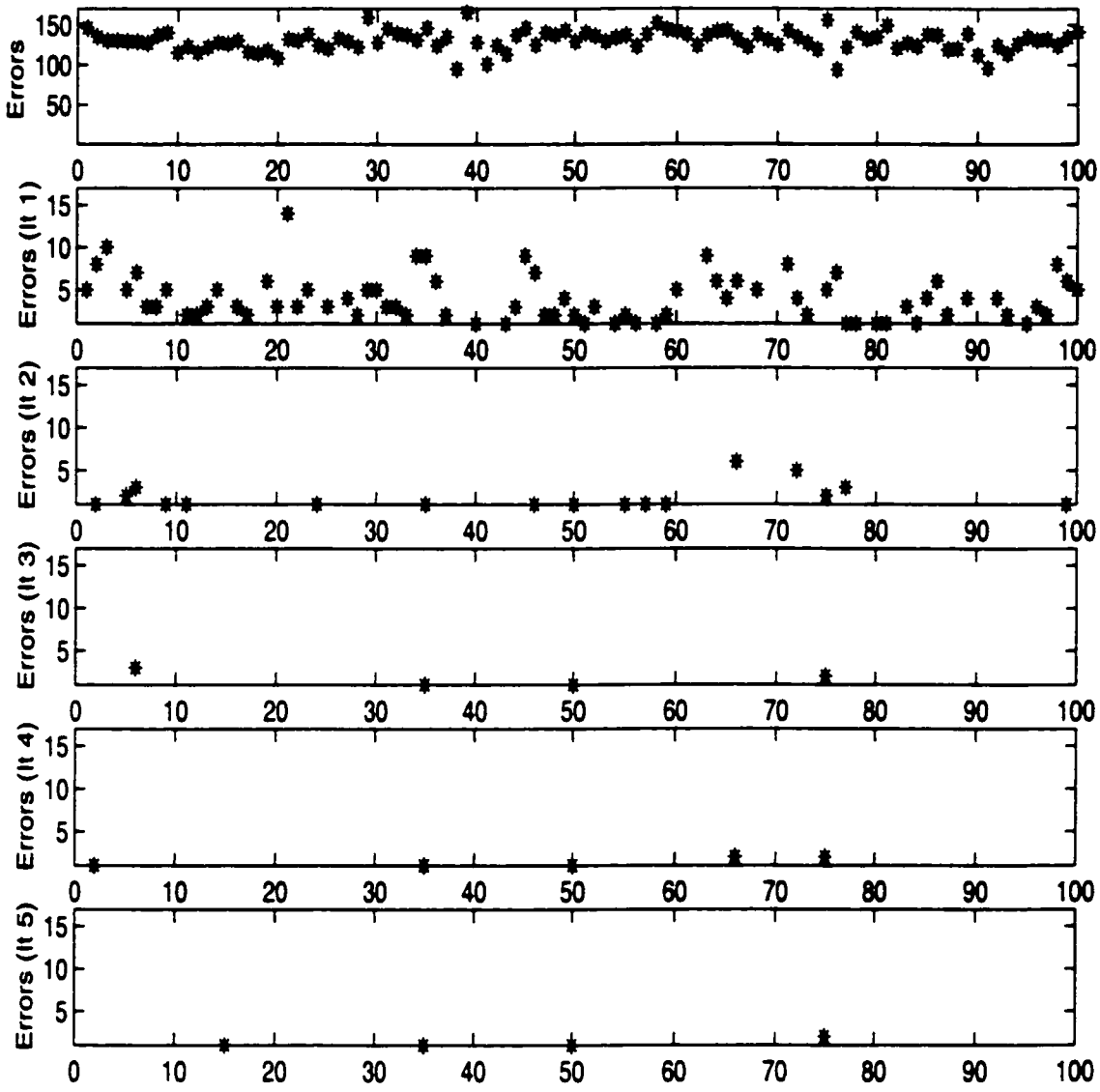

Figure 5.2: Number of errors vs packets in T-BLAST, n_T=8 and n_R=6 with convolutional code of rate $R = 1/2$ and constraint length 3, and $\pi/4$-shifted QPSK modulation.

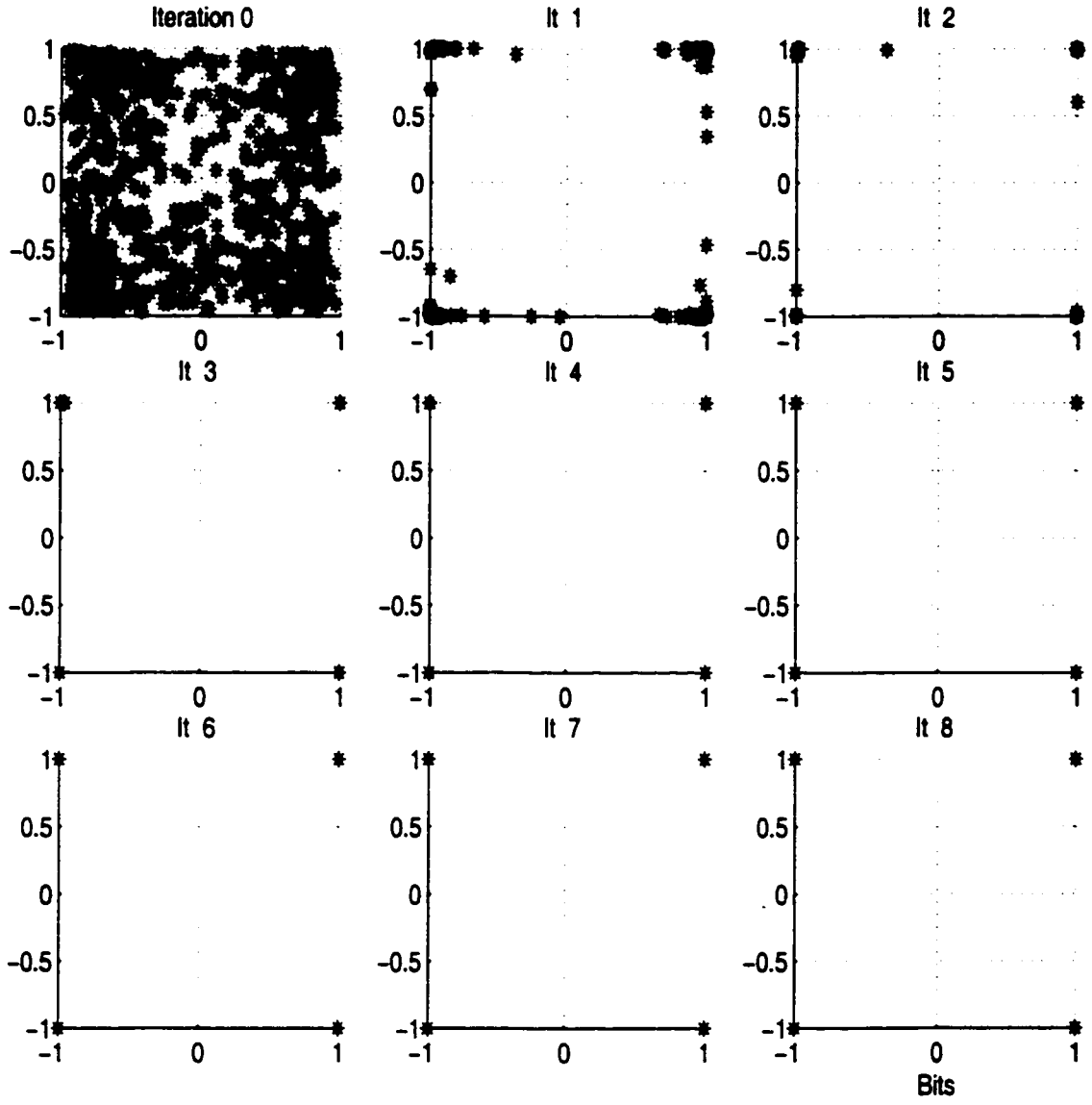

Figure 5.3: Signal-space diagram at the receiver output in T-BLAST for packet 1, n_T=8 and n_R=6 with convolutional code of rate $R = 1/2$ and constraint length 3, and $\pi/4$-shifted QPSK modulation.

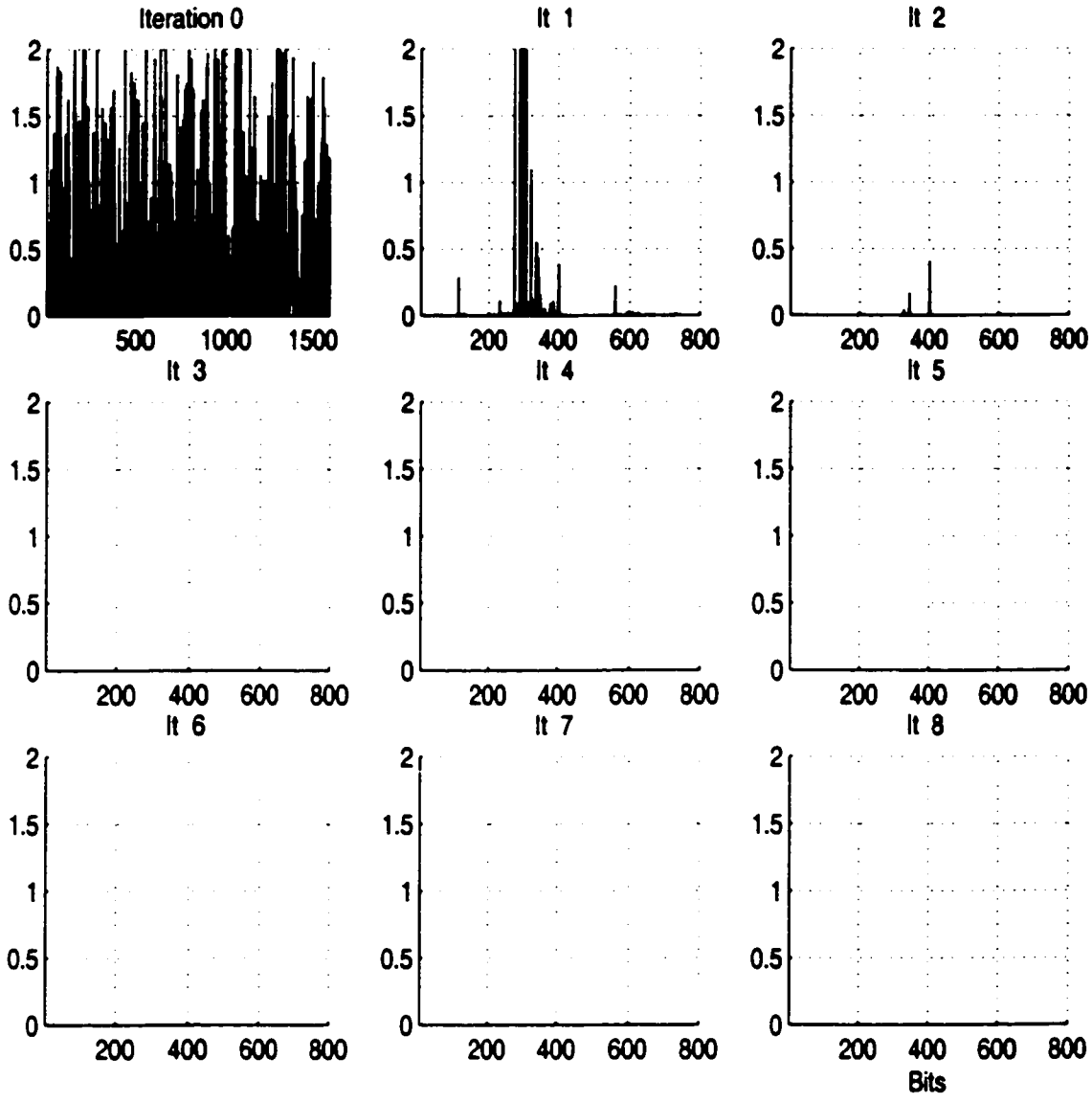

Figure 5.4: Mean-squared error at the receiver output of T-BLAST for packet 1, n_T=8 and n_R=6 with convolutional code of rate $R = 1/2$ and constraint length 3, and $\pi/4$-shifted QPSK modulation.

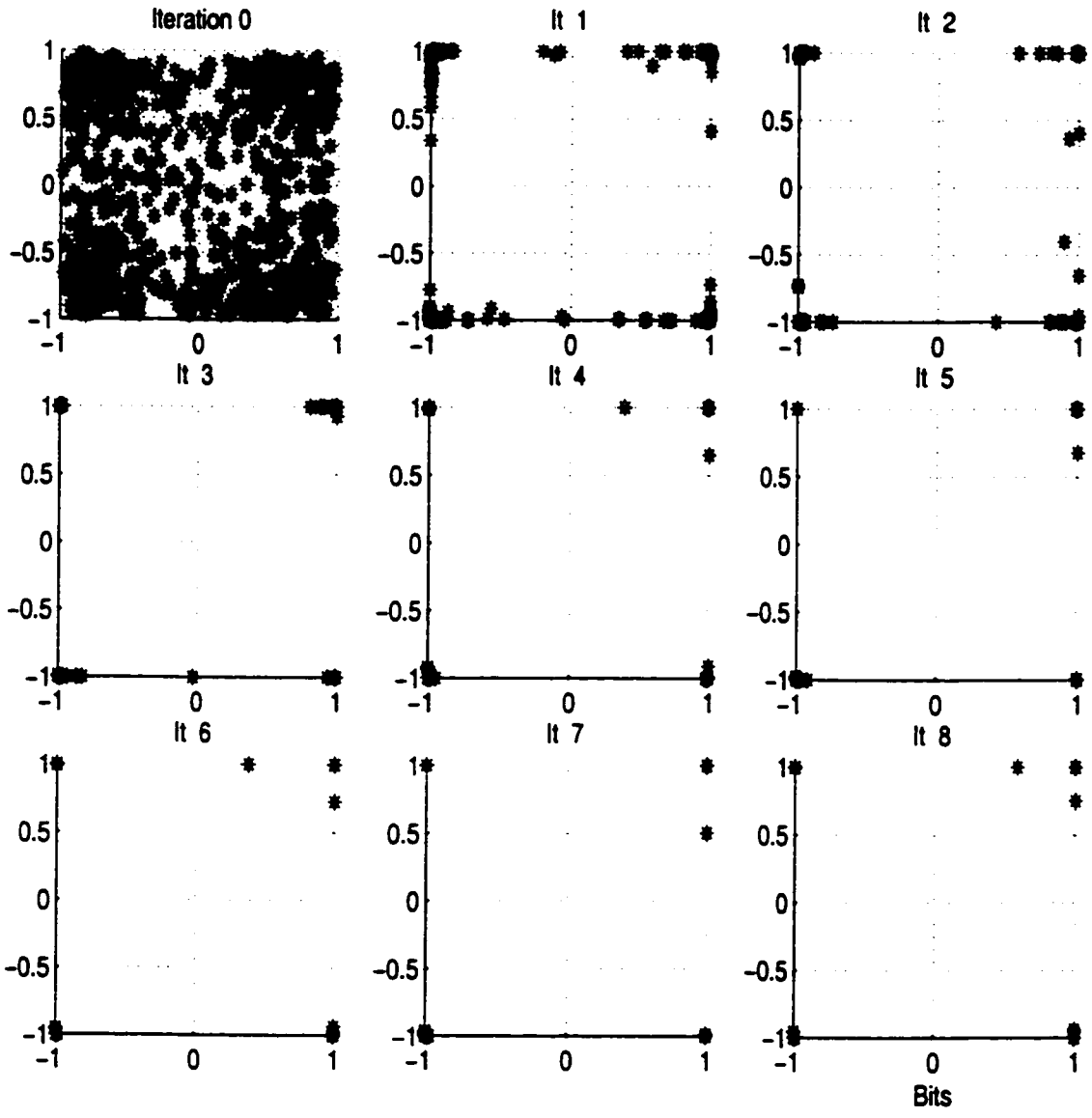

Figure 5.5: Signal-space diagram at the receiver output for packet 2 in T-BLAST, n_T=8 and n_R=6 with convolutional code of rate $R = 1/2$ and constraint length 3, and $\pi/4$-shifted QPSK modulation.

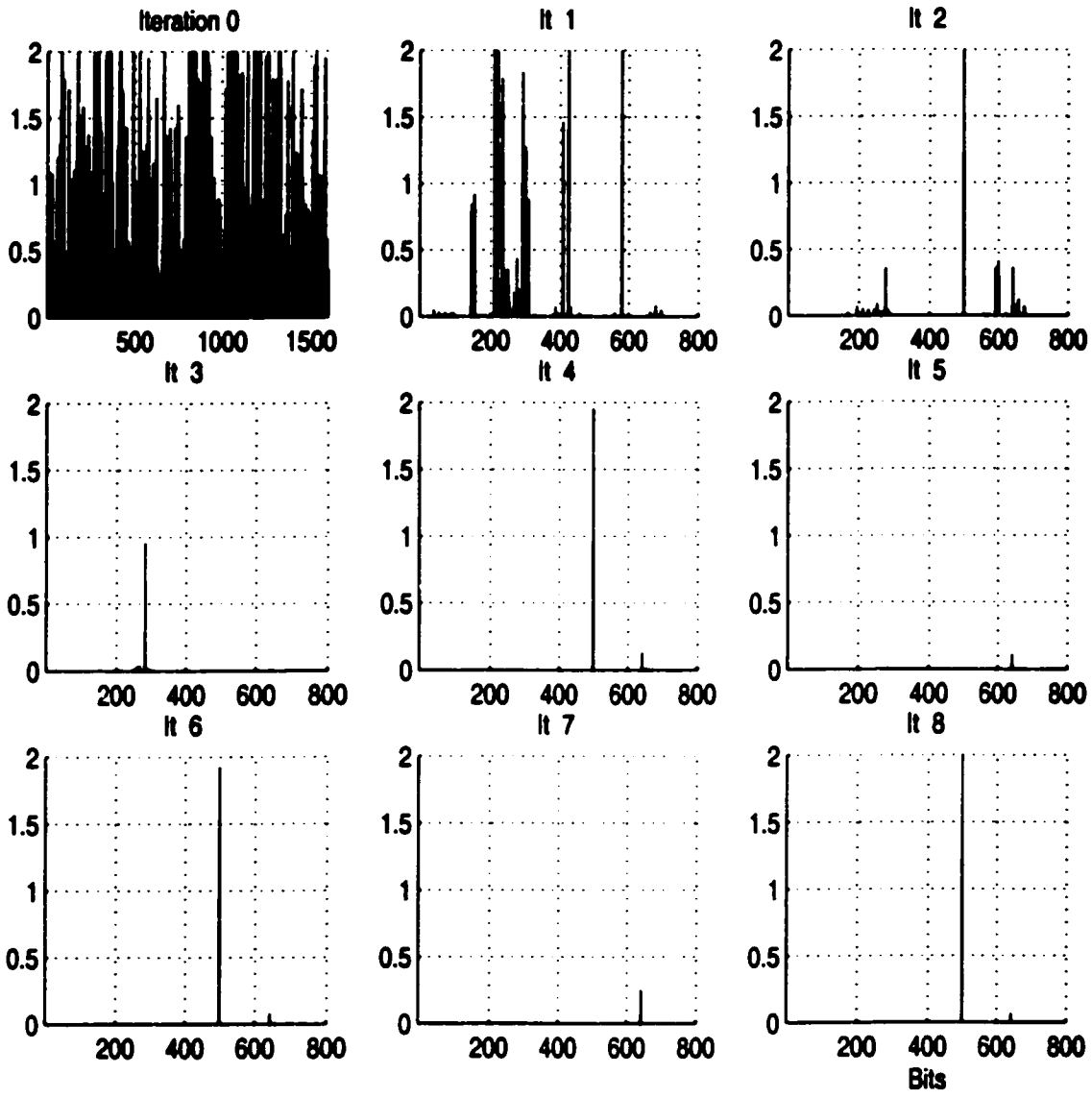

Figure 5.6: Mean-squared error at the receiver output of T-BLAST for packet 2, n_T=8 and n_R=6 with convolutional code of rate $R = 1/2$ and constraint length 3, and $\pi/4$-shifted QPSK modulation.

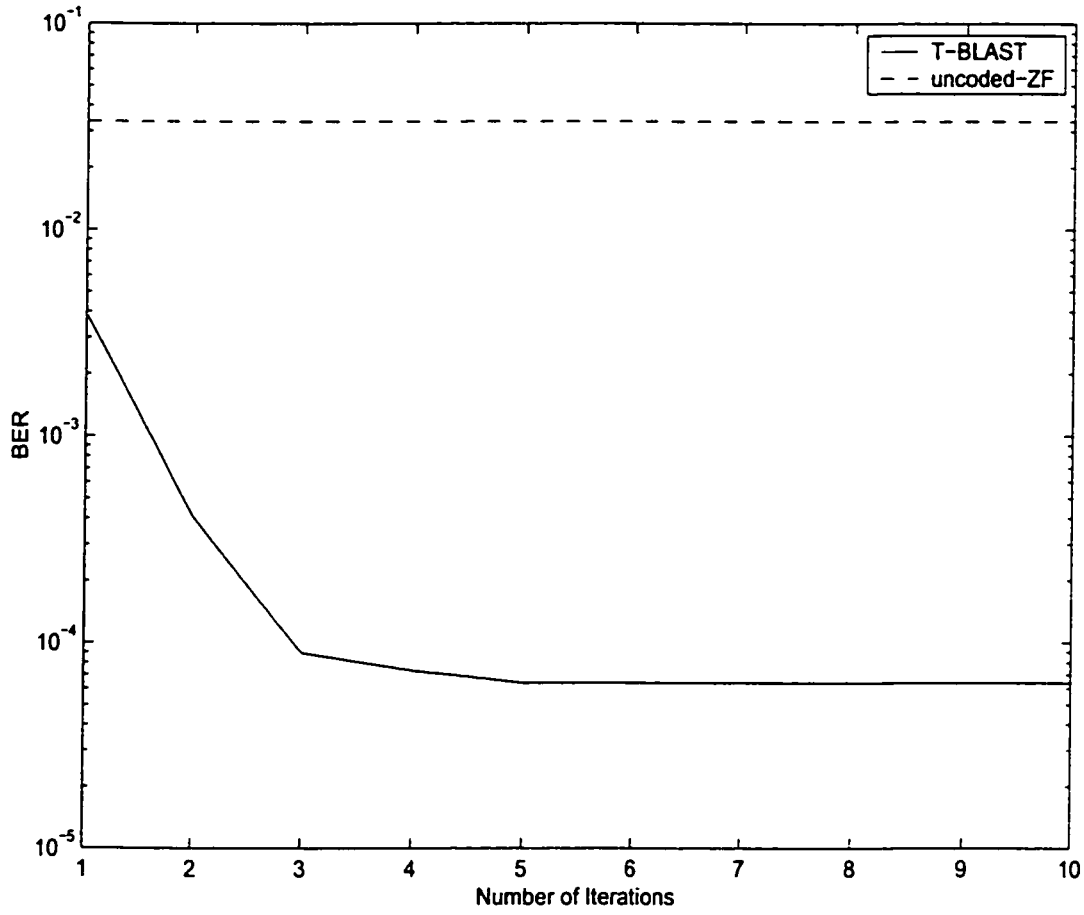

Figure 5.7: Average BER performance vs iterations of T-BLAST with and without encoding, n_T=8 and n_R=6 with convolutional code of rate $R = 1/2$ and constraint length 3, and $\pi/4$-shifted QPSK modulation.

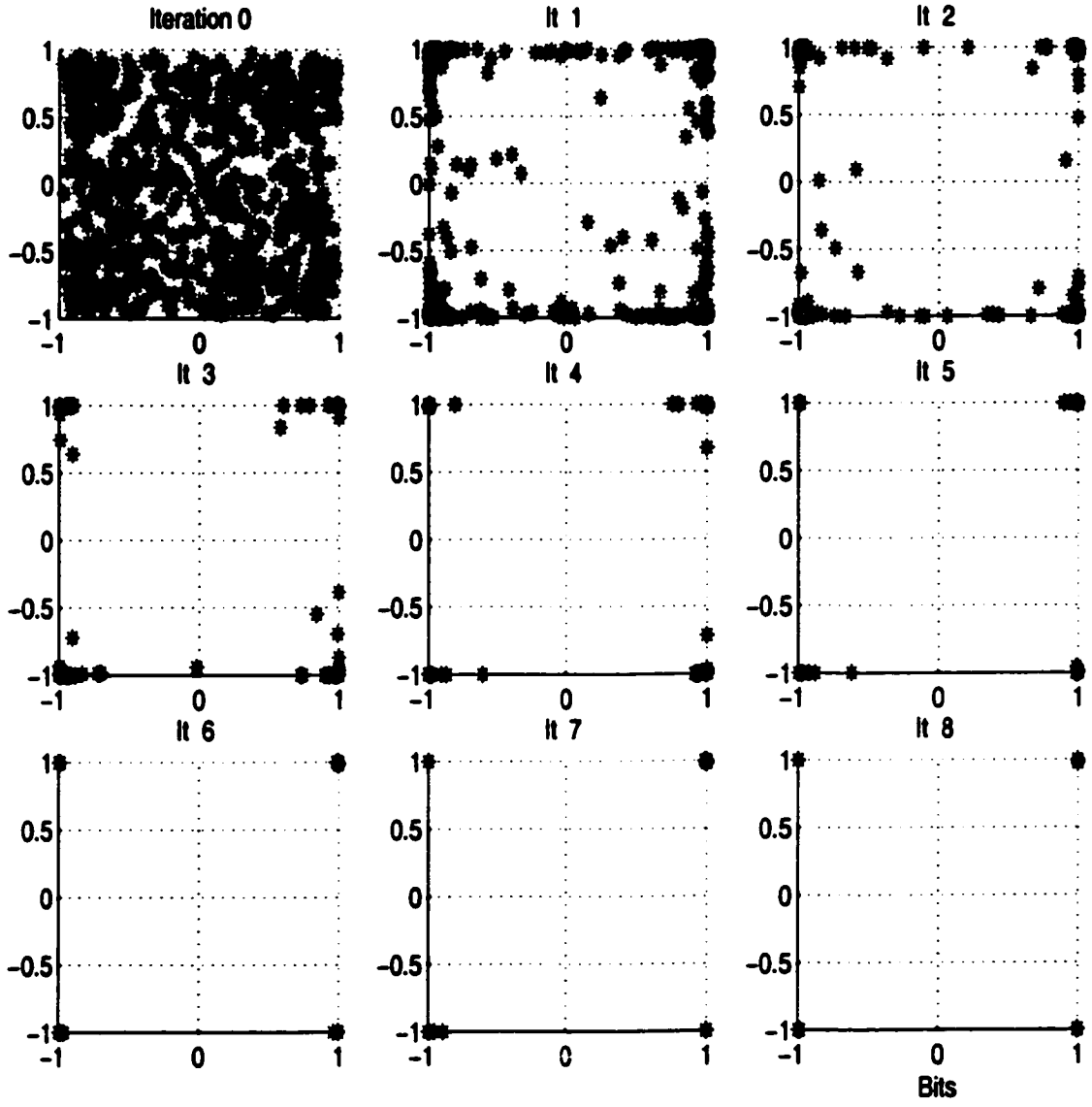

Figure 5.8: Signal-space diagram at the receiver output for packet 1 in T-BLAST, n_T=8 and n_R=5 with convolutional code of rate $R = 1/2$ and constraint length 3, and $\pi/4$-shifted QPSK modulation.

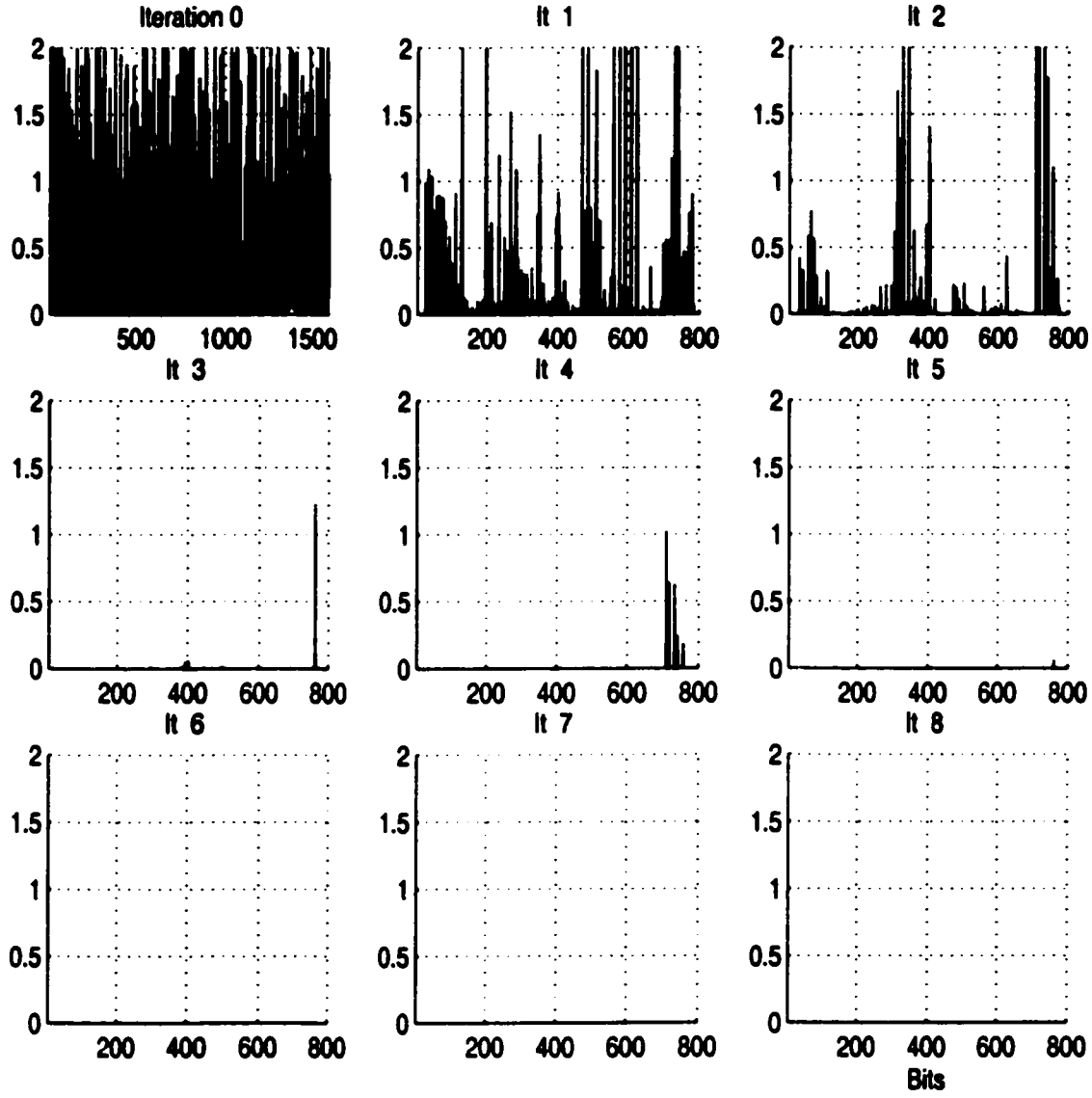

Figure 5.9: Mean-squared error at the receiver output of T-BLAST for packet 1, n_T=8 and n_R=5 with convolutional code of rate $R = 1/2$ and constraint length 3, and $\pi/4$-shifted QPSK modulation.

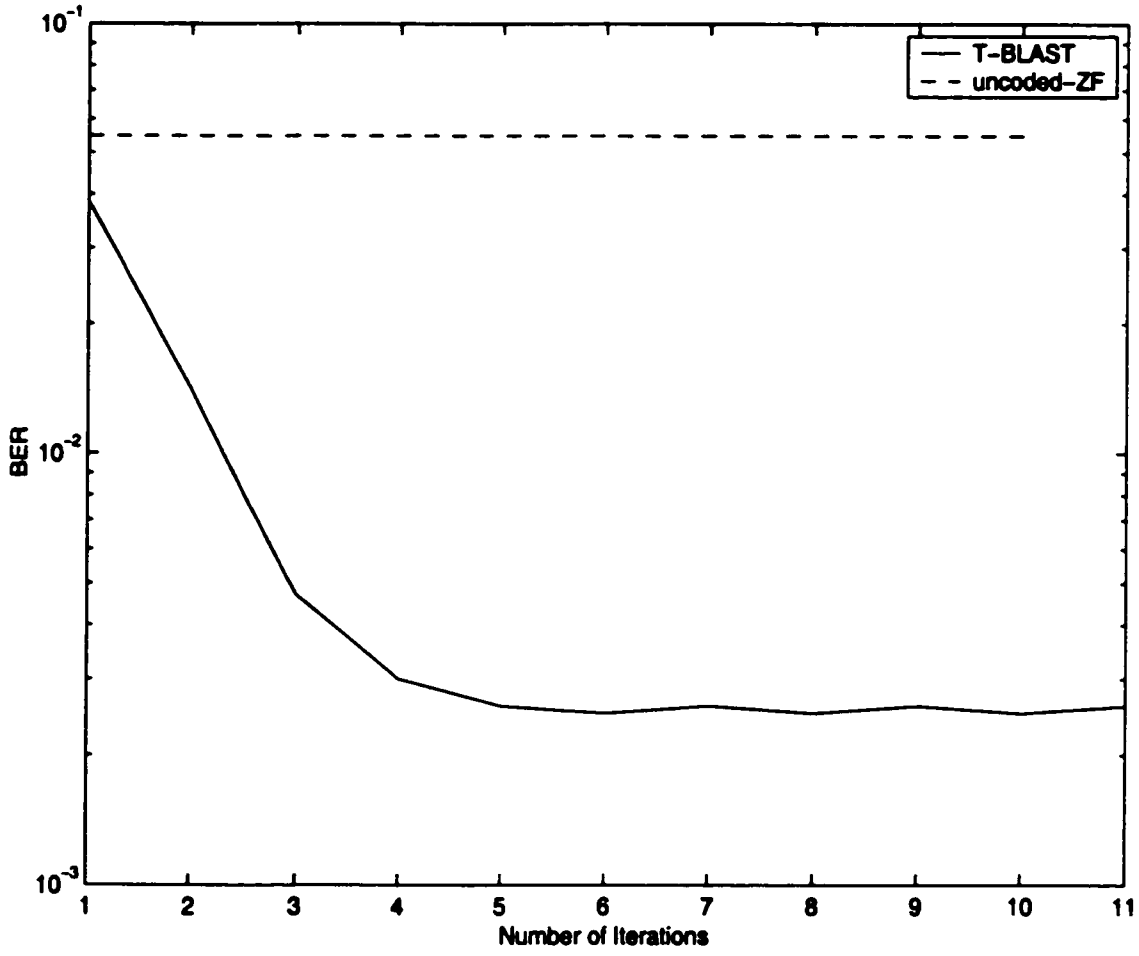

Figure 5.10: Average BER performance vs iterations of T-BLAST with and without encoding, n_T=8 and n_R=5 with convolutional code of rate $R = 1/2$ and constraint length 3, and $\pi/4$-shifted QPSK modulation.

Chapter 6

Spectral Efficiency of TURBO-BLAST

Two properties underline the hallmark of Turbo-BLAST:

- The error performance of T-BLAST improves with the number of iterations of the decoding algorithm. This is achieved by feeding extrinsic information from the output of one decoding stage to the input of the next decoding stage, which permits the iterative decoding process to take its natural course in response to the received noisy signal and channel code constraint. Most important, the system is capable of achieving performance better than V-BLAST in the course of 2-4 iterations.
- As the number of iterations approaches infinity, the performance of T-BLAST approaches the Shannon theoretical limit of channel capacity.

This chapter concentrates on illustrating the above properties of T-BLAST, for both indoor and outdoor environments, under various antenna configurations. To show the second property, we use an empirical evaluation of the spectral efficiency achievable with specified channel codes and modulation. We have taken this approach because the development of a theoretical framework for the spectral efficiency of T-BLAST is a very difficult undertaking. We proceed by fixing the target bit error rate to be achieved by T-BLAST and V-BLAST

(for comparison) and then derive the signal-to-noise ratio (SNR) necessary for the task at hand. Most important, the empirical evaluations are made using real-life data for both indoor and outdoor fixed wireless communications environments.

6.1 System Description

6.1.1 T-BLAST System

In the transmit end, each substream of 100 information bits is independently encoded using a rate 1/2 convolutional code generator (7,5) and then interleaved using space-time interleavers. The space interleavers are designed according to the diagonal-BLAST architecture but with no edge waste (see section 4.2.2). The time interleavers are chosen randomly and no attempt is made to optimize their design.

At the receiving end, an iterative decoder is used to recover the transmitted information bearing signals. In this scheme, we separate the receiver into two stages: soft interference cancellation detector, and a set of parallel soft-input/ soft-output (SISO) channel decoders. The extrinsic information learned from one stage is applied to the succeeding stage iteratively until the receiver reaches convergence. These two stages of processing are separated by the corresponding space-time interleavers and de-interleavers. See chapter 4.7.4, equation (4.77), for the algorithm used in the experiments.

6.1.2 Coded V-BLAST System

V-BLAST is typically assumed as an uncoded BLAST system, where the term "uncoded" refers to the absence of space-time or inter-substream coding. However, each antenna output could be channel encoded independently. We refer to horizontal coded V-BLAST when each of the substreams is provided with an amount of channel coding equal to that used in T-BLAST. Note that V-BLAST does not use any space-time coding or iterative decoding. The V-BLAST algorithm used here has the following major steps: finding the optimal order of detection; decoding the strongest signal using minimum mean-squared error (MMSE) nulling vectors, and maximum *a posteriori*-based SISO channel decoders;

cancellation of interference due to the decoded signal using hard decisions; finding and decoding the strongest signal component of the remaining signals, and so on.

6.2 Indoor Environment

This section describes the performance of QPSK modulated T-BLAST and the coded V-BLAST using indoor real-channel measurements on various MTMR configurations. The estimated signal-to-noise ratio of the real-life system is roughly between 9-12dB. In this chapter, we synthesize the received signal using the measured channel characteristics and evaluate the performance of T-BLAST over a wide range of SNR's using various BLAST combinations. In all the experiments presented herein, it is assumed that the exact channel matrix is known.

6.2.1 T-BLAST vs V-BLAST, $n_T = n_R = 8$

The goal of this experiment is to illustrate the superior performance of T-BLAST over V-BLAST when equal numbers of transmit and receive antenna elements are used in a BLAST configuration. In Figure 6.1, we compare the bit error rate performance of the following schemes:

- Scheme 1: T-BLAST with $n_T = n_R = 8$,
- Scheme 2: Coded V-BLAST with $n_T = n_R = 8$,
- Scheme 3: V-BLAST with $n_T = n_R = 8$,
- Scheme 4: V-BLAST with $n_T = 4$, $n_R = 8$.

Note that T-BLAST gives the best performance obtained within the first 10 iterations. The maximum possible information rate of T-BLAST and coded V-BLAST with $n_T = n_R = 8$ is 8 bits /channel use whereas the information rate of the uncoded V-BLAST with $n_T = n_R = 8$ is 16 bits/channel use. The purpose of introducing an uncoded V-BLAST

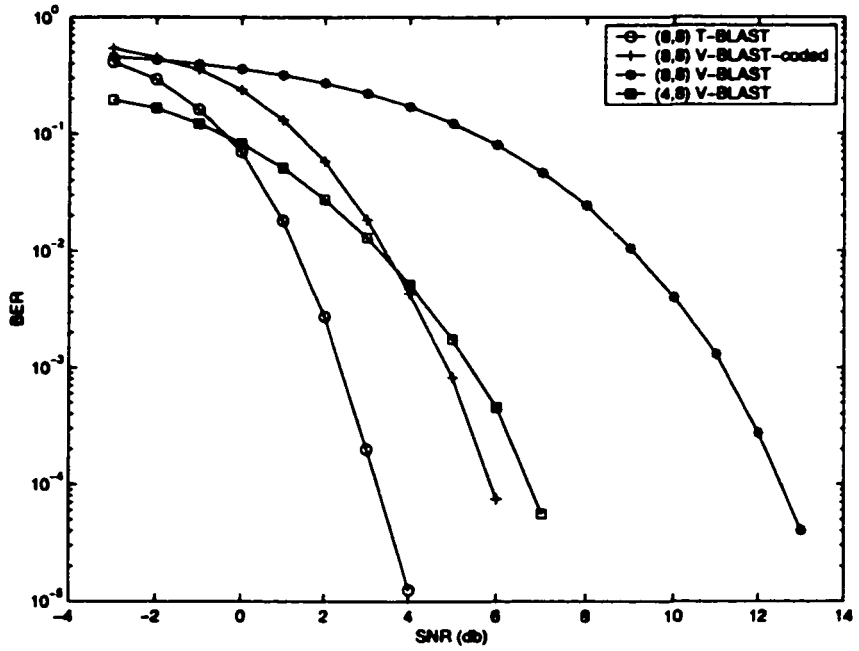

Figure 6.1: T-BLAST vs V-BLAST using real channel measurements for $n_T = n_R = 8$, using convolutional code with rate $R = 1/2$ and constraint length 3, and QPSK modulation.

with $n_T = 4$ and $n_R = 8$ is to compare the performance of T-BLAST with an uncoded system that has information rate equal to 8 bits/channel use.

As expected the performance of uncoded V-BLAST with $n_T = n_R = 8$ is inferior to all of the other schemes, whereas a significant gain (2-3dB) is achieved by the T-BLAST scheme over the coded V-BLAST with $n_T = n_R = 8$ and uncoded V-BLAST with $n_T = 4$ and $n_R = 8$. Moreover, the performance of uncoded V-BLAST with $n_T = 4$ and $n_R = 8$ outperforms that of the coded V-BLAST with 8 transmit and receive antennas for SNR between -3dB to 5dB.

The complexity of the iterative receiver used in the T-BLAST increases with the number of iterations. However, most of the iterative gain is achieved within 3 to 4 iterations. To confirm this, over a wide range of SNR values, we show in Figure 6.2 the BER performance versus SNR for T-BLAST (solid traces) at iterations 1,2,3,4 and 8 along with the performance of coded V-BLAST (broken trace).

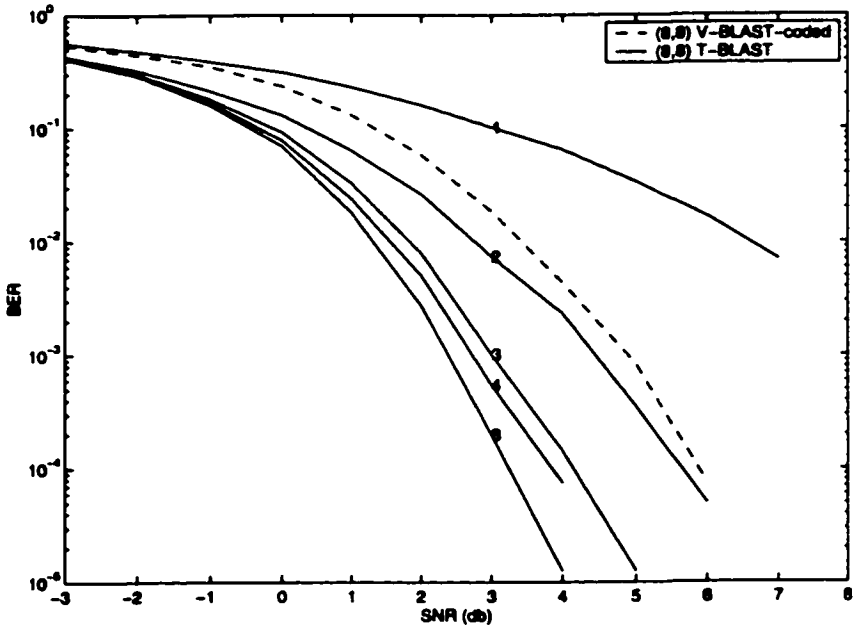

Figure 6.2: BER performance of T-BLAST with increasing iterations, using the real channel measurements for $n_T = 8$ and $n_R = 8$, using convolutional code with rate $R = 1/2$ and constraint length 3, and QPSK modulation.

The figure illustrates how the test error decreases as the number of iterations in the receiver is increased. Moreover, T-BLAST outperforms V-BLAST in two iterations. Little benefit results from increasing the number of iterations beyond three. Thus, it is reasonable to accept this number as the near optimal number of iterations in terms of both error reduction and receiver complexity.

Finally, in Figure 6.3, bit error rate (BER) versus the number of iterations at SNR = 4dB is plotted. Naturally, the V-BLAST system uses hard decisions and is therefore independent of the number of iterations. In direct contrast, the performance of both T-BLAST systems, which use soft decisions, improves with iterations and approaches the convergent limit in about 7 iterations but performance gain after iteration 3 is minimal.

Remark 10 *T-BLAST attains an information transmission rate of 8 bits /channel use at SNR=2dB. The channel capacity at SNR=2dB is 9.14 bits/channel use. Coded V-BLAST with $n_T = n_R = 8$ achieves its full information rate, that is, 8 bits/channel use at SNR=5dB.*

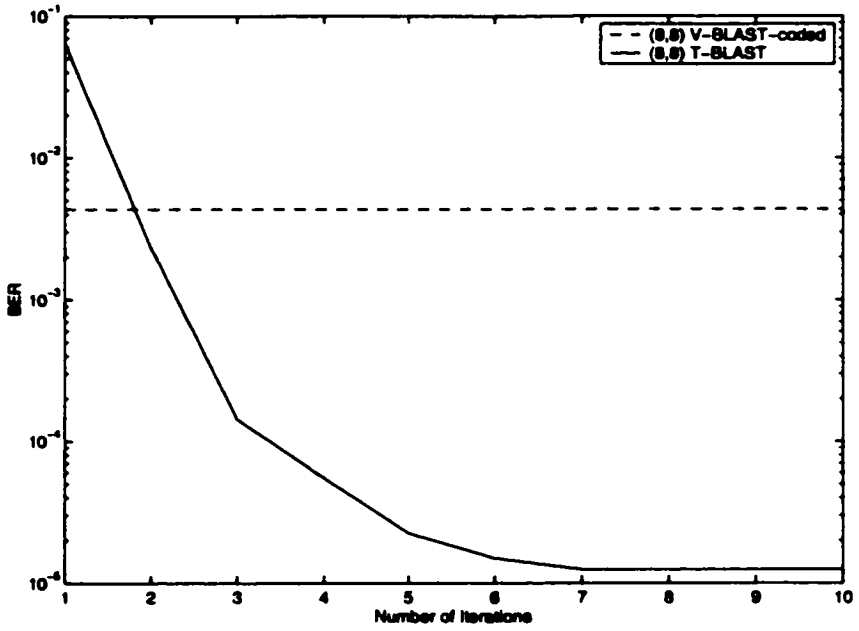

Figure 6.3: Convergence behavior of the T-BLAST receiver at SNR=4dB for (n_T=8, n_R=8), using convolutional code with rate $R = 1/2$ and constraint length 3, and QPSK modulation.

Note that the channel capacity at SNR=5dB is 13.43 bits/channel use.

6.2.2 T-BLAST vs V-BLAST, $n_T = 5, 6, 7$ and $n_R = 8$

In this section, we consider BLAST configurations with fewer transmit antennas than receive antennas. Figure 6.4 displays the bit error rate performance of T-BLAST (solid trace) and coded V-BLAST (broken trace) for antenna configurations of 8 receive and 5-8 transmit antennas. Note that the T-BLAST performance measure gives us the best performance obtained within the first 10 iterations. The following observations can be made from Figure 6.4:

- The bit error performance of both V-BLAST and T-BLAST improves with decreasing number of transmitters, with T-BLAST outperforming V-BLAST in all four cases.
- In terms of V-BLAST performance, a substantial gain in bit error rate performance

is realized with fewer transmit antennas. In particular, V-BLAST falls short of T-BLAST performance by a wide margin for more transmit antennas. For example, T-BLAST achieves 2-3dB gain over V-BLAST for $n_T = 7$ and $n_R = 8$, whereas only 0.5dB gain is attained when $n_T = 5$ and $n_R = 8$.

To see the convergence property of the iterative decoders used in T-BLAST, we plotted the BER vs number of iterations at SNR=4dB and BER vs SNR for 1,2,3,4,8 and 10 iterations in Figures 6.5 and 6.6, respectively, for (7,8) BLAST configuration. From these figures, we observe that the performance of T-BLAST exceeds that of V-BLAST in two iterations. Figure 6.5 reveals a new phenomenon observed in the T-BLAST algorithm: susceptibility to the appearance and disappearance of errors in some packets, which causes oscillations at the tail end of curve. At first glance, the oscillations may seem to be a shortcoming of T-BLAST. However, noting that the oscillations arise around a bit error rate of 10^{-5}, we do not consider this problem to be of a serious nature; at such a level of bit error rate, a wireless communications system may, for all practical purposes, considered to be "error-free."

6.2.3 T-BLAST vs V-BLAST, $n_T = 8$ and $n_R = 5, 6, 7$

In this section, we consider BLAST configurations with fewer receive antennas than transmit antennas. Results are presented in the same fashion as before with fewer transmit antennas than receive antennas.

Figure 6.7 displays the bit error rate performance of T-BLAST (solid trace) and coded V-BLAST (broken trace), provided with an amount of coding equal to that used in T-BLAST. The antenna configurations of 8 transmit and 5-8 receive antennas, and the T-BLAST gives us the best performance within the first 10 iterations. The figure reveals a major limitation of V-BLAST system: the inability to work with fewer receive antennas than transmit antennas. In terms of T-BLAST performance, the following observations can be made from Figure 6.7:

- The bit error performance of T-BLAST improves with increasing number of receivers,

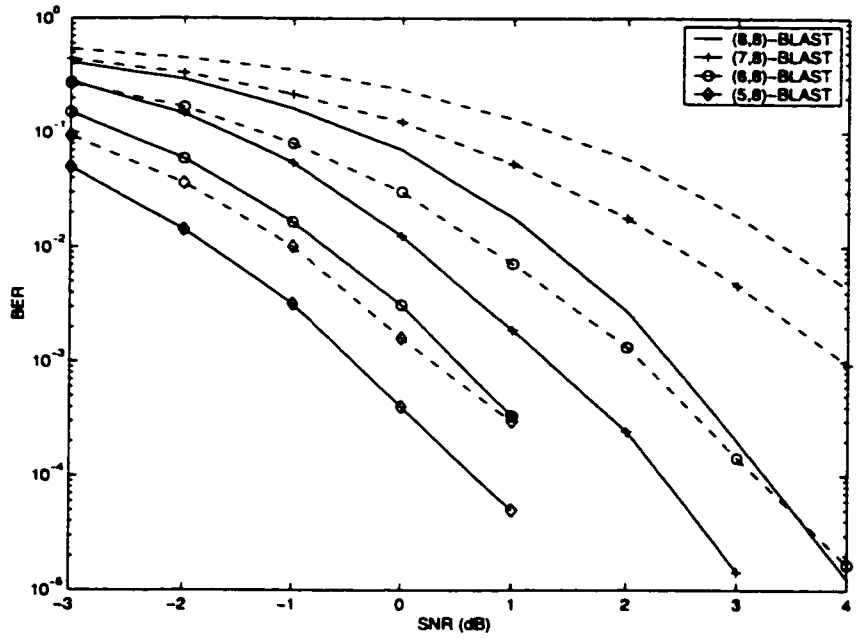

Figure 6.4: Bit error performance for n_T=5,6,7 and 8 and n_R=8, using convolutional code with rate $R = 1/2$ and constraint length 3, and QPSK modulation.

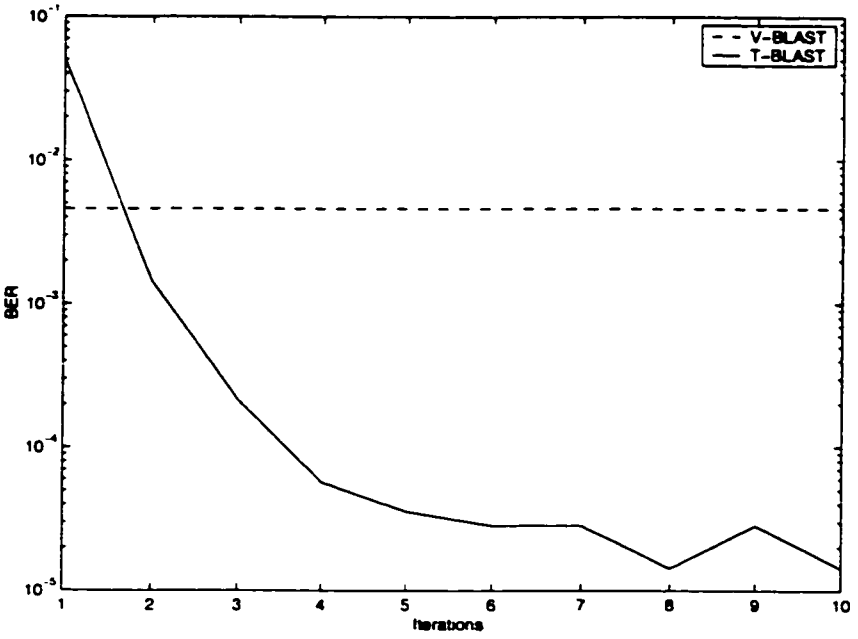

Figure 6.5: Convergence behavior of the T-BLAST receiver at SNR=4dB for n_T=7 and n_R=8, using convolutional code with rate $R = 1/2$ and constraint length 3, and QPSK modulation.

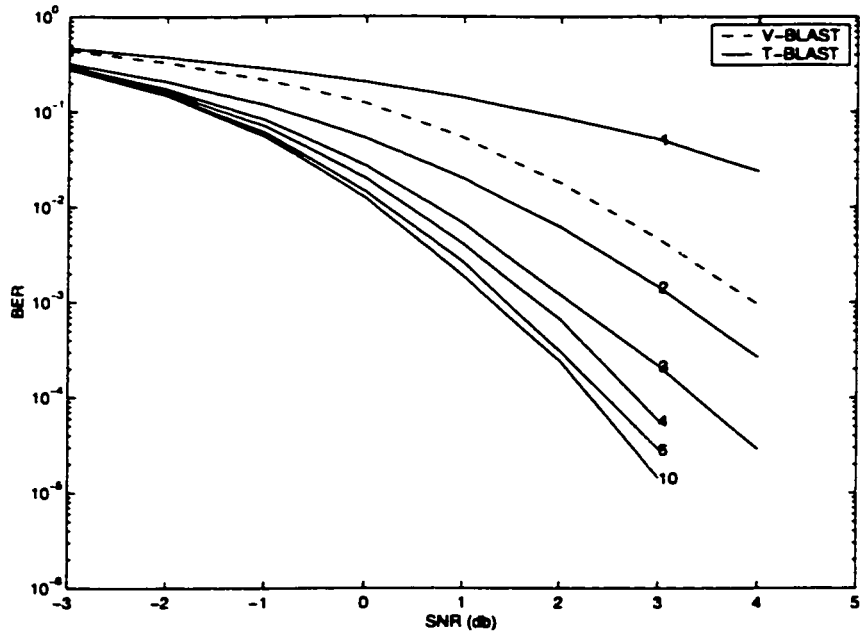

Figure 6.6: BER performance of T-BLAST with increasing iterations, for $n_T = 7$ and $n_R = 8$, using convolutional code with rate $R = 1/2$ and constraint length 3, and QPSK modulation.

with T-BLAST outperforming V-BLAST in all four cases.

- Increasing the number of receivers from 7 to 8 offers little benefits.

Further, in Figures 6.8 and 6.9, we have plotted the BER versus the number of iterations at SNR=4dB and BER versus SNR for 1,2,3,4,8 and 10 iterations for T-BLAST of (8,7) antenna configuration, respectively. As the results show the performance of T-BLAST exceeds that of V-BLAST in two iterations. Little benefit results from increasing the number of iterations beyond five; thus it is reasonable to accept this number as the optimal number of iterations in terms of both error reduction and receiver complexity.

The tail end of Figure 6.8 again displays the oscillating behavior of T-BLAST; however, as in the case of Figure 6.5, this oscillations are of no practical significance due to the low level of bit error rate (below 10^{-4}).

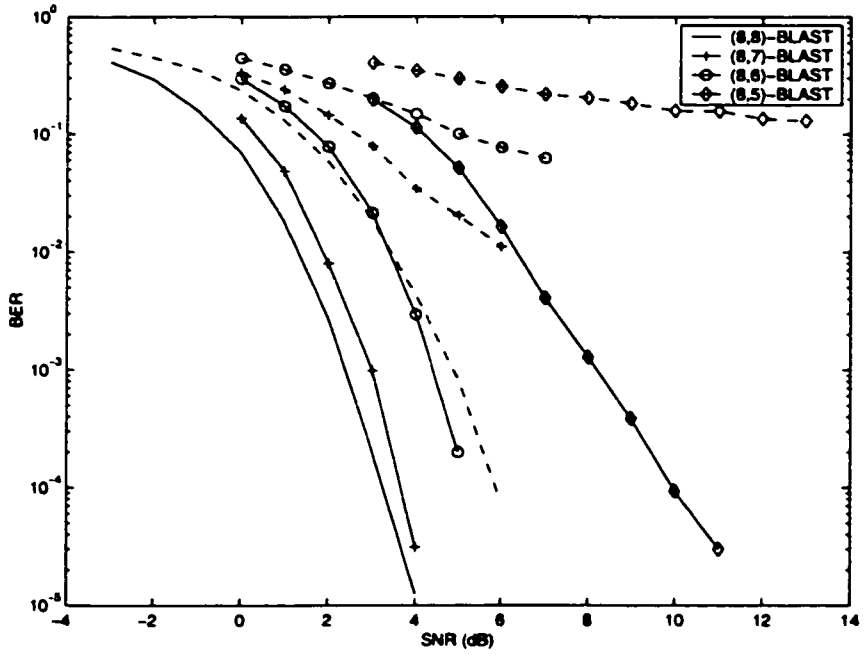

Figure 6.7: Bit error performance for n_T=8 and n_R=5,6,7 and 8, using convolutional code with rate $R = 1/2$ and constraint length 3, and QPSK modulation.

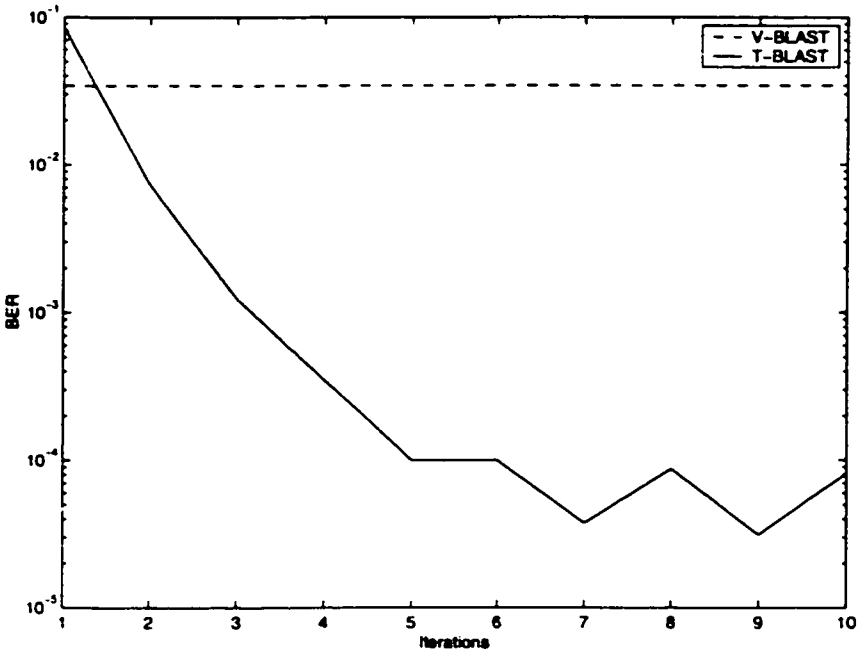

Figure 6.8: Convergence of the T-BLAST receiver at SNR=4dB for (n_T=8, n_R=7), using convolutional code with rate $R = 1/2$ and constraint length 3, and QPSK modulation.

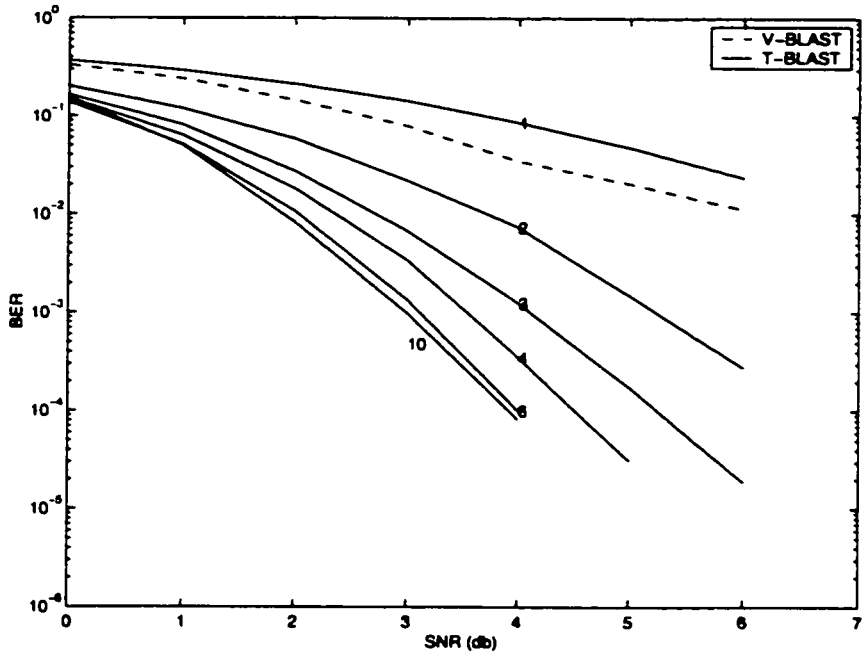

Figure 6.9: Bit error performance with number of iterations for n_T=8 and n_R=7, using convolutional code with rate $R = 1/2$ and constraint length 3, and QPSK modulation.

6.2.4 Spectral Efficiency

Another measure of performance is the information transmission rate of T-BLAST with the given channel code (convolutional code with rate $R = 1/2$ and constraint length 3), block size (100 symbols/transmission), and modulation (QPSK). The information rate of T-BLAST and V-BLAST with the given channel code is evaluated as follows: We fix the target BER for error-free communication to be achieved as 10^{-3} and we derive the SNR necessary to achieve this targeted BER for both V-BLAST and T-BLAST receivers.

Table 6.1 summarizes the signal-to-noise ratio necessary to achieve this targeted BER 10^{-3}, information rate of T-BLAST, the actual capacity of (8,8) matrix channel and the percentage of channel capacity achieved by T-BLAST referenced to the capacity of (8,8) matrix channel, for the various antenna configurations considered herein. The corresponding values for V-BLAST are given in Table 6.2. In terms of T-BLAST performance, we note the following:

- a power gain of 0.5-4dB achieved over the V-BLAST system, and
- 88% of the channel capacity is attained with T-BLAST using the antenna configuration (8,8), and a corresponding value of 60% for V-BLAST.

Moreover, the maximum possible information transmission rate of the T-BLAST and V-BLAST systems is 8 bits/channel use. At SNR=1.1dB, the channel capacity is 8 bit/channel use. Given this reference, T-BLAST and V-BLAST attain the Shannon theoretical capacity limit within 0.9dB and 3.9dB of average signal-to-noise ratio, respectively.

Configuration (n_T, n_R)	SNR ρ dB	Capacity of T-BLAST C_T bits/channel use	Channel Capacity C bits/channel use	Percentage capacity
(5,8)	0.0dB	5	6.80	74 %
(6,8)	0.5dB	6	7.36	81 %
(7,8)	1.0dB	7	7.93	88 %
(8,8)	2.0dB	8	9.14	88 %
(8,7)	3.0dB	8	10.46	76 %
(8,6)	4.0dB	8	11.89	67 %

Table 6.1: Spectral efficiency of T-BLAST in an indoors environment.

Configuration (n_T, n_R)	SNR ρ dB	Capacity of V-BLAST C_V bits/channel use	Channel Capacity C bits/channel use	Percentage capacity
(5,8)	0.5dB	5	7.36	67 %
(6,8)	2.5dB	6	9.70	61 %
(7,8)	4.0dB	7	11.89	59 %
(8,8)	5.0dB	8	13.40	60 %
(8,7)	-	-	-	-
(8,6)	-	-	-	-

Table 6.2: Spectral efficiency of V-BLAST in an indoors environment.

6.3 Outdoor Environment

This section compares the performances of T-BLAST and V-BLAST in an outdoor fixed-wireless environment. The experiments presented herein are based on the preliminary outdoor channel measurements acquired through the Department of Wireless Communications Research, Lucent Technologies, Bell Laboratories at Holmdel, New Jersey and were collected using a BLAST configuration with 5 transmit and 7 receive antennas. The distance between the measurement location of transmitter and receiver is roughly 2km. The system operates at a carrier frequency of 1.95 GHz with 30 kHz signal bandwidth.

6.3.1 T-BLAST vs V-BLAST

Figures 6.10 - 6.12 display the bit error rate performance of T-BLAST (solid trace) and coded V-BLAST (broken trace) provided, for antenna configurations (5,7), (4,7) and (3,7). In all three figures, T-BLAST provides the best performance within the first 6 iterations. The following observations can be made from these figures:

- The performances of both V-BLAST and T-BLAST improves with increasing SNR, and T-BLAST outperforms V-BLAST significantly.
- The performance of both T-BLAST and V-BLAST improves significantly with decreasing number of transmitters.

6.3.2 Spectral Efficiencies

In this section, we investigated the information transmission rate of T-BLAST with the given channel code (convolutional code with rate $R = 1/2$ and constraint length 3), block size (100 symbols/transmission) and modulation (QPSK), for outdoor fixed-to-fixed channel measurements. Again, the information rates of T-BLAST and V-BLAST with the given channel code were evaluated as follows: We fix the targeted BER for error-free communication to be achieved as 10^{-3} and then derive the SNR necessary to achieve the targeted BER for both V-BLAST and T-BLAST receivers.

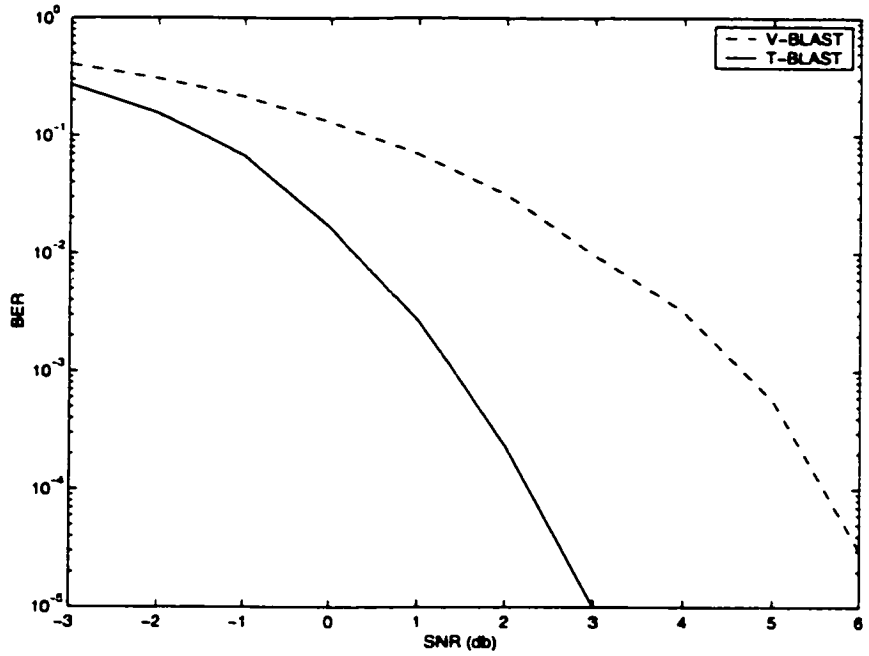

Figure 6.10: Bit error performance for $n_T = 5$ and $n_R = 7$, using convolutional code with rate $R = 1/2$ and constraint length 3, and QPSK modulation for outdoor channels.

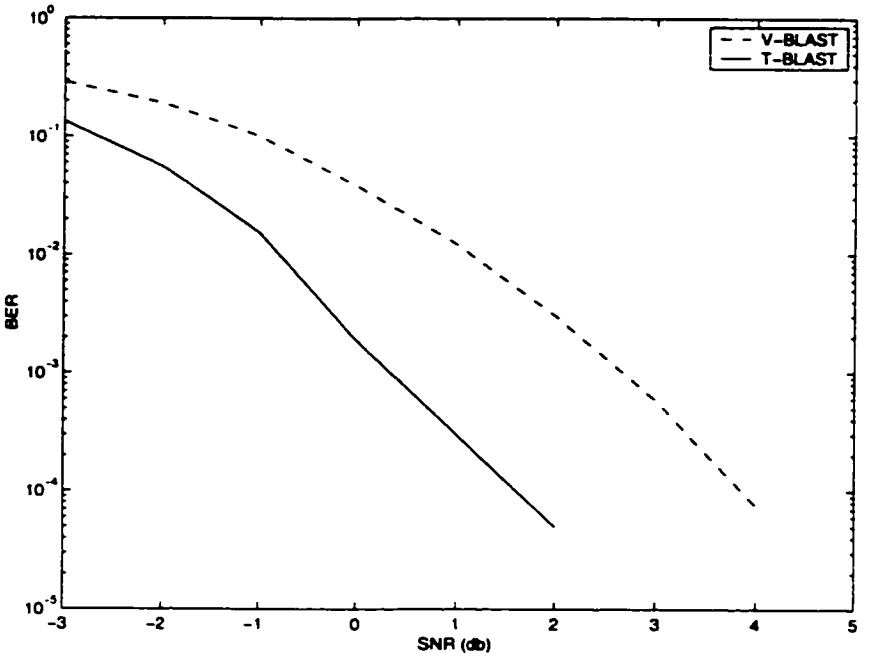

Figure 6.11: Bit error performance for n_T=4 and n_R=7, using convolutional code with rate $R = 1/2$ and constraint length 3, and QPSK modulation for outdoor channels.

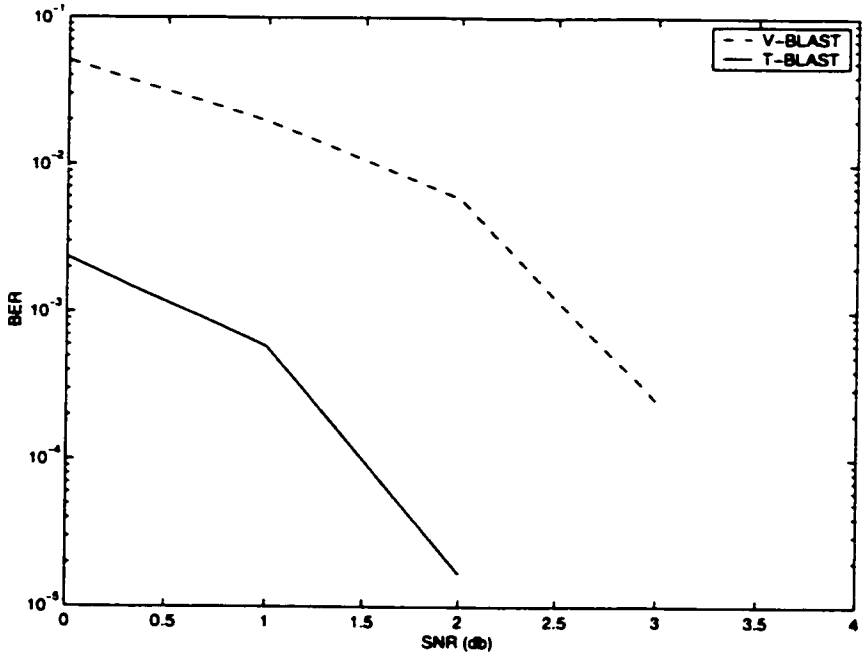

Figure 6.12: Bit error performance for n_T=3 and n_R=7, using convolutional code with rate $R = 1/2$ and constraint length 3, and QPSK modulation for outdoor channels.

Table 6.3 shows the SNR necessary to achieve this targeted BER of 10^{-3}, information rate of T-BLAST, the actual capacity of (5,7) matrix channel, and the percentage of system capacity achieved by T-BLAST referenced to the capacity of (5,7) matrix channel, for the antenna configurations considered in the experiments. The corresponding values of V-BLAST are listed in Table 6.4. In terms of T-BLAST performance, a power gain of 2-3.5dB is achieved over the V-BLAST system. Moreover, T-BLAST attains 86% of the channel capacity with antenna configuration (5,8), whereas V-BLAST attains only 57% of the channel capacity with the same configuration.

Further, the maximum possible information transmission rate of T-BLAST and V-BLAST is 5 bits/channel use. Meanwhile, at SNR=0.2dB, the channel capacity is 5 bit/channel use. Given this reference, T-BLAST and V-BLAST attain the Shannon theoretical capacity limit within 1.3dB and 4.8dB of average signal-to-noise ratio, respectively.

Configuration (n_T, n_R)	SNR ρ dB	T-BLAST C_T bits/channel use	Channel C bits /channel use	Percentage capacity
(5,7)	1.5dB	5	5.82	86 %
(4,7)	0.5dB	4	5.13	78 %
(3,7)	0.5dB	3	5.13	58 %

Table 6.3: Spectral efficiency of T-BLAST in an outdoors environment.

Configuration (n_T, n_R)	SNR dB	V-BLAST C_V bits/channel use	Channel C bits /channel use	Percentage capacity
(5,7)	5.0dB	5	8.73	57 %
(4,7)	3.0dB	4	6.91	58 %
(3,7)	2.5dB	3	6.54	43 %

Table 6.4: Spectral efficiency of V-BLAST in an outdoors environment.

6.4 Summary

In this chapter, we studied the bit error performance and spectral efficiency of T-BLAST systems empirically. Our analysis includes performance evaluation of the T-BLAST wireless communication system using the channel measurements acquired through the narrowband BLAST test-bed at the Bell-Labs of Lucent Technologies, Crawford Hill, New Jersey, in both indoor and outdoor environments.

The results of the real-life experiments demonstrate that:

- the Shannon capacity of MTMR schemes is achieved within a few dB's of average SNR within 3 to 5 iterations of the receiver, when one includes the losses due to practical coding schemes, and
- a power gain of 0.5-4dB is achieved over the coded V-BLAST system described in [3].

It should noted that this performance is not necessarily the best achievable, since we have used only simple channel coding with short block lengths. Moreover, a better gain may be attained by using turbo or low-density parity-check (LDPC) codes.

Chapter 7

Conclusions

This thesis is devoted to research into the BLAST (Bell Labs Layered Space-Time) architecture, which involves the use of multiple antennas at both transmitter and receiver. The attractive feature of the BLAST for wireless communications is the fact that the information capacity and spectral efficiency of the system grow linearly with the number of transmit antennas for a fixed amount of transmit power. The challenging task is to design space-time encoders and decoders realizing the full benefits of BLAST in a computationally feasible manner.

In this thesis, we have proposed and studied a new multi-transmit and multi-receive (MTMR) system called Turbo-BLAST or, for short, T-BLAST. Specifically, we showed that the combination of BLAST and turbo principles in an intelligent manner provides a reliable and practical solution to high data-rate transmission for wireless communication.

In the transmitter, we have proposed two novel space-time coding designs: a random space-time coding and a diagonal space-time coding by using conventional one-dimensional channel codes and space-time interleavers. In other words, a two-dimensional space-time cyclic code is designed via a one-dimensional channel coding approach. A major bonus of this unified approach is that it enables us to readily extend the space-time setting of the proposed system to much of the large body of results and insights developed over the last several decades in conventional coding theory.

The second major result of the proposed space-time encoding techniques is that they lead to an iterative space-time decoder that is turbo-like in operation, and capable of achieving a high spectral efficiency in the course of 3 to 4 iterations of the receiver. By representing the proposed space-time codes as a concatenation of inner and outer codes, the iterative space-time receiver decodes the inner and outer codes in a successive and iterative manner. The iterative decoder, which uses the *extrinsic* and *intrinsic* information concepts inherent to the turbo principle, is a close approximation to the global maximum likelihood decoding of the space-time codes.

Three turbo-like iterative decoders, assuming knowledge of the channel matrix, have been derived so as to reduce the complexity of the iterative decoder with some sacrifice in overall performance. In particular, joint channel estimation and decoding of the proposed space-time codes are performed in an iterative and simple fashion. Consequently, the complete system is constructed using building blocks of separately coded one-dimensional subsystems of equal capacity that allow one-dimensional signal processing at the receiving end, and yet the system is capable of closely attaining the Shannon capacity limit. It is important, however, to note that this new scheme does not use the turbo principle in a traditional manner. Rather, it uses the fundamental ideas underlying the turbo principle to decode the proposed random space-time coding in a near-optimal way and with low complexity. Hence, we call the new random space-time code a "turbo space-time code" and the MTMR wireless system that uses it "Turbo-BLAST".

The above unique properties and the excellent performance of T-BLAST have been demonstrated in a Rayleigh slow-fading environment, using computer simulations. Three different BLAST algorithms, T-BLAST, D-BLAST with no edge waste, and V-BLAST, were evaluated and we found T-BLAST to be superior to the other two by a wide margin (2-7dB).

Most important, we demonstrated the performance of T-BLAST and studied the convergence behavior using real-life wireless channel data. Specifically, the experimental analysis includes performance evaluation of the T-BLAST wireless communication system using a narrow-band BLAST test-bed at the Bell-Labs of Lucent Technologies, Crawford Hill, New

Jersey, in both indoor and outdoor environments:

- We empirically evaluated Turbo-BLAST with an antenna configuration of eight transmit and six receive antennas. In contrast to V-BLAST systems, T-BLAST accommodates any multiple antenna configuration, including the case of fewer receive antennas than transmit antennas with manageable computational complexity. The experimental results obtained under these conditions confirmed the practical virtues of T-BLAST.

- We have shown that, by using real-life data, the theoretical capacity limit of MTMR schemes is reached within a few dBs of average signal-to-noise ratio (SNR) for various antenna configurations, including the losses due to practical coding schemes at the target 10^{-3} bit-error-rate. Moreover, a power gain of 2 to 4dBs is achieved over the corresponding coded V-BLAST system.

Bibliography

[1] J. G. Foschini and M. J. Gans, "On limits of wireless communications in a fading environment when using multiple antennas", *Wireless Personal Communications*, 6: 311-335, 1999.

[2] J. G. Foschini, "Layered space-time architecture for wireless communication in a fading environment when using multi element antennas", *Bell Labs Technical Journal*, Autumn 1996.

[3] P. W. Wolniansky, J. G. Foschini, G. D. Golden, and R. A. Valenzuela, "V-BLAST: An architecture for realizing very high data rates over the rich-scattering wireless channel", *Proceedings of ISSSE*, Pisa, Italy, September 1998.

[4] G. D. Golden, J. G. Foschini, R. A. Valenzuela, and P. W. Wolniansky, "Detection algorithm and initial laboratory results using V-BLAST space-time communication architecture", *Electronics Letters*, vol. 35, pp. 14-15, January 1999.

[5] G. J. Foschini, G. D. Golden, R.A. Valenzuela, and P.W. Wolniansky, "Simplified processing for high spectral efficiency wireless communications employing multi-element array", *IEEE J. Selected Areas in Communications*, vol. 17, no. 11, November 1999.

[6] M. Sellathurai and S. Haykin, "Turbo-BLAST for high speed wireless communications", *Proceedings of wireless communications and network conf.*, Chicago, IL, September 2000.

[7] M. Sellathurai and S. Haykin, "A nonlinear iterative beamforming technique for wireless communications", *33rd ASILOMAR conf. on signals, systems, and computers*, Pacific Grove, CA, vol. 2, pp. 957-961, November, 1999.

[8] M. Sellathurai and S. Haykin, "Turbo-BLAST: A novel technique for multi-transmit multi-receive wireless communications", *Multiaccess, Mobility, and Teletraffic for Wireless Communications*, vol. 5, pp. 13-24, Kulwer Academic Publishers, ISBN 0-7923-7275-1.

[9] M. Sellathurai and S. Haykin, "A simplified diagonal BLAST architecture with iterative parallel-interference cancellation", to be presented in *IEEE Int. conf. on communications*, Helsinki, Finland, June 2001.

[10] M. Sellathurai and S. Haykin, "Further results on D-BLAST architecture", to be presented in *IEEE vehicular technology conf.*, Greece, May 2001.

[11] M. Sellathurai and S. Haykin, "Joint beamformer weight estimation and interference cancellation technique for TURBO-BLAST", to be presented in *IEEE Int. conf. on acoustics, speech and signal processing*, Salt Lake City, Utah, May 2001.

[12] M. Sellathurai and S. Haykin, "Random space-time codes with iterative decoders for BLAST architectures", to be presented in *IEEE Int. symposium on information theory*, June 2001.

[13] M. Sellathurai and S. Haykin, "TURBO-BLAST: First experimental results", to submit to *IEEE Trans. on Vehicular Technology.*

[14] M. Sellathurai and S. Haykin, "On the experimental verification of TURBO-BLAST", submitted to *IEEE vehicular technology conf.*, New Jersey, September 2001.

[15] E. Ayanoglu, K. Y. Eng, M. J. Karol, Z. Liu, P. Pancha, M. Veeraraghavan, and C. B. Woodworth, "Mobile Infrastructure", *Bell-Labs Technical Journal*, pp. 143-161, Autumn 1996.

[16] S. Ohmori, Y. Yamao, and N. Nakajima, "The future generations of mobile communications based on broadband access technologies", *IEEE Communications Magazine*, pp. 134-149, December 2000.

[17] M. Zeng, A. Annamalai, and V. K. Bargava, "Harmonization of third-generation mobile systems", *IEEE Communications Magazine*, pp. 94-104, December 2000.

[18] W. Mohr and W. Konhauser, "Access network evaluation beyond third-generation mobile communications", *IEEE Communications Magazine*, pp. 122-133, December 2000.

[19] W. C. Jakes, Jr., *Microwave Mobile Communications*, John Wiley and Sons, New York, 1974.

[20] T. S. Rappaport, *Wireless Communications: Principles & Practice*, Prentice Hall, 1996.

[21] R. B. Ertel, P. Cardieri, K. W. Sowerby, T. S. Rappaport, and J. H. Reed, "Overview of spatial channel models for antenna array communications systems", *IEEE Personal Communications*, pp. 10-27, February 1998.

[22] P. A. Bello, "Characterization of randomly time-variant channels", *IEEE Trans. on Communication Systems*, vol. CS-11, pp. 360-393, 1963.

[23] E. Biglieri, J. Proakis, and S. Shamai, "Fading channels: Information-theoretic and communications aspect", *IEEE Trans. on Information Theory*, vol. 44, no. 6, pp. 2619-2651, October 1998.

[24] Simon Haykin, *Communication Systems*, 4th Edition, John Wiley, 2000.

[25] D. Gesbert, H. Bolcskei, D. Gore, and A. Paulraj, "MIMO wireless channels: capacity and performance prediction", *Proceedings of IEEE Globecom*, San Francisco, CA, vol. 1, pp. 1083-1087, November 2000.

[26] H. Zheng and D. Samardzija, "H.263 Video over BLAST Wireless Test-Bed", to be presented in *the 35th annual conference on information sciences and systems*, Baltimore, Maryland, March 2001.

[27] P. Kiritsi, P. Wolniansky, and R. A. Valenzuela, "Indoor BLAST measurements: Capacity of multi-element antenna systems", *Multiaccess Mobility and Teletraffic for Wireless Communications*, vol. 5, pp. 49-60, Kulwer Academic Publishers, ISBN 0-7923-7275-1.

[28] C. Martin, J. H. Winters, and N. R. Sollenberger, "Multiple-Input Multiple-Output (MIMO) Radio Channel Measurements", in *Proceedings of vehicular technology conference*, Boston, MA, 0-7803-6507-0, September 2000.

[29] A. Paulraj, "Diversity Techniques", *Chapter in CRC Handbook on Communications*, Ed. J. Gibson, CRC press, 11:213-223, December 1996.

[30] J. G. Proakis, *Digital Communications*, 3rd Ed., McGraw-Hill, 1995.

[31] A. Paulraj and C. Papadias, "Space-time processing for wireless communications", *IEEE Signal Processing Magazine*, pp. 49-83, November 1997.

[32] B. Lu and X. Wang, "Space-time code design in OFDM systems", *Proceedings of IEEE Globecom*, San Francisco, CA, vol. 1, pp. 1000-1004, November 2000.

[33] Z. Wang and G.B. Giannakis, "Wireless multicarrier communications: Where Fourier meets Shannon", *IEEE Signal Processing Magazine*, pp. 29-48, May 2000.

[34] S. N. Diggavi, "Communication in the Presence of Uncertain Interference and Channel Fading", *Ph.D. Thesis*, Stanford University, 1998.

[35] A. F. Naguib, "Adaptive Antennas for CDMA Wireless Networks", *Ph.D. Thesis*, University of Stanford, 1996.

[36] Lennart Rade and Bertil Westergren, *Mathematics Handbook for Science and Engineering*, Third ed., Studentlitteratur, 1995.

[37] C. Papadias, "On the spectral efficiency of space-time spreading schemes for multiple antenna CDMA systems", *33rd Asilomar conference on signals, systems, and computers*, Pacific Grove, CA, pp. 639-643, 24th-27th October 1999.

[38] P. Dent, G. E. Bottomley, and T. Croft, "Fading mobile radio systems", *Electronics Letters*, vol. 29, no. 13, pp. 1162-1163, 24th June 1993.

[39] E. Teletar, "Capacity of multi-antenna Gaussian channels", *Technical Report., AT &T Bell Laboratories*, Murray Hill, NJ,1995.

[40] C. E. Shannon, "A Mathematical Theory of Communication", *Bell System Technical Journal*, vol. 27, pp. 379-423, 623-656, October 1948.

[41] R. G. Gallager, *Information Theory and Reliable Communications*, New York: John Wiley and Sons, 1968.

[42] D. J. C. MacKay, "Good error-correcting codes based on very sparse matrices", *IEEE Trans. on Information Theory*, vol. 45, no. 2, pp. 399-431, March 1999.

[43] B. J. Frey and D. J. C. MacKay, "Irregular Turbo codes", *In proceedings of the 37th Allerton conf. on communication, control, and computing*, Allerton House, Illinois, 1999.

[44] D. J. C. MacKay, S. T. Wilson, and M. C. Davey, "Comparison of constructions of irregular Gallager codes", *IEEE Trans. on Communications*, vol. 47, no. 10, pp. 1449-1454, October 1999.

[45] H. Krim and M. Viberg, "Two Decades of Array Signal Processing Research", *IEEE signal processing magazine*, pp. 67-94, July 1996.

[46] P. Balaban and J. Salz, "Optimum Diversity Combining and Equalization in Digital Data Transmission with Applications to Cellular Mobile Radio-Part I: Theoretical Considerations", *IEEE Trans. on Communications*, vol. 40, no. 5, pp. 885-893, May 1992.

[47] J. H. Winters, "Optimum combining in digital mobile radio with cochannel interferences", *IEEE J. Selected Areas in Communications*, vol. SAC-2, no. 4, pp. 528-539, july 1984.

[48] S. M. Alamouti, "A simple transmitter diversity scheme for wireless communications", *IEEE J. Selected Areas of Communications*, vol. 6, pp. 1451-1458, October 1998.

[49] A. Narula, M. Trott, and G. Wornell, "Information theoretic analysis of multiple-antenna transmission diversity", in *IEEE Int. symposium on information theory and its applications*, September 1996.

[50] A. Narula, M. Trott, and G. Wornell, "Performance limits of coded diversity methods for transmitter antenna arrays", *IEEE Trans. on Information Theory*, pp. 2418-2433, vol. 45, November 1999.

[51] S. L. Ariyavisitakul, "Turbo space-time processing to improve wireless channel capacity", *IEEE Trans. on Communications*, vol. 48, no. 8, pp. 1347-1359, August 2000.

[52] S. L. Ariyavisitakul, J. H. Winters, and I. Lee, "Optimum space-time processors with dispersive interference: Unified analysis and required filter span" *IEEE Trans. on Communications*, vol. 47, no. 7, pp. 1073-1083, July 1999.

[53] B. Hassibi, "High-rate codes that are linear in space and time", *Technical Memorandum, Bell Laboratories, Lucent Technologies*, 2000.

[54] S. Haykin, *Adaptive Filter Theory*, 3rd ed., Englewood Cliffs, N.J: Prentice-Hall, 1996.

[55] G. H. Golub and C. F. Van Loan, *Matrix Computations*, Johns Hopkins Press, 3rd Ed, 1996.

[56] M. O. Damen, "Joint Coding/Decoding in a Multiple Access System, Application to Mobile Communication", *Ph.D. Thesis*, ENST, October 1999.

[57] X. Li, H. Huang, G. J. Foschini, and R. A. Valenzuela, "Reduced-complexity detection algorithms for systems using multi-element arrays", *Proceedings of IEEE Globecom*, San Francisco CA, vol. 1, pp. 1072-1076, November 2000.

[58] X. Li, H. Huang, G. J. Foschini, and R. A. Valenzuela, "Effects of iterative detection and decoding on the performance of BLAST", *Proceedings of IEEE Globecom*, San Francisco, CA, vol. 1, pp. 1062-1066, November 2000.

[59] B. Hassibi, "An efficient square-root algorithm for BLAST", *Technical Memorandum*, Bell Laboratories, Lucent Technologies, 1999.

[60] V. Tarokh, N. Seshadri, and A. R. Calderbank, "Space-time codes for high data rate wireless communications: performance criterion and code construction", *IEEE Trans. on Information Theory*, vol. 44, pp. 744-765, March 1998.

[61] V. Tarokh, H. Jafarkhani, and A. R. Calderbank, "Space-time block codes from orthogonal design", *IEEE Trans. on Information Theory*, vol. 45, pp. 1456-1567, July 1999.

[62] R. A. Monzingo and T. W. Miller, *Introduction to Adaptive Arrays*, New York: Wiley, 1980.

[63] C. Berrou and A. Glavieux, "Near optimum error- correcting coding and decoding: Turbo codes", *IEEE Trans. on Communications*, vol. 44, pp. 1261-1271, October 1996.

[64] C. Berrou, A. Glavieux, and P.Thitmajshima, "Near Shannon Limit Error-Correcting Coding and Decoding: Turbo codes", *Proceedings of Int. conf. on communications*, Geneva Switzerland, pp. 1064-1070, May 1993.

[65] C. Berrou and M. Jezequel, "Non-binary convolutional codes for turbo coding", *Electronics Letters*, vol. 35, no. 1, pp. 39-40, 7th January, 1999.

[66] C. Berrou and M. Jezequel, "Frame oriented convolutional turbo codes", *Electronics Letters*, vol. 32, no. 15, pp. 1362-1364, 18th July, 1996.

[67] R. G. Gallager, *Low-Density Parity-Check Codes*, MIT Press, 1963.

[68] T. Richardson and U. Urbanke, "Efficient encoding of low-density parity-check codes", *Technical Memorandum* Bell-Laboratories, Lucent Technologies, 1999.

[69] J. Hagenauer, "The turbo principle: Tutorial introduction and state of the art", *Int. symposium on turbo codes*, Best, France, September 1997.

[70] R. J. McEliece, E. R. Rodemich, and J. Cheng, "The turbo decision algorithm", in *33rd Allerton conf. on communication, control, and computing*, Allerton House, Illinois, October 1999.

[71] B. Sklar "Primer on turbo code concept", *IEEE Communication Magazine*, pp. 94-102, December 1997.

[72] S. Haykin, "Adaptive Digital Communication Receiver", *IEEE Communications Magazine*, pp. 106-114, December 2000.

[73] S. Benedetto, D. Divsalar, G. Montorsi, and F. Pollara, "A soft-input soft-output maximum a posteriori (MAP) module to decode parallel and serial concatenated codes", *TDA Progress Report 42-127.*

[74] S. Benedetto, D. Divsalar, G. Montorsi and F. Pollara, "Analysis, design, and iterative decoding of double serially concatenated codes with interleavers", *IEEE J. Selected Areas in Communications*, February 1998.

[75] M. C. Reed and P. D. Alexander, J. A. Asenstorfer, and C.B. Schlegel, "Near single user performance using iterative multiuser detection for CDMA with turbo-codes decoders", *Proceedings of PIMRC'97*, pp. 750 -744, September 1997.

[76] J. Lodge and M. Gertsman, "Joint detection and decoding by turbo processing for fading channel communications", *Proceedings of the int. symposium of turbo codes and related topics*, September 1997.

[77] M. Moher, "An iterative multiuser decoder for near capacity communications", *IEEE Trans. on Communications*, vol. 46, pp. 870-880, July 1998.

[78] M. Moher, "Cross-Entropy and Iterative Decoding", *Ph.D. Thesis*, Carleton University, Ottawa, Canada, May 1997.

[79] X. Wang and V. Poor, "Iterative (TURBO) soft interference cancellation and decoding for coded CDMA", *IEEE Trans. on Communications*, vol. 47, no.7, pp. 1046-1061, July 1999.

[80] H. El Gamal and A. R. Hammons, Jr, "New approach for space-time transmitter/receiver design", *37th Allerton conf. on communication, control, and computing*, Allerton House, Illinois, pp. 186-194, September 1999.

[81] H. El Gamal and E. Geraniotis, "Iterative multiuser detection for coded CDMA signals in AWGN and fading channel", *IEEE J. on Selected Areas in Communications*, vol. 18, no. 1, pp. 30-41, January 2000.

[82] C. Douillard, M. Jezequel, C. Berrou, A. Picart, P. Didier, and A. Glavieux, "Iterative correction of inter-symbol interference: Turbo-equalization", *European Transactions on Telecommunications*, vol. 6, no.5, pp. 507-511, September/October 1995.

[83] P. Robertson, and Th. Woerz, "A novel bandwidth efficient coding scheme employing turbo-codes", *Proceedings of IEEE Int. conference on communications*, Dallas, USA, June 1996.

[84] Kimmo Kettunen, "Iterative multiuser receivers utilizing soft decoding information", *Proceedings of Int. Conference on Communications*, pp. 942-946, June 1999.

[85] M. C. Valenti, "Iterative detection and decoding for wireless communications", *Ph.D. Thesis*, Virginia Polytechnic Institute of State University, July 1999.

[86] G. D. Forney, Jr., "Shannon Lecture", *Int. symposium on information theory*, September 17-22, 1995, British Columbia, Canada.

[87] E. R. Berlekamp, *Algebraic Coding Theory* New York, McGraw-Hill, 1968.

[88] G. D. Forney, Jr., *Concatenated Codes*, Cambridge, Massachusetts: Massachusetts Institute of Technology, 1966.

[89] R. M. Fano, "A heuristic discussion of probabilistic decoding", *IEEE Trans. on Information Theory*, vol. 15, pp. 122-127, January 1969.

[90] R. Johannesson and K. Sh. Zigangirov, *Fundamentals of Convolutional Coding*, IEEE Press, 1999.

[91] A. J. Viterbi, "Error bounds for convolutional codes and an asymptotically optimum decoding algorithm", *IEEE Trans. on Information Theory*, vol. 13, pp. 260-269, April 1967.

[92] G. D. Forney, Jr, "The Viterbi Algorithm", *IEEE Trans. on Information Theory*, vol. IT-61, no 3, pp. 268-278, March 1973.

[93] L. R. Bahl, J. Cocke, F. Jelinek and J. Raviv, "Optimal decoding of linear codes for minimizing symbol error rate", *IEEE Trans. on Information Theory*, vol. 20, pp. 284-287, March 1974.

[94] R. W. Chang and J. C. Hancock, "On receiver structures for channels having memory", *IEEE Trans. on Information Theory*, vol. IT-12, pp 463-468, October 1966.

[95] K. Abend and B. D. Fritchman, "Statistical detection for communications channels with inter-symbol interference", *Proceedings of the IEEE*, vol. 58, no. 5, pp. 779-785, May 1970.

[96] J. Hagenauer and P. Hoeher, "Viterbi algorithm with soft-decision outputs and its applications", in *Proceedings of IEEE Globecom*, pp. 1680-1686, 1989.

[97] R. Robertson and P. Hoeher, "Optimal and sub-optimal maximum a posteriori algorithms suitable for turbo coding", *European Transactions on Telecommunications*, vol.8, pp. 119-125, March/April 1997.

[98] S. Verdu, "Minimum probability of error for asynchronous Gaussian multiple-access channels", *IEEE Trans. on Information Theory*, vol.32, no. 1, pp. 85-96, January 1986.

[99] S. L. Loyka, "Channel capacity of two-antenna BLAST architecture", *IEE Electronics letters*, vol.35, no. 17, pp. 1421-1422, 19th August 1999.

[100] M. B. Pursley and C. S. Wilkins, "Adaptive-rate coding for frequency-hop communications over Rayleigh fading channels", *IEEE J. Selected Areas in Communications*, vol. 17, no. 7, pp. 1224-1232, July 1999.

[101] O. Tirkkonen and A. Hottinen, "Complex space-time block codes for four Tx antennas", *Proceedings of IEEE Globecom*, San Francisco, CA, vol. 1, pp. 1005-1009, November 2000.

[102] S. Wishwanath, W. Yu, R. Negi, and A. Goldsmith, "Space-time turbo codes: Decorrelation properties and performance analysis for fading channels", *Proceedings of IEEE Globecom*, San Francisco, CA, vol. 1, pp. 1016-1020, November 2000.

[103] L. Hang, C. Jason, and R.S. Cheng, "Low complex turbo space-time code for system with large number of antennas", *Proceedings of IEEE Globecom*, San Francisco, CA, vol. 1, pp. 990-994, November 2000.

[104] D. Tujkovic, "Recursive space-time trellis codes for turbo coded modulation", *Proceedings of IEEE Globecom*, San Francisco, CA, vol. 1, pp. 1010-1014, November 2000.

[105] Y. Liu, Michale P. Fitz, and O. Y. Takeshita, "QPSK space-time turbo codes", *Proceedings of Int. Conference on Communications*, pp. 292-296, 2000.

[106] A. Stefanov and T. M. Duman, "Turbo coded modulation for wireless communications with antenna diversity", *Proceedings of IEEE vehicular technology conf.*, pp. 1565-1569, 1999.

[107] A. G. Burr, "On space-time turbo-codes", *2nd International symposium on turbo codes & related topics*, Best, France, 2000.

[108] H. Su and E. Geraniotis, "Spectrally efficient turbo-codes with with full antenna diversity", *Proceedings of Multi access Mobility and Teletraffic for Wireless Communications*, Venice, Italy, October 1999.

[109] S. Baro, G. Bauch, A. Pavlic, and A. Semmler, "Improved BLAST performance using space-time block codes and turbo decoding", *Proceedings of IEEE Globecom*, San Francisco, CA, vol. 1, pp. 1067-1071, 2000.

[110] G. Jongren and M. Skoglund, "Utilizing quantized feedback information in orthogonal space-time block coding", *Proceedings of IEEE Globecom*, San Francisco, CA, vol. 1, pp. 995-999, 2000.

[111] K. Cavalec-Amis and R. Pyndiah, "Block turbo codes for space-time systems", *Proceedings of IEEE Globecom*, San Francisco, CA, vol. 1, pp. 1021-1025, 2000.

[112] P. Lancaster and M. Tismenetsky, *The Theory of Matrices with Applications*, second edition, Academic press, 1985.

[113] M. Sellathurai and S. Haykin, "Statistical learning and layered space-time architecture for point-to-point wireless communication", *32nd ASILOMAR conf. on signals, systems, and computers*, Pacific Grove, CA, vol. 2, pp. 1084-1088, November 1998.

[114] B. A. Bjerke and J. G. Proakis, "Multiple-antenna diversity techniques for transmission over fading channels", *Proceedings of wireless communications and network conference*, Vancouver, Canada, September 1999.

[115] B. M. Hochwald and T. L. Marzetta, "Unitary space-time modulation for multiple-antenna communications in Rayleigh flat fading", *IEEE Trans. on Information Theory*, vol. 46, no.2, March 2000.

[116] T. L. Marzetta and B. M. Hochwald, "Fundamental limitations on multiple-antenna wireless links in Rayleigh fading", *Proceedings of Int. symposium on information theory*, pp. 310, 1998.

[117] A. R. Hammons, Jr and H. El Gamal, "On the theory of space-time codes for PSK modulation", IEEE Trans. on Information Theory, vol. 46, no. 2, pp. 524-542, March 2000.

[118] R. D. Wesel and J. M. Cioffi, "Trellis code design for periodic interleavers", *IEEE Communications letters*, vol. 3, no. 4, pp. 103-105, April 1999.

[119] E. Biglieri, G. Caire, and G. Taricco, "Designing codes for the wireless channel", *Proceedings of the 6th Canadian workshop on information theory*, pp. 1-4, Kingston, Ontario, June 1999.

[120] P. F. Driessen and G. J. Foschini, "On the capacity formula for multiple input-multiple output wireless channels: A geometric interpretation", *IEEE Trans. on Communications*, vol. 47, no. 2, pp. 173-176, February 1999.

[121] S. Verdu, *Multiuser Detection*, Cambridge university Press, 1999.

[122] T. M. Cover and J. A. Thomas, *Elements of Information Theory*, 2nd edition, John Wiley and Sons, Inc., 1991.